Mitochondrial Dysfunction And Oxidative Stress In Osteoarthritis

Christos Gavriilidis

A thesis submitted in partial fulfillment of the requirements for the degree of Doctor of Philosophy

Institute of Cellular Medicine

Newcastle University

August 2012

Abstract

Mitochondria are considered the powerhouse of the cell being the major site of ATP production but in addition to this function they also regulate ROS production and inhibition, calcium handling and apoptosis. Previous studies have reported a downregulation in the levels of superoxide dismutase 2 (SOD2), an inhibitor of mitochondrial superoxide ($O_2^{\cdot-}$), in osteoarthritic (OA) hip cartilage compared to that from healthy joints (neck of femur fracture; NOF). This finding provides the opportunity to characterise the functional effects of SOD2 downregulation in OA in the context of oxidative damage and mitochondrial dysfunction.

SOD2 depletion increased the mitochondrial $O_2^{\cdot-}$ levels in human articular chondrocytes (HAC). Measurement of lipid peroxidation levels in OA and NOF cartilage showed that OA cartilage has higher levels of lipid peroxidation compared to NOF. SOD2 depletion in a chondrosarcoma cell-line, SW1353, also led to a significant increase in lipid peroxidation levels. Additionally, SOD2 depletion led to a significant increase in mtDNA strand breaks in SW1353 cells although there was no difference detected in OA compared to NOF mtDNA. However, large-scale mtDNA deletions were identified in OA cartilage and other OA joint tissues but the low levels of mutated mtDNA observed were not considered to be pathologically relevant.

Mitochondrial respiratory function was also determined in OA and NOF isolated chondrocytes. OA chondrocytes showed less spare respiratory capacity (SRC), higher non-phosphorylating respiration and higher proton leak compared to NOF. SOD2-depleted HAC also showed a lower SRC and higher proton leak. Additionally, HAC demonstrated a very low mitochondrial/glycolysis ratio, suggesting that HAC are highly glycolytic cells. SOD2 depletion caused depolarization of the $\Delta\psi m$.

NLRX1, a mitochondrially localised gene involved in innate immunity signalling was also identified to regulate basal levels of matrix metalloproteinase 13 (MMP-13) and double stranded RNA- induced ROS levels in chondrocytes.

These findings suggest that SOD2 depletion in chondrocytes leads to oxidative damage and mitochondrial dysfunction caused by increasing ROS levels and can potentially lead towards alterations in cell signalling pathways, cellular dysfunction and cartilage degradation.

Acknowledgements

I would like to thank my supervisors Dr. David Young and Prof. Robert Taylor for their guidance and advice and their continuous patience and support throughout this study.

I would also like to thank Profs Bob Lightowlers and Drew Rowan for useful guidance and Drs Marta Radwan, Matt Barter, Kim Krishnan, Satomi Miwa, Laura Greaves and Trevor Booth for advice, assistance and for sharing their expertise throughout this study. Also special thanks to Arthritis Research UK for funding this project.

Thanks to the students and postdocs of both MRGs for the great working and social environment and everyone's contribution to the permanent supply of sweets!

I would like to thank my family and friends for their understanding and continuous support over the last few years and especially during the last months of writing. I especially thank my wife Kamila for her love and ongoing support and having to put up with me throughout the last few years!

Contents

List of Figures and Tables

Abbreviations used in this thesis

•OH	Hydroxyl radical
ADAM	A disintegrin and metalloproteinase
ADP	Adenosine diphosphate
AP-1	Activator protein-1
ATP	Adenosine triphosphate
B2M	β-2-microglobulin
BAC	Bacterial Artificial Chromosome
Ca^{2+}	Calcium ion
COX	Cytochrome *c* oxidase
DHR-123	Dihydrorhodamine-123
DMSO	Dimethyl sulfoxide
DNA	Deoxyribonucleic acid
dsDNA	Double-stranded DNA
ECAR	Extracellular acidification rate
ECM	Extracellular matrix
ER	Endoplasmic reticulum
FACS	Fluorescent activated cell sorting
FAD	Flavin adenine dinucleotide
FCCP	Carbonyl cyanide-p-trifluoromethoxyphenylhydrazone
Fe-S	Iron-sulphur cluster
FMN	Flavin mononucleotide
g	Relative centrifugal force
H_2O_2	Hydrogen peroxide
HAC	Human articular chondrocyte
IL	Interleukin
iNOS	Inducible nitric oxide synthase
JAK/STAT	Janus kinase/ Signal transducer and activator of transcription
JNK	c-Jun N-terminal kinase
LA-PCR	Long amplification Polymerase chain reaction
MAPK	Mitogen-activated protein kinase
MDA	Malondialdehyde
MDA5	Melanoma differentiation-associated gene 5

MMP	Matrix metalloproteinase
MnSOD	Manganese superoxide dismutase
MRC	Mitochondrial respiratory chain
mtDNA	Mitochondrial DNA
NAC	N-acetyl-L-cysteine
NAD^+	Nicotinamide adenine dinucleotide
NF-κB	Nuclear factor kappa-light-chain-enhancer of activated B cells
NLR	Nucleodite oligomerisation domain (NOD)-like receptor
NLRP3	Nucleodite oligomerisation domain (NOD)-like receptor family, pyrin domain containing 3
NO	Nitric oxide
NOD	Nucleotide-binding oligomerisation domain-containing protein
NOF	Neck of femur fracture
$O_2^{\cdot-}$	Superoxide
OA	Osteoarthritis
OCR	Oxygen control rate
$ONOO^-$	Peroxynitrite
OSM	Oncostatin M
OXPHOS	Oxidative phosphorylation
PAMP	Pathogen-associated molecular patterns
PCR	Polymerase chain reaction
POLG	Polymerase gamma
poly(I:C)	Polyinosinic : polycytidylic acid
PRR	Pattern recognition receptors
RA	Rheumatoid arthritis
RCR	Respiratory control ratio
RIG-I	Retinoic acid-inducible gene I
RLR	RIG-I like receptor
RNA	Ribonucleic acid
ROS	Reactive oxygen species
rRNA	Ribosomal RNA
RT-PCR	Reverse-transcription PCR
SDH	Succinate dehydrogenase

SEM	Standard error of mean
siRNA	Small-interfering RNA
SOD	Superoxide dismutase
SRC	Spare respiratory capacity
ssDNA	Single-stranded DNA
TBARS	Thiobarbituric Acid Reactive Substances
TCA	Tricarboxylic acid cycle, Krebs cycle, citric acid cycle
TIMP	Tissue inhibitor of metalloproteinases
TLR	Toll-like receptor
TMRM	Tetramethyl Rhodamine Methyl Ester
TNF-α	Tumor necrosis factor-alpha
tRNA	Transfer RNA
UCP	Uncoupling protein
VISA	Virus-induced signalling adapter
Δψm	Mitochondrial membrane potential

Chapter 1. Introduction

1.1 Mitochondria

Mitochondria are small organelles that are present in large (but variable) numbers in cells of all eukaryotic organisms. Mitochondria are considered the powerhouse of the cells as they are the main sites of adenosine triphosphate (ATP) production of the cells via oxidative phosphorylation (OXPHOS). Mitochondria are also involved in mitochondrial membrane potential (Δψm) regulation, Ca^{2+} handling and apoptosis and in the regulation of cell toxicity by mainly regulating reactive oxygen species (ROS) production as well as inhibition (Cadenas et al 1977; Landolfi et al 1998; Mitchell, & Moyle 1969; Newmeyer et al 1994; Turrens, & Boveris 1980). In humans, they have their own, maternally inherited, 16,569bp extrachromosomal DNA (mtDNA) that encodes for 13 polypeptides, 22 tRNAs and 2 rRNAs, which are responsible for the translation of those polypeptides (Anderson et al 1981; Andrews et al 1999). Mitochondrial functions are regulated both by nuclear and mitochondrial transcripts (Lister et al 2005).

1.1.1 Mitochondrial structure

Mitochondria have a diameter size of 0.5-1μm and occupy a large portion of the volume of the cell cytoplasm (Frey, & Mannella 2000). They are dynamic organelles as they can move within cells via microtubules or microfilaments and they can also fuse and divide (fission) (Ligon, & Oswald 2000; Morris, & Hollenbeck 1995). They normally form a reticular network of fused mitochondria or a fragmented arrangement of discrete organelles (Bereiter- Hahn 1994). These processes are maintained by the co-ordination of fission and fusion machinery (Liesa et al 2009; Palmer et al 2011; Westermann 2010). Mitochondrial fusion is controlled by three nuclear-encoded proteins; mitofusin 1 (Mfn1), Mfn2 and optic atrophy 1 (Opa1) (Alexander et al 2000; Chakraborti et al 2003; Chen et al 2003; Delettre et al 2000). Dynamin related protein 1 (Drp1) regulates mitochondrial fission (division) (Smirnova et al 2001). These processes are essential for the maintenance of respiratory activity required by the cells as well as to regulate processes such as inheritance and stability of

mtDNA, transmission of energy, cellular differentiation, metabolite maintenance, apoptosis, Ca^{2+} signalling and embryonic development (Chang et al 2006; Chen, & Chan 2005; Chen et al 2010; Ishihara et al 2009; Tanaka et al 2010).

Mitochondria are composed of 2 lipid membranes (inner and outer) and 2 internal compartments; the intermembrane space and the mitochondrial matrix (Figure 1.1).

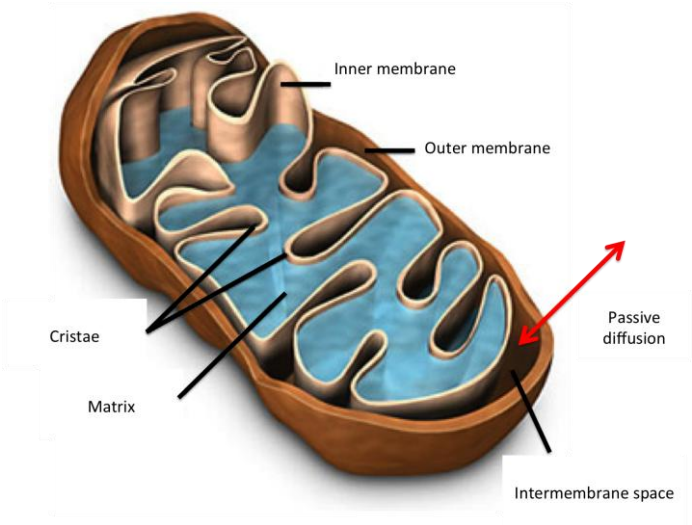

Figure 1.1 The general organisation of the mitochondrion

Figure shows the major compartments of the mitochondrion; the outer membrane, the intermembrane space, the inner membrane folded into cristae and the mitochondrial matrix. (Image taken from of http://micro.magnet.fsu.edu/)

Outer membrane

The outer membrane is a porous membrane that allows passive diffusion of low molecular weight molecules (less that 5kDa) between the cytosol and the intermembrane space (Colombini 1979). This is achieved by the presence of porin that forms large aqueous channels through the lipid bilayer of the membrane (Colombini 1979; Mihara et al 1982). It also contains enzymes that are involved in lipid synthesis, import receptors and the enzymatic machinery responsible for division and fusion of the mitochondrion (Heiden et al 2000).

Inner membrane

The inner membrane contains enzymes that are essential for the activity of the mitochondrial respiratory chain (MRC), the site of OXPHOS of the

mitochondrion, to facilitate the production of ATP by ATP synthase. A proton gradient has to be established in order for OXPHOS to function and as a result the inner membrane is very impermeable compared to the outer membrane, especially to ions (Mitchell, & Moyle 1967). It also contains transport proteins to facilitate the movement of molecules in and out of the matrix (Voos et al 1999; Schleyer, & Neupert 1985). The inner membrane is folded into cristae that project into the matrix in order to increase the surface area of the membrane. The amount of folding of the membrane is determined by the energy requirements of the cell (Daems 1966).

Intermembrane space

The intermembrane space is located between the outer and inner membrane and facilitates the transfer of ATP molecules out of the matrix and into the cytosol (Koehler et al 1998).

Mitochondrial matrix

The mitochondrial matrix is enclosed within the inner membrane. It contains enzymes required in other processes such as the tricarboxylic acid (TCA or Krebs) cycle (carbohydrate metabolism), β-oxidation (fat metabolism) and for the oxidation of pyruvate (Frey, & Mannella 2000). The matrix also contains mitochondrial ribosomes, tRNAs, multiple copies of the mtDNA as well as enzymes required for mitochondrial gene expression.

1.1.2 Oxidative Phosphorylation (OXPHOS)

A major process performed by the mitochondria is OXPHOS. It is the production of ATP from adenosine diphosphate (ADP) and inorganic phosphate (Pi). It generates 15 times more ATP than glycolysis alone. This process takes place at the MRC, in the inner membrane. In the mitochondrial matrix, pyruvate produced by glycolysis is converted together with fatty acids to Acetyl CoA (Krebs, & Eggleston 1940). Acetyl CoA is essential for the initiation of the TCA cycle that produces the high-energy electrons that are transferred to the inner membrane where they enter the MRC to facilitate OXPHOS. These electrons

are carried by NADH and $FADH_2$ molecules and are required by the MRC to create the electrochemical gradient to drive ATP synthesis (Mitchell 1961).

1.1.3 Mitochondrial Respiratory chain and OXPHOS

As mentioned above, NADH and $FADH_2$ molecules carry the high energy electrons produced by the TCA cycle to the MRC at the inner membrane (Vogel et al 2007). These electrons are transferred from NADH and $FADH_2$ to oxygen by four respiratory enzyme complexes (Complex I-IV) in order to reduce oxygen to water (Figure 1.2). Electron transfer from one complex to the next is possible due to the fact that each complex along the chain has a greater affinity for electrons compared to the previous one (Moser et al 1992). Three of these complexes (Complex I, III and IV) also act as proton pumps driven by the electron transport, pumping protons to the intermembrane space thus creating an electrochemical proton gradient. Proton pumping is coupled to ATP synthesis and the proton gradient is utilised by the ATP synthase (Complex V) during ATP synthesis (Mitchell 1961).

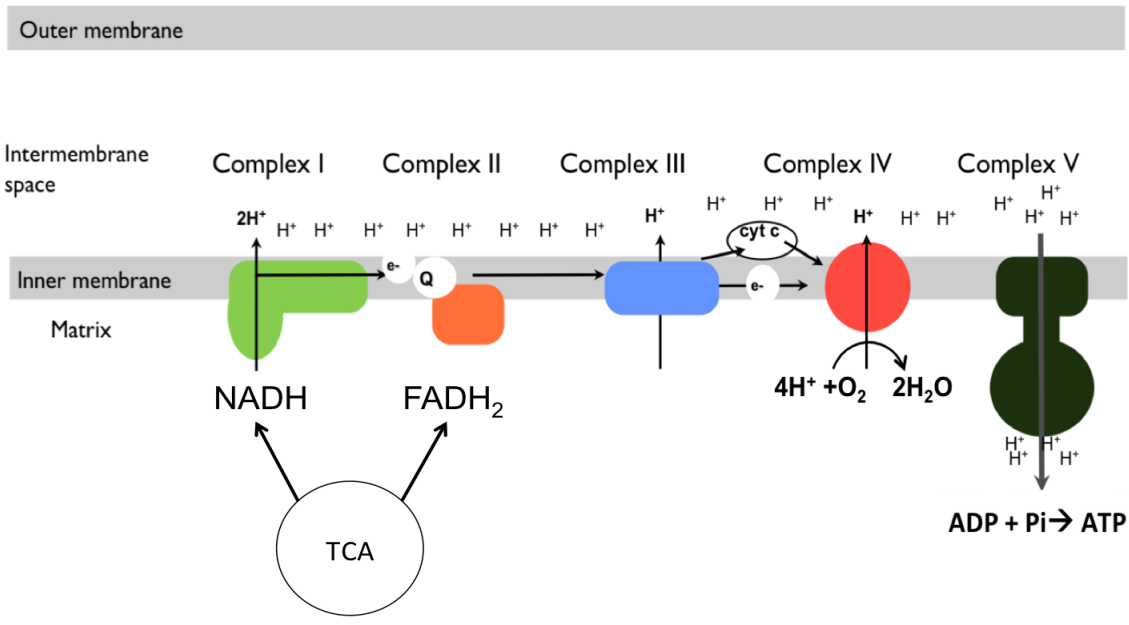

Figure 1.2 OXPHOS in mitochondria

Schematic representation of OXPHOS taking place at the MRC. Protons are pumped into the intermembrane space from complexes I, III and IV to create a net proton gradient that is utilised by ATP synthase to produce ATP.

Complex I (NADH:ubiquinone oxidoreductase)

Complex I is the first and largest enzyme complex of the MRC. It has a mass of 980kDa and is made up of around 45 polypeptide chains, seven encoded by mitochondrial DNA (*mtND1-mtND6*, *mtND4L*) and the remaining by nuclear DNA (Schultz, & Chan 2001). Complex I consists of a hydrophilic and a membrane domain. The hydrophilic domain consists of eight subunits and contains the non-covalently bound flavine mononucleotide (FMN) and iron-sulphur (Fe-S) clusters as prosthetic groups (Sazanov, & Hinchliffe 2006; Schultz, & Chan 2001). The membrane domain consists of six subunits with 55 transmembrane helices, which along with conserved polar residues facilitate proton translocation from the matrix into the intermembrane space.

The main function of Complex I is to accept electrons from the oxidation of NADH via non-covalent binding of FMN. These electrons are then transferred through Fe-S clusters to ubiquinone (Coenzyme Q_{10}) and thus reduce it to ubiquinol. In this process, the energy released drives the translocation of four protons from the mitochondrial matrix to the intermembrane space thus facilitating the accumulation of the electrochemical proton gradient (Ragan, & Racker 1973a; Ragan, & Racker 1973b; Efremov et al 2010). The reaction is summarized in the equation:

$$\mathbf{NADH + Q + 5H^{+}_{(matrix)} \rightarrow NAD^{+} + QH_2 + 4H^{+}_{(intermembrane\ space)}}$$

It is also considered to be a major site of superoxide ($O_2^{\cdot-}$) production in the mitochondria as described in more detail in section 1.1.7 (Cadenas et al 1977; Turrens, & Boveris 1980).

Complex II (Succinate:ubiquinol oxidoreductase)

Complex II is the second enzyme that enables entry of high-energy electrons to the MRC. It is smaller than Complex I as it is composed of four subunits (SDHA, SDHB, SDHC and SDHD) and has a mass of 124kDa (Cecchini 2003). It contains a covalently bound flavin adenine dinucleotide (FAD), and a 27kDa Fe-S protein that binds three Fe-S clusters (Ohnishi, & Salerno 1976). Complex II

has major differences compared to the other complexes. It is the only enzyme of the MRC that is entirely nuclear-encoded. Also, it has a role in both the TCA cycle and the MRC processes catalysing the oxidation of succinate to fumarate to reduce ubiquinone to ubiquinol shown in the equations (Ackrell et al 1975):

$$\textbf{succinate } (C_4H_6O_6) + FAD + Q + 2e^- + 2H^+_{matrix} \rightarrow \textbf{fumarate } (C_4H_4O_6) + FADH_2 + QH_2$$

Oxidation of succinate takes place at the SDHA subunit. Then electrons are transferred via the SDHB subunit and the Fe-S clusters and then to ubiquinone via the SDHC/SDHD subunits (Lemarie et al 2011; Sun et al 2005). Due to the low energy released by this reaction, no protons are translocated to the intermembrane space (Rich, & Maréchal 2010).

Complex III (Ubiquinol:cytochrome c oxidoreductase)

Complex III is a homodimer with each half composed of eleven subunits encoded by both nuclear and mitochondrial genes (Berry et al 2000). The largest subunit, cytochrome *b*, is mitochondrially-encoded. Complex III contains four redox-active prosthetic groups; an [2Fe–2S] iron-sulphur cluster, haem C (cytochrome *c*) and two haems B (cytochrome *b*) (Rich, & Maréchal 2010). These groups catalyse the oxidation of ubiquinol and the reduction of cytochrome *c* in a reaction known as the Q-cycle, which was first proposed by Peter Mitchell (Mitchell 1976). The reaction consumes two protons from the matrix and facilitates the translocation of four protons to the intermembrane space, contributing to the overall proton gradient. The Q-cycle reaction is summarised in the equation:

$$2QH_2 + 2\text{cyt } c^{3+} + Q + 2H^+_{(matrix)} \rightarrow 2Q + 2\text{cyt } c^{2+} + QH_2 + 4H^+_{(intermembrane\ space)}$$

Complex IV (cytochrome c oxidase)

Complex IV is also a homodimer with each monomer composed of thirteen polypeptides encoded by both nuclear and mitochondrial genes (Rich, & Maréchal 2010). Cytochrome c oxidase subunits I (COI), II (COII) and III (COIII)

are mtDNA encoded while the remaining genes are encoded by nuclear DNA. It also houses one copper centre (Cu_A) where electrons enter the complex, two haems, (haem *α* and haem *α3)* and a binuclear centre (BNC) where Cu_B interacts with haem *α3* to reduce oxygen (Iwata et al 1995; Muramoto et al 2007). Complex IV is the final electron transporting complex of the MRC and it (mainly COI and COII) catalyses the transfer of the electrons from the reduced cytochrome *c* to oxygen (Rich, & Maréchal 2010). The reaction consumes eight protons from the matrix and translocates four protons to the intermembrane space thus facilitating greatly to the proton gradient (Wikstrom et al 2009; Wikstrom 1977). The net reaction is summarised in the equation (Wikstrom 1977):

$$\mathbf{4\ cyt\ c^{2+} + O_2 + 8\ H^+_{(matrix)} \rightarrow 4\ cyt\ c^{3+} + 2\ H_2O + 4\ H^+_{(intermembrane\ space)}}$$

The mechanism for the reduction of O_2 to water involves the transfer of electrons from cytochrome c to Cu_A and then to haem *α*. Then electrons are transferred to Cu_B and haem *α3* and subsequently to molecular oxygen.

ATP synthase (Complex V)

ATP synthase is the final enzyme of the MRC and the OXPHOS process. It has a mass of 500kDa and consists of two functional domains, factor oligomycin, (F_o) located in the inner membrane and factor 1 (F_1) located in the mitochondrial matrix (Abrahams et al 1994; Collinson et al 1994b; Collinson et al 1994a). The F_1 catalytic domain in the mitochondrial enzyme consists of nine subunits with the stoichiometry $\alpha_3\beta_3\gamma_1\delta_1\varepsilon_1$. Subunits γ, δ and ε form a central stalk linking the $\alpha_3\beta_3$ subcomplex of F_1 to the membrane domain, F_o (Stock et al 2000). The $\alpha_3\beta_3$ subcomplex and F_o are also linked by a peripheral stalk (or stator) that holds the $\alpha_3\beta_3$ subcomplex stationary against the torque of the rotating central stalk (Carbajo et al 2005; Dickson et al 2006; Rees et al 2009).

ATP synthase uses the energy created by the electrochemical proton gradient to facilitate the phosphorylation of ADP to ATP (Boyer et al 1973). ATP synthase provides a hydrophilic pathway across the inner membrane to facilitate the transfer of protons to the matrix. These protons are used to drive the phosphorylation of ADP to ATP, an energetically unfavourable reaction, thus

ATP synthase uses physical rotation of its subunits to catalyse the reaction (Boyer 1975; Abrahams et al 1994; Yoshida et al 2001). ATP synthase can also function in reverse to hydrolyse ATP and pump protons to the intermembrane space (Hisabori et al 1999; Kato-Yamada et al 1998; Noji et al 1997). This is to maintain the ATP:ADP ratio of the cell and also the Δψm that depends on the proton gradient (Schultz, & Chan 2001).

1.1.4 Proton motive force and Δψm

The proton translocation across the inner membrane, facilitated by the electron transport chain and ATP synthase, creates a proton circuit across the inner membrane. This proton circuit can be described in terms of a driving force or potential/proton motive force (pmf, in mV) and flux (the proton current in nmol of protons/min). The pmf has two major components, ΔpH and Δψm. The ΔpH represents the pH gradient across the inner membrane and Δψm is the difference in electrical potential between the cytoplasm and the mitochondrial matrix (Mitchell, & Moyle 1969). Other processes that depend on the pmf include Ca^{2+} handling across the mitochondrial inner membrane, metabolite transport and protein import (Jouaville et al 1999; Nicholls 2005; Brand, & Nicholls 2011).

1.1.5 Proton leak

As discussed above, proton pumping is coupled to respiration through ATP synthesis. However, this coupling is not complete since protons can leak across the membrane and lower the coupling efficiency of the reaction (Figure 1.3).

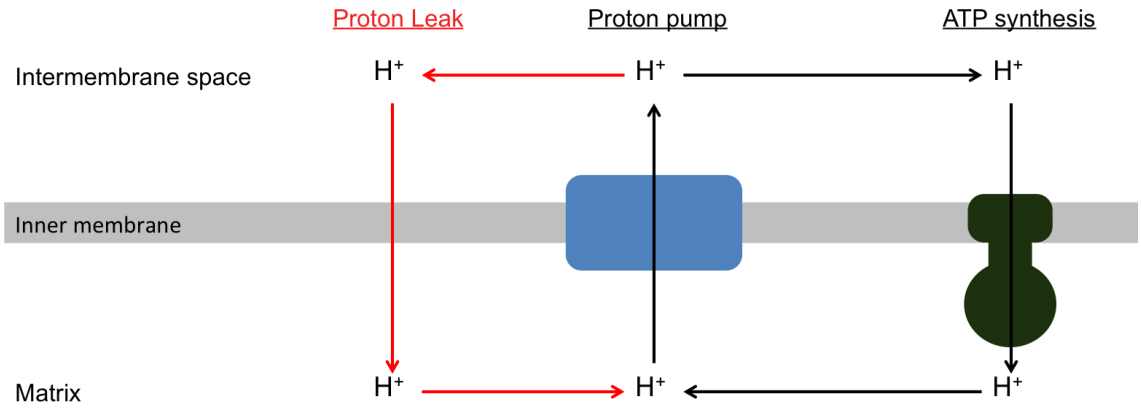

Figure 1.3 Mitochondrial coupling and basal proton leak

Figure shows a representation of how mitochondrial proton pumping is coupled to ATP synthesis. As shown by the black arrows, protons are pumped into the mitochondrial intermembrane space, thus creating a proton gradient, which is utilised by the ATP synthase during ATP synthesis. However, as shown in by the red arrows, some protons are not utilised into ATP production and flow back to the mitochondrial matrix.

This process is termed as proton leak (Brand et al 1994). There are two types of proton leak; basal and inducible leak. Basal proton leak regulation is not fully understood. It mainly depends on anion carriers present on the inner mitochondrial membrane and on the adenine nucleotide translocase (ANT) content (Brookes et al 1998; Brand et al 2005) It is also cell-type specific and correlates with the metabolic rate of the cell (Hafner et al 1988; Brand et al 1991). Basal proton leak contributes significantly to the increase of basal metabolic rate of the cells (Brand et al 1991).

Inducible leak is regulated by ANT and UCPs (uncoupling proteins) and can be activated by fatty acids, $O_2^{\cdot-}$ or lipid peroxidation products (Parker et al 2008). Literature suggests that increased proton leak can be a reaction to counteract the effects of increasing ROS levels (Korshunov et al 1997; Longo et al 1999; Skulachev 1996) or even as a consequence of damaged membranes due to lipid peroxidation (Kokoszka et al 2001). Inducible leak through UCP1 in mammalian brown adipose tissue regulates heat production and can be ROS dependent (Dlasková et al 2010; Oelkrug et al 2010). The exact roles of UCP2 and UCP3 are not yet resolved. UCP3 has been identified to reduce ROS production in isolated mitochondria (Toime, & Brand 2010). Also, UCP2 has recently been suggested to regulate human pluripotent stem cell (hPSC) differentiation (Zhang et al 2011). In this study the authors showed that UCP2

prevented mitochondrial glucose oxidation by inhibiting the utilisation of pyruvate from the KREBS cycle (thus inhibiting OXPHOS) and converting it to lactate instead, promoting glycolysis. This process also inhibits hPSC differentiation. Upon differentiation, UCP2 is repressed, glycolysis is decreased and mitochondrial glucose oxidation is either constant or increased.

1.1.6 Mitochondrial genetics

mtDNA is a 16,569 bp, double-stranded, circular molecule and the mtDNA sequence was first deduced in humans in 1981 (Anderson et al 1981). It is the only extrachromosomal DNA within the mammalian cell and there are multiple copies of it in every mitochondrion (Steuerwald et al 2000). The two mtDNA strands are different in terms of their base composition. The heavy strand is rich in guanines and the light strand is rich in cytosines. Human mtDNA is inherited exclusively through the maternal line, with only one case of paternal inheritance been reported in only muscle tissue of the subject (Schwartz, & Vissing 2002).

Mitochondria-encoded genes and their function

The mitochondrial genome encodes for 37 genes. For 28 of them the heavy strand is the sense strand and for 9 the light strand (Figure 1.4). mtDNA encodes for 13 polypeptides that are synthesised in mitochondrial ribosomes, all related to the OXPHOS process as they encode for subunits of the MRC complexes. It also encodes for 22 tRNAs and 2 rRNAs that are responsible for the translation of those polypeptides. The mitochondrial genome contains very little non-coding regions and completely lacks introns (Anderson et al 1981). The coding sequences of each gene are very close to each other and in some cases overlap (ATPase 6 and ATPase 8). The displacement (D) loop region is the only non-coding region of the mtDNA.

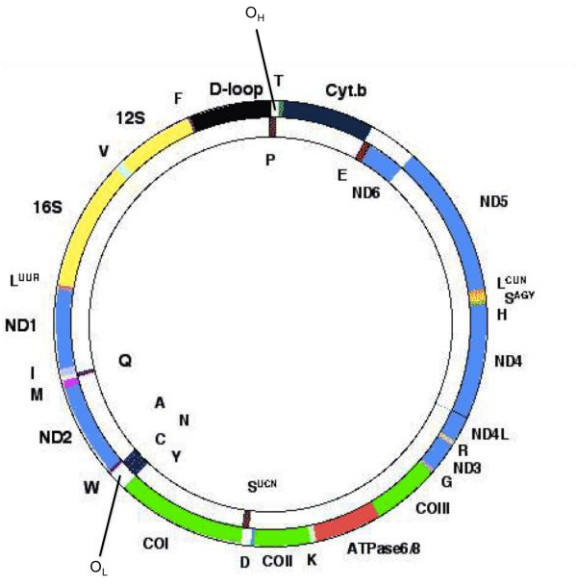

Figure 1.4 mtDNA map

Figure shows a representation of a mtDNA molecule. On the outside circle it shows the genes encoded with the heavy strand as a sense strand and on the inside circle the genes that are encoded with the light strand as a sense strand. Complex I genes are shown in blue, complex III in dark blue, complex IV in green and ATP synthase genes are in red. tRNAs and rRNAs are shown in single letters. The origins of replication O_H and O_L are also shown. (Figure adapted from MITOMAP ([NO STYLE for: Mitomap 2006])).

mtDNA replication

mtDNA is replicated by polymerase γ (POLG), which also functions as a repair enzyme. In addition to POLG, mitochondrial replication requires TWINKLE, a 5'-3' helicase (Korhonen et al 2003) and the mitochondrial single-stranded binding protein (mtSSB). Reconstruction of a minimal mtDNA replisome *in vitro* confirmed biochemically the need for both POLG and TWINKLE, as a helicase, in order to form ssDNA molecules from dsDNA (Korhonen et al 2004). However, this reaction can only synthesise about 2kb of ssDNA. In the same study, the authors showed that addition of the mtSSB stimulates replication further thus generating molecules of about 16kb, the size of the mammalian mtDNA molecule, at a rate of 180bp/min compared to 270bp/min calculated for *in vitro* replication (Korhonen et al 2004; Clayton 1982).

However, the exact mechanism of mtDNA replication has been an unclear and controversial topic. There are two main theories of mtDNA replication; strand-asynchronous replication (Robberson, & Clayton 1972; Yasukawa et al 2006) and coupled leading-lagging strand (synchronous) replication (Figure 1.5) (Holt

et al 2000). In brief, the strand asynchronous replication model (or strand displacement) proposed by Robberson *et al* in 1972 suggests that replication begins at the O_H origin of replication and displaces the light-lagging strand from the heavy-leading strand and the leading strand synthesis occurs in the absence of lagging strand synthesis (Robberson, & Clayton 1972). Lagging strand synthesis begins in the opposite direction when the O_L origin of replication is exposed from the leading strand synthesis. This suggests that leading and lagging strand replication are uncoupled. The process ends with the creation of two daughter molecules made of two linked DNA rings. The coupled leading-lagging strand replication model suggests that similarly to nuclear DNA replication, mtDNA replication takes place in both directions from a specific replication site, the zone of replication (OriZ) and thus requires the synthesis of short fragments on the lagging strand (Okazaki fragments) (Holt 2009; Holt et al 2000).

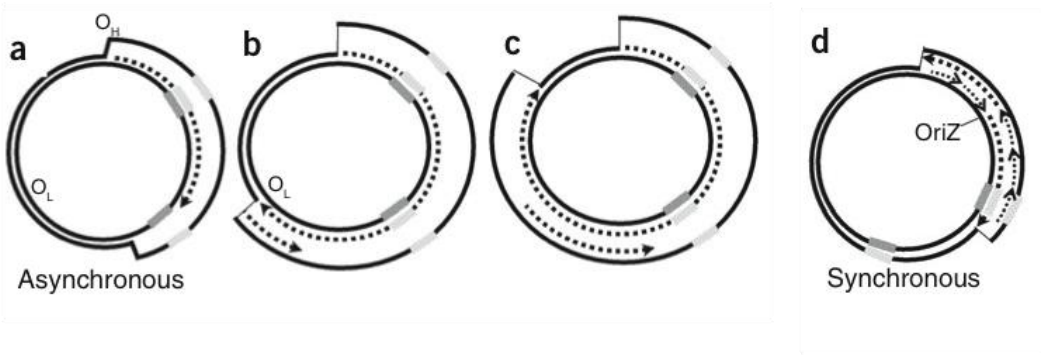

Figure 1.5 Illustration of the strand asynchronous and coupled leading-lagging strand (synchronous) replication models

(a–c) Strand-asynchronous replication. (a) mtDNA replication begins at the O_H and displaces the light-lagging strand from the heavy-leading strand and leading strand synthesis takes place. The lagging strand synthesis starts when the leading strand exposes O_L. (b,c) Lagging strand replication starts in the opposite direction until both strands have been fully replicated. (d) Synchronous or coupled replication. Replication begins from a zone of replication (OriZ) on the genome and replicates in both directions via conventional coupled leading- and lagging-strand synthesis thus requiring the formation of short (Okazaki) fragments on the lagging strand. (adapted from Krishnan *et al*, (Krishnan et al 2008))

mtDNA transcription

mtDNA gene transcription is initiated at three initiation sites, two on the heavy strand and one on the light strand to generate polycistronic transcripts of mRNA, tRNA and rRNA molecules (Montoya et al 1982). The promoters for

each strand, heavy (HSP) and light strand promoters (LSP), each includes a short (15 bp) consensus sequence that is essential for transcription (Chang 1984). Transcription of the heavy strand initiates at nucleotide 561 within the HSP or less often at nucleotide 638, whereas light strand transcription initiates at nucleotide 407 within the LSP (Parisi, & Clayton 1991; Chang 1984). For transcription to take place, a mitochondrial RNA polymerase (POLRMT) is recruited alongside mitochondrial transcription factor A (TFAM), and one of the transcription factor B1 (TFB1M) or B2 (TFB2M) (Falkenberg et al 2002; Fisher et al 1987). Transcription termination is facilitated by the mitochondrial transcription termination factor 1 (MTERF1), which affects elongation by stalling transcription downstream of the mitochondrial rRNA genes (Fernandez-Silva et al 1997; Kruse et al 1989). Another member of the MTERF family, MTERF3, has also been linked with transcriptional regulation however, MTERF3 negatively regulates mtDNA transcription initiation (Park et al 2007).

mtDNA translation

mt-mRNA is translated in the mitochondrial matrix by the mitochondrial ribosome which is composed of mitochondrially encoded 12S and 16S rRNAs and more than 85 ribosomal proteins encoded from the nucleus (Matthes et al 1982). mt-tRNAs punctuate the mRNA to mediate its processing (Ojala et al 1981). Translation is suggested to start directly after the mt-tRNA sequence as mt-mRNA lacks the 5' non-coding (5'UTR) sequences and the 7-methylguanylate cap that enable ribosome binding and recognition in nuclear RNA (Grohmann et al 1978; Montoya et al 1981). Translation termination in the mitochondria takes places when the mitoribosomes facilitate a -1 frameshift at the AGA and AGG codons, which have previously been predicted to terminate the open reading frames (ORFs) of MTCOI and MTND6 respectively (Temperley et al 2010; Barrell et al 1979). Consequently, both ORFs terminate at the standard UAG stop codon (Temperley et al 2010).

mtDNA deletions, point mutations and repair

mtDNA is prone to mutations. Due to the high gene density of the mitochochondrial genome, there is a high chance that a mutation will affect the coding sequence of mitochondrial genes. Furthermore, mtDNA has no histones

and therefore the DNA is exposed and thus prone to damage from molecules such as ROS. mtDNA is close to the MRC machinery and free radical production sites and therefore directly exposed to oxidative damage as described in more detail in section 1.1.7 (Beckman, & Ames 1999).

The mitochondrial genome, due to its polyploid nature, is exposed to homoplasmy and heteroplasmy. Homoplasmy refers to the situation where all copies of the mitochondrial genome are identical, whereas heteroplasmy is when there is coexistence of two (or rarely more) stable mitochondrial genotypes within the same cell, tissue, or organism. When some mutations affect all copies of the mtDNA they are referred as homoplasmic mutations, while when they only occur in some copies of the mitochondrial genome they are referred as heteroplasmic mutations. Evidence suggests that mtDNA constantly acquires mutations, which undergo clonal expansion and then extinction (Coller et al 2001). It is evident that there is variability between the mtDNA of siblings as well as different tissues (Lightowlers et al 1997). Different cells, tissues or organisms can have different levels of mutated (and stable) and wildtype mtDNA. Studies have suggested that the mutated form of mtDNA is functionally recessive and for a biochemical phenotype to be apparent, a threshold (on average 60% of the mtDNA has to contain a mutation) for mutated mtDNA must be exceeded (Chinnery et al 1997; Sciacco et al 1994).

Errors in mtDNA repair have been linked with the higher mutation rate in ageing tissues. POLG is a nuclear encoded mtDNA polymerase responsible for copying and proofreading of mtDNA and the only one targeted to the mitochondria (Hansen et al 2006). Experiments on mice with an error-prone POLG, resulted in a 3-8 times higher number of somatic mtDNA mutations in most tissues compared to the wildtype. They have also shown premature ageing features such as kyphosis, hair loss and graying and a loss of muscle mass (sarcopenia) and reduced lifespan (Trifunovic et al 2004; Trifunovic et al 2005; Kujoth et al 2005). Despite the fact that MRC deficiencies have been identified in these mice, there was no increase in the amount of ROS produced in these cells and only a minor increase in oxidative damage (Trifunovic et al 2005; Kujoth et al 2005). These data suggest that errors in the repair process of

mtDNA affect the function of the MRC but do not result in an increase in oxidative damage in the cells.

In tissues composed of mitotic cells, e.g. kidney, spleen, skin and liver, mtDNA point mutations are more common than deletions (Cortopassi et al 1992). In addition, accumulation of mtDNA point mutations in human colonic crypt stem cells results in MRC deficiency in their progeny however, no mtDNA deletions were observed (Taylor et al 2003).

Deletions are the primary cause of somatic mtDNA mutation in post-mitotic tissues, e.g. skeletal muscle, heart and brain possibly due to the fact that these cells are non-dividing and therefore less exposed to purifying selection of mtDNA deletions (Cortopassi et al 1992). Purifying selection of mtDNA refers to the condition where mutated mtDNA from a mother cell is not transferred to the daughter cell, and it most commonly associated with mitotic cells and inherited mtDNA mutations, especially via the maternal germ line (Stewart et al 2008a; Stewart et al 2008b). The higher levels of ROS in these tissues due to their high metabolic rate might also contribute to the higher incidence of mtDNA deletions (Cortopassi et al 1992). What causes somatic mtDNA deletions is also currently controversial. The main theories describing the mechanism of mtDNA deletions are recombination (Schon et al 1989; Mita et al 1990), slip-replication (Shoffner et al 1989) and double-strand break repair (Krishnan et al 2008). The common features of deletions created by these mechanisms are that most are located in the major arc of the mtDNA, and approximately 85% are flanked by direct repeat sequences, suggesting that these repeats have a role in the generation of these deletions. However, recently a study analysing the incidence of the 13bp repeat sequence in the common mtDNA deletion, has suggested that mtDNA deletions are not caused by direct repeats but due to stable secondary structures that can form between distant segments of the mitochondrial genome (Guo et al 2010). Alternatively, the same study suggested that the deletions depend on long and stable duplexes between distant mtDNA segments and the fact that there were variations in the breakpoint distribution implies that different mechanisms could be involved in mtDNA deletion generation.

mtDNA deletions can be observed more often in aged post-mitotic tissues and individuals with neurodegenerative diseases like Parkinson disease (Bender et al 2006; Kraytsberg et al 2006; Cortopassi et al 1992). Defects can also be caused by nuclear DNA mutations in genes involved in mitochondrial nucleotide metabolism, mtDNA maintenance, copy number and MRC function (Hudson, & Chinnery 2006).

MtDNA haplogroups

mtDNA haplogroups are defined as single nucleotide polymorphisms (SNP) in the mtDNA that are fixed in the normal population. There are 38 major human mtDNA haplogroups identified and they reflect the evolution of a particular maternal linage and ultimately can be traced back to a common matrilineal ancestor, or Mitochondrial Eve, that lived approximately 200 000 years ago in Africa (Behar et al 2008; [NO STYLE for: Phylotree 2009]; Oven, & Kayser 2009). Different haplogroups have been associated with a number of polymorphisms (Torroni et al 1997) and different predisposition towards the ageing process (Benedictis et al 2000).

1.1.7 Reactive oxygen species

ROS include hydrogen peroxide (H_2O_2), $O_2^{\cdot-}$, hydroxyl free radical (•OH) and peroxynitrite (ONOO-), which is formed from the reaction of nitric oxide with H_2O_2. ONOO- is sometimes regarded as a reactive nitrogen species (RNS) but for the purpose of our discussion we will consider RNS as ROS.

ROS production

Mitochondrial ROS production accounts for approximately 90% of the total ROS production in a cell (Balaban et al 2005). Mitochondrial complex I and complex III are the major sites of ROS production in the mitochondria (Murphy 2009; Ott et al 2007; Turrens, & Boveris 1980; Cadenas et al 1977). Complex II has also been reported as a site of $O_2^{\cdot-}$ production however its contribution to the overall ROS levels is minor (Zhang et al 1998). $O_2^{\cdot-}$ is the major ROS produced at these sites by the single electron reduction of O_2. $O_2^{\cdot-}$ is then dismutased to H_2O_2 in a reaction catalyzed by the superoxide dismutases (SOD).

$$2\ O_2^{-} + 2\ H_2O \rightarrow O_2 + H_2O_2 + 2\ OH^{-}$$

H_2O_2 is scavenged by catalase (CAT) in the cytosol or glutathione peroxidase (GPx) and decomposes into water in the reaction represented by the equation:

$$2\ H_2O_2 \rightarrow 2\ H_2O + O_2$$

Oxidative damage

Reactive oxygen species (ROS), when present in excess amounts, are the main source of oxidative damage in the cell. ROS production and ROS-induced damage increase with age in humans. Also, ROS have been shown to be triggered by cytokines, growth factors and hormones such as interleukin-1β (IL-1β), IL-3, IL-6, tumour necrosis factor a (TNF-α), transforming growth factor β (TGF-β) and angiotensin II (ANGII) (Thannickal, & Fanburg 2000). ROS have the capacity to oxidize proteins, lipids, nuclear and mtDNA (Golden, & Melov 2001; Beckman, & Ames 1999). Oxidative damage from ROS includes base modifications, single and double strand breaks and cross-linking.

Complex I is thought to be responsible for most of the increased $O_2^{\cdot-}$ production in ageing and Parkinson's disease and is also the main source of $O_2^{\cdot-}$ in the brain under normal physiological conditions (Barja, & Herrero 1998; Turrens 2003). The decline in the activity of antioxidant enzymes Cu/ZnSOD, CAT and GPx with age as well as a decrease in the activity of MnSOD at a later stage (after approximately 65 years) also contribute to the increased ROS levels (Lu et al 1999).

Complex III is the primary source of $O_2^{\cdot-}$ in heart and lung mitochondria (Turrens, & Boveris 1980; Turrens 2003). Excess ROS production occurs due to alterations in the normal function of enzymes of the MRC and it is also related to the concentration of potential electron donors in the mitochondria (Murphy 2009).

There are different mechanisms in which ROS can cause DNA damage. The hydroxyl radical ($^{\bullet}OH$) can react with the DNA by the addition to double bonds of DNA bases, e.g. by reacting with the C5-C6 double bond of pyrimidines leading to C5-OH- and C6-OH- adduct radicals and abstraction of an H atom

from thymine resulting in allyl radicals (Cooke et al 2003). The redox properties of adduct radicals can differ since C5-OH adduct radicals are reducing and C6-OH adduct radicals oxidising (Steenken 1987).

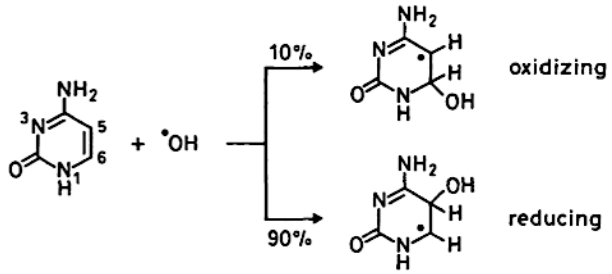

Figure 1.6 Diagrammatic representation of the reaction of •OH with C5-C6 double bonds of pyrimidines

•OH reacts with C5-C6 double bond of cytosine and depending on the localisation of the radical and the OH, the product is either reducing or oxidising. Also the percentage of reducing and oxidising adducts produced from the reaction is show. (Figure adapted from Steenken S, (Steenken 1987))

•OH also reacts with the sugar moiety of DNA by the mechanism of abstraction of an H atom to form DNA strand breaks and altered sugars as end groups (Beesk et al 1979). Another reaction of base radicals is the addition to an aromatic amino acid of proteins leading to DNA-protein crosslinking (Dizdaroglu et al 2002). A thymine-tyrosine cross-link was reported in mammalian chromatin *in vitro* and in cells exposed to H_2O_2 (Olinski et al 1992; Dizdaroglu et al 1989). The mechanism involves the addition of the allyl radical of thymine to the carbon 3 position of the tyrosine ring in a protein, followed by oxidation of the adduct radical (Margolis et al 1988; Dizdaroglu et al 1989).

ROS can also attack polyunsaturated fatty acid residues of phospholipids on cell and mitochondrial membranes, which are extremely sensitive to oxidation, thus forming unstable peroxyl radicals (ROO•) that are precursors of the final and more stable product of the peroxidation process, malondialdehyde (MDA) (Valko et al 2007). This process is defined as lipid peroxidation (Figure 1.7). The process is a chain reaction that is initiated by the reaction of unsaturated lipids with ROS (such as •OH and hydroperoxyl (HO_2) radicals) thus producing unstable lipid radicals. These radicals react with oxygen to produce an unstable lipid peroxyl radical. The lipid peroxyl radical undergoes an intermediate cyclisation step and either by a second cyclisation or by the reaction with

unsaturated lipids it produces a lipid peroxide, and another lipid radical that contributes to the continuation of the chain reaction (if it reacts with unsaturated lipids). MDA is a more stable product of the lipid peroxidation process.

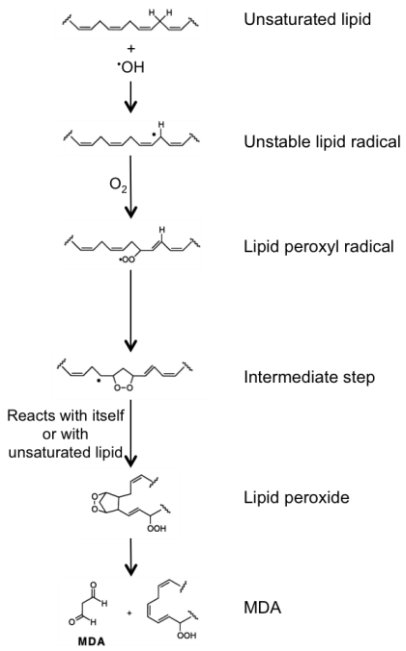

Figure 1.7 Diagrammatic representation of lipid peroxidation reaction

An unsaturated lipid is oxidised by ROS to an unstable lipid radical, which then reacts with O_2 to produce a lipid peroxyl radical. The peroxyl radical then, via an intermediate cyclisation step, reacts with itself through a second cyclisation event or with an unsaturated lipid to produce an unstable lipid peroxide. The peroxide, through chemical conversion of the bicyclic peroxide group, forms the more stable MDA and another fatty acid by-product. (Figure adapted from Marnett LJ (Marnett 1999))

MDA has been shown to be mutagenic in mammalian cells and carcinogenic in rats as it reacts with DNA to form adducts to deoxyguanosine and deoxyadenosine (Fedtke et al 1990; Wang et al 1996; Marnett 1999). 4-hydroxy-2-nonenal (HNE) is another major product of lipid peroxidation but its mutagenic effect is weaker than MDA (Valko et al 2007; Siems et al 1995).

ROS in intracellular signalling

ROS are not simply involved in oxidative damage in cells. When at normal physiological levels, ROS can act as signalling molecules and stimulate several intracellular pathways, which include mitogen-activated protein kinase (MAPK) signalling, HIF-1, NF-κB and AP-1 signalling pathways (Dröge 2002; Valko et al

2007), many of which have important roles in controlling chondrocyte phenotype (section 1.2.5).

Mitochondrial ROS (mtROS) have been reported to inhibit the activity of different phosphatases including protein tyrosine phosphatase 1B, phosphatase & tensin homolog (PTEN) and MAPK phosphatases (Kwon et al 2004; Lee et al 1998; Levinthal, & Defranco 2005; Meng et al 2002). mtROS can also induce TNF-α-mediated cell death in the absence of active NF-κB, however, when active, NF-κB-induced SOD2 counteracts this effect (Kamata et al 2005).

ROS can also regulate tumour initiation, maintenance and metastasis and have also been suggested as a possible anti-cancer treatment (Gao et al 2007; Ishikawa et al 2008; Ma et al 2009).

Pattern recognition receptors (PRRs) are recruited as part of an innate immune response to detect microbial motifs upon infection. They include Toll-like receptors (TLRs), C-type lectins (CTLs) and NOD-like receptors (NLRs), which recognize pathogen-associated molecular patterns (PAMPs) (Schroder, & Tschopp 2010). Some PRRs assemble into high-molecular weight, caspase-1-activating platforms called ‘‘inflammasomes’’ that control maturation and secretion of interleukins such as IL-1b and IL-18, thus regulating host responses to infection and injury (Martinon et al 2002; Schroder, & Tschopp 2010). The NLRP3- inflammasome is activated by PAMPs and ROS to trigger innate immune responses in the cell (Zhou et al 2011).

Three recent studies pointed out the role of ROS as signalling molecules in both NLRP3-inflammasome dependent and independent pro-inflammatory cytokine release (IL-6, IL-1β and IL-18) and caspase activation (Bulua et al 2011; Nakahira et al 2011; Zhou et al 2011). Bulua *et al* demonstrate that mtROS induce MAPK activation (increased levels of phosphorylated p38 and JNK) and also regulate transcription of IL-6 in a NLRP3 inflammasome independent manner (Bulua et al 2011). Alternatively, two other studies by Nakahira *et al* and Zhou *et al*, suggest that autophagy (or mitophagy in this case) reduces immune responses by “self-digestion” of damaged mitochondria thus inhibiting NLRP3 inflammasome and ROS induced release of mtDNA in the cytoplasm and subsequent IL-1β and IL-18 secretion and caspase activation (Nakahira et al

2011; Zhou et al 2011). Therefore, mitophagy inhibition is required for damaged mitochondria to accumulate thus increasing mtROS levels, for mtDNA to be released in the cytoplasm, and for the NLRP3 inflammasome to be activated in order activate proinflammatory signalling. ROS levels have also been shown to be regulated by NOD-like receptor X1 (NLRX1) in response to TNF-α, *Shigella* infection and double stranded RNA (dsRNA or poly(I:C), a dsRNA mimic) treatment resulting in amplified NF-κB and JUN dependent signalling pathways thus suggesting that NLRX1 is a positive regulator of the innate immunity signalling (Tattoli et al 2008). The role of NLRX1 in innate immunity is further described in section 1.1.10.

1.1.8 Antioxidant mechanisms

ROS levels are regulated mainly by three superoxide dismutases (SODs), catalase (CAT) and Glutathione peroxidase (GPx). The SODs encode for 3 different superoxide dismutases; SOD1 encodes for the cytosolic Cu/ZnSOD, SOD2 for the mitochondrial MnSOD and SOD3 for the extracellular EC-SOD. All three SODs spontaneously dismutase $O_2^{\cdot-}$ to H_2O_2 at an approximate rate of $2x\ 10^9\ M^{-1}\ s^{-1}$ (Klug et al 1972; Rotilio et al 1972). Glutathione peroxidase and catalase scavenge the H_2O_2 at the mitochondrial matrix and the cytosol respectively, to produce H_2O.

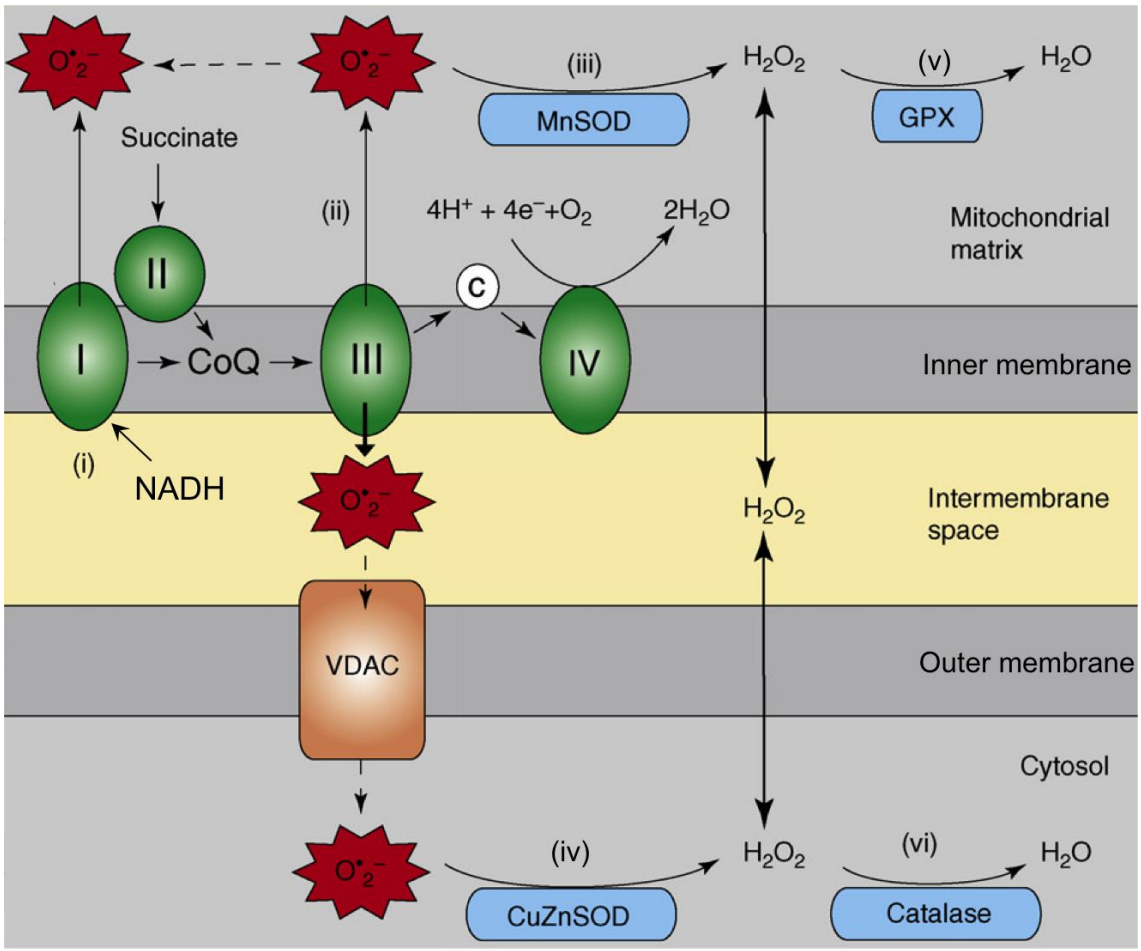

Figure 1.8 ROS production and scavenging in the cell and mitochondria

(i) and (ii) $O_2^{\cdot-}$ is mainly produced at complex I and complex III of the MRC and released into the mitochondrial matrix, the intermembrane space and the cytosol. (iii) MnSOD (SOD2) catalyses the dismutation of $O_2^{\cdot-}$ to H_2O_2 in the mitochondrial matrix and (iv) Cu/Zn SOD (SOD1) catalyses the dismutation of $O_2^{\cdot-}$ to H_2O_2 in the cytosol. H_2O_2 is scavenged by (v) GPx in the mitochondrial matrix and by (vi) catalase in the cytosol, to produce H_2O. (Figure adapted from Poyton *et al*, (Poyton et al 2009))

1.1.9 Superoxide Dismutase 2 (Manganese superoxide dismutase)

As mentioned above, SOD2 is localized in the mitochondrial matrix and dismutases $O_2^{\cdot-}$ to the less reactive H_2O_2 in a spontaneous reaction.

Human SOD2 gene expression

SOD2 is located on chromosome 6q25.3. It encodes for three transcript variants, two for isoform A (NM_000636.2 and NM_001024465.1) and one for isoform B (NM_001024466.1). Isoform A and isoform B transcripts translate to 222 amino acid and 183 amino acid proteins respectively. The *SOD2* gene has five exons interrupted by four introns.

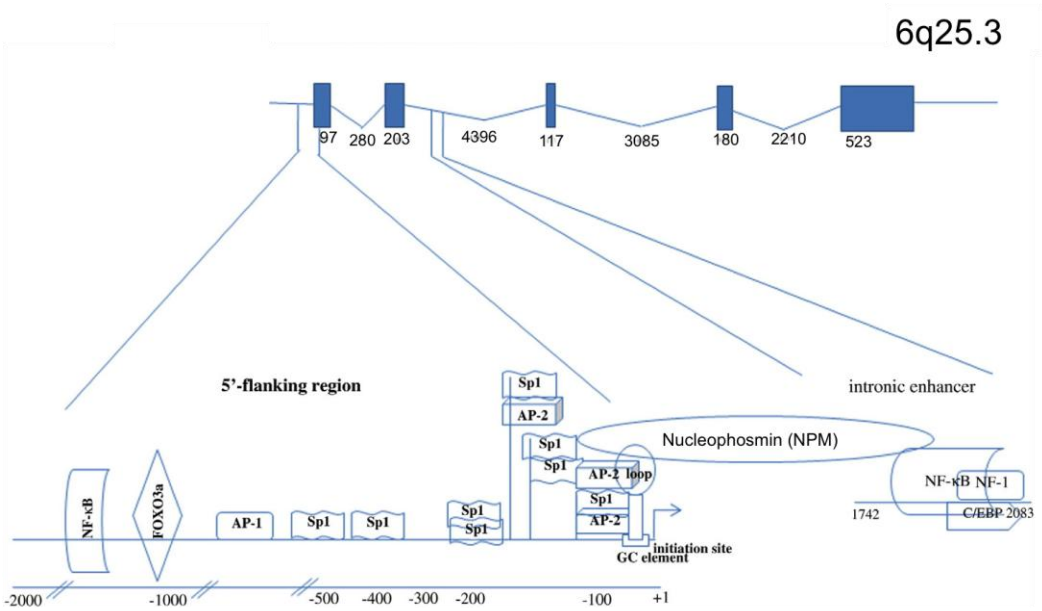

Figure 1.9 Organisation of the *SOD2* gene (Entrez gene ID #6648)

Solid blue boxes and the associated numbers indicate exons and the exon size in base pairs. Lines and numbers between each exon indicate introns and the corresponding size. The regulatory elements identified in the 5′ flanking region and the second intron of the human sod2 are expanded and shown at the bottom. Corresponding positive and negative numbers indicate their location relative to the start site, which is designated +1. (Figure was adapted from Miao *et al*, (Miao, & Clair 2009))

The promoter of the *SOD2* gene lacks TATA and CAAT boxes but contains GC-rich motifs and binding sites for several transcription factors. An intronic enhancer found within the second intron of the *SOD2* gene also regulates *SOD2* gene expression (Xu et al 1999; Miao, & Clair 2009). *SOD2* has one NF-κB binding site in its proximal promoter and one found in the intronic enhancer region (Xu et al 1999). NF-κB is one of the major transcription factors regulating *SOD2* gene expression upon cytokine stimulation. On the contrary, p50 (a member of the NF-κB family) negatively regulates *SOD2* expression upon exposure to the tumour promoter 12-O-tetradecanoylphorbol-13-acetate possibly due to the formation of p50-p50 homodimers that inhibit NF-κB signalling (Dhar et al 2007). This indicates that NF-κB mediated SOD2 expression is differentially regulated depending on the stimulus and as a result it can both promote and inhibit SOD2 expression. A binding site for the forkhead transcription factor FOXO3a is also found on the *SOD2* proximal promoter and it has been shown that it increases *SOD2* expression to protect cells from oxidative stress (Kops et al 2002). In a separate study the interaction of FOXO3a with PGC-1α has been shown to be required for the activation of

SOD2 (Olmos et al 2009). Several Sp1 binding sites are also found in the *SOD2* promoter region and are needed to induce *SOD2* expression via the proximal promoter and the intronic enhancer element. An 11-G (guanine) single-stranded loop is found in the *SOD2* promoter region. Nucleophosmin (NPM), an RNA-binding protein, binds to this loop structure (due to its G-rich nature) and intergrades the *SOD2* response to Sp1 and NF-κB. Disruption of the loop structure alters *SOD2* transcription (Xu et al 2007). The *SOD2* promoter has one binding site for the AP-1 transcription factor and several sites for the AP-2 transcription factor. AP-1 activated via the JNK and MAPK pathway increases *SOD2* expression whereas AP-2 decreases *SOD2* expression by inhibiting SP-1 dependent transcription (Qadri et al 2004; Zhu et al 2001).

Structure of human MnSOD

MnSOD (SOD2) protein has a mass of 32kDa and assembles into a tetramer, by the formation of a dimer of asymmetric dimers to create two identical four-helix bundles. Each subunit has one N-terminal helical hairpin domain that is made up of a loop and two α helices and one C-terminal α/β domain made up of five α helices and three β strands (Figure 1.10A) (Borgstahl et al 1992). Its active site is located between the N and C terminal domains of each subunit. It contains a single manganese ion and it is stabilised in a five-coordinate trigonal bipyramidal structure by two N-terminal and two C-terminal amino acids and by one water molecule (Figure 1.10B) (Borgstahl et al 1992). The manganese ions (Mn^{2+}) are located near the dimer interface site (Figure 1.10C). The $O_2^{\cdot-}$ reaches the active site through a narrow tunnel that limits the access to the active site to small ions (Figure 1.10D). $O_2^{\cdot-}$ is attracted by the net positive charge of the tunnel side chains (Borgstahl et al 1992; Perry et al 2010).

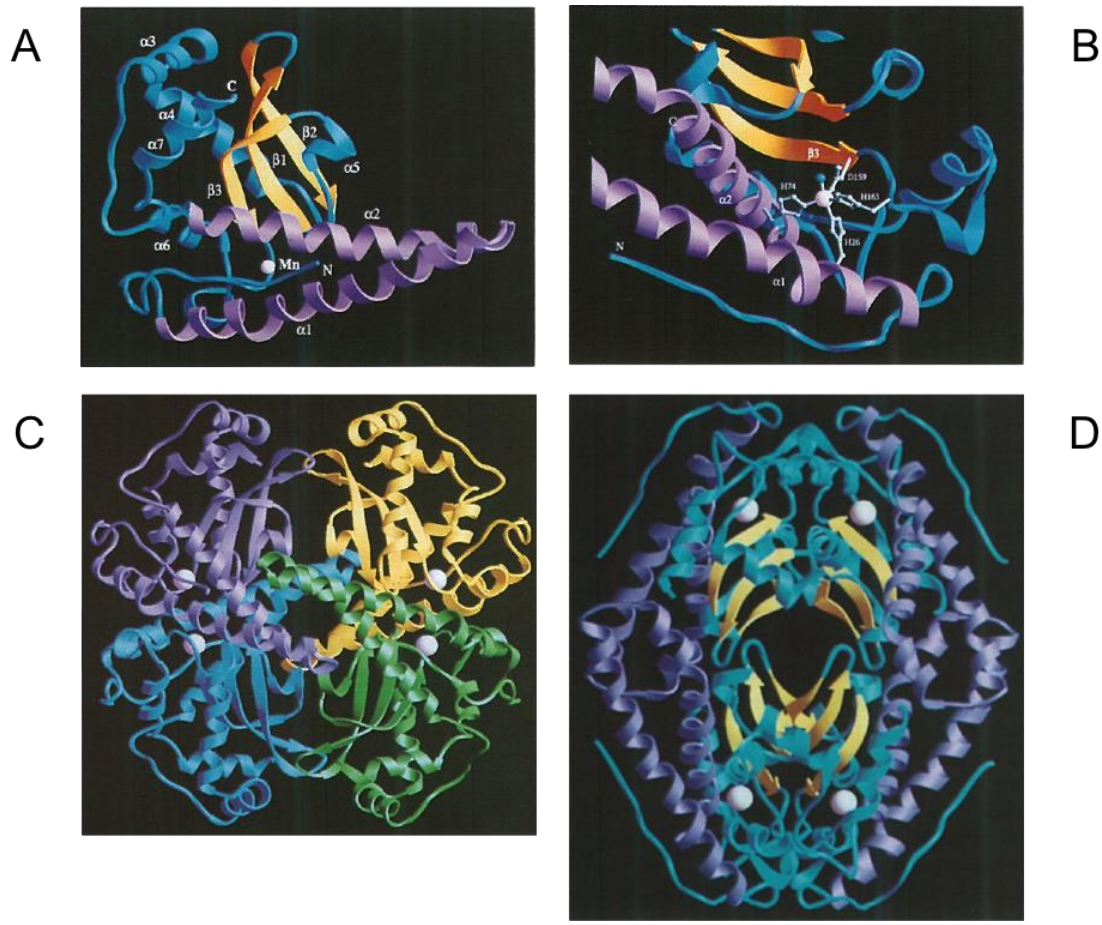

Figure 1.10 Stereo diagrams of human MnSOD subunit fold, active site geometry and tetramer assembly

Mn^{2+} are shown as light pink spheres. (A) MnSOD subunit. The N terminal domain (bottom) is made up of a loop (blue) and two α helices (α1-α2; purple). The C-terminal α/β domain (top) is made up of five α helices (α3-α7; blue) and three β strands (β1-β3; yellow). Mn^{2+} lies between the two domains. (B) Active site geometry of MnSOD. The active site is located between the N and C terminal domains of each subunit. The manganese ion (pink) is stabilised in a five-coordinate trigonal bipyramidal structure (ball and stick) by two N-terminal (His-26 and His-74) and two C-terminal (Asp-159 and His-163) amino acids and by one water molecule (blue sphere). (C) Tetrameric structure of MnSOD. Each subunit is coloured differently. Mn^{2+} are located near the dimer interface (blue-purple dimer; yellow-green dimer). (D) Tetrameric structure of MnSOD showing the positively charged tunnel from when $O_2^{\cdot-}$ reaches the active site. The C terminal domain (yellow β-sheets and blue α-helices and loops) surrounds the central tunnel. (Figure adapted from Borgstahl *et al*, (Borgstahl et al 1992))

SOD2 role in cell physiology

SOD2 is important for cell homeostasis as well as cell survival since 90% of the ROS are produced at the MRC. SOD2 (-/-) mice experience prenatal (C57BL/6J background) or neonatal lethality (CD1, DBA/2J and B6D2F1 backgrounds), associated with severe neurological and cardiac phenotypes and metabolic acidosis (Huang et al 2001; Li et al 1995; Lebovitz et al 1996). These differences in phenotype between strains can be attributed to the different

sensitivities and mitochondrial damage caused by the increased levels of $O_2^{\cdot-}$ in the mitochondria of SOD2 (-/-) mice. Lipid accumulation in the liver and skeletal muscle as well as metabolic acidosis (indicating impairment of fatty acid metabolism) and reduction in succinate dehydrogenase (complex II) activities have been reported in SOD2 (-/-), CD1 background, mice lacking exon 3 which encodes 39 amino acids involved in homodimerisation and manganese binding (Li et al 1995). Homozygous SOD2 mutant mice (of the same CD1 genetic background) exhibit decreased Complex I and II activity, high levels of oxidative DNA damage in the form of oxidative base modifications (8-oxo-guanine/adenine/cytosine) as well as deficiencies of the tricarboxylic acid cycle enzyme aconitase in brain and heart (Melov et al 1999). mtDNA damage was also reported in livers of SOD2 heterozygous mice (C57BL/6 background) at 2–4 months of age (Williams et al 1998). Higher levels of lipid peroxidation were also reported in heterozygous SOD2 mutant mice from the C57BL/6 genetic background (Strassburger et al 2005). Treatment of SOD2 null CD1 mice with SOD2 mimetics increases their lifespan and attenuates spongiform encephalopathy and mitochondrial defects (Melov et al 2001; Melov et al 1998). These findings indicate the importance of tight regulation of mitochondrial $O_2^{\cdot-}$ levels, as it is essential to maintain normal cell homeostasis.

1.1.10 Mitochondria and their role in innate immunity

Mitochondria have been identified as a signalling platform that regulates different processes and signalling events such as Ca^{2+} signalling and handling, ROS signalling, apoptosis and innate immunity signalling.

Ca2+ signalling

Mitochondria maintain and dictate cytosolic Ca^{2+} concentrations through their ability to accumulate, buffer and release Ca^{2+} into and from the cytoplasm. Ca^{2+} uptake by the mitochondria increases ATP production (Jouaville et al 1999). Active ATP production by the mitochondria is also required for the Ca^{2+} uptake by the endoplasmic reticulum (ER) (Landolfi et al 1998; Dumollard et al 2004). Ca^{2+} handling in the ER and the mitochondria relies on mitochondrial-ER interactions that are regulated by p38 MAPK and PKD (Szanda et al 2008;

Koncz et al 2009). Ca^{2+} has also been suggested to regulate mitochondrial biosynthesis by increasing PGC-1α expression (Handschin, & Spiegelman 2006).

Apoptosis

Mitochondria play a major role in apoptosis. “Death signals” such as TNF-α, IL-1β and NF-κB activation, facilitate the recruitment of members of the Bcl-2 family of proteins such as Bid and Bad (Kamata et al 2005; Wachlin et al 2003). These proteins are activated by undergoing conformational changes and translocate to the mitochondria where they inhibit the anti-apoptotic Bcl-XL and activate Bax and Bax-like proteins thus facilitating release of cytochrome c into the cytoplasm (Desagher et al 1999; Eskes et al 2000; Griffiths et al 1999). Cytochrome c then activates caspase-9 by binding to Apaf-1 and dATP and thus inducing other downstream caspases and apoptosis (Newmeyer et al 1994).

Innate Immunity signalling

Mitochondria have recently been linked with signalling pathways associated with anti-viral responses. In 2005, four different groups identified a protein, the ‘virus-induced signalling adapter’ (VISA/IPS-1/MAVS/Cardif) to play a role in regulating interferon α (IFNα) and IFNβ production through the NF-κB, Interferon regulatory factor 3 (IRF3) and IRF7 pathways as a response to viral dsRNA (Seth et al 2005; Kawai et al 2005; Meylan et al 2005; Xu et al 2005). dsRNA is sensed by TLR3 (Toll-like receptor 3) or two retinoic acid inducible gene 1-like receptors (RLRs), RIG-I (retinoic acid inducible gene 1) and MDA5 (melanoma differentiation associated gene 5). VISA is found on the mitochondrial outer membrane, it interacts with RIG-I and MDA5 and recruits IKKα, IKKβ and IKKε kinases leading to NF-κB and IRF3 activation in a RLR dependent pathway (Kawai et al 2005; Kawai, & Akira 2006). VISA has also been suggested to interact with TRIF and TRAF6 to mediate activation of the TLR3 mediated activation of NF-κB and IRF3 pathways (Xu et al 2005). Activation of VISA has recently been suggested to be regulated by NLRX1, a newly identified member of the NOD-like receptor family (NLR). NLRX1 is also localized on the mitochondrial outer membrane and negatively regulates the

activity of VISA and thus downregulating the RLR dependent anti-viral response described above (Tattoli et al 2008; Moore et al 2008). NLRX1 has also been identified to increase ROS production in response to TNF-α, *Shigella* infection and dsRNA stimulation, resulting in amplified NF-κB and JNK dependent signalling pathways and therefore suggesting that NLRX1 is additionally a positive regulator of the immune system (Tattoli et al 2008). Controversially in 2009, the same group suggested that NLRX1 is localized in the mitochondrial matrix thus speculating that it does not interact with VISA to block signaling (Arnoult et al 2009). Another recent report, using NLRX1 knockout mice, has shown that NLRX1 deficiency does not alter VISA-dependent responses but identified a mitochondrial complex III subunit to be binding with NLRX1 thus suggesting that NLRX1 can regulate the activity of the MRC and alter ROS production (Rebsamen et al 2011).

NF-κB has likewise been identified as a positive regulator of the SOD2 activity upon stimulation with TNF-α and IL-1β (Xu et al 1999; Miao, & Clair 2009). This suggests a link between NLRX1, ROS levels and SOD2 in the context of NLRX1 regulating the ROS levels directly and also indirectly via the NF-κB pathway.

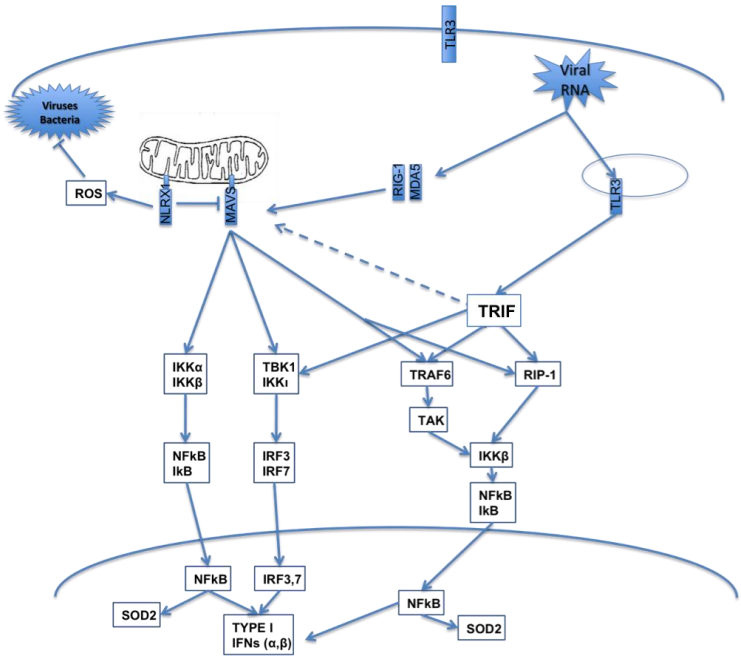

Figure 1.11 NLRX1 and TLR3 in innate immunity signalling

Graphical representation of the role of TLR3 dependent and independent pathways (NLRX1 and VISA), in innate immunity signalling regulation.

1.2 Osteoarthritis

1.2.1 Disease pathology

Osteoarthritis (OA) is a degenerative joint disease that causes progressive loss of joint function. It is characterised by the loss of articular cartilage but also from changes to the periarticular bone, synovial lining and adjacent connective tissue elements (Brandt et al 2006). It is strongly associated with ageing since it affects mostly people over the age of 65. The most commonly affected joints are the knees, hips, hands and the spine. The symptoms of OA include inflammation, pain, stiffness and loss of mobility (Hunter, & Felson 2006). There are a number of risk factors associated with OA including age, obesity, injury, previous surgery, bending and lifting, joint instability, peripheral neuropathy, muscle, weakness as well as genetic factors (Hunter, & Felson 2006; Goldring, & Goldring 2007). OA can be detected mainly using radiographs and magnetic resonance imaging (MRI) by quantifying changes of articular cartilage morphology, volume and thickness (Goldring, & Goldring 2007).

1.2.2 Cartilage

Cartilage is the tissue that covers and protects the ends of bones in synovial joints and enables friction-less movement between the joints (Figure 1.12). It is elastic, filled with fluid and supported by a layer of calcified cartilage and bone (Lane et al 1977). Cartilage is composed of two main extracellular matrix (ECM) macromolecules, aggrecan and type II collagen along with a resident single cell type, the chondrocyte. Type II collagen, a fibrillar collagen, is the predominant form of collagen present in the cartilage and provides the resistance of the tissue to tensile and shear forces. Aggrecan is responsible for the resistance of cartilage to compression by hydrating and swelling against the type II collagen scaffold. Aggrecan with highly sulfated glycosaminoglycan content (chondroitin sulfate and keratin sulfate) forms proteoglycan aggregates in association with hyaluronan and link protein, that stabilises the interaction of aggrecan and hyaluronan (Roughley 2001; Doege et al 1991).

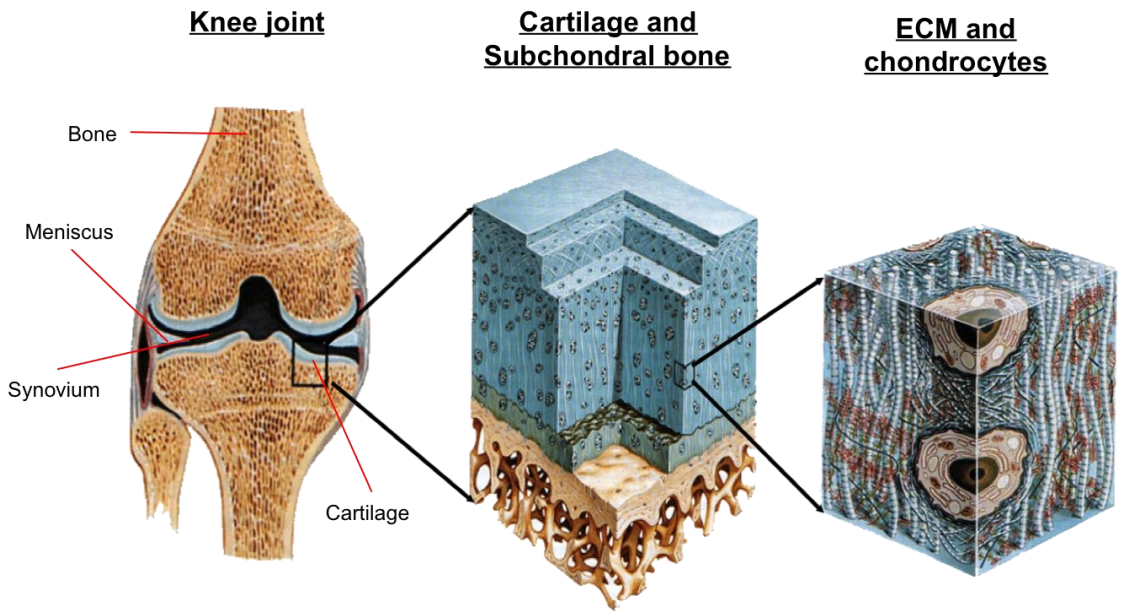

Figure 1.12 Representation of a knee joint and cartilage with its extracellular matrix and chondrocytes

Figure shows the main parts of a knee joint and concentrates on the structure of cartilage and the subchondral bone as well as the structure of the extracellular matrix of cartilage with the chondrocytes. (Figure adapted from David A. Young, unpublished figure)

Chondrocytes only make up 5% of the volume of the cartilage (Stockwell 1967). They are the main sites of production of the components of the ECM. There is a fine balance between the anabolic (synthetic) activity of the chondrocytes and their catabolic (degradative) activity. Catabolic events are mediated by pro-inflammatory agents whereas the anabolic events are mediated by anti-inflammatory agents. These events are controlled by the production of growth factors and cytokine cascades as well as physical factors, for example mechanical stress (Rowan, & Young 2007).

In OA there is a change in the molecular structure and the composition of the ECM (Buckwalter, & MANKIN 1997). There is an increase in the production of matrix metalloproteinases (MMPs) and inflammatory mediators, for example IL-1, IL-8, IL-6, prostaglandin E2 (PGE2) and nitric oxide (NO) as well as an increase in the ECM-degrading proteins and the pro-inflammatory cytokines (Pelletier et al 2001). The net result is a decrease of the anabolic, or synthetic, activity of the chondrocytes and an increase of the catabolic, or degradative, activity (Aigner et al 1997; Aigner et al 2001; Fay et al 2006). Proteoglycans are lost and newly synthesized proteoglycans are smaller, therefore the water

concentration of the matrix is decreased and the collagen network is broken down and as a result, cartilage has less resistance to compression. The replacement of chondrocytes and the ECM is a very slow process, especially of type II collagen, leaving cartilage prone to damage accumulation with age and could be partially responsible for the development of OA (Yudoh et al 2005; Loeser et al 2002).

1.2.3 Matrix metalloproteinases

MMPs

Matrix metalloproteinases (MMPs) comprise a family of 23 Zinc-dependent and calcium dependent endopeptidases that modulate interactions between cells and between cells and the ECM (Murphy et al 2002). Together the enzyme family is able to degrade all components of the ECM. They are regulators of cell differentiation, migration, proliferation and survival (Baker et al 2002). They have been associated with osteoarthritis and rheumatoid arthritis (RA), cardiovascular diseases and cancer. In cartilage, chondrocytes in response to the biomechanical stresses as well as traumatic injuries secrete MMPs, thus regulating the turnover of matrix components and the production of inflammatory cytokines (Goldring, & Goldring 2007; Kurz et al 2005; Fitzgerald et al 2004). There are 5 main groups of MMPs (Murphy et al 2002): collagenases, gelatinases, stromelysins, metrilysins and membrane type MMPs, all involved in the cleavage and degradation of different ECM components. MMPs (except membrane bound MMPs) are secreted by both the resident cells, e.g. chondrocytes in cartilage, and invading cells e.g. neutrophils. MMPs are first synthesized as inactive precursors (Pro-MMPs) and outside the cell become activated by proteolytic cleavage of an N-terminal polypeptide (Knäuper et al 1996; Eeckhout, & Vaes 1977). MMPs are also able to cleave aggrecan (Fosang et al 1996; Struglics et al 2006).

Collagenases

Triple helical fibrillar collagens include type I collagen, type II collagen and type III collagen and consist of three α chains that wind around each other in a right-handed twist to form a triple helical structure (Murphy et al 2002; Nagase, &

Fushimi 2008). There are three collagenases; collagenase-1 (MMP-1), collagenase-2 (MMP-8) and collagenase-3 (MMP-13). Collagenases consist of three major domains; a propeptide that keeps the enzymes in a latent state and two domains that are required for collagen hydrolysis: a catalytic domain that contains the catalytic zinc and via a linker region is linked at the C-terminal of a hemopexin (Hpx) domain (Nagase, & Fushimi 2008).

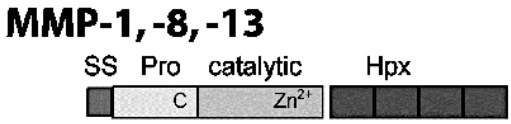

Figure 1.13 Domains of collagenases MMP-1, MMP-8 and MMP-13.

Domain components of collagenases are indicated by different shades. SS: signal peptide; pro: propeptide; Hpx: hemopexin. (Figure adapted from Nagase *et al*, (Nagase, & Fushimi 2008)).

They act by first unwinding triple helical collagen to present each α chain to the active site in a mechanism that involves contact of the catalytic and Hpx domain with collagen (Chung et al 2004). Then the α chains of the unwound collagen are cleaved at a single site approximately three-quarters from the N-terminus, thus generating one-quarter and three-quarter fragments (Miller et al 1976; Mitchell et al 1996).

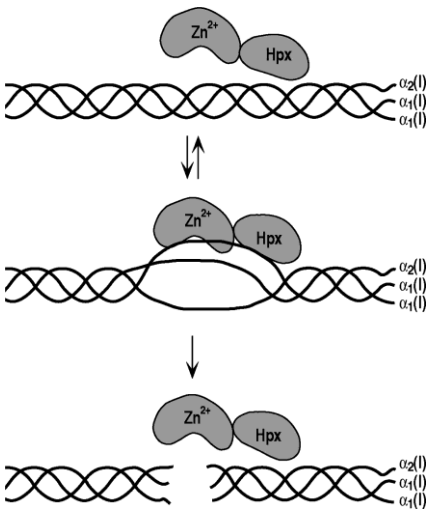

Figure 1.14 Triple helical collagen cleavage by collagenases

Collagenases bind to collagen and unwind collagen to present the three α chains to the active site. The unwound α chains are then cleaved at a single site approximately three-quarters from the N-terminus. (Figure adapted from Nagase *et al*, (Nagase, & Fushimi 2008))

ADAMTS

The 'A disintergrin and metalloproteinase with thombospondin motifs' (ADAMTS) family of secreted proteases comprises 19 genes in humans. ADAMTS are responsible for collagen processing as procollagen-N-propeptide, cleavage of aggrecan (aggrecanases) as well as processes such as inhibition of angiogenesis, blood coagulation homeostasis, inflammation and fertility. As a result, they have been linked with arthritis and cancer (Porter et al 2005). A major subgroup of ADAMTS is the aggrecanases (ADAMTS-1, 4, 5, 8, 9, 15). They have a major role in cartilage aggrecan cleavage, with ADAMTS-5 being identified as the major aggrecanase in murine OA (Glasson et al 2005; Stanton et al 2005). ADAMTS expression is dysregulated in OA cartilage. The aggrecanases ADAMTS-1,5,9 and 15 have been shown to be downregulated whereas a number of other ADAMTSs (ADAMTS-2,12,14 and 16) are upregulated (Kevorkian et al 2004). ADAMTS and membrane-bound MMPs have furin recognition motifs that facilitate activation to occur through the endoplasmic reticulum and Golgi apparatus thus enabling secretion of an active proteinase in the extracellular matrix. This mechanism ideally localises these proteinases to effect proteolysis close to the cell, an event thought to occur in arthritic disease (Itoh, & Seiki 2006; Basbaum, & Werb 1996).

TIMPs

The activity of MMPs and ADAMTS is also regulated by inhibition mainly by the tissue inhibitors of metalloproteinases (TIMPs) and α2-macroglobulin. There are four TIMPs (1-4) and they bind metalloproteinases to control their activity. They are secreted proteins but they can also be found at the cell surface in association with other membrane bound proteins. In general most MMPs and ADAMTS-1, 4 and 5 can be inhibited by TIMPs although the extent of inhibition varies (Baker et al 2002; Kashiwagi et al 2001; Rodriguez-Manzaneque et al 2002). α2-macroglobulin is synthesized in the liver and inhibits endoproteinases like MMPs and ADAMTS. It is also a major inhibitor of MMPs in the plasma (Baker et al 2002). TIMP-2 has also been identified to be involved in proMMP-2 activation by forming a complex with MT1-MMP and pro-MMP-2 at the cell surface (Butler et al 1998; Wang et al 2000; Worley et al 2003).

1.2.4 Cartilage destruction and disease

Cartilage destruction by collagen breakdown is considered a slow and irreversible process that occurs at latter stages of disease pathology. Aggrecan degradation is a faster process and occurs early in the cartilage degradation process (Little et al 2002; Caterson et al 2000). Collagenases MMP-1, MMP-8 and MMP-13 degrade collagen in cartilage. However, not all collagenases are predominant in all cartilage-related diseases. MMP-8 is not expressed highly by human chondrocytes but is expressed highly by neutrophils in septic arthritis (Rajasekhar et al 2004). Both MMP-1 and MMP-13 are expressed by chondrocytes. However, MMP-1 is considered more predominant in RA where MMP-13 is presumed as the major collagenase in OA (Tetlow et al 2001; Billinghurst et al 1997). A recent study has demonstrated convincing evidence of the role of MMP-13 in OA by demonstrating reduced OA cartilage lesions in MMP-13 deficient mice (Little et al 2009). In the same study, aggrecan loss was high throughout the experiment, but cartilage erosion was not detected on the MMP-13 deficient mice suggesting that aggrecan depletion cannot drive cartilage erosion by itself. An earlier study on ADAMTS-5 deficient mice demonstrated the role of ADAMTS-5 in cartilage breakdown (Glasson et al 2005). Also, Little *et al* identified the interglobular domain (IGD) of aggrecan is an important cleavage site by ADAMTS-5 (Little et al 2007). In this study, they generated mice with a knockin mutation that provided resistance of the IGD to ADAMTS-5 cleavage. This mutation reduced aggrecan loss and cartilage erosion in mouse model of surgically induced osteoarthritis and a model of inflammatory arthritis and also appeared to stimulate cartilage repair following inflammation.

1.2.5 Regulation of MMP-13 and MMP-1 gene expression in cartilage

In arthritic disease, several pro-inflammatory mediators have been associated with the induction of collagenase gene expression. These include IL-1, IL-17 and TNF-α. Although OA is considered a non-inflammatory disease, many of these molecules are released by articular chondrocytes following mechanical stress, thus inducing MMP gene expression (Mitchell et al 1996). Other molecules that are involved in the induction of MMP-1 and MMP-13 include IL-6

and oncostatin M (OSM). Both work in synergy with IL-1, IL-17 and TNF-α to stimulate collagenase expression and collagen breakdown in RA but probably not OA (Manicourt et al 2000; Catterall et al 2001; Heinrich et al 2003; Hui et al 2003; Hui et al 2005; Koshy et al 2002). Cytokines mediate their effect by activating several intracellular signalling pathways that regulate MMP activation and repression. The major pathways associated with arthritic disease include the MAPK (Malemud 2004), NF-κB (Feldmann et al 2002), and the Janus kinase/ signal transducers and activators of transcription (JAK/STAT) pathway (Heinrich et al 2003; Ivashkiv 2003).

MAPK

The MAPK family consists for three serine/threonine kinases; c-Jun N-terminal kinases (JNKs), the extracellular signal-regulated kinases (ERKs) and the p38 kinases (Vincenti, & Brinckerhoff 2002). The MAPK pathway in chondrocytes can activate the AP-1 family members, c-Jun and c-Fos and therefore activate expression of MMPs (Rowan, & Young 2007). Both JNKs and ERKs activate c-Jun, which dimerises with c-Fos to induce MMP expression (Karin 1995).

NF-κB

Both IL-1 and TNF-α signal via the NF-κB pathway. In chondrocytes, NF-κB mainly regulates MMP-13 expression (Liacini et al 2002; Liacini et al 2003). In a recent study, AP-1 was also identified to regulate MMP-13 expression by binding an evolutionary conserved region approximately 20kb 5' of relative to the MMP-13 transcription start site (Schmucker et al 2012). In the same study, the authors suggest that chromosome looping brings this region close to the MMP-13 transcriptional start site. Despite the presence of an NF-κB binding site on its promoter, it is not clear whether MMP-1 expression is regulated by NF-κB in chondrocytes (Catterall et al 2001) (Rowan, & Young 2007).

JAK/STAT

As with the NF-κB pathway, OSM and IL-6 members (plus leptin) signal via the JAK/STAT pathway to induce MMP-1 and MMP-13 expression (Heinrich et al 1998; Li et al 2001). IL-6 has also been shown to activate STATs and ERK to

drive MMP-1 and MMP-13 expression in bovine chondrocytes (Legendre et al 2005). However, it has also been suggested that OSM does not or only modestly induces MMP-1 mRNA expression (Catterall et al 2001).

1.2.6 OA and ageing

OA has been strongly associated with the ageing process. Alterations in the size of proteoglycan aggregates have been observed with increasing age (Martin, & Buckwalter 2002). This is due to both increased proteoglycan degradation and altered proteoglycan synthesis leading to a shorter aggrecan protein core and chondroitin sulfate chains, thus decreasing the resistance of cartilage to compression (Martin, & Buckwalter 2002; Thonar et al 1986).

Chondrocytes have been shown to undergo senescence with age. Cartilage is a long-lived tissue and it has a slow turnover of cells and type II collagen (Verzijl et al 2000). Premature senescence and chondrocyte apoptosis can result from the increase in ROS and NO production (Loeser 2006; Afonso et al 2007). A report by Martin *et al*, suggested that mechanical stress promotes the release of ROS, which then induce senescence in chondrocytes with age (Martin et al 2004). It has been reported that excess levels of peroxynitrite induce telomere erosion and extrinsic senescence in chondrocytes (Yudoh et al 2005). Telomere erosion beyond the main length necessary for replication (5-7kb) also induces cell cycle arrest and replicative senescence of chondrocytes (Martin, & Buckwalter 2002).

1.3 Mitochondria in cartilage and OA

In recent years the involvement of mitochondria in the pathogenesis of OA has been considered. Their direct role in ROS regulation, ATP production, senescence and apoptosis has been linked to cartilage degeneration.

1.3.1 Mitochondrial activity in healthy cartilage

The activity of mitochondria and ATP production in chondrocytes, although not very extensively studied, has been a topic of interest but with contradicting results. Chondrocytes have no blood supply due to the absence of blood vessels in articular cartilage. Therefore, the major source of nutrients and oxygen comes from the synovium and the bone vessels on either side of joint with oxygen possibly transferred to the cells by diffusion of water from the synovium (Greenwald, & Haynes 1969; Lim et al 2006; Mauck et al 2003; O'Hara et al 1990). Chondrocytes can survive for many days without oxygen, however the rates of matrix synthesis and energy production are reduced in an oxygen tension dependent manner (Grimshaw, & Mason 2000). Oxygen tension was estimated, using knee synovial fluid samples, to be between 20 and 80 mm Hg at the surface of articular cartilage (Falchuk et al 1970). Further studies suggested that an oxygen gradient exists across articular cartilage since chondrocytes at the surface of cartilage receive 5-10% oxygen compared to approximately 1-2% at the deepest regions (Grimshaw, & Mason 2000; Marcus 1973; Zhou et al 2004). As a result ATP production in cells in the superficial and middle zones of articular cartilage by OXPHOS is 18 times more efficient than glycolysis (Blanco et al 2004). However, although mitochondrial OXPHOS in chondrocytes is active, 80% of glucose is metabolized by glycolysis (Blanco et al 2004). Similarly, it has been reported that OXPHOS is not entirely inactive in chondrocyte mitochondria and is responsible for 25% of the chondrocytes' ATP production as well as to maintain the $\Delta\psi m$ (Stockwell 1983; Lee, & Urban 1997). The rate of glycolysis is reduced under anoxic conditions (64% less lactate production compared to aerobic condition) suggesting the presence of a negative Pasteur effect in bovine articular cartilage (Lee, & Urban 1997). The negative (or reverse) Pasteur effect describes the situation in which carbohydrate breakdown is suppressed under anoxia and as a result could

make the chondrocytes prone to a shortage of energy due to a reduction in O_2 supply (Lee, & Urban 1997). Another study performed on chicken epiphyseal growth plate cartilage suggests that in the same population, cells with and without mitochondrial activity were detected suggesting that chondrocytes utilize OXPHOS as well as glycolysis for their ATP production (Yamamoto, & Gay 1988). Human normal chondrocytes in culture have also been shown to have activity of the MRC similar to other mesenchymal cells (Maneiro et al 2003; Blanco et al 2004). Additionally, a 20-fold increase in the concentration of mitochondrial transcripts for cyt B, CO II and CO III has been reported in chondrocytes in culture compared to the levels in cartilage suggesting that the mitochondrial properties of chondrocytes change when transferred in an artificial culture environment (Mignotte et al 1991).

In general, the information available and the number of studies performed on mitochondrial respiratory activity of chondrocytes are limited and therefore it is difficult to reach any conclusions regarding OXPHOS in chondrocytes without more extensive studies.

1.3.2 Mitochondrial dysfunction and OA

A decrease in complex II and III activity has been observed in OA chondrocytes as well as an increase in the mitochondrial mass, possibly as a mechanism to compensate for the decrease in the MRC activity. In OA, there are more chondrocytes with depolarised mitochondria than in healthy chondrocytes and this can be due to the lower activity of the mitochondrial complex III possibly due to the reduced proton pumping from complex III into the mitochondrial matrix during electron transport along the MRC (Maneiro et al 2003). Depolarisation can lead to swelling of the mitochondria, disruption of the outer mitochondrial membrane and therefore alteration of physiological functions of the mitochondria as described previously; the release of pro-apoptotic factors such as cytochrome *c* and as a result apoptosis and ATP-depletion can take place (Susin et al 1999; Liu et al 1996).

Inflammatory cytokines have also been associated with mitochondria dysfunction. TNF-α and IL-1β have been shown to regulate the function of mitochondria in chondrocytes by inhibiting complex I activity either due to

modification of complex I proteins or due to reduced substrate availability. Mitochondrial depolarization was observed as well as an increase in mRNA and protein expression of the genes of the Bcl-2 family, indicating a possible role of TNF-α and IL-1β in apoptosis and cartilage degradation (López-Armada et al 2006). Inhibition of complexes III and V of the MRC in human chondrocytes lead to an NF-κB mediated increase of cyclo-oxygenase 2 and prostaglandin E_2 (PGE_2), both of which are inflammatory mediators involved in the joint tissue inflammation (Cillero-Pastor et al 2008).

Another study has shown that the OA chondrocytes have a diminished mtDNA repair capacity as well as decreased mtDNA integrity (Grishko et al 2008). OA chondrocytes were shown to be more sensitive to ROS and NO-induced mtDNA oxidative damage. Also, the mtDNA repair capacity (following oxidative damage) of the chondrocytes in general, and especially OA chondrocytes is limited (Grishko et al 2008). In OA knee cartilage as well as non-OA aged tissue, accumulation of a 4977bp (nucleotide positions 8468 - 13446) mtDNA deletion (a common deletion identified in mtDNA) has been observed, suggesting a role of mtDNA deletions in the development and progression of OA (Chang et al 2005; Cortopassi et al 1992; Schon et al 1989; Shoffner et al 1989). This deletion is considered a common cause of Pearson's syndrome, a childhood multisystem disorder, Kearns-Sayre syndrome (KSS), the symptoms of which include external ophthamoplegia, mitochondrial myopathy, ptosis and retinitis pigmentosa, and chronic progressive external ophthalmoplegia (CPEO), a late-onset KSS (Goto et al 1990; Lestienne, & Ponsot 1988; McShane et al 1991; Mita et al 1989; Rötig et al 1990). It has also been associated with neuromuscular dysfunction in ageing (Cortopassi et al 1992). The evidence of the 4977bp common deletion in OA mitochondria can support and can be supported by the hypothesis that mtDNA deletions in post-mitotic tissues (like cartilage) arise during inefficient mtDNA repair (Krishnan et al 2008).

Another interesting observation is that different mitochondrial haplogroups have different risks of OA progression and therefore could be used as biomarkers for OA. Two studies using subjects from the Spanish population, representing the European population, have identified that carriers of haplogroup J might have a decreased risk of knee and hip OA progression due to odds ratios (OR, odds of

carrying each allele in OA patients as compared with controls) of 0.460 (knee OA) and 0.661 (hip OA) (Rego-Perez et al 2008; Rego et al 2009). Also, carriers of haplogroup J might also have a decreased risk of developing high severity knee OA compared to low severity knee OA (OR=0.351) (Rego-Perez et al 2008). Conversely, the same study suggested that carriers of haplogroup U might have an increased risk for a more severe progression of knee OA (OR= 1.788).

More recently, the same group assessed the influence of mtDNA haplogroups on the serum levels of collagenases and type II collagen markers (ELISA assays) (Rego-Perez et al 2010; Rego-Perez et al 2011). OA patients carrying haplogroup H had 33% higher serum levels of MMP-3 compared to OA patients carrying haplogroup J (Rego-Perez et al 2011). Analysis of type II collagen markers identified that OA patients carrying haplogroup H had higher serum levels of type II collagen (89% and 85%), nitrated type II collagen (230% and 178%) and procollagen type II C-terminal propeptide (200% and 165%) compared to OA patients carrying haplogroup J and U respectively (Rego-Perez et al 2011). Carriers of haplogroup H had 19% higher serum levels of MMP-13 compared to haplogroup J carriers as well 27% higher levels of type II collagen, 28% higher levels of nitrated type II collagen, 135% higher levels of a C-terminal neoepitope generated by the collagenase-mediated cleavage of type II collagen and 96% higher levels of procollagen type II C-terminal propeptide (Rego-Perez et al 2010). Taken together, these findings suggest that carriers of haplogroup H also have an increased risk of OA progression and could possibly be used, in combination with other markers, as a biomarker for OA (Rego-Perez et al 2010; Rego-Perez et al 2011).

1.3.3 Chondrocyte Senescence

It has been demonstrated in other cell types (fibroblasts and melanocytes) that oxidatively damaged mitochondria can lead to growth arrest and replicative senescence (Toussaint et al 2000). As mentioned before, premature senescence could result from the increase in ROS and NO production (Afonso et al 2007; Loeser 2006). The number of senescent human chondrocytes has been shown to increase with age. The chondrocytes have shortened telomeres

as well as high levels of senescence-accumulated β-galactosidase and their replicative capacity is decreased (Martin, & Buckwalter 2003; Price et al 2002). By treating the human articular chondrocytes with the anti-oxidant ascorbic acid, telomere length and lifespan remained constant with time (Yudoh et al 2005).

1.3.4 Chondrocyte apoptosis

Chondrocyte apoptosis has been linked to the reduced number of cells in OA cartilage and is considered to contribute to cartilage degradation (Blanco et al 1998; Hashimoto et al 1998; Stockwell 1967). Hashimoto *et al*, reported that 22% of OA chondrocytes undergo apoptosis and they are mostly localised in the superficial and middle zones of cartilage (Hashimoto et al 1998). Blanco *et al*, reported that 51% of OA chondrocytes undergo apoptosis and that the majority are also localised in the superficial and middle zones of cartilage (Blanco et al 1998). However, a later study contradicted these findings and suggested that apoptosis does not play a role in OA as they identified very low levels of apoptotic chondrocytes (Aigner et al 2001). An alternative hypothesis was suggested, chondroptosis, a variant of apoptotic cell death in chondrocytes (Roach et al 2004). Chondroptosis shares some features with classical apoptosis, such as cell shrinkage, chromatin condensation and involvement of caspases. However, in chondroptotic cells, the plasma membrane is deformed and the Golgi and ER are degraded, whereas in apoptotic cells, the plasma membrane and the organelles shrink but are intact. Also they suggest that there is no formation of apoptotic bodies in chondroptosis and therefore the degraded cellular material is left as debris. Some degradation also takes place into autophagic vacuoles suggesting a mechanism involving autophagy as well. Two recent reports associate autophagy with OA, suggesting that activation of autophagy by rapamycin inhibits chondrocyte apoptosis and ROS levels, reduces IL-1β-induced *MMP-13* and *ADAMTS-5* expression and also recovers IL-1β-mediated reduction of *COL2A1* and *aggrecan* expression (Caramés et al 2011; Sasaki et al 2011).

The poor repair capacity of ROS induced mtDNA damage in OA chondrocytes compared to healthy chondrocytes correlates with increased susceptibility of OA chondrocytes to ROS- induced apoptosis compared to healthy chondrocytes

(Grishko et al 2008). Previous studies from the same group suggested that targeting DNA repair enzymes (8-oxoguanine DNA glycosylase/apurinic lyase (OGG1), endonuclease III and endonuclease VIII) into mitochondria could enhance the repair of mtDNA damage and also increase the viability of the treated cells and protect them against apoptosis (Rachek et al 2002; Rachek et al 2004). Cells overexpressing Bcl-2 have been show to be resistant to apoptosis induced by serum withdrawal or retinoic acid (Feng et al 1998). An increase in chondrocyte apoptosis has been linked with a decrease in the Bcl-2 expression in OA (Kim et al 2000). The regulation of Bcl-2 has also been associated with TGFβ1. TGFβ1 has a possible anti-apoptotic effect on chondrocytes by acting via protein phosphatase A and thus increasing the Bcl-2:Bax ratio by increasing Bcl-2 expression (Lires-Dean et al 2008). TGFβ1 supplementation has also been shown to enhance cartilage repair, however side effects like fibrosis and osteophyte formation were observed (Blaney Davidson et al 2007). Caspase inhibitors have been suggested as a possible therapy as they have been shown to inhibit apoptosis induced by mechanical injury in human cartilage and horse cartilage discs (D'Lima et al 2001; Huser et al 2006).

1.3.5 ROS and MMPs

Reactive oxygen species have also been implicated in matrix degradation (Henrotin et al 2005) and have been shown to lead to the cleavage of collagen and hyaluronan (Gao et al 2008; Petersen et al 2004). $^{\bullet}OH$ can react with proline residues and lead to peptide bond cleavage in collagen (Schuessler, & Schilling 1984). Also $O_2^{\bullet-}$ has been reported to directly cleave peptide bonds (Monboisse et al 1988). MMP-1 activation can also be regulated indirectly by the effect of H_2O_2 on the MAPK pathway. Proinflammatory cytokines, such as IL-1 and TNF-α, increase SOD2 activity and therefore SOD2 can generate more H_2O_2 (Ranganathan et al 2001). H_2O_2 enhances the phosphorylation and activation of MAPKs, including ERK 1/2, JNK and p38 (Clerk et al 1998). JNK then phosphorylates c-Jun and JunD, whereas ERK 1/2 phosphorylates c-Jun and Fos family members (such as c-Fos) (Han et al 2001). Dimerization of Jun–Jun or Jun–Fos factors, promotes translocation of these transcription factors into the nucleus where they regulate *MMP-1* transcription (Han et al 2001;

Nelson, & Melendez 2004). MMP-1 transcription has also been reported to be enhanced by SOD2 via the H_2O_2 dependent activation of AP-1.

Analysis of murine MMP-13 expression in *SOD1* -/- mice suggested that ROS regulate collagen degradation in murine fibroblasts via the ROS-induced phosphorylation of MAPK kinases (ERK, JNK and p38) and the subsequent transcriptional activation of MMP-13. A study by the same group suggested that H_2O_2 regulates senescence-associated MMP-1 expression in human lung fibroblasts via JNK phosphorylation and recruitment of c-Jun to the MMP-1 promoter (Dasgupta et al 2010). Additionally, type-I collagen fragmentation has been shown to promote ROS production and ROS-mediated MMP-1 expression in aged human skin fibroblasts via AP-1 and α2β1 integrin (a cell surface receptor for ECM) activation (Fisher et al 2009). H-Ras, NADPH oxidase and ROS have also been shown to mediate IL-1 and TNF-α-induced MMP-13 gene and protein expression in human chondrocytes via a mechanism that possibly involves the MAPK, AP-1 and NF-κB pathways (Ahmad et al 2011).

1.3.6 Nitric oxide

iNOS (inducible NO synthase) is up-regulated in OA, resulting in production of NO (Amin et al 1995). NO also inhibits proteoglycan and collagen synthesis (Taskiran et al 1994). Maneiro *et al*, (Maneiro et al 2005), have shown that nitric oxide mediates apoptosis by increasing caspase 3 and 7 levels and decreasing Bcl-2 levels. In the same study NO has also been demonstrated to inhibit the activity of the complex IV in human articular chondrocytes and to contribute to the depolarization of the Δψm. Elevated levels of nitrotyrosine, which is oxidized tyrosine in the presence of nitrous oxide (a product of NO+ROS), have been identified in OA and aged cartilage from human subjects and macaques (Loeser et al 2002). NO's interference with the mitochondrial function has also been demonstrated. A gradual 2-fold increase in NO levels in guinea pig chondrocytes has resulted in a 50% decrease in the levels of ATP produced (Johnson et al 2004). In the same study, to confirm that the cause of ATP depletion was mitochondrial dysfunction, they found an increase in the lactate: pyruvate ratio, a compensation reaction to mitochondrial dysfunction. A different study also showed that treatment with the antioxidant N-Acetyl-cysteine

prevents NO-Induced apoptosis and cartilage degradation in a white rabbit chondrocyte model of OA (Nakagawa et al 2010). Nitric oxide has also been shown to affect OA synoviocytes. Cillero Pastor *et al* demonstrated that NO induced mitochondrial depolarization and cell death in human OA synoviocytes (Cillero-Pastor et al 2011). Also NO induced the activities of mitochondrial complex I and III possibly as an adaptive response to produce more energy. However, NO treatment also reduced mitochondrial mass and ATP turnover and decreased Bcl-2, Mcl-1 and pro-caspase-3 protein expression in the same cells (Cillero-Pastor et al 2011).

1.3.7 ROS inhibitors and OA

All three major inhibitors of $O_2^{\cdot-}$ in the cell, superoxide dismutase 1 (SOD1), SOD2 and SOD3, have decreased expression in OA cartilage compared to control both at the mRNA and protein level (Scott et al 2010; Ruiz-Romero et al 2009; Aigner et al 2006). SOD2 downregulation in OA could be partially explained by the increase in the number of partially methylated CpG sites in OA compared with NOF cartilage. An increase of intracellular ROS levels in OA chondrocytes compared to healthy chondrocytes has also been reported, suggesting that this is a consequence of the decrease of SODs in OA and therefore higher $O_2^{\cdot-}$ levels (Ruiz-Romero et al 2009).

As described in detail in section 1.1.9, SOD2 deficiency increases mitochondrial $O_2^{\cdot-}$ levels in mice and leads to prenatal or neonatal lethality. This phenotype is associated with severe neurological and cardiac phenotypes and linked to decreased Complex I and II activity as well as mitochondrial aconitase deficiencies, lipid peroxidation and oxidative gDNA damage in brain, heart, skeletal muscle and liver (Huang et al 2001; Li et al 1995; Lebovitz et al 1996; Melov et al 1999; Morten et al 2006). Treatment of SOD2 null CD1 mice with SOD2 mimetics increases their lifespan and attenuates spongiform encephalopathy and mitochondrial defects (Melov et al 2001; Melov et al 1998). The effect of exercise on cartilage in heterozygote SOD2-deficient mice (C57BL/6 x Sv129/Ola background) was recently assessed (Baur et al 2011). Elevated levels of 15-F2t-isoprostane (17%) and nitrotyrosine (25%) were detected in articular cartilage of SOD2 +/- mice compared to wild type possibly

due the increased $O_2^{\cdot-}$ levels in SOD2 +/- mice. The levels of these molecules in articular cartilage were increased in both SOD2 +/+ (15-F2t-isoprostane: 40%; nitrotyrosine: 33%) and SOD2 +/- (15-F2t-isoprostane: 40%; nitrotyrosine: 29%) after aerobic running exercise due to the fact that ROS levels were possibly induced by electron leakage from the MRC during aerobic exercise (Baur et al 2011). However, these changes had no effect on cartilage morphology, structure and function and both SOD2 +/+ and SOD2 +/- mice did not show any features of OA.

EC-SOD (or SOD3) levels have been shown to have a 4-fold reduction in OA chondrocytes compared to normal chondrocytes (Regan et al 2005). SOD3 levels are also reduced in synovial joint fluid of OA subjects compared to normal (Regan et al 2008).

Pro-inflammatory cytokines IL-1/4/6 and TNF-α are potent activators of SOD2. IL-1β reduces type II collagen expression and increases MMP-1 and MMP-3 expression. It also stimulates NO production and as a consequence (provided ROS are present) peroxynitrite expression that can target the telomeres (guanine repeats) and can induce extrinsic senescence (Yudoh et al 2005; Afonso et al 2007). IL-1β stimulation in bovine cartilage enhanced SOD2 and GPX gene expression but decreased the expression of SOD1 (Cu/Zn SOD), SOD3 and CAT, suggesting a possible role of IL-1β in ROS production (Mathy-Hartert et al 2008). However, depletion of SOD2 in human chondrocytes reduced basal MMP-1 and IL-1α induced MMP-1 and MMP-13 mRNA levels (Scott et al 2010) possibly due to reduced H_2O_2 levels, a known MMP-1 inducer (Ranganathan et al 2001). This can suggest that the reduction of SOD2 levels in OA has a potential chondroprotective role.

A study evaluating the relationship of oxidative stress and age reported that increased oxidative stress with ageing makes chondrocytes more susceptible to ROS-mediated cell death (Carlo, & Loeser 2003). They studied this by assessing the levels of GSH (Glutathione), a ROS scavenger with anti-oxidative activity, in human chondrocytes. GSH affects the ECM of articular cartilage via regulation of H_2O_2 production, which has been shown to inhibit hyaluronic acid and proteoglycan synthesis (Bates et al 1985b; Bates et al 1985a). Additionally,

a decrease in GSH causes a decrease in proteoglycan and hyaluronic acid synthesis (essential components of the ECM) (Carlo, & Loeser 2003). GSSH, the oxidized form of GSH, was 4-fold increased in chondrocytes from older donors compared to chondrocytes from young donors, while the levels of GSH remained constant. The overall GSSH:GSH ratio was double in old donors compared to young donors and this could contribute to the increased ROS levels and oxidative stress in aged chondrocytes (Carlo, & Loeser 2003).

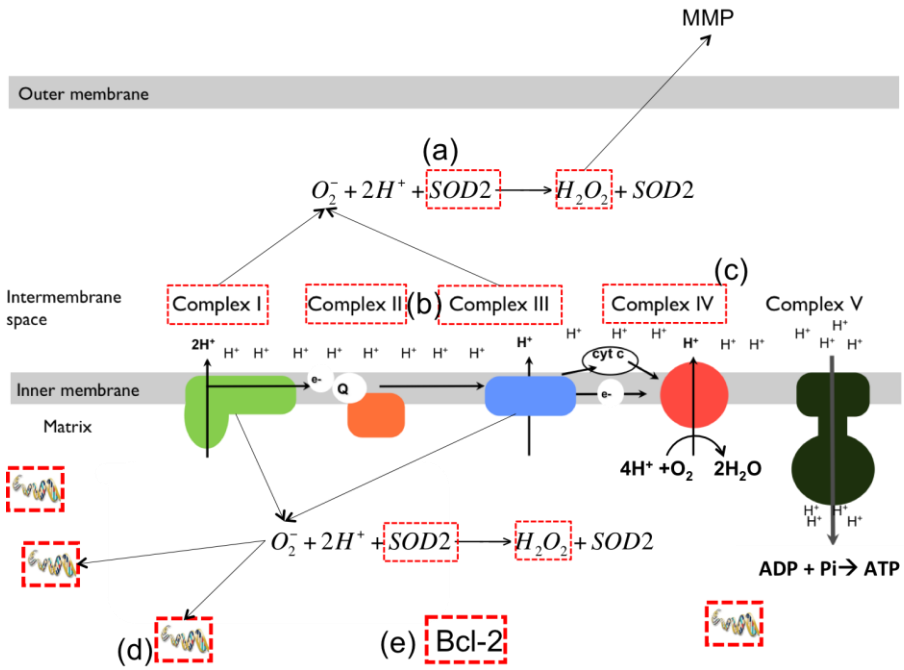

Figure 1.15 Mitochondrial dysfunction in osteoarthritic cartilage.

(a) SOD2 is downregulated in OA and its inhibition is related to MMP regulation in fibroblasts. (b) Complex II and Complex III activity is downregulated and inhibition of complex III causes mitochondrial depolarization. (c) NO inhibits complex IV and interferes with ATP production. (d) 4977bp mt DNA deletion found in osteoarthritic mitochondria. (e) Bcl-2 is downregulated in OA and is also thought to be regulated by TGF-β. TGF-β regulation is also altered in OA.

1.3.8 OA, TLRs and mitochondria

As described in section 1.1.7, PRRs are recruited by the innate immune system to detect microbial motifs as a response upon infection. They include TLRs, CTLs and NLRs, which recognize pathogen-associated molecular patterns (PAMPs) (Schroder, & Tschopp 2010). Toll-like receptor 3 (TLR3) is, as mentioned before, a positive regulator of the NF-κB signalling. In a recent study, TLR3 expression has been shown to be significantly increased in OA cartilage

compared to normal healthy (NOF, neck of femur) cartilage (Zhang et al 2008). In the same study, TLR3 ligands have been shown to upregulate NF-κB mediated MMP-1 and MMP-13 induction suggesting a role in matrix degradation. As described in section 1.1.10, TLR3-independent NF-κB activation by dsRNA is thought to be regulated by the mitochondrial localized VISA (Seth et al 2005; Kawai et al 2005; Meylan et al 2005; Xu et al 2005). Another mitochondrial localised protein, NLRX1, was identified to be involved in non-TLR3 dependent dsRNA stimulation via the inhibition of VISA (Tattoli et al 2008; Moore et al 2008). Other studies have linked NLRX1 with the regulation of TNF-α, *Shigella* infection and dsRNA induced ROS production thus amplifying the NF-κB and JNK pathways in a non-VISA dependent response thus suggesting that NLRX1 does not inhibit VISA but it is just a regulator of ROS levels upon infection (Tattoli et al 2008; Rebsamen et al 2011; Arnoult et al 2009). Two studies from our laboratory reported differential expression of both NLRX1 and TLR3 in OA and NOF cartilage and that TLR3 activation induced MMP-13 expression in chondrocytes, suggesting a possible role of these proteins in end-stage OA (Zhang et al 2008)(David A. Young, unpublished data).

1.3.9 Mitochondria and RA

Mitochondrial dysfunction and excess ROS have also been associated with RA (Filippin et al 2008). SOD1 and SOD3 are inhibited by TNF-α in RA leading to an increase in ROS production. An increase in peroxynitrite increased MMP-3 and MMP-13 activity and decreased TIMP levels as well as type II collagen production (Afonso et al 2007). Also, more amino acid changing mutations where identified in MTND1 in RA synovium samples compared to OA synovium controls (Sylva et al 2005). DaSylva *et al*, also suggested that there are 5 possible peptides that are altered due to mitochondrial mutations and can be presented by MHCII and recognized as non-self thus inducing an inflammatory response (Sylva et al 2005). Mitochondrial depolarization, increased levels of lipid peroxidation as well as high levels of lactate dehydrogenase (indicator of cytotoxicity) have also been observed in lymphocytes and serum samples from RA patients compared to non-RA controls (Moodley et al 2008).

1.4 Scope of this thesis

SOD2 mRNA and protein expression has been demonstrated to be downregulated in OA cartilage compared to NOF (Scott et al 2010; Ruiz-Romero et al 2009; Aigner et al 2006). The functional role of SOD2 depletion in OA has been examined in terms of MMP-1 and MMP-13 mRNA expression (Scott et al 2010). Also, intracellular ROS levels have been shown to be upregulated in OA chondrocytes compared to healthy chondrocytes (Ruiz-Romero et al 2009). The effects of SOD2 depletion in mice have been previously characterized in terms of life expectancy, organ failures, mitochondrial dysfunction and oxidative damage due to increased $O_2^{\cdot-}$ levels (Huang et al 2001; Li et al 1995; Lebovitz et al 1996; Melov et al 1999; Strassburger et al 2005; Melov et al 2001; Williams et al 1998). Recently, it has been reported that SOD2 depletion decreases mitochondrial spare respiratory capacity (SRC) in mouse synaptosomes (Flynn et al 2011). Mitochondrial dysfunction and mtDNA damage have been identified in OA chondrocytes compared to healthy controls (Maneiro et al 2003; Grishko et al 2008; Chang et al 2005). Inflammatory cytokines have also been associated with mitochondria dysfunction in OA (López-Armada et al 2006; Cillero-Pastor et al 2008). ROS have also been shown to regulate MMP-1 and MMP-13 expression in human and murine lung fibroblasts as well as human chondrocytes (Ahmad et al 2011; Dasgupta et al 2010; Dasgupta et al 2009; Nelson, & Melendez 2004).

In this thesis the functional effects of SOD2 downregulation in OA will be further examined, in the context of oxidative damage and mitochondrial dysfunction. The effect of SOD2 depletion on mitochondrial $O_2^{\cdot-}$ levels will be assessed in HAC. This will provide a basis for examining the downstream effects of SOD2 downregulation in chondrocytes. OA cartilage will be screened for mtDNA damage and lipid peroxidation levels, which can be potentially caused by SOD2 depletion and compared to NOF cartilage. Since SOD2 is vital in regulating oxidative damage in the cells, the effect of SOD2 depletion on lipid peroxidation and mtDNA damage will also be examined. Also mitochondrial function will be assessed in NOF and OA chondrocytes and SOD2-depleted chondrocytes in order to determine differences in mitochondrial function in NOF and OA chondrocytes and then assess the possible role of SOD2 in the regulation of

mitochondrial function in chondrocytes. In addition, the potential role of mitochondria as an innate immunity signalling platform in chondrocytes will be assessed by examining the role of NLRX1 in the regulation of MMP-13 expression and ROS production. Also the effect of dsRNA and NLRX1 in the regulation of the differential expression of SOD2 in OA and NOF will be assessed.

Chapter 2. Materials and Methods

2.1 Materials

2.1.1 Antibodies

MnSOD (SOD2) rabbit polyclonal antibody (#110E) was purchased from Stressgen Bioreagents (Cambridge, UK). Alexa Fluor® 488 goat anti-rabbit IgG, (A-11034) was purchased from Invitrogen (Paisley, UK). NLRX1 mouse polyclonal antibody was kindly donated by Dr Stephen Girardin (University of Toronto, Canada).

2.1.2 SW1353 cell line

The SW1353 chondrosarcoma cell line was initiated from a primary grade II chondrosarcoma of a 72-year-old female Caucasian in 1977. SW1353 cells (HTB-94) were purchased from the (American Type Culture Collection) ATCC. SW1353 chondrosarcoma cells are considered a substitute for a chondrocytic experimental system. However, a study comparing the gene expression profile of SW1353 cells and HAC reported that SW1353 cells have very limited similarities in gene expression compared to HAC (Gebauer et al 2005). The authors suggested that SW1353 cells could be used to study the induction of MMPs however their potential to mimic HAC function is limited. The results acquired in this thesis using SW1353 chondrosarcoma cells as a model system for chondrocytes have to be interpreted carefully in terms of their relevance to mimic the function in HAC and the use of these cells in some experiments is a limitation of this thesis and therefore the use of this cell line was minimal and restricted to the optimisation of methods and when HAC availability was limited.

2.1.3 Cell Culture Reagents

DMEM medium and foetal bovine serum (FBS) were obtained from Invitrogen (Life technologies, Paisley, UK). Penicillin-streptomycin solution (10000 U/mL and 10 mg/mL respectively), L-glutamine solution (200 mM), Nystatin suspension (10000 U/mL), trypsin-EDTA solution (0.5g porcine trypsin and 0.2g EDTA per L), hyaluronidase (from bovine testes, 439 U/mg), trypsin (from

porcine pancreas, 1020 U/mg) and collagenase (from Clostridium histolyticum type I) were obtained from Sigma-Aldrich Ltd (Poole, UK). Phosphate buffered saline (PBS) was purchased from Lonza (Wokingham, UK). Tryptone, yeast extract and bacto-agar were purchased from Difco Laboratories (Detroit, MI, USA).

2.1.4 Commercially Available Kits

QIAquick® GelExtraction Kit and QIAquick DNA extraction kit were purchased from Qiagen (Crawley, UK). The TOPO TA Cloning® Kit for sequencing pCR®4-TOPO® vector was purchased from Invitrogen. E.Z.N.A Tissue DNA extraction kit was purchased from Omega Bio-Tek (Norcross, GA, USA). TBARS assay kit was purchased from Cayman Chemical (Ann Arbor, MI, USA)

2.1.5 Molecular Biology Reagents

GeneRuler™ 100kb and 1kb DNA ladders, *Eco*RI, *Bgl*II and *Hind*III were purchased from Fermentas Life Sciences (York, UK). Deoxyribonucleotide triphosphate (dNTP) and 5-bromo-4-chloro-3-indolyl β-D-galactopyranoside (X-GAL) were purchased from Bioline (London, UK). VECTASHIELD mounting medium with DAPI was purchased from Vector Labs. Cryo-M-Bed compound was purchased from Bright (Huntingdon, UK) and SuperFrost® Plus Gold slides by Menzel Glaser were purchased from Fisher Scientific (Loughborough, UK). pGL3-Basic Vector (E1751) was purchased from Promega (Southampton, UK). Advantage® GC 2 PCR Kit, TITANIUM™ Taq DNA Polymerase and LA Taq were purchased from Takara Biomedicals (Wokingham, UK). Accuprime Pfx, TMRM and Mitosox Red were purchased from Invitrogen. Paraquat dichloride, N-Acetyl-L-cysteine, Antimycin A from Streptomyces sp., rotenone and Saponin from quillaja bark were purchased from Sigma-Aldrich Ltd (Poole, UK).

All other standard laboratory chemicals and reagents, unless otherwise indicated, were commercially available from Sigma-Aldrich Ltd, Fisher Scientific, Invitrogen or BDH Chemicals (Poole, UK).

Methods

2.2 Human Articular Cartilage sample collection

Human articular cartilage samples were obtained from patients undergoing joint (hip or knee) replacement surgery due to end-stage osteoarthritis. Normal cartilage (NOF) was obtained from neck of femur fracture patients (with no history of osteoarthritis) undergoing joint replacement surgery. This study was performed with ethical committee approval from Oxford Radcliffe Hospitals NHS Trust and Newcastle and North Tyneside Health Authority and all patients provided informed consent.

Cartilage was processed to extract chondrocytes or dissected and snap-frozen in liquid nitrogen or super cooled isopentane for DNA extraction and immunohistochemistry respectively.

For OA chondrocyte cultures, cells were extracted from the remaining cartilage present on end-stage OA knee or hip specimens and therefore included lesions as well as macroscopically normal areas. Human cartilage used for immunohistochemistry was obtained from end-stage OA knee or hip specimens and exhibited differing degrees of damage.

A difference of the OA and NOF cartilage is that the majority of the surface layer of cartilage is missing in OA samples due to disease progression. As a result, only surface layer HAC, which have higher mitochondrial activity compared to the middle and deep layers, could be isolated from NOF cartilage and not OA (Blanco et al 2011). Additionally, NOF patients are not completely “normal” and healthy, however due to their similar age to OA patients they were the best controls available for comparison. These are limitations of the sampling and have to be taken into consideration when analysing the results.

2.2.1 Human articular chondrocyte (HAC) extraction

Reagents:

- PBS containing 200IU/mL penicillin, 200µg/mL streptomycin and 40IU/mL Nystatin

- DMEM culture medium containing 10% FBS, 2mM L-glutamine, 200IU/mL penicillin, 200µg/mL streptomycin and 40IU/mL Nystatin

Method:

Macroscopically normal cartilage was removed from the subchondral bone and washed in PBS. Cartilage was cut in small pieces and sequentially digested with 1mg/mL hyaluronidase in PBS for 15 min at 37°C, 2.5mg/mL trypsin in PBS for 30 min at 37°C and 2.5mg/mL collagenase (from Clostridium histolyticum type I) in DMEM for 16 hours at 37°C. Cartilage pieces were washed three times in either PBS or DMEM between each of the incubations. Following digestion, cell suspensions were left for 15 min to allow undigested material to settle and the supernatant was removed and spun at 250 x *g* in a bench top centrifuge to pellet the cells. The cell pellet was washed with PBS and re-suspended in culture medium. HAC were seeded at an appropriate density in vented tissue culture flasks prior to experimentation, approximately at the density of 4×10^4 cells/cm^2 in a T25 cm^2 or T75 cm^2 culture flask.

2.2.2 Preparation of frozen sample blocks for sections

Cartilage sections were used to identify cytochrome c oxidase (COX) -positive and COX-negative chondrocytes by the COX-SDH assay described in section 2.6.1 and then their mtDNA screened for deletions.

Method:

Cartilage chips were snap frozen in super-cooled isopentane prior to sectioning. Samples were then mounted onto the stage using Cryo-M-Bed embedding compound.

2.2.3 Homogenisation of tissue for DNA extraction

Cartilage total DNA was screened for mtDNA deletions, mtDNA strand breaks and mtDNA copy number.

Method:

Cartilage was weighed and 1.0-1.5g ground in a pre-cooled mixer mill (Retsch MM200, Retsch UK ltd, Castleford, West Yorkshire, UK). Cartilage was ground for 4 cycles of 1.25 min grinding at an impact frequency of 20 Hz and 2 min cooling in liquid nitrogen.

2.3 Cell culture

2.3.1 Routine cell culture

HAC

Reagents:

- HAC culture medium- DMEM culture medium containing 10% FBS, 2mM L-glutamine, 200IU/mL penicillin, 200µg/mL streptomycin and 40IU/mL Nystatin.

Method:

Cells were cultured in vented T25 cm^2 or T75 cm^2 flasks in a humidified incubator with 5% CO_2 (v/v) at 37°C (Scott et al 2010). Cells were cultured until they reached 70% - 80% confluency. Cell monolayers were washed with PBS before incubation with trypsin-EDTA solution to release the cells. Cells were split into appropriate culture vessels for experimentation.

SW1353 chondrosarcoma cell line

Reagents:

- SW1353 culture medium- DMEM culture medium containing 10% (v/v) FBS, 2mM L-glutamine, 100IU/mL penicillin, 100µg/mL streptomycin
- Freezing medium containing 90% (v/v) FBS and 10% (v/v) DMSO.

Method:

SW1353 cells were cultured like HAC. Cells were split into appropriate culture vessels for experimentation or into further T25 cm^2 or T75 cm^2 flasks to continue the cell lines (Zhang et al 2008).

Excess SW1353 cells were frozen down for long term storage in liquid nitrogen by re-suspending cell pellets in freezing medium. Cells were transferred to cryovials and frozen slowly (1°C /min) in a cell freezing container overnight at -80°C prior to transfer to liquid nitrogen store.

2.3.2 siRNA transfection

Cells were seeded in appropriate culture vessels at a density of 1.5 x 10^4 cells/cm^2 or 2.5 x 10^4 cells/cm^2 for SW1353 and HAC respectively. The following day, cells were transfected with 100nM of the appropriate siRNA or siGENOME non-targeting siRNA pool #2 (siControl2) using DharmaFECT® 1 according to manufacturer's instructions (Dharmacon, Lafayette, CO, USA) as described previously (Zhang et al 2008). After 48 hours cells were used for the experimentation or were washed with PBS and incubated in serum-free medium for a further 24 hours and stimulated with 0.5ng/ml Interleukin-1α (IL-1α) or poly(I:C). SOD2-targeting siRNA sequences (sense and antisense) and the NLRX1 and VISA target sequences are shown in Table 2.1.

SMARTpool® Duplex	Target Strand	Sequence
SOD2- 1	Sense	5'-GGACAAACCUCAGCCCUAAUU
	Antisense	5'-PUUAGGGCUGAGGUUUGUCCUU
SOD2- 2	Sense	5'-GGAGCACGCUUACUACCUUUU
	Antisense	5'-PAAGGUAGUAAGCGUGCUCCUU
SOD2- 3	Sense	5'-AAAGAUACAUGGCUUGCAAUU
	Antisense	5'-PUUGCAAGCCAUGUAUCUUUUU
SOD2- 4	Sense	5'-GUAAUCAACUGGGAGAAUGUU
	Antisense	5'-PCAUUCUCCCAGUUGAUUACUU
NLRX1- 1	Target sequence	5'-GCACGGGACUUUGUAGUGA
NLRX1- 2	Target sequence	5'-CAUCAGAGCUCCUUGACCA
NLRX1- 3	Target sequence	5'-GAUCUGCGGUUUCUCUGAU
NLRX1- 4	Target sequence	5'-GCACAUCUUCCGUCGGGAU
VISA- 1	Target sequence	5'-AAGUAUAUCUGCCGCAAUU
VISA- 2	Target sequence	5'-GCUGUGAGCUAGUUGAUCU
VISA- 3	Target sequence	5'-CAAGAGACCAGGAUCGACU
VISA- 4	Target sequence	5'-AGAAUGAGUAUAAGUCCGA

Table 2.1 Table Sequences of SOD2, NLRX1 and VISA-targeting siGENOME® SMARTpool® siRNA (Scott et al 2010).

2.3.3 Plasmid transfection

NLRX1 was overexpressed in SW1353 cells and its effect on NF-κB activity was assessed after IL-1α and poly(I:C) stimulation.

Method:

SW1353 cells were seeded in 6 well or 48 well plates at a density of 1.5 x 10^4 cells/cm^2. The following day, cells were transfected for 24 hours with 0.3μg/ml NLRX1- mammalian expression plasmid DNA (Tattoli et al 2008). For luciferase assays cells were co-transfected for the same 24 hours with 0.15μg/ml NF-κB-luciferase reporter using 3 μl Fugene HD (Promega) per 1μg of DNA. Cells were washed with PBS and incubated in serum-free medium for a further 24 hours and stimulated with 0.5ng/ml IL-1α or poly(I:C) for 6 hours.

2.3.4 dsRNA stimulation and transfection

dsRNA mimic poly(I:C) is a ligand for TLR3 and potentially the RIG-I like receptors (RLR) MDA5 and RIG-I. Stimulation with extracellular (naked) poly(I:C) has been shown to activate TLR3, whereas transfected poly(I:C) bypasses TLR3 activation and activates RIG-I or MDA5 in a cell-type specific manner (Kato et al 2005; Kato et al 2006; Gitlin et al 2006). poly(I:C) was used to determine the effect of innate immunity signalling on *MMP-13* and *SOD2* expression and ROS production in HAC and SW1353 cells.

Method:

Cells were stimulated with 0.5μg/ml poly(I:C) or transfected with 0.5μg/ml Poly(I:C) for 24 hours using Lyovec (or Lipofectamine 2000) dsRNA mimics and ligands of TLR3 and MDA5/RIG-I respectively (Zhang et al 2008). Cells were then washed twice in cold PBS and lysed in Ambion Cells-II-cDNA buffer to analyse mRNA expression as described in section 2.4.7 or cell-lysis buffer for protein extraction as described in section 2.5.1.

2.4 Nucleic Acid extraction and analysis

2.4.1 Extraction of total DNA from cartilage homogenates

DNA from OA and NOF cartilage was screened for deletions and strand breaks in the major arc of the mtDNA and mtDNA copy number was assessed as described later on in this section.

Method:

DNA was extracted from powdered cartilage homogenate using the E.Z.N.A. DNA/RNA Isolation Kit (Omega Bio-Tek Inc, Norcross, GA, USA). The DNA extraction procedure was performed according to the manufacturers instructions. DNA samples were quantified using the NanoDrop® spectrophotometer (NanoDrop Technologies, Wilmington, Delaware, USA) and stored at -20°C.

2.4.2 Extraction of total DNA from cell cultures

Total DNA from SW1353 cells was screened for strand breaks in the major arc of the mtDNA.

Method:

Cells were trypsinised, washed in serum containing media to neutralise the trypsin and then washed twice in PBS. DNA was extracted from using the QIAmp DNA mini kit (Qiagen, Crawley, UK). The DNA extraction procedure was performed according to the manufacturers instructions. DNA samples were quantified using the NanoDrop® spectrophotometer (NanoDrop Technologies, Wilmington, Delaware, USA) and stored at -20°C.

2.4.3 Total DNA extraction from single cells

Total DNA from single cells was screened for deletions in the major arc of the mtDNA and also mtDNA copy number was assessed in the same samples.

Method:

Freshly extracted HAC were cytospun on membrane-microscope slides for 10min at 250 x *g*. Single cells were isolated using laser capture microdissection as described in section 2.4.4. Cells were lysed using a 15µl single cell lysis buffer prepared as follows: In a total volume of 500µl, 250µl 1% (v/v) Tween 20 (0.5% (v/v) final concentration), 195µl dH_2O, 50µl 0.5M Tris-HCl pH 8.5 (50mM final concentration) and 5µl Proteinase K (200µg/ml final concentration). Lysate was used for mtDNA deletion and mtDNA copy number analysis described below.

2.4.4 Laser capture microdissection

This technique was used to isolate single cells that were selected according to their COX activity in order for their mtDNA to be screened for large-scale deletions.

Method:

Cells were cytospun on PEN-membrane slides and stained for COX and SDH as in section 2.6. Cells were then visualized using the Leica AS LMD system and COX-positive or COX- negative cells were selected (Krishnan et al 2010). These cells were then isolated using the laser capture tool of the Leica AS LMD system and placed into 0.5ml Eppendorf tubes in order to be lysed as described in 2.4.

2.4.5 DNA isolation from Bacterial artificial chromosome (BAC)

BAC containing the RP-11 56L9 region of the human DNA, which includes the *SOD2* gene, was used in order to isolate the SOD2 promoter region to identify the changes that lead to differential SOD2 expression in NOF and OA.

Bacterial cell culture

Reagents:

- Luria Broth (LB) containing 10 g NaCl, 10 g tryptone and 5 g yeast extract per litre dH_2O. Adjust pH to 7.5 with NaOH.

- LB Agar – 10 g NaCl, 10 g tryptone, 5 g yeast extract and 15 g agar per litre dH_2O. Adjust pH to 7.5 with NaOH.

Method:

A 100µL aliquot of *Escherichia coli* (*E.coli*) cells containing a BAC with the human RP-11 56L9 DNA region, that contained the human genetic locus including SOD2 gene promoter DNA, was spread on LB-agar plates containing 12µg/mL chloramphenicol. Plates were incubated for 16 hours at 37°C in order for colonies to develop. A single isolated bacterial colony was selected and added to 2mL of LB media supplemented with 60µM chloramphenicol. Cultures were shaken at 220 rpm and 37°C for 16 hours in an orbital shaker.

DNA isolation

Reagents:

- P1 (filter sterilized, 4°C)
- 15mM Tris-HCl, pH 7.5
- 10mM EDTA
- 10µg/mL RNase A
- P2 (filter sterilized, room temperature)
- P3 (autoclaved, 4°C)

Method:

Cultures were centrifuged at 4000 x *g* for 10 min and the supernatant discarded. Each pellet was resuspended in 100µL P1 solution by gently tapping the tubes. 100µL P2 was then added, the contents were mixed thoroughly by inverting the tubes 5 times and let to stand for 5 min. 100 µL P3 was then added while shaking the tubes gently to mix thoroughly and the tubes were placed on ice for 5 min. The contents were centrifuged for 10 min at 13000 x *g* at 4°C and the supernatant mixed with 0.8mL ice-cold isopropanol. Samples were placed on

ice for 5 min and then centrifuged for 15 min at 13000 x *g* at 4°C. Supernatant was removed mixed with 0.5 mL 70% ethanol to wash the DNA pellets. The tubes were centrifuged for 5 min at 13000 x *g* at 4°C, and the pellets allowed to air-dry before resuspension in 50µL dH_2O.

BAC DNA digestion

Method:

To confirm the presence of the *SOD2* gene in the RP-11 56L9 sequence, a 12.5µL aliquot of each DNA isolation was digested using the restriction enzymes *Bam*HI and *Hind*III in separate reactions. DNA was combined with 25U restriction enzyme (2.5µL), 5µL 10x restriction enzyme buffer appropriate for each reaction and dH_2O in a final volume of 50µL and incubated at 37°C for 2 hours. A 20µL aliquot of each digest was electrophoresed on a 1% (w/v) agarose-TAE (x1, Tris/Acetate/EDTA) gel as described in section 2.4.6.

2.4.6 Agarose gel electrophoresis

Reagents:

- x1 Tris-acetate-ethylenediamine tetra-acetic acid (TAE) containing 0.04 M Tris (pH 7.5), 5.7% (v/v) glacial acetic acid and 0.001M EDTA.
- Loading buffer containing Tris 0.125 M (pH 7.5), 2% (w/v) SDS, 10% (v/v) glycerol and 0.001% (w/v) bromophenol blue.

Method:

0.8-3% (w/v) agarose gels are prepared by dissolving the required amount of agarose in x1 TAE buffer through boiling. 10mg/ml ethidium bromide (3,8-Diamino-5-ethyl-6-phenylphenanthridinium bromide) solution was added to cooled agarose at a final concentration of 0.2 µg/mL. Gels were poured, allowed to set and the required amount of DNA loaded in loading buffer. Amplicons were separated at 100V for approximately 40 min and visualised on a ChemiGenius II BioImager (Syngene, Cambridge, UK).

2.4.7 Extraction of total RNA from HAC and SW1353 cells and reverse transcription

RNA was extracted from HAC and SW1353 cells and the reverse transcribed to cDNA in order to assess differential gene expression by real-time polymerase chain reaction (PCR) after specific treatments as described later in this section.

Ambion Cells-II-cDNA Kit

Method:

The *Cells-to-cDNA™ II Kit* was used for cell numbers of less than 1 x 10^4 seeded in a 96-well plate (Zhang et al 2008). Cell monolayers were washed with ice-cold PBS and lysed directly by addition of 30 µL Cells-to-cDNA™ II Cell Lysis Buffer. Lysates were mixed briefly, transferred to an ice-cold 96-well PCR plate and incubated at 75°C for 15 min to inactivate RNases. DNA digestion was performed by addition of 2 U DNase I per well followed by incubation at 37°C for 15 min and 75°C for 5 min.

Reverse transcription PCR (RT-PCR)

Method:

An 8µL aliquot of each RNA sample was transferred to a new 96-well PCR plate for reverse transcription. RNA samples were combined with 0.625 mM dNTP and 0.2 µg $p(dN)_6$ and incubated at 70°C for 5 min. Samples were placed on ice and a reaction mixture containing 10 mM DTT, 100 U M-MLV, 4 µL 5X First-Strand Buffer (Invitrogen) and 1.5 µL dH_2O added to each sample giving a final reaction volume of 20 µL. The reactions were incubated at 37°C for 50 min and then 75°C for 15 min. Samples were diluted by addition of 30 µL dH_2O for quantification of target genes and 5 µL aliquots where further diluted 1:10 in H_2O for quantification of housekeeping genes (Zhang et al 2008). The cDNA was stored at -20°C prior to analysis and 5 µL aliquots were used in real-time PCR reactions as described in section 2.4.8.

2.4.8 Polymerase Chain Reaction

Conventional PCR

SOD2 promoter amplification

The human SOD2 promoter would be isolated in order to subclone it into a luciferase reporter plasmid pGL3-Basic (Promega). Transcriptional activation of the promoter generates luciferase enzyme from the reporter and when incubated with substrate luciferase results in the production of light. The intensity of the light produced is proportional to the amount of enzyme produced and therefore gene activation. This construct would be used to identify signalling changes that cause differential expression of SOD2 in OA and NOF.

Primer design

A series of primers were designed to amplify a highly CpG rich region of the SOD2 promoter sequence as well as the 342bp NF-κB-responsive enhancer I2E within the second intron of the SOD2 gene. Forward primers SOD2- 2987, SOD2- 1605, SOD2- 1240, SOD2- 555 and SOD2- 210 and reverse primer SOD2R +24 were taken from a previous publication (Xu et al 1999) and both the forward and reverse primers had the *Bgl* II and *Hind* III restriction site sequence respectively attached to them. Primers SOD2 F1-F7, SOD2 R1-R7 and SOD2 I2E F and SOD2 I2E R were designed using the PrimerSelect software (DNAstar, Madison, WI, USA) and were based on the GenBank reference assembly sequence NC_000006.10. Primers SOD2 I2E F and SOD2 I2E R had a *Sal*I were synthesised with a *Sal*I restriction site at the 5' end along with an additional number of random nucleotides. All primer sequences are shown in Table 2.2.

Primer Pair	Name	Primer	Primer sequence
1	sod2-2987	Forward	5'-CGGAGATCTGACCATGAGGCAGCTTTGAAGACA-3'
	SOD2R +24	Reverse	5'-CGGAAGCTTGCCGAAGCCACCACAGCCACGAGT-3'
2	sod2-1605	Forward	5'-CGGAGATCTAGATCACTTGAGGTCAGGCGTTCG-3'
	SOD2R +24	Reverse	5'-CGGAAGCTTGCCGAAGCCACCACAGCCACGAGT-3'
3	sod2-1240	Forward	5'-CGGAGATCTCCTGTTGTGAAGCCAAGTTCAGGT-3'
	SOD2R +24	Reverse	5'-CGGAAGCTTGCCGAAGCCACCACAGCCACGAGT-3'
4	SOD2 I2E F	Forward	5'-CGGGTCGACCGGGGTTATGAAATTTGTTGAGTA-3'
	SOD2 I2E R	Reverse	5'-CGGGTCGACCCACAAGTAAAGGACTGAAATTAA-3'
5	SOD2-F1	Forward	5'-ACTGTGGTTGGATCTGTTACTGG-3'
	SOD2-R1	Reverse	5'-CTCCGTTTTCTTTTTCTTTTTGTC-3'
6	SOD2-F2	Forward	5'-ACATGAGCCCAGCAAGTCG-3'
	SOD2-R2	Reverse	5'-AGTGGTTTTTCAGGCAAGGTGGTC-3'
7	SOD2-F3	Forward	5'-AGACCACCTTGCCTGAAAAACCAC-3'
	SOD2-R3	Reverse	5'-AACAGTCAGGCGAAGAGGAACCAC-3'
8	SOD2-F4	Forward	5'-GGTTCCTCTTCGCCTGACTGTTTT-3'
	SOD2-R4	Reverse	5'-ACGACGTGCCCGAGACTGC-3'
9	SOD2-F5	Forward	5'-GCACCTGCTACCTTCCATCAT-3'
	SOD2-R5	Reverse	5'-AGCGCCCTTCCAACCCGTATTCAG-3'
10	SOD2-F6	Forward	5'-TTAGGCAGCCGGTGGGGACAAAG-3'
	SOD2-R6	Reverse	5'-CCAGGGCACGGGAGAAAGGAG-3'
11	SOD2-F7	Forward	5'-ACCAGCAGCTAGGCCCCGTCTTC-3'
	SOD2-R7	Reverse	5'-CTCAACATGCTGCTAGTGCTGGTG-3'

Table 2.2 Sequences of primers used for analysis of SOD2 promoter

Optimisation of cycling conditions

Method:

SOD2 promoter amplification was firstly attempted using primer pairs 1-3. However, due to unsuccessful amplification, different sections of the promoter region were amplified using primer pairs 5-11. Primers pairs 5-10 amplified the SOD2 promoter region successfully however primer pair 11 did not amplify the SOD2 promoter region fully and deletions were present possibly due the presence of GC-rich regions (section 6.4.8 and (Xu et al 2007)).

For primer pairs 1-3 and 5-10, different 20µL PCR reactions were performed by combining the BAC RP-11 56L9 DNA and the Advantage® GC 2 PCR Kit (1-3) or TITANIUM™ Taq DNA Polymerase kit (5-10) following the manufacturer's recommended concentrations and cycling conditions. A 5µL aliquot of each reaction was electrophoresed on a 1% (w/v) agarose-TAE (x1) gel (section 2.4.6) to determine the optimal annealing temperature and other conditions to amplify the PCR product. Optimum amplification of primer pairs 1-3 was achieved using the GC-2 PCR kit under the following cycling conditions: 94°C for 3 min, 35 cycles of [94°C for 30 sec, 68°C for 3 min], 68°C for 3 min. Optimum amplification of primer pairs 5-10 was achieved using the TITANIUM™ Taq DNA Polymerase kit and the following cycling conditions: 95°C for 1 min, 35 cycles of [95°C for 30 sec, 60°C for 30 sec, 68 for 2min], 68°C for 5 min.

For primer pair 11, 20µL PCR reactions were performed by combining the BAC RP-11 56L9 DNA and the TITANIUM™ Taq DNA Polymerase kit and 5% or 10% DMSO or 1.25M betaine. Optimum amplification was achieved following the manufacturer's recommended concentrations, and using 1.25M betaine and the following cycling conditions: 95°C for 1 min, 35 cycles of [95°C for 30 sec, 67 or 68°C for 30 sec, 68 for 2min], 68°C for 5 min.

For primer pair 4, 20µL PCR reactions were performed by combining the BAC RP-11 56L9 DNA and the Accuprime Pfx kit. Optimum amplification was achieved following the manufacturer's recommended concentrations and using the following cycling conditions: 94°C for 2 min, 30 cycles of [94°C for 15 sec, 60°C for 30 sec, 68 for 90 sec], 68°C for 5 min.

PCR product purification

Method:

SOD2 PCR products obtained were purified using the QIAquick® Gel extraction Kit according to manufacturer's instructions. PCR products were electrophoresed a 1% (w/v) agarose-TAE (x1) gel (section 2.4.6) and the required amplicon was excised. Gel was dissolved in Buffer QG and the PCR

products extracted and purified using QIAquick® spin columns prior to elution in 30µL dH_2O.

Long amplification PCR (LA-PCR)

LA-PCR was used to amplify a 9.9kb fragment of the mtDNA (major arc). In the presence of large-scale deletions in this region, the size of the PCR product is smaller than 9.9kb. This can suggest the presence of mtDNA deletions in the samples. However, this technique is not quantitative since the reaction preferentially amplifies smaller fragments instead of larger fragments.

mtDNA deletions

Method:

PCR analysis was performed using the Takara LA PCR System (Krishnan et al 2010). In order to amplify mtDNA, each PCR reaction was prepared by combining 2.5 U (0.5 µL) Takara LA Taq™, 5 µL 10x LA PCR™ Buffer II (Mg^{2+} plus), 0.4 mM dNTP, 300nM Long 10F primer, 300nM Long 10R primer and 50ng DNA sample in a final volume of 50 µL. The primers used were designed to amplify a 9.9Kb region (9,931 bp) of the mitochondrial genome (GenBank ID NC_001807) between nucleotides 6222 and 16153 (see Table 2.3). PCR reactions were performed using a GeneAmp® PCR system 9700 (Applied Biosystems). Cycling conditions were: 94°C for 1 min, 35 cycles of [94°C for 30 sec, 58°C for 30 sec, 68°C for 11 min], 72°C for 10 min. A 25µL aliquot of each PCR reaction was electrophoresed on a 0.8% (w/v) agarose-TAE (x1) gel as described in section 2.4.6. Single amplicons smaller than 9.9kb were gel purified and cloned into a TOPO-TA vector (Invitrogen) and chemically transformed into Mach-I competent cells following the manufacturer's protocol. A 100µL aliquot of each transformation was spread onto a pre-warmed agar plate containing 100µg/mL ampicillin. 40µl of 40mg/ml X-gal were spread on the plate to select for colonies containing an insert. Plates were incubated at 37°C for 16 hours in order for colonies to develop. Single colonies were picked for overnight cultures and then quick minipreps were performed as described in section 2.4.10. A 2µL aliquot from each miniprep was digested using *EcoR*I and

if positive for the insert sequenced and analysed using the CLC sequence Viewer software.

Primer name	Primer	Primer sequence	Position
Long 10F	Forward	5'-CCCTCTCTCCTACTCCTG-3'	6222-6239
Long 10R	Reverse	5'-CAGGTGGTCAAGTATTTATGG-3'	16133-16153

Table 2.3 Primers used to amplify part of the major arc of the mitochondrial genome

mtDNA strand breaks

In order to assess mtDNA strand breaks a modification of the LA-PCR reaction was performed. An 11Kb amplicon was amplified using a real-time PCR method.

Method:

SW1353 cells were seeded in 6cm dishes at a density of 1.5 x 10^6/dish. After 24 hours cells were transfected with 100nM siRNA as in section 2.3.2 for 48 hours and serum starved for 16 hours. Cells were also treated with 200nM H_2O_2 for 1 hour as a positive control for the reaction. Cells were checked and looked normal after treatment with H_2O_2 and then trypsinised, washed and a dry cell pellet was collected. Total DNA was extracted using the QIAmp DNA mini kit as described in section 2.4.2. Extracted DNA was equalised using the Nanodrop system and the levels of mtDNA damage were assessed by real-time PCR by the amplification of part of the major arc of the mtDNA using the primers in Table 2.4. The long PCR was performed in 50µl reactions using the Expand Long Template PCR System (Roche). PCR reaction mixture contained: 200ng template DNA, 10mM buffer, 10µM primer, 5x SYBR Green, high grade PCR water, 10mM dNTP and 3.75U of Expand Long Template enzyme. Cycling conditions were as follows: 94°C for 2 mins, 10 cycles of 15 seconds denaturation at 94°C, 30 seconds annealing at 60°C and 9 mins extension at 72°C; then 25 cycles of 15 seconds denaturation at 94°C, 30 seconds annealing at 60°C and 8.5 mins extension (+10 seconds/cycle) at 68°C.

MTND1 was used as a housekeeping marker. Real-time products were then subjected to 0.8% (v/v) agarose gel electrophoresis to screen for large mtDNA deletions.

This method has been previously validated by Dr Matthew Birket in the Dermatology Department, Newcastle University and is published (Passos et al 2007).

Primer name	Primer	Primer sequence	Position
OLA	Forward	5'-ATGATGTCTGTGTGGAAAGTGGCTGTGC-3'	5756-5781
D1B	Reverse	5'-GGGAGAAGCCCCGGCAGGTTTGAAGC-3'	282-255

Table 2.4 Primers used to amplify the part of the major arc of the mitochondrial genome to screen for mtDNA strand breaks

Real time RT-PCR

Fluorescence-based, real-time reverse transcription PCR (RT-PCR) was used to measure steady-state mRNA expression in cells through real-time detection of sequence amplification. In real-time PCR, the amount of PCR product is measured at each cycle by the use of fluorescent markers that are incorporated into the PCR product and therefore enables accurate detection of the initial amount of target.

When analysed with a stably expressed gene, e.g. *18S*, the relative expression of a gene of interest was determined. Both the TaqMan probe-based and SYBR Green real-time PCR detection systems were used.

Real-Time RT-PCR Primer Design

Method:

Primers and probes used for the TaqMan® probe-based RT-PCR method were designed using Primer Express 1.0 software from Applied Biosystems unless indicated otherwise. Primers used for the SYBR® Green real-time RT-PCR method were designed using ProbeFinder software (available at Universal ProbeLibrary Assay Design Centre and based on Primer3) from Roche

Diagnostics unless indicated otherwise. The *18S* ribosomal RNA (rRNA) gene was used as an endogenous control (unless otherwise specified) and measured using a TaqMan probe-based reaction (with FAM™ reporter and TAMRA quencher) (Zhang et al 2008). All primers were designed to span an intron-exon boundary where possible, to prevent amplification of any contaminating DNA.

TaqMan® Probe-Based Real-Time RT-PCR

The TaqMan® system requires a pair of PCR primers in addition to a probe. The probe is designed to bind to the sequence amplified by the primers. In addition the probe contains a 5' reporter dye and, in some cases a 3' quencher dye attached which when intact and bound to the DNA template, emit fluorescence.

Method:

PCR reactions were prepared by combining 3µL cDNA with 5µL of TaqMan® Gene Expression Master Mix (Applied Biosystems), 300nM of each primer and 150nM probe in a final volume of 10 µL. Cycling conditions were: 50°C for 2 min, 95°C for 10 min and 40 cycles of [95°C for 15 sec, 60°C for 1 min]. The primers and probes for *18S* and *MMP-13* amplification were taken from from a previous publication (Zhang et al 2008) and are shown in Table 2.5.

Primer name	**Primer**	**Primer sequence**
MMP-13	Forward	5'-AAATTATGGAGGAGATGCCCATT-3'
	Reverse	5'-TCCTTGGAGTGGTCAAGACCTAA-3'
	Probe	5'-FAM-CTACAACTTGTTTCTTGTTGCTGCGCATGA-TAMRA-3'
18S	Forward	5'-CGAATGGCTCATTAAATCAGTTATGG-3'
	Reverse	5'-TATTAGCTCTAGAATTACCACAGTTATCC-3'
	Probe	5'-FAM-TCCTTTGGTCGCTCGCTCCTCTCCC-TAMRA-3'

Table 2.5 MMP-13 and *18S* TaqMan real time PCR primers and probes

SYBR® Green Real-Time qRT-PCR

SYBR® Green dyes bind to dsDNA. The intensity of the fluorescent signal is very little in solution since its intensity depends to the amount of dsDNA present

in the reaction. Therefore as dsDNA accumulates, the dye, when excited, emits a fluorescent signal proportional to the amount of dsDNA present.

Method:

PCR reactions were prepared by combining 3 µL cDNA with 4.8 µL SYBR® Advantage® qPCR Premix (Clontech Laboratories Inc, Mountain View, CA, USA), 0.2 µL ROX Reference Dye II, and 400 nM of each primer in a final volume of 10 µL. Cycling conditions were: 95°C for 10 min and 40 cycles of [95°C for 15 sec, 60°C for 1 min], standard dissociation curve. A dissociation curve analysis was performed at the end of the reaction to ensure amplification of one specific product. Final PCR products were also electrophoresed a 3% (w/v) agarose-TAE (x1) gel (section 2.4.6) to confirm the presence of a single product. Primers for *SOD2* amplification were taken from a previous publication (Scott et al 2010) and are shown in Table 2.6.

Primer name	**Primer**	**Primer sequence**
SOD2	Forward	5'-CTGGACAAACCTCAGCCCTA-3'
	Reverse	5'-TGATGGCTTCCAGCAACTC-3'

Table 2.6 SOD2 SYBR Green real-time PCR primers

TaqMan gene expression assays

TaqMan gene expression assays are made of a ready mix of primers and probe required for real-time PCR detection that is based on the Taqman Probe-based real-time RT-PCR system described above. The method and reaction conditions are the same as described previously in the Taqman Probe-based real-time RT-PCR section. *NLRX1* and *VISA* gene expression was assessed using this method (FAM reporter), and the product codes of the TaqMan assays (Applied Biosystems) used are "Hs00226360_m1 NLRX1" and "Hs_00325038_m1 VISA" for *NLRX1* and *VISA* respectively.

Gene expression analysis

For both TaqMan® probe-based and SYBR® Green qRT-PCR methods the relative quantification of gene expression was performed using the ABI PRISM

7900HT Sequence Detection System (Applied Biosystems). Target gene expression was normalised to the level of *18S* gene expression using the calculation $2^{-\Delta C}{}_T$, were ΔC_T represents C_T (target gene) – C_T (*18S*).

mtDNA deletions from single cells

HAC were screened for mitochondrial respiratory activity using the COX/SDH activity protocol as in section 2.6.2. Single cells were then isolated using laser capture microdissection (section 2.4.4), lysed and were screened for deletions in the major arc of the mtDNA. This experiment would be used to identify differences in the mtDNA of COX-positive and COX-negative cells and also differences between NOF and OA mtDNA.

Method:

Chondrocytes were extracted from cartilage as described in section 2.2.1 and total DNA isolated as in section 2.4.3. Real Time PCR was performed on DNA extracts and mtDNA standards (10^2-10^9 MTND1 and MTND4 molecules per µL) using primers and probes for MTND1 and MTND4, two mitochondrial encoded genes (Krishnan et al 2010). MTND1 was used as the control and MTND4 as the deletion marker as it is more commonly deleted in post-mitotic tissues (MITOMAP) ([NO STYLE for: Mitomap 2006]). Wildtype blood DNA was used for normalisation. A multiplex qPCR reaction was then performed using two different probes (VIC and FAM) for the two genes of interest. The amount of deleted DNA (MTND4) was normalised to MTND1 levels and the blood control (supplied by Dr Kim Krishnan) using the calculation $(1\text{-}2^{-\Delta C}{}_T)$ x 100%, where ΔC_T represents C_T (MTND4) – C_T (MTND1) -C_T (blood control, ΔC_T of MTND4 - MTND1). The primer and probe sequences are shown in Table 2.7 (Krishnan et al 2010).

Primer name	Primer	Primer sequence
L3485-ND1	Forward	5'- CCCTAAAACCCGCCACATCT -3'
H3532-ND1	Reverse	5'- GAGCGATGGTGAGAGCTAAGGT -3'
	Probe	5'-VIC- CCATCACCCTCTACATCACCGCCC -3'
L12087-ND4	Forward	5'- CCATTCTCCTCCTATCCCTCAAC -3'
H12170-ND4	Reverse	5'- CACAATCTGATGTTTTGGTTAAACTATATTT -3'
	Probe	5'-FAM- CCGACATCATTACCGGGTTTTCCTCTTG- 3'

Table 2.7 MTND1 and MTND4 primers and probes

mtDNA copy number

This experiment was performed in order to identify differences in the mtDNA copy number between NOF and OA hip cartilage and also compare it to the mtDNA copy number of OA knee cartilage and other joint tissues.

Single cells

Method:

Single chondrocytes were isolated as described in 2.2. Fifty cells were pooled and then lysed with 15µL lysis buffer (0.5% Tween 20, 50mM Tris-HCl pH8.5, 200µg/ml Proteinase K) to extract the DNA. Real Time PCR was performed on DNA extracts and mtDNA standards (10^2-10^9 MTND1 molecules per µL) using primers and probes for MTND1 (Krishnan et al 2010). The copy number per sample was then calculated according to the standard curve derived from the amplification of the standards (10^2-10^9 MTND1 molecules per µL).

Whole tissue

Method:

DNA from OA and NOF cartilage homogenates was isolated as described previously in section 2.4.1. MTND1 was used as the mitochondrial marker and β-2-microglobulin (B2M) as a nuclear reference gene (Krishnan et al 2010). Primers used for the preparation of B2M templates (used to prepare the standards) and standards and SYBR Green real-time PCR amplification are shown in Table 2.8.

Primer name	Primer	Primer sequence
B2M (standards)	Forward	5'- CGCAATCTCCAGTGACAGAA -3'
	Reverse	5'- GCAGAATAGGCTGCTGTTCC -3'
B2M (real-time PCR)	Forward	5'- CACTGAAAAAGATGAGTATGCC -3'
	Reverse	5'- AACATTCCCTGACAATCCC -3'

Table 2.8 B2M primers for template and standards preparation and real-time PCR amplification

Template and standards preparation

Standard curves were prepared for each primer set to ensure the efficiency of each reaction and to allow accurate quantification.

Method:

PCR templates covering the region to be amplified by qPCR were generated using standard PCR techniques and gel extracted and purified. DNA was then quantified using the NanoDrop 1000 spectrophotometer and the number of DNA copies was calculated using the following equation, where C is DNA concentration in g/L, L is the amplicon length in bp and A is Avogadro's number.

$$\textbf{\textit{Copy number} = [C \div (L \times 2 \times 330)] \times A}$$

Templates were serially diluted 1/10 with H_2O to generate standard curves with 10^9 to 10^2 copies of MTND1 and B2M.

2.4.9 Purification of PCR products

QIAquick Gel purification kit

Method:

SOD2 PCR products obtained were purified using the QIAquick® Gel extraction Kit according to manufacturer's instructions. PCR products were electrophoresed a 1% (w/v) agarose-TAE (x1) gel (section 2.4.6) and the required amplicon was excised. The gel was dissolved in Buffer QG and the PCR products extracted and purified using QIAquick® spin columns prior to elution in 30µL dH_2O.

2.4.10 Cloning of PCR products

Ligation

Method:

Purified PCR products were cloned using the appropriate vector. For the products from primers 1-3 the pGL3 basic vector was used. In brief, purified DNA and pGL3 basic vector were digested in separate reactions. 30ng DNA was combined with 10U (1µL) of *Bgl*II restriction enzyme and 10U (1µL) of *Hind*III restriction enzyme, 6µL 10x restriction enzyme buffer M and dH_2O in a final volume of 60µL. 5µL pGL3 basic vector (5µg/µL) was combined with 10U (1µL) of *Bgl*II restriction enzyme and 10U (1µL) of *Hind*III restriction enzyme, 6µL 10x restriction enzyme buffer M and dH_2O in a final volume of 60µL. The two reactions mixtures were incubated for 3 hours at 37°C and then heat inactivated at 68°C for 15 min. Then ligation reactions were prepared by combining 10ng digested vector, 4µL 5X Ligase Buffer, 1U T4 DNA Ligase (Invitrogen, Paisley, UK), 5µL digested DNA and dH_2O in a final volume of 20µL. Ligations were incubated at room temperature for 16 hours.

For the PCR products from primer pair 11, the TOPO TA Cloning® pCR®4-TOPO® vector was used according to manufacturer's instructions.

Transformation

Method:

For pairs 1-3, 5 µL of the ligation reaction was added to 50 µL Mach1™-T1® chemically competent *E. coli*. Reactions were incubated on ice for 30 min prior to transformation by heat-shock at 42°C for 2 min followed by immediate removal to ice. Using sterile technique, a 250 µL aliquot of S.O.C. medium (Invitrogen, Paisley, UK), a nutrient-rich bacterial growth medium, was added to each vial and cultures were shaken (220 rpm) at 37°C for 1 hour. A 100µL aliquot of each transformation was spread onto a pre-warmed agar plate containing 100 µg/mL Ampicillin. Plates were incubated at 37°C for 16 hours in order for colonies to develop.

For pair 11, 5µL of the ligation reaction was added to 50 µL One shot® DH5α™chemically competent *E. coli*. The same protocol was performed as with pairs 1-3. A 100µL aliquot of each transformation was spread onto a pre-warmed agar plate containing 100µg/mL ampicillin as well 40µg/mL X-GAL in dimethylformamide (DMF) and 100mM IPTG spread on each plate. Plates were incubated at 37°C for 16 hours in order for colonies to develop.

Preparation of Overnight Cultures

Method:

White colonies were selected and added to 5 mL LB containing 100 µg/mL Ampicillin. Cultures were shaken at 220 rpm and 37°C for 16 hours in an orbital shaker.

Quick Minipreps of Plasmid DNA

Method:

A 1.5 mL aliquot of a bacterial culture was transferred to an Eppendorf and centrifuged for 15 sec at 12000 x *g*. The supernatant was discarded and cells resuspended in 100 µL Buffer P1 (Qiagen) by vortexing. Subsequently, 200 µL Buffer P2 (Qiagen) was added to cells and mixed thoroughly by inverting 6 times. A 150 µL aliquot of Buffer P3 (Qiagen) was then added and mixed immediately by inverting 6 times. Lysates were centrifuged for 3 min at 12000 x *g* and the supernatant removed to a new Eppendorf containing 1 mL 100% (v/v) ethanol. Samples were vortexed for 10-15 sec to mix thoroughly and centrifuged for 10 min at 12000 x *g*. All ethanol was removed and pellets allowed to air-dry before resuspension in 50 µL dH_2O.

Restriction endonuclease digestion

Method:

A 2µL aliquot of each miniprep was restriction endonuclease-digested, in order to identify any DNA insert, using the appropriate restriction enzymes. Plasmid DNA was combined with 2.5 U of the appropriate restriction enzyme, 1.5 µL 10x of the appropriate buffer and 11 µL dH_2O and incubated at 37°C for 1 hour.

10µL of each digest was electrophoresed on a 1% (w/v) agarose-TAE (x1) gel (section 2.4.6) to determine if it contained an insert of the correct size compared to 1kb DNA ladder (Bioline, London, UK). 20µL aliquots of the isolated DNA were sent for DNA sequencing using the appropriate sequencing primer (generally SP6, GATTTAGGTGACACTATAG). Sequencing results were analysed using the CLC sequence Viewer software.

2.5 Protein isolation and analysis

Protein levels were assessed using western blotting and fluorescent immunocytochemistry and compared to the different conditions used in the experiments.

2.5.1 Preparation of Cell Lysates

Reagents:

Lysis buffer containing 50 mM Tris-HCl (pH 7.5), 10% (v/v) glycerol, 1 mM EDTA (pH 8), 1 mM EGTA, 1 mM Na_3VO_4, 5 mM NaF, 10 mM β glycerol phosphate, 5 mM $Na_4P_2O_7$, 1% (v/v) Triton X-100, 1 µM microcystin-LF and 1x Complete -EDTA free mini protease inhibitor cocktail tablet (Roche Diagnostics, Burgess Hill, UK)

Method:

Total protein was isolated from cells in a 6-well plate (approximately 2.5 x 10^4 cells/cm^2) (Scott et al 2010). After the experimental period, culture medium was removed and cells were washed with ice-cold PBS. Cells were scraped into ice-cold lysis buffer added to cells at a volume of 100 µL/well. Lysates were transferred to a 1.5ml Eppendorf, mixed for 20 min at 4°C using a rotary mixer and centrifuged for 3 min at 10,000 x *g* and 4°C. Supernatants were removed and stored at -80°C prior to use.

2.5.2 Bradford protein assay

Method:

A 2mg/ml stock bovine serum albumin (BSA) protein standard solution (Pierce & Warriner, Chester, UK) was diluted to 0.4mg/ml BSA in dH_2O. A range of standards from 0-4mg/ml, with 0.4mg/ml increment increases, was added to a flat-bottomed 96-well plate. Cell lysates and equal qualities of cell lysis buffer to act as blanks, were added to the 96-well plate. Bradford assay reagent was then added to all the wells according to the manufacturer's instructions. The samples were then gently mixed upon a flat-bed vortex, left to stand for 5 minutes and the absorbance read at 595nm using a Tecan Sunrise microplate absorbance reader and protein levels measured based on the standard curve (Scott et al 2010).

2.5.3 Western blotting

Reagents:

- Laemmli sample buffer containing 0.1 M Tris-HCl (pH 7.5), 0.35 M SDS, 20% (v/v) glycerol, 0.01% (w/v) bromophenol blue and 5% (v/v) β-mercaptoethanol.
- Transfer buffer containing 20 mM Tris-HCl (pH 7.5), 0.6 M glycine and 20% (v/v) methanol.
- TBS-Tween (TBS-T) containing 150 mM NaCl, 10 mM Tris-HCl (pH 7.5) and 0.1% (v/v) Tween-20.
- 4% (w/v) paraformaldehyde in PBS

Method:

Cell lysates were thawed on ice and combined with Laemmli sample buffer in a 5:1 ratio. Lysates were heated to 100°C for 5 min, cooled on ice and electrophoresed on appropriate 10 or 12.5% SDS-polyacrylamide gels at 180V for approximately 1 hour. Proteins were transferred to polyvinylidene fluoride (PVDF) membrane using a Scie-Plas V20-SDB 20 x 20cm semi-dry blotter for 1.5 hours at $1mA/cm^2$ in transfer buffer. Membranes were incubated in a blocking buffer containing 5% (w/v) non-fat dry milk powder in TBS-T for 1 hour. Membranes were subsequently washed 3 times in TBS-T prior to incubation with primary antibody solution overnight at 4°C with gentle agitation. Primary antibody solutions were prepared according to manufacturer's instructions.

Following incubation, membranes were washed for 3 x 5 min in TBS-T and then incubated with a horseradish peroxidase (HRP)-conjugated secondary antibody for 1 hour at room temperature. Secondary antibodies were diluted in a solution of 5% (w/v) milk powder in TBS-T. The membranes were washed 3 x 5 min in TBS-T before visualisation on high-speed X-ray film (Sigma-Aldrich) using Amersham ECL detection reagents (GE healthcare, Little Chalfont, UK) according to manufacturer's instructions.

2.5.4 Immunocytochemistry

SOD2

Reagents:

- PBG-Triton solution containing 0.2% (v/v) fish skin gelatine, 0.5% (w/v) BSA and 0.5% (v/v) Triton-X-100 in PBS.
- PBG-Saponin solution containing 0.2% (v/v) fish skin gelatine, 0.5% (w/v) BSA and 0.5% (v/v) Saponin in PBS.

Method:

Cell monolayers were washed twice in PBS for 5 min and then fixed for 10 min in ice cold 4% (w/v) paraformaldehyde in PBS at room temperature. Cells were permebilised and blocked with PBG-Saponin solution for 10 min or PBG- Triton solution for 45 mins at room temperature. Cells were incubated with anti-human SOD2 primary antibody at a final concentration of 1µg/ml for 45mins. Cells were then incubated with a secondary antibody (Alexa 488) diluted in 1:1000 (v/v). Cells were washed twice in between the antibody incubations with PBG-Saponin or PBG-Triton. Slides were washed twice in PBS and mounted in Vectashield with DAPI. Cells were visualised using confocal and fluorescent microscopy and their fluorescence was analysed as described in section 2.10.

2.6 Cytochrome C oxidase/ Succinate Dehydrogenase (COX/SDH) reaction

COX/SDH sequential histochemistry reveals respiratory-deficient cells harbouring mtDNA mutations. An active COX produces a brown reaction

product whereas when COX is not active (possibly due to mtDNA mutations) cells can react with (nuclear-encoded) SDH and produce a blue product (Krishnan et al 2010).

Reagents:

- Cytochrome *c* oxidase (COX) incubation medium containing 100 µM cytochrome *c,* 4 mM diaminobenzidine tetrahydrochloride (DAB) in 0.2 M phosphate buffer (pH 7.0).
- Succinate dehydrogenase (SDH) incubation medium containing 130 mM sodium succinate, 200 µM phenazine methosulphate, 1 mM sodium azide and 1.5 mM nitroblue tetrazolium in 0.2 M phosphate buffer (pH 7.0).

2.6.1 Cartilage Sections

Cartilage chips were snap frozen in super-cooled isopentane prior to sectioning. Samples were mounted in Cryo-M-Bed embedding compound and 12 µm serial sections were prepared through the full thickness of each sample using a HM 560 Cryo-Star cryostat (MICROM International, Welwyn Garden City, UK). Sections were then mounted onto SuperFrost® Plus Gold slides and allowed to air-dry for 1-2 hours.

Sequential histochemical reactions for COX and SDH were performed on 12µm cartilage sections. Attempts at optimal reactions were determined by incubating cartilage sections at 37°C for 40, 50, 60, 70, 80, 90 or 120 min with either COX incubation medium or SDH incubation medium. Sections were washed for 3 x 5 min in PBS and subsequently dehydrated in a graded ethanol series (2x 99%, 95%, 70% and 50% (v/v)), cleared in 2 changes of Histoclear II (National Diagnostics, GA, USA) and mounted in DPX (Distrene-80, Plasticiser Xylene)(Sigma Aldrich, Poole, UK).

COX or SDH activity could not be detected in cartilage sections at any time point.

2.6.2 Human Articular Chondrocytes

HAC were enzymatically extracted from the macroscopically normal cartilage as described previously in section 2.2.1.

Cultured HAC

HAC were seeded at a density of 2 x 10^4 per well of a chamberslide and left to adhere for 24 hours. After 24 hours media was removed and cells washed twice with PBS. All PBS was removed and cell monolayers allowed to air-dry for 30 min before the COX-SDH reaction. This procedure lysed the cells and they became fixed to the chamberslide. Optimal incubation times were determined as with the cartilage sections. Optimal COX reactivity was achieved by incubating for 90 min, 37°C and SDH reactivity when incubating for 50min, 37°C although cell morphology was altered after the COX reaction. Cells, which had exhibited COX activity, produced a brown reaction product whereas those deficient in COX produced a blue product. Cells were then visualized under a brightfield microscope.

Freshly extracted HAC

Freshly extracted cells were cytospun at a density of 1x10^4 cells per slide and washed twice in PBS. Optimal reaction times were determined by incubating HAC at 37°C for 60, 70, 80, 90 min with COX incubation medium and for 35, 45, 55 and 65 mins with SDH incubation medium. Optimum reactivity was achieved when incubating for 60 minutes at 37°C with COX medium and 65 minutes at 37°C with SDH medium. Cells were then visualized under a brightfield microscope and COX-positive and COX-negative cells were microdissected as described in section 2.4.4. Then cells were lysed and analysed for mtDNA deletions as described in section 2.4.8.

2.7 Reactive oxygen species analysis

2.7.1 Mitosox staining

Mitosox-Red is a cationic dye that is rapidly oxidized by $O_2^{\cdot-}$ but not by other reactive oxygen species (ROS) and reactive nitrogen species (RNS). The

oxidized product is highly fluorescent upon binding to nucleic acid. Due its lipophilic and cationic nature it is specifically attracted in the mitochondria and therefore oxidised by $O_2^{\cdot-}$ specifically in the mitochondria. Mitosox-Red was used to assess the $O_2^{\cdot-}$ levels in chondrocytes mitochondria after SOD2 depletion.

Reagents:

- 5mM Mitosox Red in DMSO

Microscopy

Method:

Cells were seeded into chamberslides at a density of 2 x 10^4 cells/ cm^2. After 24 hours cells were either transfected with targeted siRNA against SOD2 or serum starved for 16 hours overnight and stained the next day. Cell monolayers were stained with different concentrations of mitosox-red (1μM, 2.5μM and 5μM) in serum free media for 15 min at 37°C. Cell monolayers were washed twice in PBS for 5 min and then fixed in 4% (w/v) cold preparation of paraformaldehyde in PBS for 10 min at room temperature. Slides were washed two times in PBS and mounted in Vectashield with DAPI. Cells were visualised using confocal and fluorescent microscopy.

Flow cytometry

Method:

Cells were serum starved 16 hours before experimentation, washed with Trypsin-EDTA for 5 min, resuspended in serum free media and split into 1.5ml Eppendorf tubes at a density of 1x10^6cells/ml. Cells were spun at 250x *g* in between stainings and washes. Cells were then stained with 1μM and 5μM concentrations of mitosox-red in serum free media for 15 min at 37°C, washed twice in PBS and then fluorescence was assessed using flow cytometry (FL-3 channel, red) as described in section 2.11.

2.7.2 Dihydrorhodamine 123 (DHR-123)

DHR-123 is an uncharged and nonfluorescent ROS indicator that can passively diffuse across membranes where it is oxidized by H_2O_2 and to cationic rhodamine 123, which localizes in the mitochondria and exhibits green fluorescence.

Reagents:

- 5mM DHR-123 in DMSO

Method:

Cells were seeded into chamberslides at a density of 2 x 10^4 cells/ cm^2. After 24 hours cells were serum starved for 16 hours overnight and stained the next day. Cell monolayers were stained with 75µM DHR-123 in serum free media for 30 min at 37°C. For live cell imaging, cells were washed twice with warm media and visualised immediately. For analysis of fixed cells, cell monolayers were washed twice in PBS for 5 min and then fixed in 4% (w/v) cold preparation of paraformaldehyde in PBS for 10 min at room temperature. Slides were washed two times in PBS and mounted in Vectashield with DAPI. Cells were visualised using confocal and fluorescent microscopy.

2.7.3 Reactive oxygen species stimulation and inhibition

ROS production was stimulated or inhibited in order to assess the efficiency of the Mitosox-Red dye and its responsiveness to changes in ROS levels within cells.

Method:

Cells were seeded into chamberslides at a density of 3 x 10^4 cells/ cm^2. After 24 hours cells were serum starved for 16 hours overnight. Cells were then stimulated with 3 different ROS inducers and one ROS scavenger in serum free media and then stained with 2.5µM Mitosox Red. The concentrations and times of stimulation are shown in Table 2.9. Cell monolayers were washed twice in PBS for 5 min and then fixed in a cold preparation of 4% (w/v) paraformaldehyde in PBS for 10 min at room temperature. Slides were washed

two times in PBS and mounted in Vectashield with DAPI. Cells were visualised using confocal microscopy and their fluorescence analysed as described in section 2.10.

Reagents	Inducer/ Inhibitor	Mode of action	Final concentration	Incubation time
Paraquat	Inducer	Paraquat redox reaction	100μM and 200 μM	1 hour
Antimycin A	Inducer	Complex III inhibition	10μM and 100 μM	1 hour
Rotenone	Inducer	Complex I inhibition	2.5 μM and 10 μM	24 hour
N-Acetyl-L-Cysteine	Inhibitor	Increases levels of ROS scavengers	5mM and 10mM	24 hour

Table 2.9 ROS inducers and inhibitors

2.7.4 Mitochondria superoxide and SOD2 dual staining

This technique was used to allow simultaneous visualization of Mitosox-Red and SOD2 protein levels in chondrocytes where SOD2 expression was depleted using RNAi to mimic the downregulation of SOD2 in OA compared to NOF (Scott et al 2010; Ruiz-Romero et al 2009; Aigner et al 2006).

Reagents:

- PBG-Saponin and PBG-Triton solutions
- Mitosox Red 5mM in DMSO.

Microscopy

Method:

Mitosox Red has been reported to be non-fixable and can leak into the nucleus and the cytoplasm after triton-mediated permebilisation (Robinson et al 2008), therefore a dual Mitosox-SOD2 staining protocol had to be established that retains Mitosox-Red in the mitochondrial after fixation, in order to be able to compare $O_2^{\cdot-}$ and SOD2 levels simultaneously. The criteria for selecting the

optimum time were sufficient antibody staining as well as clear and specific Mitosox-Red staining within the same cells.

Cells were seeded into chamberslides at a density of 2 x 10^4 cells/ cm^2. After 24 hours, cells were serum starved for 16 hours overnight and stained the next day. Cell monolayers were washed twice in PBS for 5 min and then cells were stained with 2.5μM Mitosox-red in serum free media for 15 min at 37°C.

Cell monolayers were washed twice in PBS for 5 min and then fixed in a cold preparation of 4% (w/v) paraformaldehyde in PBS for 10 min at room temperature. Optimal permebilisation and blocking times for PBG-Saponin and Triton-X buffer were determined by incubating the cells with PBG-Saponin or Triton at room temperature for 5, 10, 15, 45 min. Optimal permeabilisation was achieved and cells were permebilised and blocked with PBG-Triton or PBG-Saponin solution for 45 min and 10 min respectively at room temperature.

Optimal incubation times for primary and secondary antibodies diluted in PBG-Saponin or Triton were determined by incubating the cells for 30, 45 and 60 min. For SOD2 antibody staining, a final SOD2 antibody concentration of 1μg/ml was used. Secondary antibody (Alexa 488) was diluted in 1:1000 (v/v). Cells were washed twice in between the antibody incubations with permeabilising buffer. Optimal antibody incubation times in Saponin buffer were achieved at 45 min for each antibody (primary and secondary). Triton permeabilisation and antibody incubation resulted in non-specific mitochondrial staining. Slides were washed twice in PBS and mounted in Vectashield with DAPI. Cells were visualised using confocal and fluorescent microscopy and their fluorescence was analysed as described in section 2.10. Detailed results of the antibody optimisation are shown in section 3.4.4.

Flow cytometry

Method:

Cells were serum starved 16 hours before experimentation, washed with Trypsin-EDTA for 5 min at room temperature, resuspended in serum free media and split into 1.5mL Eppendorf tubes at a density of 1x10^6cells/mL. The same

optimised staining procedure was followed as described before in this section. Cells spun at 250x *g* in between stainings and washes. Fluorescence was assessed using flow cytometry as described in section 2.11, and confocal microscopy on cells spun onto a microscope slide using a cytospin and mounted in Vectashield with DAPI. Fluorescence of cytospun cells was analysed as described in section 2.10.

2.8 Lipid peroxidation analysis

Cell and mitochondrial lipid peroxidation is a reaction that takes place due to high levels of ROS in cells. In order to assess the levels of lipid peroxidation in OA and NOF cartilage as well as to establish the role of SOD2 depletion lipid peroxidation in SW1353 cells, the thiobarbituric acid reactive substances (TBARS) assay was performed. This assay quantifies the levels of malondialdehyde (MDA) in tissues or cells. MDA is a stable byproduct of lipid peroxidation and under acidic conditions and high temperatures (90-100°C) it forms adducts with Thiobarbituric acid (TBA) that can be measured spectrophotometrically. Other assays that measure 4-HNE levels are also available however they were not used, as the effect of 4-HNE on lipid peroxidation is weaker than the effect of MDA (Valko et al 2007; Siems et al 1995). Therefore, the TBARS assay was chosen as the most appropriate method for measuring lipid peroxidation in cartilage and cells.

Reagents:

- Supplied by manufacturer
    - Colour reagent (contains TBA, it is acidic and is used in the detection of MDA as it changes colour according to MDA concentration)
        - Thiobarbituric acid (TBA)
        - TBA acetic acid
        - TBA sodium hydroxide
    - TBA MDA standard
    - TBA SDS solution

- RIPA buffer (50mM Tris-HCl pH 7.0, 150mM NaCl, 1% (v/v) Triton-X 100, 0.5% (v/v) sodium deoxycholate, 0.1% (v/v) SDS, 1mM EDTA, 1x Complete -EDTA free mini protease inhibitor cocktail tablet)

2.8.1 TBARS assay on tissue homogenates

Method:

The tissue was homogenized and the assay was performed following the manufacturer's instructions. In brief, 250µl of RIPA buffer was added to the cartilage in a 1.5ml Eppendorf tube. The samples were sonicated for 3x5 seconds over ice. The tubes were centrifuged at 1600x *g* for 10mins at 4°C. Standards of 0µM, 0.625µM, 1.25µM, 2.5µM, 5µM, 10µM, 25µM, and 50µM MDA concentration were also prepared according to manufacturer's protocol. 100µl of the supernatant or each standard were then transferred into a 15ml falcon tubes and 100µl of SDS was added to each sample and standard. 4ml of the colour reagent were added into each sample and the tubes were added to boiling water for 1 hour. Samples were incubated on ice for 10mins and then centrifuged at 1600x *g* for 10 mins at 4°C. 150µl (in triplicate) were loaded from each vial to a 96-well plate. Absorbance was measured at 535nm and MDA concentration was determined using the standard curve.

Assay optimisation

In order to determine the optimum quantity of cartilage homogenate required to obtain readings within the standard curve, 10mg, 50mg and 100mg of cartilage were assessed for MDA levels as described above. As shown in section 3.4.7, 50mg of cartilage showed the highest MDA concentration, and it was within the lower range of the standard curve. However, the presence of cartilage in the supernatant probably could have inhibited the reactions. Therefore, 50mg were selected as the optimum amount of cartilage to be assayed however, extra care was taken in order to avoid the presence of any cartilage in the supernatant.

MDA levels in OA compared to NOF

11 OA and 11 NOF cartilage samples (50mg each) were assayed as described above. Absorbance was measured at 535nm and MDA concentration was

determined using the standard curve. Statistical significance of the difference in MDA levels between NOF and OA cartilage samples was evaluated using the Mann-Whitney U test.

2.8.2 TBARS assay on SW1353 cells treated with targeted siRNA against SOD2

Method:

SW1353 cells were seeded in 75cm^2 flasks at a density of 1.5 x 10^6 cells/flask. After 24 hours cells were transfected with 100nM of targeted siRNA against SOD2 or with a non-targeting control as described in section 2.3.2. Cells were then trypsinised, washed in PBS, counted and 4 x 10^6 cells were re-suspended in 200µl of PBS. Cells were then sonicated for 3x5 seconds over ice. The whole homogenate was used in the assay and PBS was used as a sample blank. The assay was then performed as described above (after and including the addition of 100µl of SDS). Absorbance was measured at 535nm and MDA concentration was determined using the standard curve. Statistical significance of the fold difference in MDA levels between cells treated with siRNA against SOD2 and controls was evaluated using the Mann-Whitney U test.

2.9 Mitochondrial bioenergetics

2.9.1 Mitochondrial respiration

Respirometry was used to evaluate differences in mitochondrial respiratory activity between NOF and OA chondrocytes and also the effect of SOD2 depletion on mitochondrial respiration in chondrocytes.

Reagents

- Galactose containing media [500ml DMEM (no glucose, Gibco catalog no. 11966.25), 10% Fetal Bovine Serum, 450mg galactose, 1mM sodium pyruvate, 1ml uridine (25mg/ml stock solution), 5ml non essential amino acids]
- MRC inhibitors
    - 5mM oligomycin (ATP synthase inhibitor)

- 10mM Carbonyl cyanide-*p*-trifluoromethoxyphenylhydrazone (FCCP, Protonophore, uncoupler)
- 10mM Rotenone (Complex I inhibitor)
- 25mM Antimycin A (Complex III inhibitor)

Oroboros Oxygraph- 2K

The Oroboros Oxygraph-2K respirometer is based on the Clark electrode system where the cells are placed in a closed chamber and their oxygen consumption is assessed using the decay of oxygen concentration in the chamber.

Method:

Primary human chondrocytes were extracted from NOF and OA femoral heads as in section 2.2.1. Cells were plated in 75cm^2 flasks and cultured for 96 hours. Cells were then washed with Trypsin-EDTA for 5 mins and resuspended in galactose containing media [500ml DMEM (no glucose), 10% Fetal Bovine Serum, 450mg galactose, 1mM sodium pyruvate, 1ml uridine (25mg/ml stock solution), 5ml non essential amino acids]. Chambers were washed sequentially with 70% and 100% (v/v) ethanol and then with water. 2.5ml galactose media was then added into each chamber and the respirometer calibrated according to manufacturer's protocol. In brief oxygen levels are measured prior to the addition of cells in the chamber at 37^{o}C and this was set as the background oxygen consumption in the software and was substracted from the oxygen consumption values calculated. Cells were then added in each chamber (1x10^6/chamber) and then counted using a haemocytometer to normalise respiration values. 2.5μM oligomycin, a titration of 0.5μM FCCP (until peaks no longer increase), 0.5μM Rotenone and 2.5μM Antimycin A were added in the chamber and the oxygen consumption/flow recorded. The oxygen levels in the chamber were checked in order to remain higher than 150nmol/ml. Oxygen flow values after each treatment were analysed further as described later on in this section.

Seahorse XF-24

Seahorse XF-24 is a multi-well plate based respirometry system that measures oxygen consumption and pH levels by lowering a piston-like probe into each well to amplify the changes in oxygen concentration and pH.

Method:

Primary human chondrocytes were extracted from NOF and OA femoral heads as in section 2.2.1. Cells were plated in Seahorse XF-24 plates at a density of $1.5x10^5$ cells/well and cultured for 96 hours. 4 wells were left empty for calibration purposes according to the manufacturer's instructions. A Seahorse cartridge was rehydrated 24 hours before the experiment. Cells were washed before the experiment in seahorse media and incubated for 1 hour in Seahorse media containing 5% Fetal Bovine serum and 1mM/10mM pyruvate in 0% (v/v) CO_2 incubator for 1 hour. The machine was then calibrated according to manufacturer's instructions. In brief, the fluorescent intensities within each well were normalized to the oxygen levels of each well before the addition of cells at 37^oC. A special calibration plate containing calibration media was used. The system assigns 10000 fluorescence units to ambient oxygen concentration and pH during its internal calibration procedure by setting the intensity of the light emitting diode used to excite the sensor. The cells were treated sequentially with 2.5µM oligomycin, 1.5µM FCCP, 0.5µM Rotenone and 2.5µM Antimycin A. Oxygen flow values and pH changes were calculated after every treatment. Oxygen flow values were used to assess mitochondrial respiratory activity and pH levels were used to assess glycolytic activity. Analysis of oxygen flow values was performed as outlined later on this section.

Effect of SOD2 depletion on mitochondrial respiration

In order to assess the effect of SOD2 depletion on mitochondrial respiration in HAC, cells were plated in the Seahorse plates at a density of $3x10^4$ cells/well and transfected as described in section 2.3.2. Respiration was then assessed as described above and respiratory activity parameters were calculated to determine the effect of SOD2 depletion on different parameters of the mitochondrial respiration.

The efficiency of the siRNA transfection was assessed by measuring *SOD2* gene expression. RNA was isolated, reverse transcribed and amplified by SYBR Green real-time PCR amplification as described in 2.4.8.

Respiratory activity parameters

The following respiratory activity parameters were calculated using the oxygen flow values from the Oroboros 2K or the Seahorse XF-24 respirometers. SRC (spare respiratory capacity) is a ratio calculating how close to full capacity the MRC is functioning at. SRC is also referred to the difference between the uncoupled and basal respiration however by calculating as a ratio enables direct comparison between different samples as it normalizes for cell number. RCR (cell respiratory control ratio) is a measure of non-phosphorylating respiration and general mitochondrial function taking into account the proton leak and SRC. Proton leak is a measure of non-phosphorylating respiration, i.e. respiration that is not coupled to ATP production. ATP production is a measure of ATP generating respiration, i.e. respiration that is coupled to ATP production. The respiratory parameters were calculated as followed (Non-mitochondrial respiration (NMR) was subtracted from all the values) and shown graphically in Figure 2.1:

Spare respiratory capacity (SRC ratio) = FCCP/Resting

Cell Respiratory control ratio (RCR) =(FCCP-Oligomycin)/Resting)

Proton leak = Oligomycin insensitive respiration

ATP production= Oligomycin sensitive respiration= Resting-Oligomycin

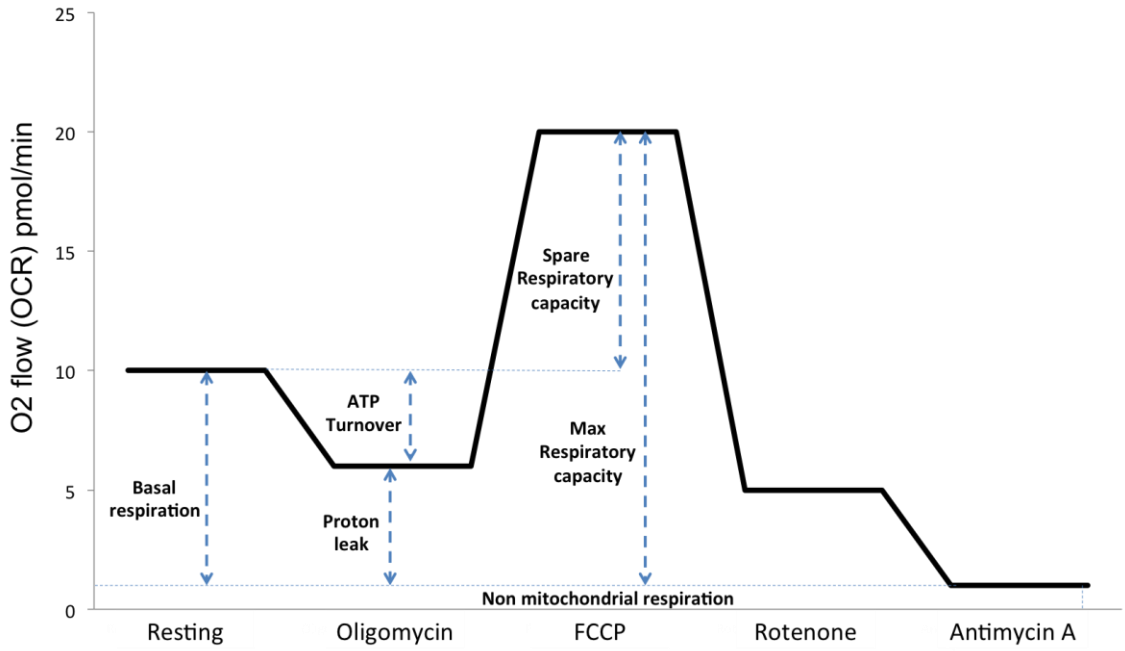

Figure 2.1 Respiratory parameters determined by mitochondrial respiration analysis

2.9.2 Mitochondrial membrane potential

These techniques were used to identify the effect of SOD2 depletion on Δψm.

JC-1

JC-1 in cells with normal Δψm forms J-aggregates, which are complexes with red fluorescence. In cells with depolarized mitochondria, JC-1 remains in its monomeric form that shows only green fluorescence.

Method:

Adherent cells were treated with 2μM FCCP (depolarisation) or 0.01% DMSO control for 10mins to alter the Δψm in order to be able to assess the dye. Cells were then treated with 50nM JC-1 for 15mins to assess the colour changes in response to mitochondrial depolarisation (more green, less red). Fluorescence was assessed with live cell confocal microscopy using the 510/527nm and 585/590nm (excitation/emission) channels.

Tetramethyl Rhodamine Methyl Ester (TMRM)

TMRM is a cationic probe that is selectively localized in the mitochondrial matrix due to the presence of a net negative charge caused by the proton gradient. Any variations in the Δψm change the intensity but not the spectra of the probe.

Method:

Adherent cells were stained with 10nM TMRM (non-quench mode). In order to estimate higher or lower Δψm, the ratio of the basal TMRM+ levels against the non-mitochondrial fluorescence (after complete mitochondrial depolarisaton by FCCP in the presence of oligomycin) was calculated. These values can only indicate differences in membrane potential but exact values cannot be calculated using this method.

2.10 Image analysis

Method:

The fluorescence detected and shown in the images was analysed using ImageJ analysis software (Wayne Rasband, NIH, USA). Individual cells were selected and the average amount of fluorescent staining present in the cells (per area) calculated. Average background levels of the stain were also measured and deducted from the cell staining values. Net values were analysed as in section 2.12.

2.11 Flow cytometric analysis

Method:

All flow cytometric analysis was performed using BD PharMingen FACScan and CellQuest software. Threshold, FSC and SSC parameters were set using unlabelled controls. Compensation was set prior to acquisition using single stained cells and ensuring that the positively stained population was aligned horizontally or vertically with the negative population on the relevant fluorescent channel dot plots. The maximum fluorescence intensities of negative and positive populations were measured in different channels. Data was analysed

using FlowJo v8.7.1 software (Tree Star, Oregon, US). Raw fluorescence values were extracted from the software and analysed as in section 2.12.

2.12 Statistical analysis

The Pearson correlation coefficient was used to determine the correlation and regression values of the SOD2-Mitosox dual staining readings.

Relative RNA levels were normalized against basal levels of housekeeping genes and then plotted as the fold induction of target gene expression over control levels. Similarly, fold change of differences between NOF and OA values and between values from siRNA treated cells and their controls were determined in the same way.

Values were given as mean ± standard error of the mean (SEM).

The Student's t-test (unpaired) and the non-parametric Mann- Whitney U test were performed between sample groups to determine any significant differences. Levels of statistical significance are shown as *$p \leq 0.05$, **$p \leq 0.01$ and ***$p \leq 0.001$.

Chapter 3. ROS and oxidative damage due to SOD2 depletion in chondrocytes and cartilage

3.1 Hypothesis

SOD2 downregulation causes an increase in the mitochondrial $O_2^{\cdot-}$ levels. This contributes to an increase in lipid peroxidation and mtDNA damage in chondrocytes and cartilage.

3.2 Introduction

Reactive oxygen species (ROS) and specifically $O_2^{\cdot-}$ are mainly produced as by products of OXPHOS in the MRC. The major sites of $O_2^{\cdot-}$ production are Complex I and Complex III (Turrens, & Boveris 1980; Cadenas et al 1977). Complex II has also been reported as a site of $O_2^{\cdot-}$ production however its contribution to the overall ROS levels is minor (Zhang et al 1998). ROS can act as signalling molecules however when at high levels they can cause oxidative damage in the form of DNA damage (base modifications, single and double strand breaks and DNA-protein crosslinking), protein and lipid oxidation (Dizdaroglu et al 2002; Cooke et al 2003; Kokoszka et al 2001; Fedtke et al 1990).

There are different mechanisms in which ROS can cause DNA damage. The hydroxyl radical ($^{\bullet}OH$) can react with the DNA by reacting with double bonds of DNA bases, e.g. by reacting with the C5-C6 double bond of pyrimidines to form C5-OH and C6-OH adduct radicals (Figure 1.6) thus leading to base modifications and giving them redox properties (Cooke et al 2003; Steenken 1987). Other reactions of base radicals include the addition to an aromatic amino acid of proteins leading to DNA-protein crosslinking (Dizdaroglu et al 2002). Also ROS can react with DNA by the mechanism of abstraction of an H atom leading to DNA strand breaks and altered sugars (Dizdaroglu et al 2002; Beesk et al 1979).

Lipid peroxidation (Figure 1.7) is a process were ROS damage lipid cell and mitochondrial membranes by attacking polyunsaturated fatty acid residues of

phospholipids on membranes, thus forming unstable peroxyl radicals (ROO•). The process is initiated by the reaction of unsaturated lipids with ROS such as the •OH and hydroperoxyl (HO_2) radicals producing unstable lipid radicals. These radicals react with oxygen to produce the unstable lipid peroxyl radical. The lipid peroxyl radical then reacts with unsaturated lipids to produce an unstable lipid peroxide and then malondialdehyde (MDA), a stable lipid peroxide. Although, MDA is a more stable product of the lipid peroxidation process, it has been shown to have mutagenic and carcinogenic properties thus causing membrane and DNA damage (Kokoszka et al 2001; Fedtke et al 1990; Wang et al 1996).

The cell houses defenses against ROS such as the superoxide dismutase family (SOD1, 2, 3), catalase and glutathione peroxidase (Zelko et al 2002). SOD2, or MnSOD, is localized in the mitochondria and, like the other SODs spontaneously dismutases $O_2^{\cdot-}$ to H_2O_2. The rate of dismutation by all three superoxide dismutases is approximately $2x\ 10^9\ M^{-1}\ s^{-1}$ (Klug et al 1972; Rotilio et al 1972).

The effects of SOD2 deficiencies in mice are described in detail in section 1.1.9. In brief, SOD2 (-/-) mice experience prenatal or neonatal lethality, depending on the genetic background of the mice, associated with severe neurological and cardiac phenotypes and linked to decreased Complex I and II activity as well as mitochondrial aconitase deficiencies and oxidative gDNA damage in brain and heart (Huang et al 2001; Li et al 1995; Lebovitz et al 1996; Melov et al 1999). In addition, lipid accumulation in the liver and skeletal muscle as well as metabolic acidosis and reduction in succinate dehydrogenase (complex II) activities have also been reported (Li et al 1995). In a separate study, heterozygous mutant mice were exposed to high levels of lipid peroxidation and apoptosis in the heart (Strassburger et al 2005). mtDNA damage was also reported in livers of SOD2 heterozygous mice (C57BL/6 background) at 2–4 months of age (Williams et al 1998). Treatment of SOD2 null mice with SOD2 mimetics increases their lifespan and attenuates spongiform encephalopathy and mitochondrial defects thus rescuing some of the pathological phenotypes mentioned above (Melov et al 2001; Melov et al 1998).

All three major inhibitors of $O_2^{\cdot-}$, SOD1, SOD2 and SOD3, have decreased expression in OA cartilage compared to control both at the mRNA and protein level (Scott et al 2010; Ruiz-Romero et al 2009; Aigner et al 2006). SOD2 downregulation regulates IL-1 induced mRNA expression of collagenases *MMP-1* and *MMP-13* suggesting that SOD2 downregulation in cartilage, as well as a role in ROS and macromolecular damage, may have a chondroprotective role. High levels of $O_2^{\cdot-}$and nitrogen oxide (NO) have been reported in OA, which lead to higher levels of H_2O_2 and $ONOO^-$ (Hiran et al 1997; Loeser et al 2002; Tiku et al 1998). The increase in ROS can potentially lead to increased levels of mtDNA and nuclear DNA damage in the form of DNA base modifications (8-oxo-guanine) and DNA strand breaks, as reported previously (Chang et al 2005; Chen et al 2008; Kim et al 2009). High levels of $O_2^{\cdot-}$, NO and inflammatory cytokines have been shown to increase lipid peroxidation and regulation of signalling pathways leading to cartilage degradation (Tiku et al 2000; Shah et al 2005; Loeser et al 2002). Also ROS have been shown to cleave collagen and hyaluronan (Gao et al 2008; Petersen et al 2004) in other systems. In the same studies EC-SOD (SOD3) attenuates oxidative fragmentation by binding directly to both collagen and hyaluronan.

3.3 Aims

- Assess the effect of SOD2 downregulation on mitochondrial $O_2^{\cdot-}$ levels using ROS- indicators and immunocytochemistry
- Determine the levels of lipid peroxidation and mtDNA strand breaks in OA and NOF cartilage
- Evaluate the contribution of SOD2 downregulation to lipid peroxidation and mtDNA damage in chondrocytes

3.4 Results

3.4.1 Effect of SOD2 RNAi on SOD2 expression

RNAi-mediated depletion of SOD2 mRNA and protein levels was used to study the role of SOD2 in the regulation of mitochondrial $O_2^{\cdot-}$ levels and determine whether its depletion causes mtDNA damage. The optimal transfection procedure and duration of siRNA incubation are described in section 2.3.2. Transfection of 100nM concentration SOD2 targeted siRNA resulted in 95% reduction in mRNA levels and a pronounced decrease in intensity of protein levels (Figure 3.1).

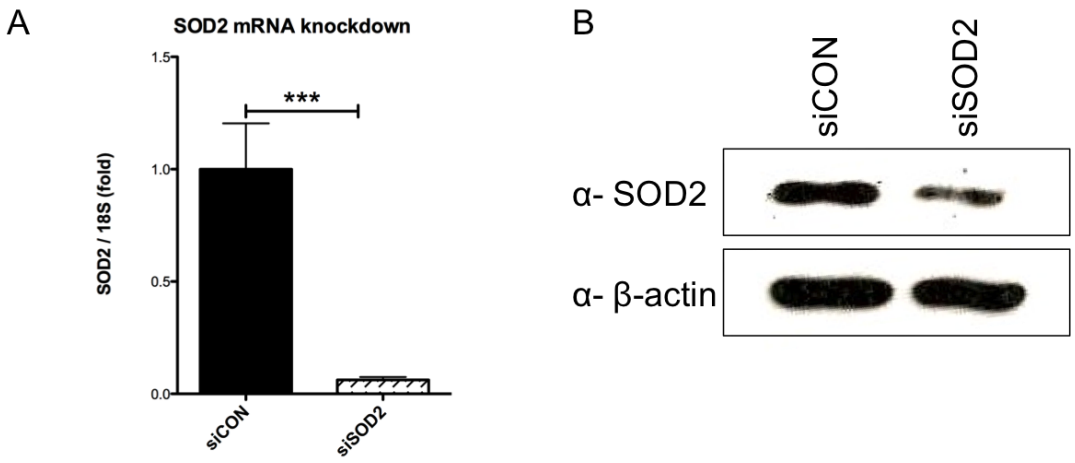

Figure 3.1 Effect of SOD2 siRNA knockdown on SOD2 mRNA and protein levels

(A) HAC isolated from knee cartilage were transfected with 100nM of SOD2 siRNA for 48 hours as described in section 2.3.2. Total RNA was extracted, reverse transcribed to cDNA and subjected to real-time RT-PCR analysis of *SOD2* gene expression as described in section 2.4.8. Values were normalised to *18S* and plotted as mean fold induction over control ± standard error of mean (SEM) (n=5). Statistical significance between siCON and siSOD2 treated cells was determined using the Mann-Whitney U test. *** p≤0.001, compared to control. (B) Human SW1353 cells were transfected as above. Total protein was extracted, resolved by SDS-PAGE and immunoblotted with the SOD2 and β-actin antibodies as described in section 2.5.3. Figure A is representative of two independent experiments and figure B is from one experiment but has been documented previously (Scott et al 2010).

3.4.2 Mitosox-Red concentration optimisation

Mitosox-Red is a cationic dye that is rapidly oxidized by $O_2^{\cdot-}$ but not by other reactive oxygen species (ROS) and reactive nitrogen species (RNS). The oxidized product is highly fluorescent upon binding to nucleic acid. Due its lipophilic and cationic nature it is specifically attracted in the mitochondria and therefore oxidised by $O_2^{\cdot-}$ specifically in the mitochondria.

In order to determine the appropriate concentration of Mitosox-Red to be used in further experiments, SW1353 chondrosarcoma cells were stained with Mitosox-Red at different concentrations and the intensity of the staining was assessed by flow cytometry as described in section 2.7.2. Cells were stained with 1μM and 5μM of Mitosox Red for 15mins at 37°C and 0.001% (v/v) DMSO was used as a negative control (Robinson et al 2006; Robinson et al 2008). Cells analysed were pre-selected from the viable cell population using forward scatter (FSC) and side scatter (SSC) selection using the FACS software. Cells treated with just DMSO only showed minor auto-fluorescence similar to untreated cells (Figure 3.2A). The population stained with 1μM Mitosox-Red showed higher numbers of cells with maximum intensity compared to the negative control. As expected the population stained with 5μM Mitosox-Red had more cells showing maximum intensity compared to the 1μM population. Cells stained with 2.5μM of Mitosox were not stained by flow cytometry.

In order to test staining saturation, SW1353 cells were also cultured in chamberslides and stained with Mitosox-Red at 1μM, 2.5μM and 5μM final concentrations for 15mins at 37°C (Figure 3.2B). Cells stained with 1μM Mitosox-Red showed very low staining intensity whereas cells stained with 5nM Mitosox-Red showed very intense staining and possibly the staining was too saturated. Cells stained with 2.5μM Mitosox-Red had average amounts of staining and minimum saturation. Therefore, in order to avoid saturation of the dye, it was decided that 2.5μM concentration of Mitosox-Red to be used in further experiments.

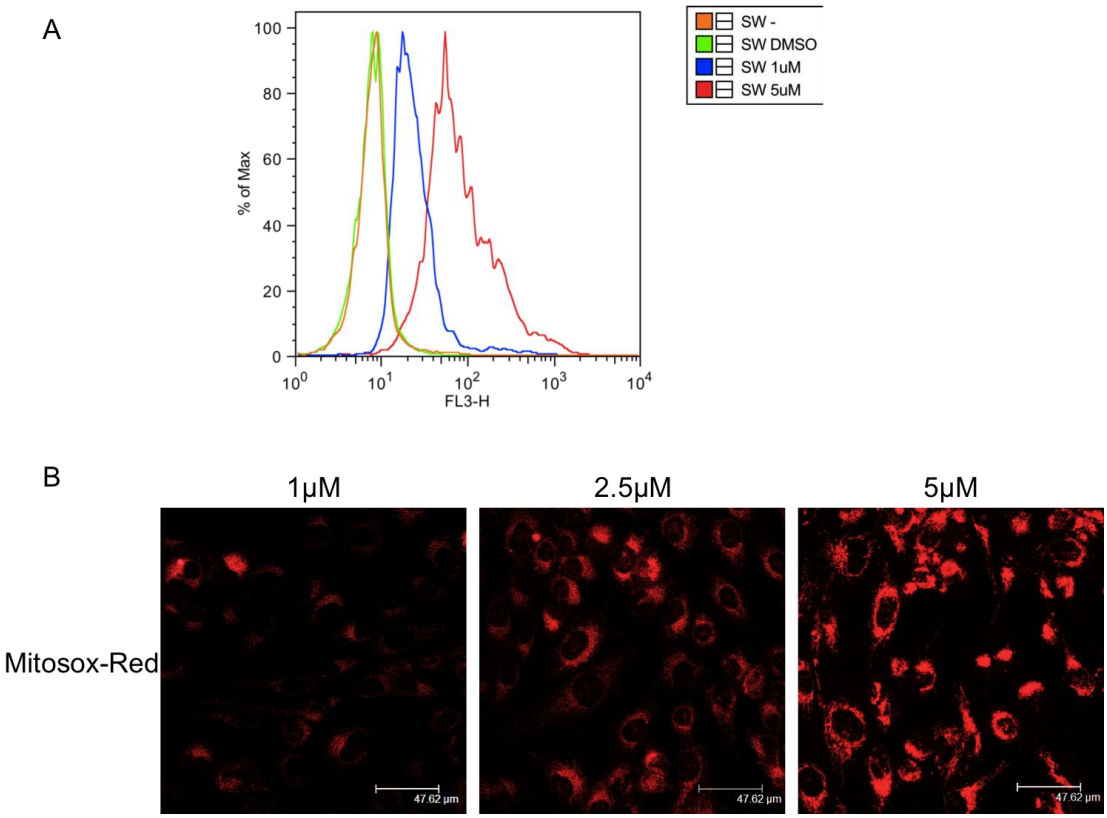

Figure 3.2 Mitosox concentration optimization

(A) SW1353 chondrosarcoma cells were resuspended in serum free DMEM media (containing phenol) and stained with the two different concentrations of Mitosox Red or 0.001% (v/v) DMSO, as a negative control for 15mins at 37°C. Cells were then washed twice and resuspended in PBS. The maximum fluorescence intensities of negative and positive populations were measured in the FL-3 channel (red) as in section 2.11. Cells analysed were pre-selected from the viable cell population using forward scatter (FSC) and side scatter (SSC) selection using the FACS software. 5000 live cells were analysed per treatment. Data was analysed using FlowJo v8.7.1 software. (B) SW1353 cells were cultured in chamberslides and stained with three different concentrations of Mitosox-Red for 15mins at 37°C. Cells were then washed twice in PBS and fixed in 4% paraformaldehyde for 10mins at room temperature. Fluorescence was assessed by confocal microscopy at 510/580 nm (absorption/emission).

3.4.3 Effect of ROS inducers and inhibitors on mitochondrial superoxide levels in chondrocytes

In order to evaluate whether quantification of mitochondrial $O_2^{\cdot-}$ in chondrocytes was possible, cells were treated with different ROS inducers and a ROS inhibitor and then stained with Mitosox Red. Different concentrations of ROS inducers rotenone, antimycin A, paraquat and a ROS inhibitor, N-acetyl-L-cysteine (NAC) were evaluated in both SW1353 chondrosarcoma cells and HAC. The chemicals were incubated for the stated time and then cells were stained with Mitosox Red for 15mins. Fluorescence was assessed with confocal microscopy and flow cytometry (FACS).

Confocal Microscopy

In SW1353 cells (Figure 3.3 and Figure 3.4), incubation with 10μM antimycin A, 100μM paraquat and 2.5μM rotenone for 1 hour resulted in an increase in ROS. Increasing the concentration of antimycin A to 100μM caused a further increase in ROS. Increasing the concentration of paraquat and rotenone to 200μM and 10μM respectively caused a reduction in ROS. Incubation with NAC at both 5mM and 10mM resulted in similar levels of ROS reduction.

In HAC (Figure 3.6 and Figure 3.6), incubation with 10μM antimycin A resulted in a reduction in ROS levels, whereas incubation with 100μM antimycin A did not change the ROS levels compared to control. Increasing concentrations of paraquat caused increasing levels of ROS similar to SW1353 cells. Similarly, increasing concentrations of rotenone increased the ROS levels. Incubation with 5mM NAC resulted in reduced levels of ROS whereas incubation with 10mM NAC caused an increase in ROS levels compared to control.

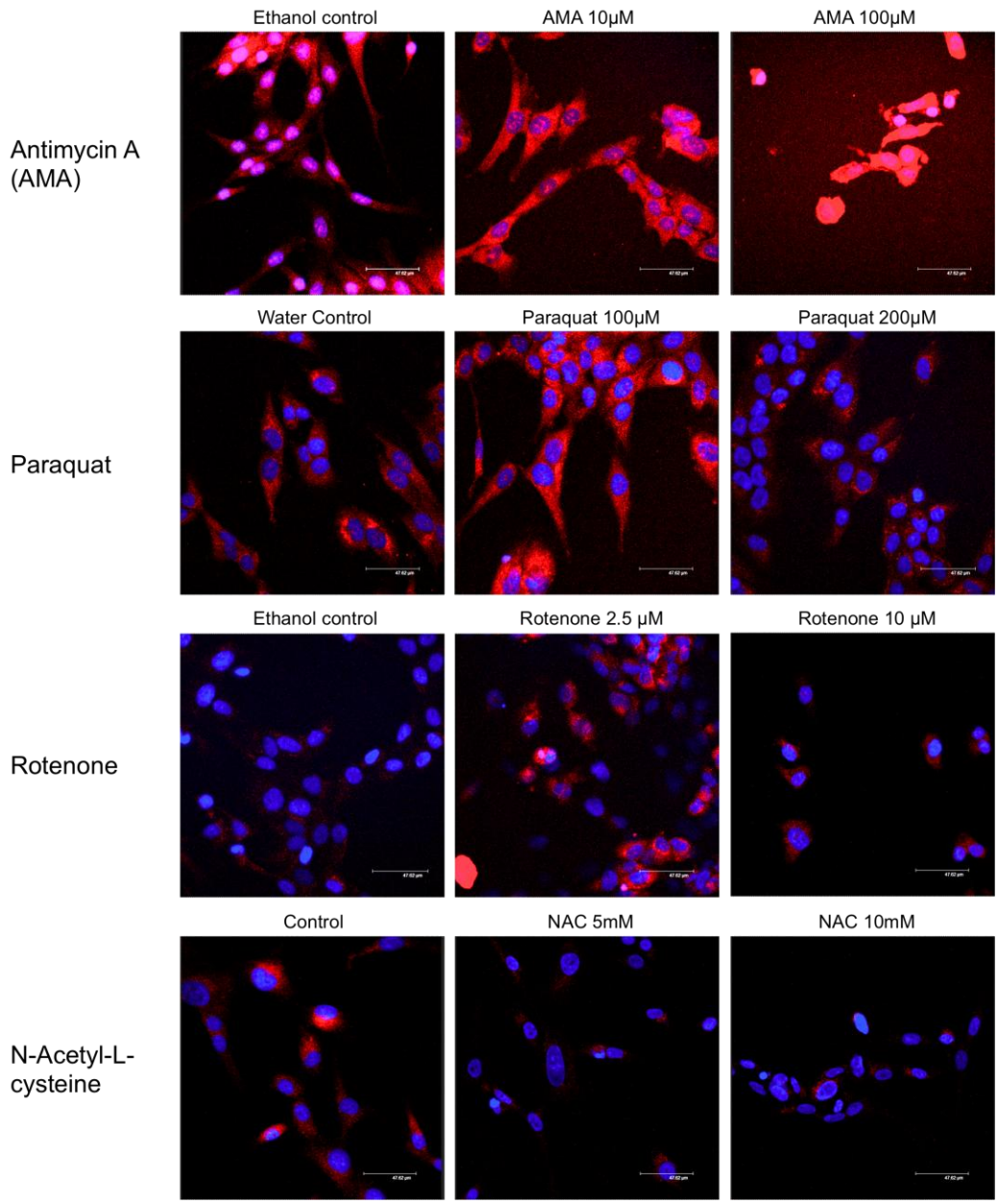

Figure 3.3 Effect of ROS inducers and inhibitors on mitochondrial $O_2^{\cdot-}$ levels in SW1353 cells

SW1353 chondrosarcoma cells were treated with the stated final concentration of antimycin A, paraquat and rotenone for 1 hour and NAC for 24 hours. Cells were then stained with 2.5μM of Mitosox-Red for 15 mins, fixed in 4% paraformaldehyde and then mounted using Vectashield containing DAPI. Fluorescence was assessed using confocal microscopy and images analysed with ImageJ. Four images were taken per treatment. Images shown are representative of a single complete experiment but individual experiments were repeated multiple times. DAPI is shown in blue and Mitosox-Red shown in red.

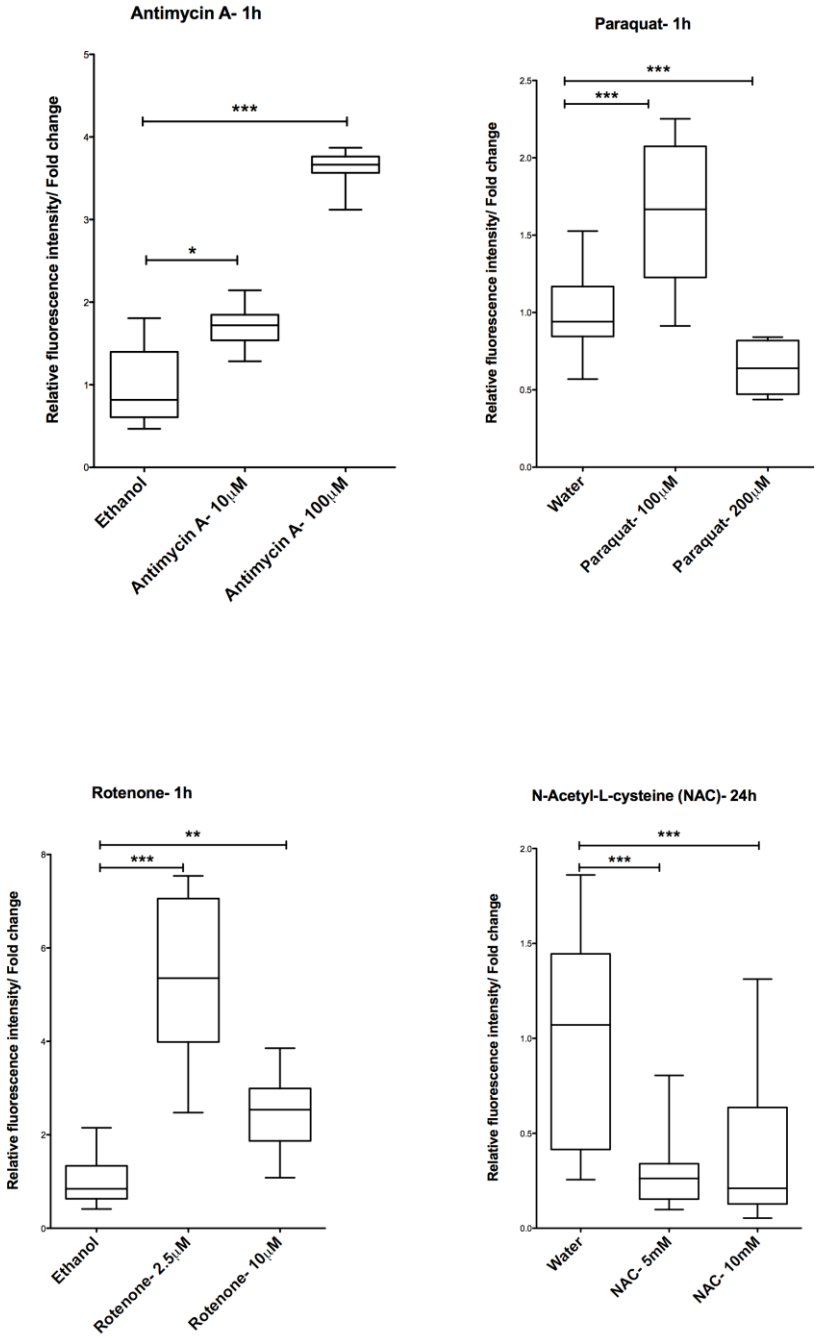

Figure 3.4 Graphical representation of effect of ROS inducers and inhibitors on mitochondrial $O_2^{\cdot-}$ levels in SW1353 cells

SW1353 cells were treated with the stated final concentration of antimycin A, paraquat and rotenone for 1 hour and NAC for 24 hours. Cells were then stained with 2.5μM of Mitosox-Red for 15 mins, fixed in 4% paraformaldehyde and then mounted using Vectashield containing DAPI. Fluorescence was assessed using confocal microscopy and images analysed with ImageJ. Four images were taken per treatment. Values were plotted as minimum, median and maximum fold induction over control ± standard deviation (SD). Statistical analysis was performed (Mann Whitney U test) to determine statistical significance between treatments and control; *p≤0.05, **p≤0.01, ***p≤0.001 compared to control. Graphs show pooled data analysis of three independent experiments.

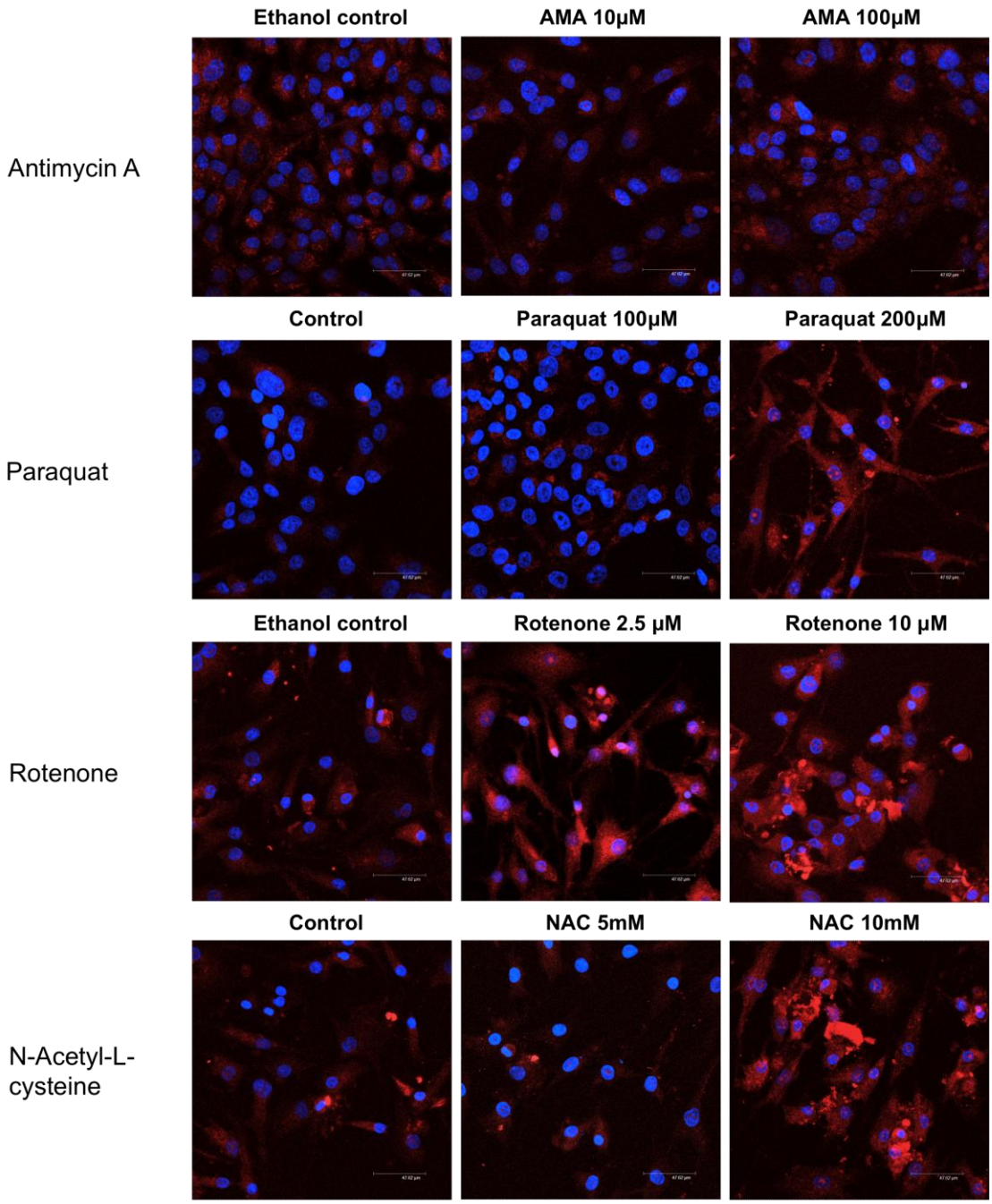

Figure 3.5 Effect of ROS inducers and inhibitors on mitochondrial $O_2^{\cdot-}$ levels in HAC

HAC isolated from knee cartilage were treated with the stated final concentration of antimycin A, paraquat and rotenone for 1 hour and NAC for 24 hours. Cells were then stained with 2.5µM of Mitosox-Red for 15 mins, fixed in 4% paraformaldehyde and then mounted using Vectashield containing DAPI. Fluorescence was assessed using confocal microscopy and images analysed with ImageJ. Four images were taken per treatment. Images shown are representative of a single complete experiment but individual experiments were repeated multiple times. DAPI is shown in blue and Mitosox-Red shown in red.

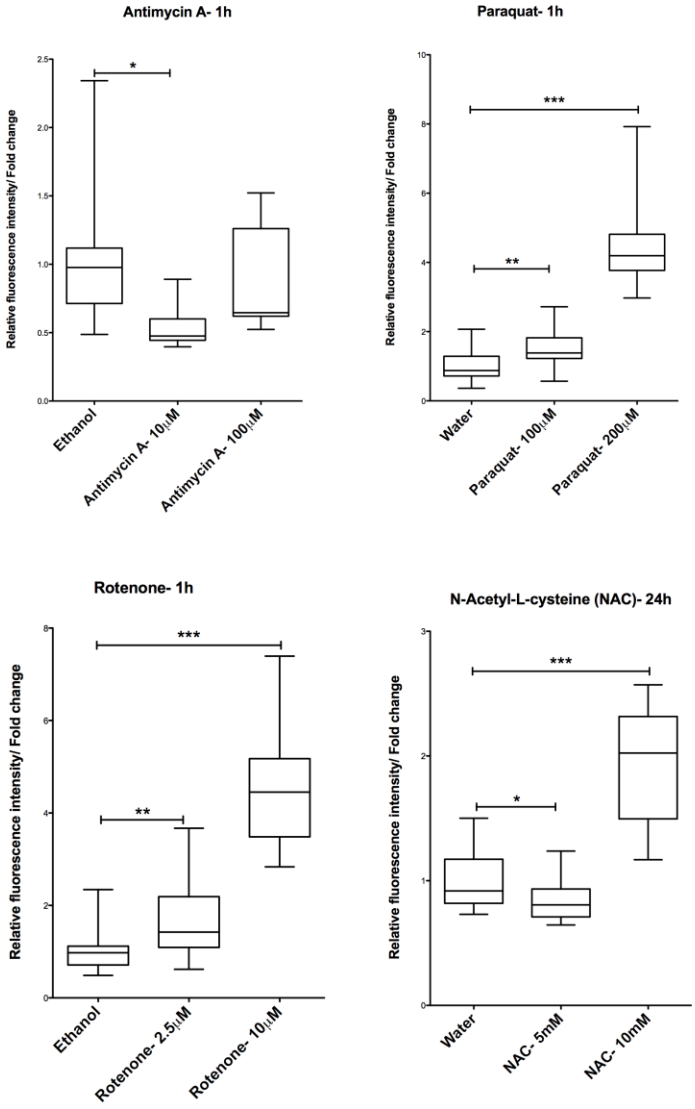

Figure 3.6 Graphical representation of effect of ROS inducers and inhibitors on mitochondrial $O_2^{\cdot-}$ levels in HAC

HAC isolated from knee cartilage were treated with the stated final concentration of antimycin A, paraquat and rotenone for 1 hour and NAC for 24 hours. Cells were then stained with 2.5µM of Mitosox-Red for 15 mins, fixed in 4% Paraformaldehyde and then mounted using Vectashield containing DAPI. Fluorescence was assessed using confocal microscopy and images analysed with Image J. Four images were taken per treatment. Values were plotted as minimum, median and maximum fold induction over control ± standard deviation (SD). Statistical analysis was performed (Mann Whitney U test) to determine statistical significance between treatments and control; p≤0.05**,** *p<0.01, ***p≤0.001 compared to control. Graphs show pooled data analysis of three independent experiments using three different patient samples.

Flow cytometry (FACS)

The effect of ROS inducers and inhibitor (NAC) on the mitochondrial $O_2^{\cdot-}$ levels was also assessed with FACS in order to determine which method (FACS or microscopy) is better to detect changes in Mitosox-Red levels in response to changes in ROS.

In SW1353 cells (Figure 3.7A and B), incubation with antimycin A and paraquat resulted in a small increase in the number of cells with high levels of Mitosox-Red staining whereas treatment with rotenone increased Mitosox-Red levels in more cells than the other inducers. Incubation with NAC resulted in a big reduction in the number of cells with high levels of Mitosox-Red staining.

In HAC (Figure 3.7C and D), incubation with antimycin A, rotenone and paraquat did not change Mitosox-Red staining in the cells at all. Incubation with NAC resulted in a very small reduction in the number of cells with high levels of Mitosox-Red staining.

These results were not consistent the results that were recorded by confocal microscopy. Therefore, some of the cells used in the FACS experiments were cytospun onto a microscope slide and their Mitosox-Red staining was assessed by confocal microscopy. As shown in the example in Figure 3.8, Mitosox-Red staining was not retained in the mitochondria and diffused into the cytoplasm of both HAC and SW1353 cells irrespective of the treatment.

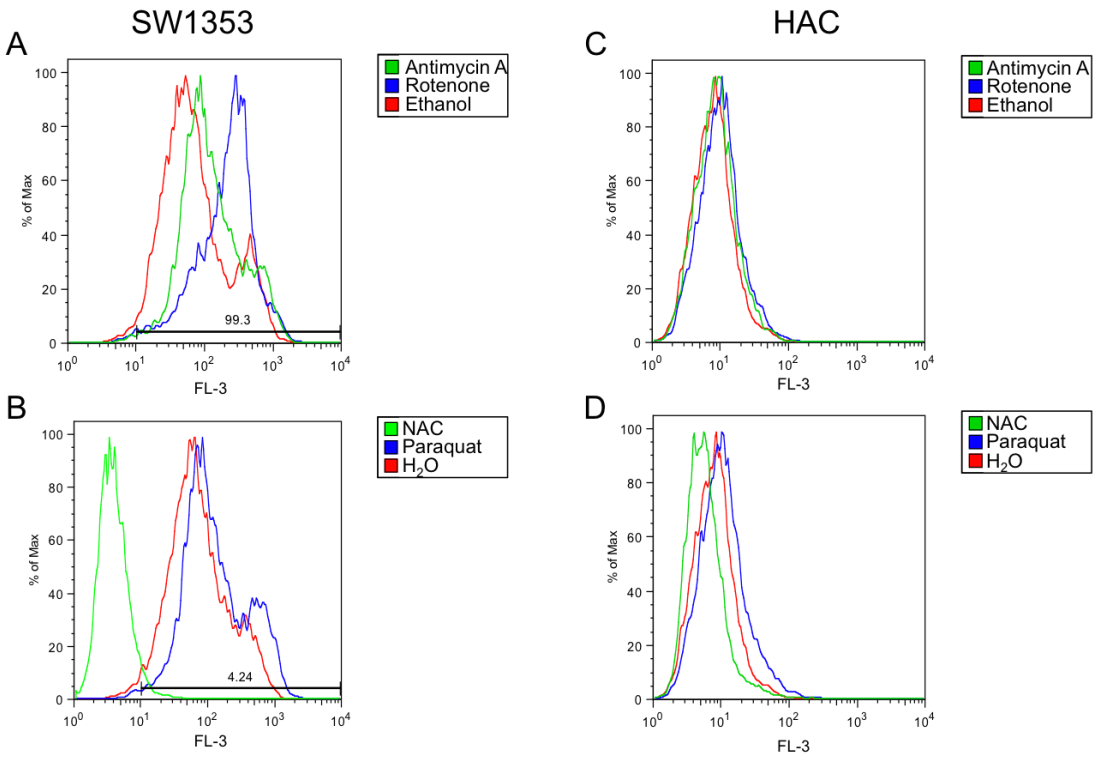

Figure 3.7 Effect of ROS inducers and inhibitors on mitochondrial $O_2^{\cdot-}$ levels in SW1353 cells and HAC assessed by FACS

SW1353 chondrosarcoma cells and HAC isolated from knee cartilage were treated with 100μM antimycin A, 100μM paraquat and 2.5μM rotenone for 1 hour and 5mM NAC for 24 hours. Cells were then resuspended in serum free DMEM media (containing phenol) and stained with 2.5nM Mitosox Red as a negative control for 15mins at 37°C. Cells were then washed twice and resuspended in PBS. The maximum fluorescence intensity was measured in the FL-3 channel (red) as in section 2.11. Cells analysed were pre-selected from the viable cell population using forward scatter (FSC) and side scatter (SSC) selection using the FACS software. 10000 live cells were analysed per treatment. Data was analysed using FlowJo v8.7.1 software. Graphs shown are representative of a single complete experiment but individual experiments were repeated twice.

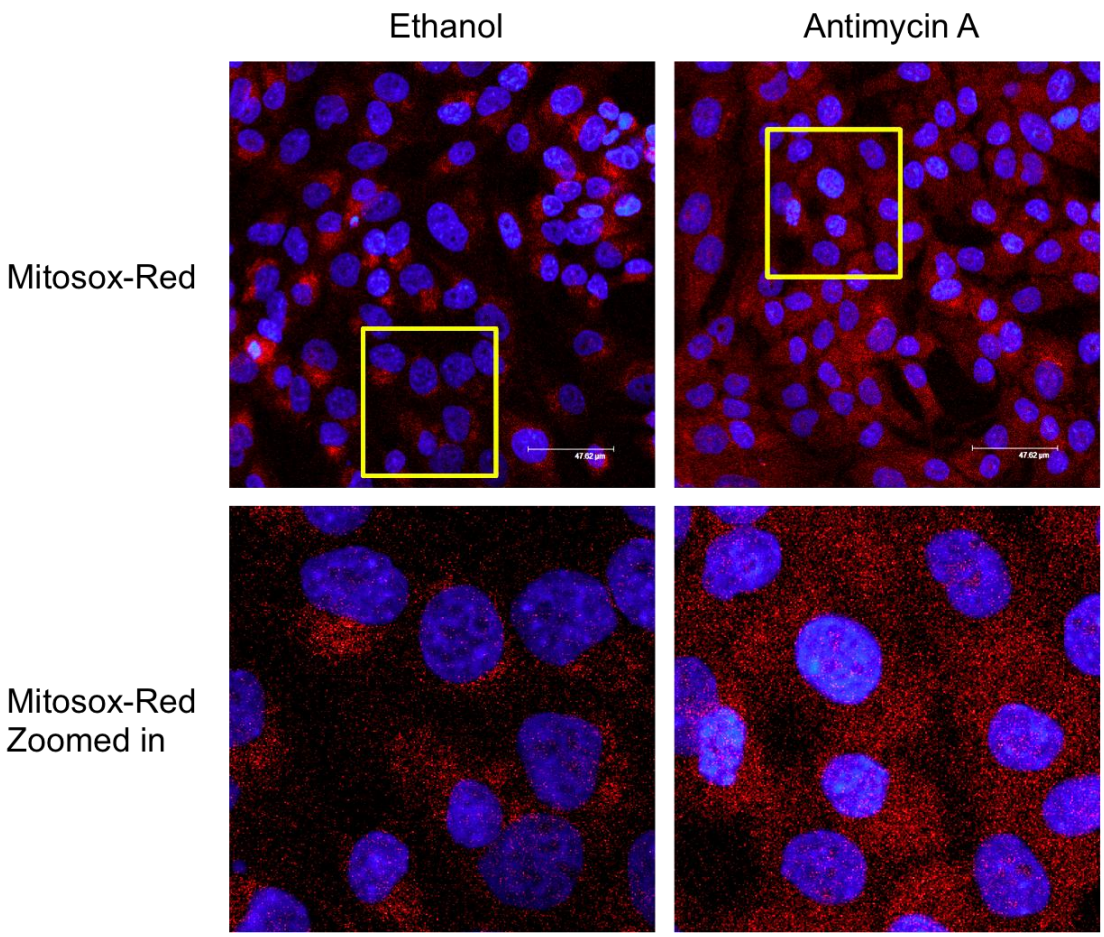

Figure 3.8 Images of cytospun cells, treated with ROS inducers and inhibitors, used for FACS.

Images show the non-specific localisation of Mitosox-Red in the mitochondria in SW1353 cells treated with antimycin A or ethanol (negative control). Cells were cytospun onto a microscope slide as described in 2.7. DAPI is shown in blue and Mitosox-Red shown in red.

3.4.4 Optimisation of Mitosox and SOD2 dual staining in HAC

In order to assess the changes in $O_2^{\cdot-}$ and SOD2 levels simultaneously in the same cells, a protocol for dual Mitosox-Red and anti-human SOD2 antibody staining had to be established. A previous study suggested that mitosox cannot be retained in the mitochondria after fixation and permeabilisation with Triton-X, procedures essential for further antibody staining (Robinson et al 2008). Therefore, in order to analyse Mitosox-Red levels and compare them to SOD1 levels, the cells were stained firstly with Mitosox-Red and the fluorescence levels were recorded by confocal microscopy. The exact position of the cells was also recorded (microscope coordinates). The cells were then stained for SOD1 antibody. The exact location of the cells assessed previously was identified using the confocal microscope and then SOD1 levels were assessed in the same cells. In this thesis, this protocol was not feasible due to inaccuracies of the confocal microscope's coordinates and therefore the exact cells could not be identified.

Therefore a protocol that enables simultaneous recording of Mitosox-Red and SOD2 antibody levels had to be established. To achieve this, Mitosox-Red had to be retained in the cells after fixing and permeabilisation. Two permeabilising chemicals were assessed, Triton-X and Saponin. The optimal staining procedure and duration are described in section 2.7.4.

Triton-X permeabilisation resulted in very good SOD2 staining however any specific Mitosox-Red staining was not specific to the mitochondria and diffused into the cytoplasm (Figure 3.9).

However, saponin permeabisation (Figure 3.10) at 30mins retained Mitosox staining but gave very weak SOD2 staining. At 45mins and 60mins, using Saponin as a permeabising agent, Mitosox-Red staining was retained within the mitochondria after fixing and permeabilisation and therefore managed to stain using the SOD2 antibody without experiencing significant amounts of Mitosox-red diffusing into the cytoplasm. Therefore, saponin incubation was used as the optimal condition for dual Mitosox-Red/SOD2 staining in chondrocytes due to the fact that SOD2 staining was satisfactory at 45mins and after permeabisation

and antibody incubation, Mitosox-Red staining was retained in the mitochondria and did not diffuse into the cytoplasm.

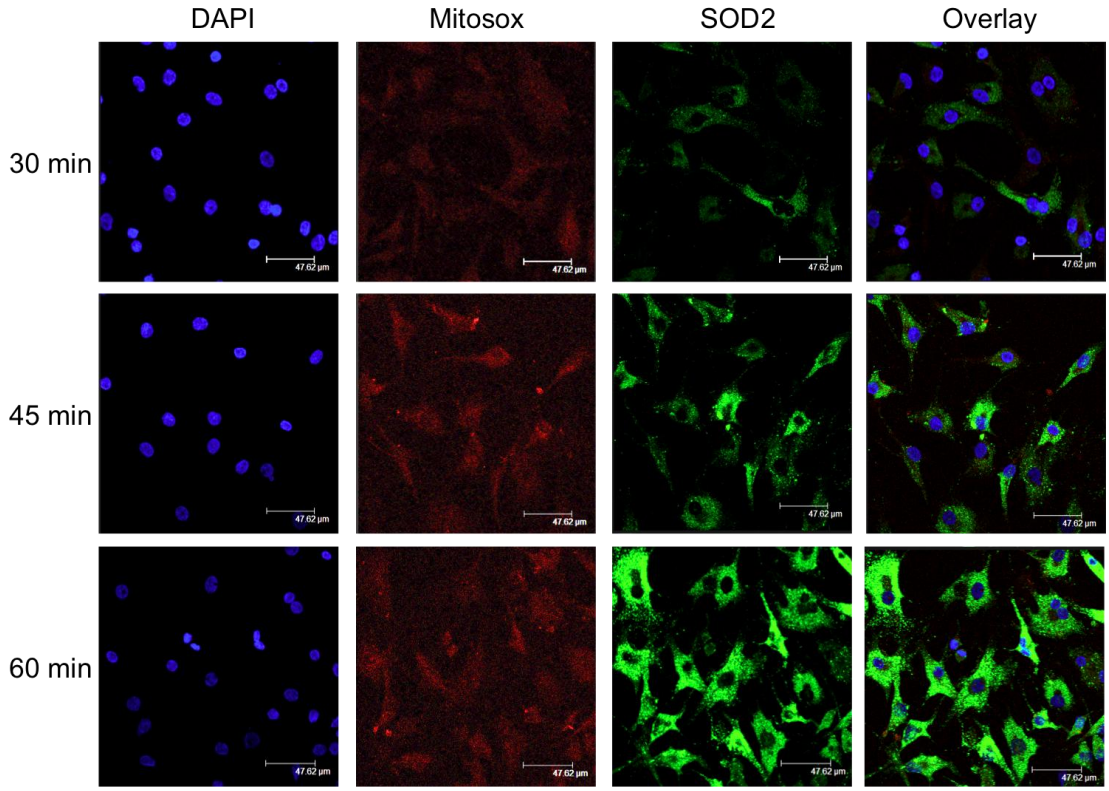

Figure 3.9 SOD2 and Mitosox Dual staining optimisation (Triton permeabilisation)

HAC isolated from knee cartilage were stained with 2.5μM Mitosox Red for 15 mins and fixed in 4% paraformaldehyde. Cells were permeabilised using a Triton-X containing buffer as described in section 2.7.4. Cells were then incubated with anti-human SOD2 antibody and an Alexa 488 secondary antibody as described in section 2.7.4. Figures are representative of two experiments.

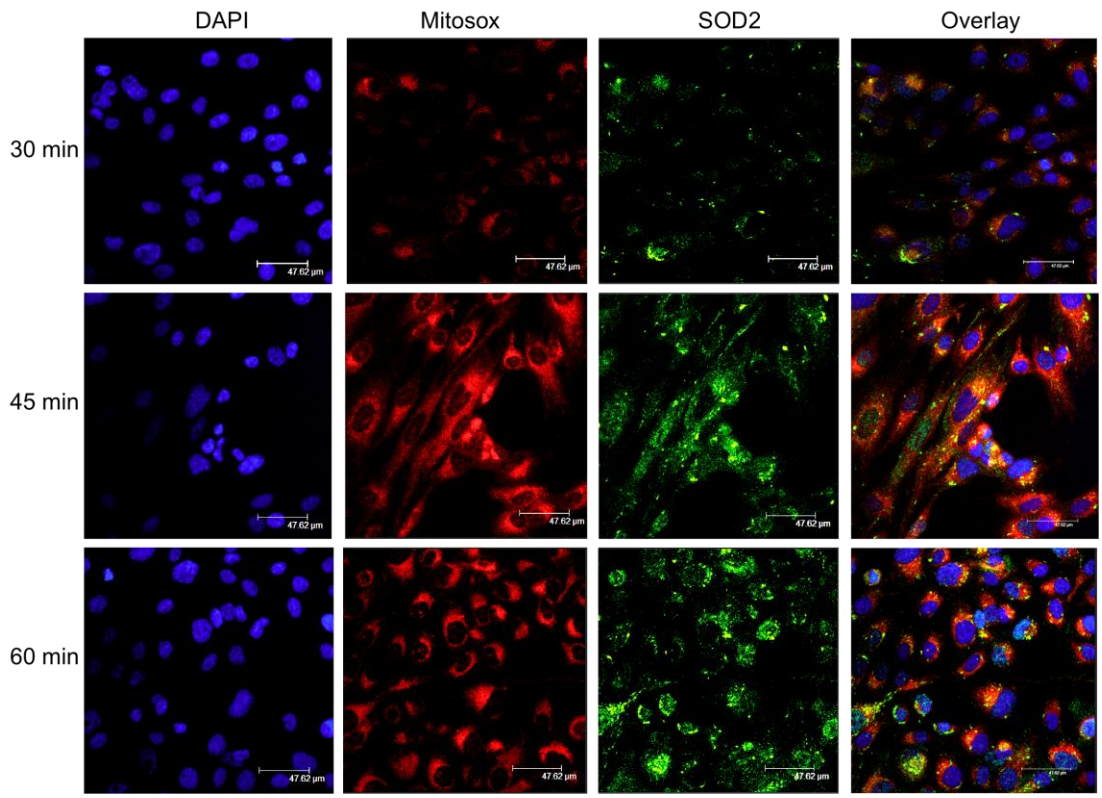

Figure 3.10 SOD2 and Mitosox Dual staining optimisation (Saponin permeabilisation)

HAC isolated from knee cartilage were stained with 2.5μM Mitosox Red for 15 mins and fixed in 4% paraformaldehyde. Cells were permeabilised using a saponin containing buffer as described in section 2.7.4. Cells were then incubated with anti-human SOD2 antibody and an Alexa 488 secondary antibody as described in section 2.7.4. Figures are representative of two experiments.

3.4.5 Comparison of mitochondrial superoxide levels and SOD2 protein levels in HAC

During optimisation of the dual staining of Mitosox-Red and SOD2, it was noticed that cells that had high levels of SOD2 protein also had low amount of Mitosox-Red as shown in Figure 3.11A. Scott *et al* reported that superficial zone chondrocytes appear to express more SOD2 than deep zone chondrocytes (Scott et al 2010). Therefore, as in this thesis, HAC are extracted from total cartilage, cells are expected to express different levels of SOD2. Therefore we decided to test this at a larger scale using HAC from seven different patients and evaluate the correlation between the SOD2 protein levels and Mitosox-Red (mitochondrial $O_2^{\cdot-}$) levels. As shown in Figure 3.11B, 5 patients showed a small negative correlation between SOD2 and Mitosox-Red as the R^2 values were very low, suggesting that cells with lower SOD2 levels had higher levels of $O_2^{\cdot-}$. However, 2 other patients showed a small positive correlation (Figure 3.11C) indicating that cells with higher SOD2 levels also had higher $O_2^{\cdot-}$ levels. These results suggest that the expected negative correlation between $O_2^{\cdot-}$ and SOD2 levels possibly exists in HAC with some exceptions, but this observation is not consistent with the whole cell population. This can be due to the differences in SOD2 expression in cells from different zones of cartilage tissue. However, as noticed previously in 3.4.3 and Figure 3.8, Mitosox-Red is not readily retained in chondrocytes after trypsinisation, therefore these results might not be reliable in terms of the Mitosox-Red levels recorded.

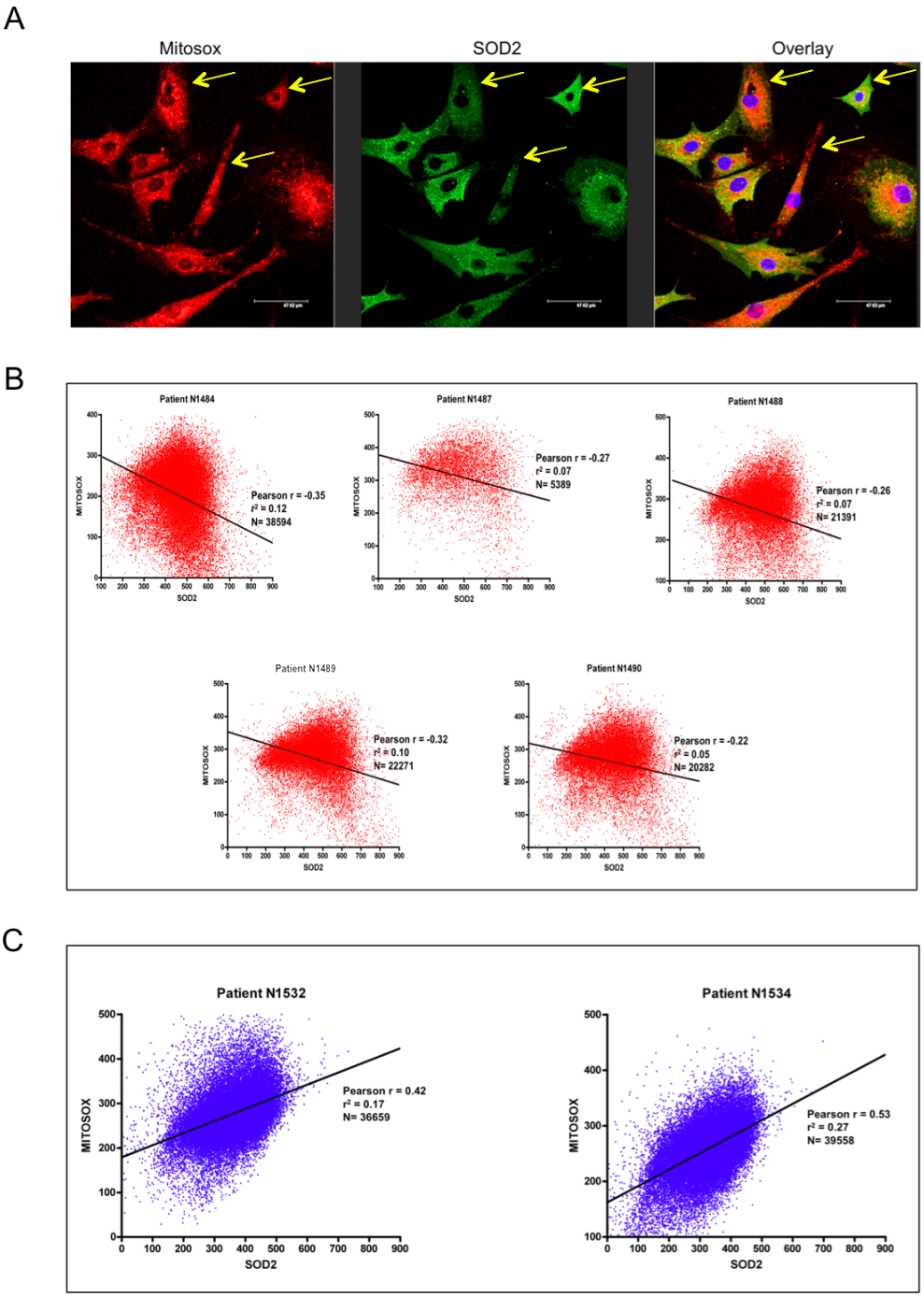

Figure 3.11 Correlation of SOD2 protein levels with Mitosox-Red levels

(A) HAC isolated from knee cartilage were stained for confocal analysis of SOD2 protein and Mitosox-Red levels as described in section 2.7.4 using saponin permeabilisation. Arrows indicate cells with low SOD2 levels and high Mitosox-red levels and cells with high SOD2 levels and low Mitosox-Red levels. (B and C) HAC were trypsinised and then stained for flow cytometric analysis of Mitosox-Red and SOD2 protein levels as described in section 2.7.4. Raw fluorescence values for each cell were exported into Microsoft Excel and the Pearson correlation coefficient and R^2 values were calculated. The correlation is also indicated by the regression line in each graph. DAPI is shown in blue, SOD2 in green and Mitosox-Red shown in red.

3.4.6 Effect of SOD2 downregulation on mitochondrial superoxide levels in HAC

As described in section 3.4.3 (Figure 3.8), Mitosox-Red was not retained in chondrocyte mitochondria after trypsinisation. This can possibly be due to the fact that trypsin and in general cell detachment, causes changes in the cytoskeleton and therefore can affect the mitochondria (Kostal, & Arriaga 2011; Badley et al 1980). Also, trypsinisation has been shown to increase ROS levels (Lim et al 2006; Aoshiba et al 2001). Therefore the Mitosox-Red levels recorded by FACS are probably partially cytoplasmic and also can be inaccurate due to the effect that trypsin has on ROS levels. Consequently, Mitosox-Red and SOD2 levels were only assessed on cells attached onto chamberslides and measured by confocal microscopy.

In order to determine whether a reduction in the protein levels of SOD2 affects the mitochondrial $O_2^{\cdot-}$ levels in human articular chondrocytes, HAC isolated from patient cartilage samples were transfected with siRNA targeted against SOD2 as in section 2.3.2. Cells were then stained for Mitosox-Red and anti-human SOD2 antibody as described in section 2.7.4. Cells were visualized using a confocal microscope and images were analysed using ImageJ (Figure 3.12, Figure 3.13A).

SOD2 depletion using RNAi resulted in a significant 33% decrease in SOD2 protein levels as analysed by confocal microscopy (Figure 3.13B). This reduction in SOD2 levels caused a pronounced 1.5-fold increase in Mitosox-Red staining in HAC (Figure 3.13B).

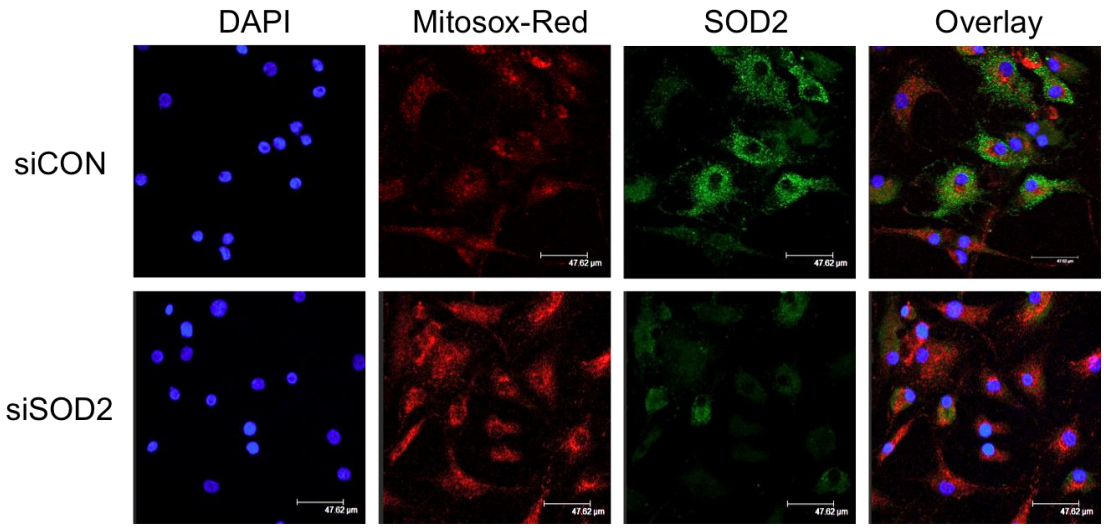

Figure 3.12 Effect of SOD2 downregulation on Mitosox-Red and SOD2 protein levels

HAC isolated from knee cartilage were transfected with 100nM of SOD2 siRNA for 48 hours. HAC were then stained with 2.5µM Mitosox Red for 15 mins and fixed in 4% Paraformaldehyde. Cells were permeabilised using a Saponin containing buffer as described in section 2.7.4. Cells were then incubated with anti-human SOD2 antibody and an Alexa 488 secondary antibody as described in section 2.7.4. Fluorescence was assessed using confocal microscopy. Figure shows DAPI staining in blue; Mitosox Red levels in red, SOD2 levels in green and an overlay of the three images. Figure is representative of four experiments.

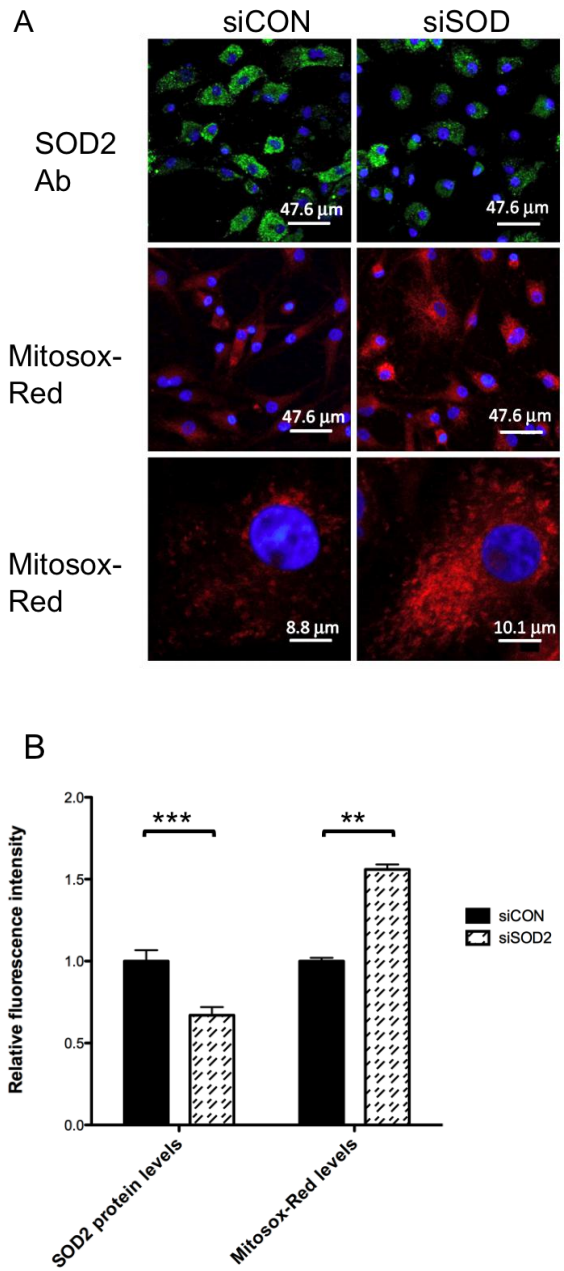

Figure 3.13 Effect of SOD2 downregulation on Mitosox-Red and SOD2 protein levels (Summary figure)

HAC from knee cartilage were transfected with 100nM of SOD2 siRNA for 48 hours. HAC were then stained with 2.5µM Mitosox Red for 15 mins and fixed in 4% Paraformaldehyde. Cells were permeabilised using a Saponin containing buffer as described in section 2.7.4. Cells were then incubated with anti-human SOD2 antibody and an Alexa 488 secondary antibody as described in section 2.7.4. Fluorescence was assessed using confocal microscopy and the images were analysed using Image J. Figure A is representative of four experiments. Figure B is pooled data analysis of four independent experiments using four different patient samples. Statistical analysis was performed (Student t-test) to determine statistical significance between treatments and control ** p≤0.01, *** p≤0.001, compared to control. (Figure adapted from Scott *et al*, 2010), DAPI is shown in blue and Mitosox-Red shown in red.

3.4.7 Lipid peroxidation in OA and NOF cartilage and the role of SOD2 in the regulation of lipid peroxidation in chondrocytes

As SOD2 levels are significantly lower in OA compared to NOF and this downregulation causes an increase in mitochondria $O_2^{\cdot-}$ levels, we assessed the level of lipid peroxidation in OA and NOF cartilage by measuring MDA concentration using the TBARS assay as described in section 2.8.

Firstly the amount of cartilage required to acquire results within the range of the standard curve suggested by the manufacturer was assessed. The cartilage used was from an OA patient. The standard curve was almost perfectly linear (Figure 3.14A). 25mg of cartilage gave a very low reading of 1.2μM MDA, which was very close to the lower end of the standard curve (Figure 3.14B). 50mg of cartilage had significantly higher concentration of MDA at 7.2μM, which was within the lower range of the standard curve (Figure 3.14B). Using 100mg of cartilage resulted in a lower MDA concentration (4.5μM) compared to 50mg. This is possibly because in the 100μl of supernatant collected after the lysis reaction of 100mg of cartilage, a lot of the cartilage homogenate was collected as well and this could have inhibited the reaction. Very small amounts of cartilage homogenate (less than the 100mg cartilage reaction) were also present in the 50mg supernatant as well so this could have a small impact in the reaction. Therefore 50mg of cartilage homogenate was considered optimum to measure MDA levels in NOF and OA cartilage, however extra care was taken in order to make sure no cartilage impurities were present in the samples.

11 OA cartilage and 11 NOF cartilage samples were assessed. No cartilage homogenate was present in the supernatants of the samples and therefore all of the values were well within the standard curve and much higher compared to the optimisation experiment. OA cartilage was found to have significantly 6.5% higher MDA levels compared to NOF (Figure 3.15). The higher values compared to the optimisation experiment can be explained from the fact that no cartilage was present in the supernatant.

To evaluate whether this increase can be caused by the depletion of SOD2 in OA, the same assay was used to evaluate the extent to which RNAi targeted depletion of SOD2 causes lipid peroxidation in SW1353 cells.

RNAi depletion of SOD2 in SW1353 cells resulted to a significant 2.5-fold increase of MDA concentration (Figure 3.16) in 3 independent experiment.

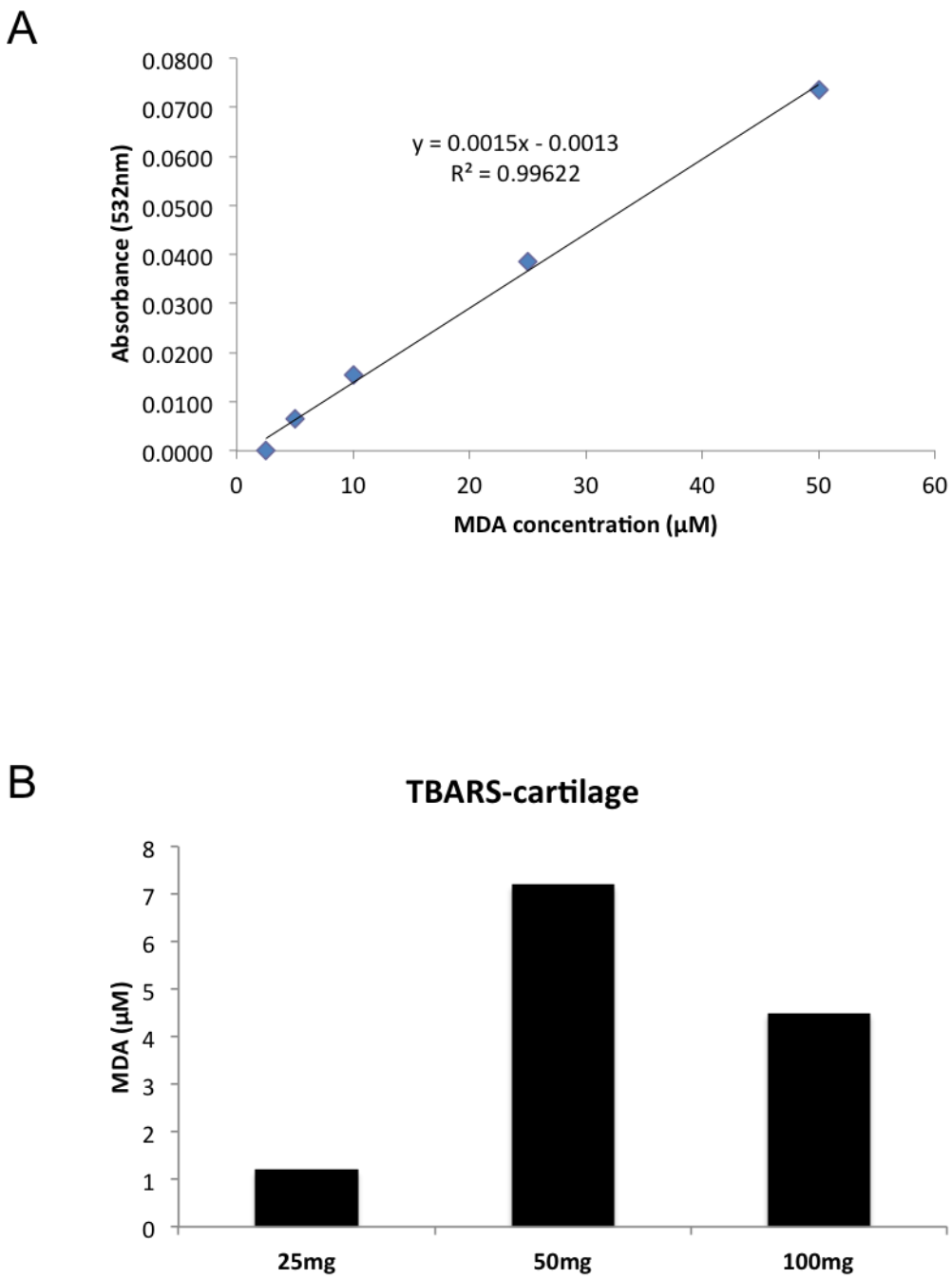

Figure 3.14 TBARS optimisation assay for cartilage homogenates

Cartilage was homogenised as described in section 2.8.1 and the assay was performed according to the manufacturer's protocol. (A) MDA standard curve reactions were set-up according to the manufacturer's protocol. (B) Three different quantities of cartilage homogenate were assayed to determine the optimum amount to be used. Figures A and B are from one independent experiment.

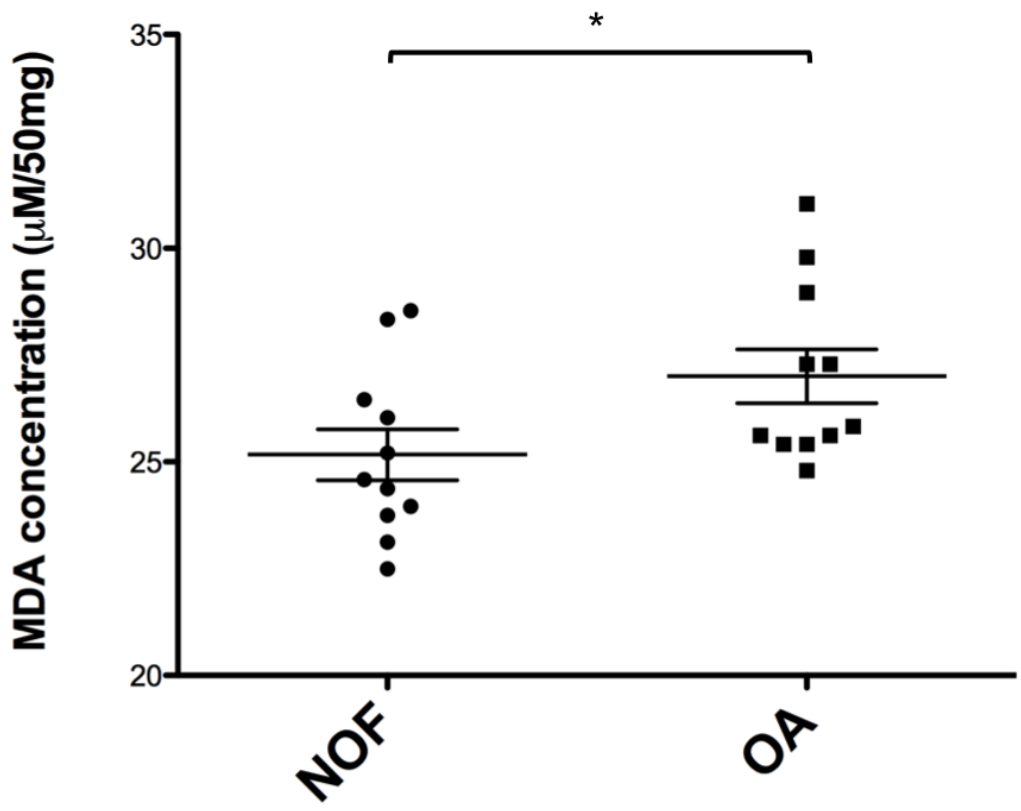

Figure 3.15 TBARS assay on human cartilage homogenates

Cartilage isolated from hip joints was homogenised as described in section 2.8.1 and the assay was performed according to the manufacturer's protocol. MDA standard curves reactions were set-up according to the manufacturer's protocol. 50mg of cartilage homogenates from eleven NOF (median age = 75yrs) and eleven OA patients (median age = 74yrs) were assayed. Each point on the graph represents the MDA concentration (μM/50mg) of each patient sample. Statistical analysis was performed (Mann Whitney U test) to determine statistical significance between treatments and control *p≤0.05 OA compared to NOF.

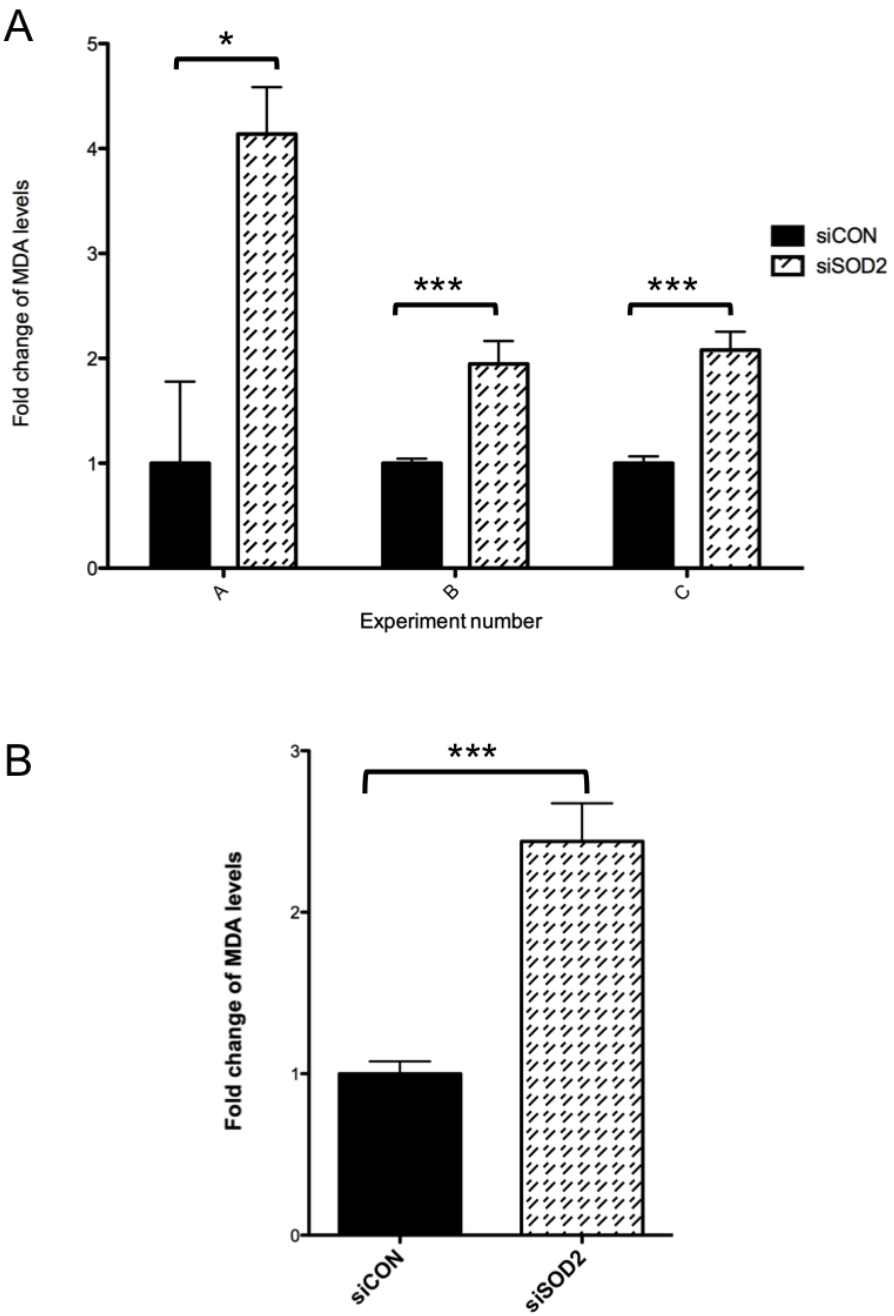

Figure 3.16 TBARS assay on SW1353 cells transfected with non-targeting siRNA control and siRNA against SOD2

SW1353 cells were seeded in 75cm^2 flasks at a density of 1.5 x 10^6/flask. After 24 hours cells were transfected with 100nM SOD2-targetted siRNA for 48 hours. Cells were then trypsinised, washed and re-suspended in 200µl of PBS and the assay was performed according to the manufacturer's protocol. (A) shows results from three independent experiments. (B) is pooled data analysis of the three independent experiments. Statistical analysis was performed (Mann Whitney U test) to determine statistical significance between treatments and control * p≤0.05, *** p≤0.001, compared to control.

3.4.8 mtDNA damage in chondrocytes due to SOD2 depletion

Previous studies in SOD2 (+/-) mice have identified higher levels of gDNA damage in various organs (Melov et al 1999; Williams et al 1998). We performed the mtDNA strand break assay, as described in section 2.4.8, in OA and NOF cartilage (described in section 4.4.1) as well as cells depleted of SOD2 by RNAi to assess the effect that SOD2 downregulation has on mtDNA damage in cartilage.

In order to identify whether SOD2 depletion in chondrocytes caused any mtDNA damage, the mtDNA strand break assay was performed in SW1353 cells depleted of SOD2 using RNAi as described in section 2.3.2. A fixed amount of total DNA was analysed by real-time PCR amplification of part of the major arc of the mtDNA. C_T values were normalized to the C_T values of MTND1 levels. RNAi depletion of SOD2 in chondrocytes resulted to a significantly 4.5-fold increase in mtDNA strand breaks compared to siCON2 transfected cells. The effect of H_2O_2 was also assessed as a positive control and caused a 42-fold increase in mtDNA strand breaks compared to its untreated control. The PCR products were subjected to agarose gel electrophoresis to screen for smaller fragments of mtDNA that may have been formed after repair of strand breaks, which can be used as an indication of large-scale deletions. However, no smaller amplicons were observed therefore no large-scale deletions were identified in these samples.

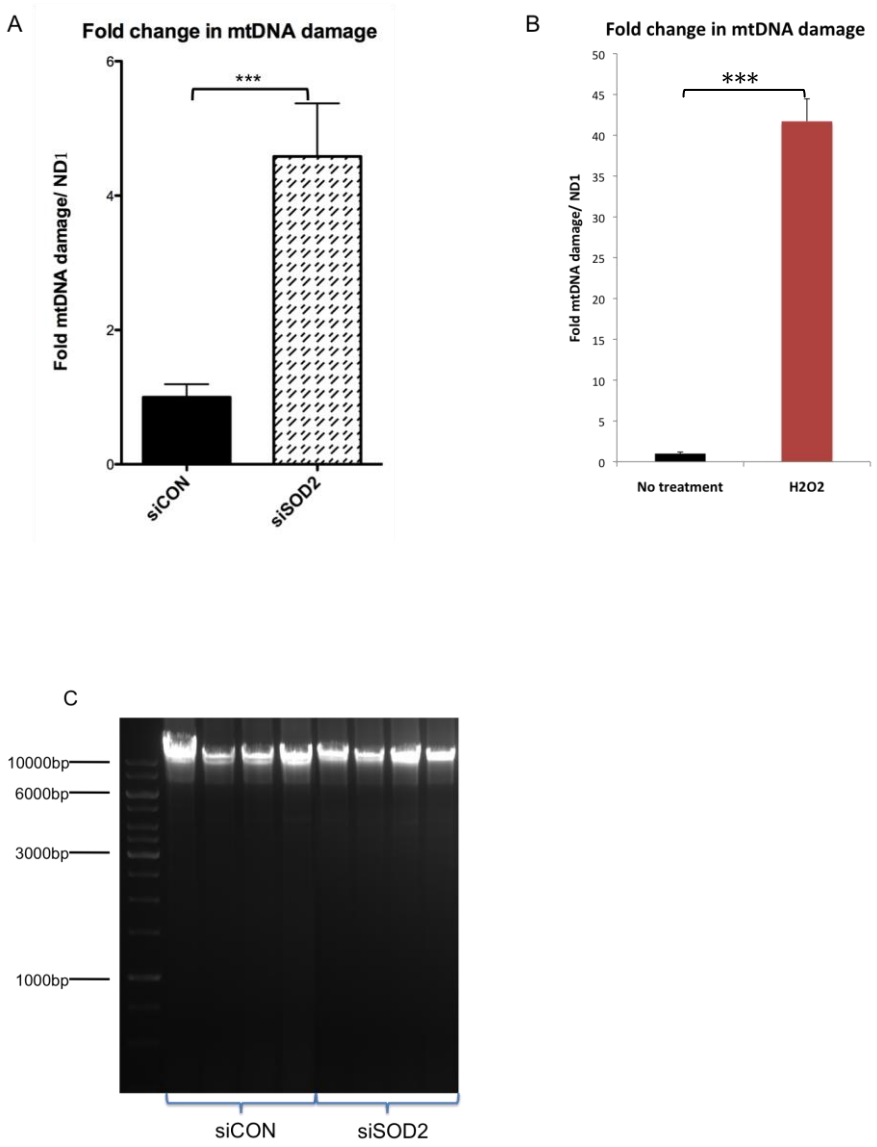

Figure 3.17 Strand break assay for mtDNA

SW1353 cells were seeded in 6cm dishes at a density of 1.5 x 10^6/dish. (A) After 24 hours cells were transfected with 100nM siRNA for 48 hours and serum starved for 16 hours. (B) Cells were serum starved for 16 hours and then treated with 200nM H_2O_2 for 1 hour as a positive control for the reaction. Cells were then trypsinised, washed and a dry cell pellet was collected. Total DNA was extracted using the QIAmp DNA mini kit. Extracted DNA was equalised using the Nanodrop system and the levels of mtDNA damage were assessed by real-time PCR as in section 2.4.8. MTND1 was used as a housekeeping marker. (C) Real-time PCR products were subjected to 0.8% agarose gel electrophoresis to screen for large mtDNA deletions. Figures A and B represent the fold change in mtDNA strand breaks after each treatment. Figure A shows results of pooled data from four independent experiments. Figure B shows pooled data of 2 independent experiments. Figure C shows the amplification products of the four experiments. *** p≤0.001, compared to control.

3.5 Discussion

As described in the introduction, the importance of SOD2 in terms of mice viability and severe neurological and cardiac phenotypes is highlighted in several studies performed using SOD2 null mice from different genetic backgrounds (Huang et al 2001; Li et al 1995; Lebovitz et al 1996). These phenotypes could be accounted to changes in mitochondrial Complex I and Complex II activity, oxidative DNA damage and the presence of lipid peroxidation (Melov et al 1999). These studies indicate that the level of $O_2^{\cdot-}$ in the mitochondria has to be kept under control in order to maintain normal cell homeostasis and cell viability.

As mentioned previously, all major inhibitors of $O_2^{\cdot-}$, SOD1, SOD2 and SOD3, are downregulated in OA compared to healthy controls, both at the mRNA and protein level (Scott et al 2010; Ruiz-Romero et al 2009; Aigner et al 2006). Other studies have also identified high levels of $O_2^{\cdot-}$ as well as nitric oxide in OA compared to control as well as higher levels of DNA damage in the form of DNA base modifications (8-oxo-guanine) and DNA strand breaks (Hiran et al 1997; Loeser et al 2002; Tiku et al 1998; Chang et al 2005; Chen et al 2008; Kim et al 2009). An increase in lipid peroxidation and intracellular signalling changes have also been reported due to high levels of $O_2^{\cdot-}$, NO and inflammatory cytokines in OA (Tiku et al 2000; Shah et al 2005; Loeser et al 2002). A recent study from our group has shown that SOD2 downregulation inhibited the IL-1 induced MMP-1 and MMP-13 expression in HAC (Scott et al 2010). However, no study has addressed the effect of SOD2 downregulation on $O_2^{\cdot-}$ levels, lipid peroxidation and mtDNA damage in HAC.

3.5.1 siRNA targeted against SOD2 reduces both SOD2 mRNA and protein level

SOD2 RNAi transfection in HAC achieved successful depletion of the cellular levels of SOD2 mRNA and protein. SOD2 mRNA was reduced by approximately 95% and there was a prominent decrease in SOD2 protein levels (Figure 3.1).

3.5.2 Mitosox-Red can detect changes in superoxide levels only in attached SW1353 cells and HAC

Previously, no other study has used Mitosox-Red, a fluorescent probe that is activated only by oxidation from $O_2^{\cdot-}$ molecules in the mitochondria (Robinson et al 2006), to quantify $O_2^{\cdot-}$ levels in chondrocyte mitochondria. Prior to the use of Mitosox-Red to evaluate the effect of SOD2 depletion on $O_2^{\cdot-}$ levels, optimisation of Mitosox-Red staining in chondrocytes had to be achieved (Figure 3.2). Initial staining was assessed by flow cytometry and increasing concentrations of Mitosox-Red resulted in more cells showing maximum intensity. Mitosox-Red staining was also evaluated by confocal microscopy. The staining was weak at 1μM but very strong at 5μM as a result of saturation of Mitosox-Red. 2.5μM of Mitosox Red were also assessed in this experiment and the intensity of Mitosox-Red was strong but not saturated. Therefore, the final concentration of 2.5μM Mitosox-Red was chosen as the concentration to be used in the experiments involving quantification of $O_2^{\cdot-}$ levels in the mitochondria as it would enable identification of both an increase and a decrease in $O_2^{\cdot-}$ levels in cells.

In order to evaluate whether Mitosox-Red staining in chondrocytes correlates with the levels of $O_2^{\cdot-}$ in the mitochondria, three known ROS inducers, rotenone, antimycin A and paraquat, and N-Acetyl-cysteine (NAC), a ROS inhibitor was used. Rotenone is a complex I inhibitor and also induces the mitochondrial ROS production by complex I (Figure 3.18a) (Votyakova, & Reynolds 2001; Hansford et al 1997). Antimycin A (AMA) is a complex III inhibitor and can also induces $O_2^{\cdot-}$ production by complex III (Figure 3.18b) (Chen et al 2003). In complex III, the semiquinone at centre “o”(IIIQo) is the major site of $O_2^{\cdot-}$ production (Cadenas et al 1977). Paraquat is a herbicide that has been also identified to increase $O_2^{\cdot-}$ levels. Paraquat is initially reduced by electrons and the reduced paraquat then reduces oxygen to $O_2^{\cdot-}$ (Figure 3.18c) (Thorneley 1974). NAC is a ROS inhibitor that is normally used in the treatment of paracetamol (or acetaminophen) overdose (Burgunder et al 1989). It acts by increasing the glutathione levels of the cells and also by binding directly to the reactive intermediate of acetaminophen (Burgunder et al 1989; Lauterburg et al 1983). It

scavenges hypochlorous acid, reacts with the $^{\bullet}OH$ and H_2O_2 but does not react with $O_2^{\bullet-}$ (Aruoma et al 1989). However, it has been reported that NAC acts as an indirect inhibitor of $O_2^{\bullet-}$ as it induced SOD2 expression in septic rat diaphragms (Figure 3.18d) (Barreiro et al 2005).

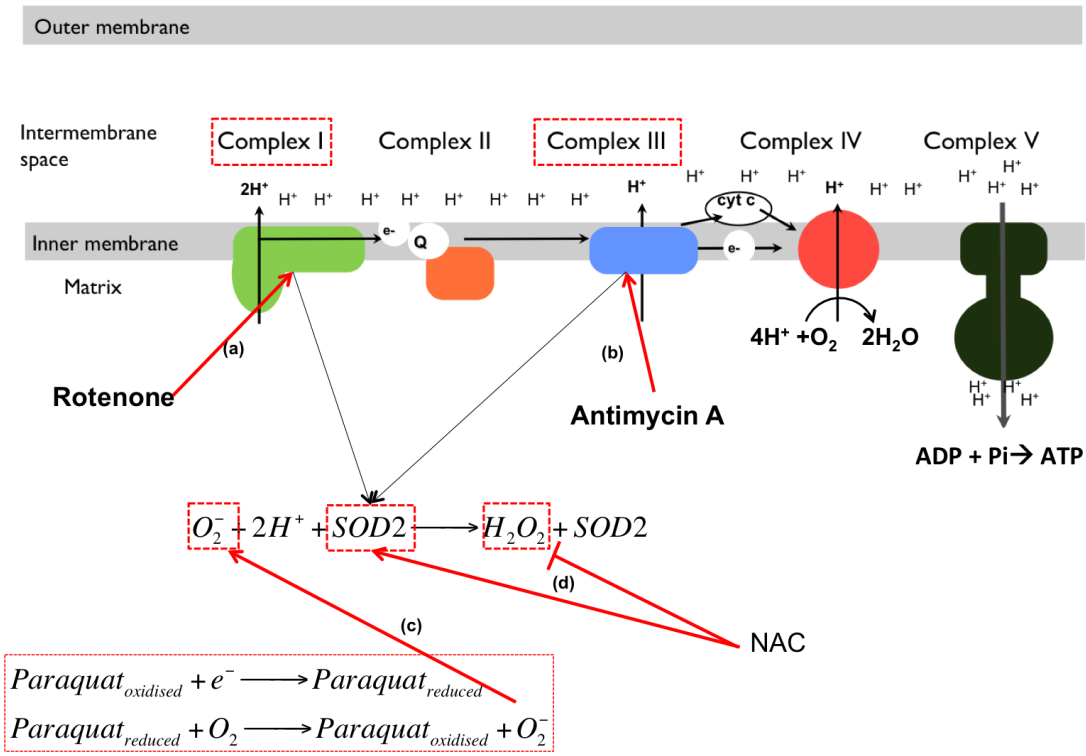

Figure 3.18 ROS regulation by ROS inducers and NAC (ROS scavenger)

Figure demonstrates the sites of action of different chemicals and how they affect the levels of ROS in the cell. (a) Rotenone is a complex I inhibitor that also increases the complex's $O_2^{\bullet-}$ production. (b) Antimycin A is a complex III inhibitor that also increases the complex's $O_2^{\bullet-}$ production. (c) Paraquat is reduced by electrons. Reduced paraquat is then oxidised by O_2 and this reaction produces $O_2^{\bullet-}$ as a by-product. (d) NAC scavenges H_2O_2 directly but also increases SOD2 levels thus reducing $O_2^{\bullet-}$ levels.

The effect of ROS inducers and NAC was evaluated both in SW1353 chondrosarcoma cells and HAC initially by confocal microscopy and FACS.

In SW1353 cells analysed by confocal microscopy (Figures 3.3 and 3.4), increasing concentrations of AMA caused an increase in ROS levels compared to control. However, the cell density after treatment with 100μM AMA was less compared to untreated and cells treated with 10μM AMA. This can suggest that high concentration of AMA may be toxic to SW1353 cells. However, this assumption was not tested. Treatment of SW1353 with a low concentration of paraquat and rotenone resulted in an increase in ROS levels compared to

control. Increasing the concentration of paraquat to 200μM caused a decrease in ROS levels both compared to the lower 100μM treatment and compared to untreated control. The exact cause of this decrease is not clear although, in leukocytes treatment with high concentration of paraquat induces SOD2 expression to dismutase the excess $O_2^{\cdot-}$ produced (Niwa et al 1990). Increasing the concentration of rotenone also caused a reduction of $O_2^{\cdot-}$ levels compared to lower concentration but the ROS levels were still significantly higher compared to control. The decrease in ROS may be due to the fact that the cell density was less after treatment with high doses of rotenone, which suggests that rotenone induces apoptosis (Li et al 2003). Treatment of cells with two different concentrations of NAC induced a similar level of reduction in the $O_2^{\cdot-}$ levels compared to control.

In HAC analysed by confocal microscopy (Figures 3.5 and 3.6), $O_2^{\cdot-}$ induction by AMA was inconsistent. Low concentrations of AMA resulted in a reduction of $O_2^{\cdot-}$ levels compared to control, whereas a higher concentration did not alter the levels of ROS. This result can possibly be due to the fact that HAC $O_2^{\cdot-}$ production is primarily dependent on complex I and therefore inhibiting the MRC at complex III using AMA does not have a pronounced effect on ROS production. However, this assumption has not been tested. Treatment of HAC with increasing concentrations of paraquat caused a proportional increase in the $O_2^{\cdot-}$ levels in the cells. Similarly, increasing concentrations of rotenone caused a proportional increase in the $O_2^{\cdot-}$ levels. Low concentration of NAC caused a reduction in $O_2^{\cdot-}$ levels compared to untreated control whereas increasing the concentration resulted in an increase in ROS levels compared to control. This can be possibly explained with the fact that high concentrations of NAC can be toxic to the cells as previously reported (Sprong et al 1998).

The data suggests that Mitosox-Red levels correlated with the $O_2^{\cdot-}$ levels in HAC and SW1353 chondrosarcoma cells. Also, we identified that NAC is effective at low concentrations in both HAC and SW1353 cells. In addition, in HAC, rotenone and paraquat were the most potent inducers of $O_2^{\cdot-}$ and therefore they can be used for future experiments if needed.

ROS levels were then analysed by FACS analysis (Figure 3.7). In SW1353 cells, only rotenone induced $O_2^{\cdot-}$ production significantly whereas, antimycin A and paraquat only induced slightly. NAC, however, highly decreased $O_2^{\cdot-}$ levels. In HAC, $O_2^{\cdot-}$ levels were not altered by either of the ROS inducers or by NAC. Cells from each treatment were then cytospun on microscope slides and their Mitosox-Red levels were also analysed by confocal microscopy in order to confirm the FACS results. In most of the cells, Mitosox-Red staining was not retained in the mitochondria and diffused into the cytoplasm of both HAC and SW1353 cells irrespective of the treatment (Figure 3.8). This can possibly be due to the fact that trypsin and in general cell detachment, causes change in the cytoskeleton and therefore can affect the mitochondria and as a result Mitosox-Red does not accumulate into the mitochondria and just diffuses into the cytoplasm (Kostal, & Arriaga 2011; Badley et al 1980).

3.5.3 Mitosox-Red and SOD2 dual staining is possible by saponin mediated permeabilisation but not by trypsin mediated permeabilisation

To examine the effect of SOD2 depletion on the $O_2^{\cdot-}$ levels in HAC, we had to be able to measure the Mitosox-Red and SOD2 protein levels simultaneously using confocal microscopy. Previous studies suggested that Mitosox-Red cannot be readily fixed due to the fact that its accumulation in the mitochondria depends partially on the $\Delta\psi m$ and fixing the cells might diminish the membrane potential and therefore the dye cannot be retained by the cell and the mitochondria (Robinson et al 2006; Robinson et al 2008). In our hands, fixing HAC and SW1353 cells did not affect Mitosox-Red staining (data not shown). Robinson *et al* recommended a protocol of staining live cells with Mitosox-Red, imaging them and at the same time recording the coordinates of the cells position relative on the microscope (Robinson et al 2008). Afterwards cells were fixed, blocked and then stained for the primary and secondary antibodies of choice. Then the cells were imaged again using the exact recorded coordinates (Robinson et al 2008). In this thesis, this protocol was attempted repeatedly however it was not successful due to technical difficulties to locate the exact position of the cells at the microscope after the antibody staining using the

coordinates recorded during the Mitosox-Red image taking. Therefore it was decided to attempt staining for both Mitosox-Red and SOD2 antibody and image them simultaneously. HAC were stained with Mitosox-Red while alive, then fixed, blocked and permeabilised using Triton-X. As described in Robinson *et al*, Mitosox-Red staining was not readily retained by the cell after Triton-X permeabilisation (Robinson et al 2008). In this thesis, this result was confirmed although SOD2 antibody staining was very clear (Figure 3.9). On the other hand, using saponin, Mitosox-Red staining was retained and the SOD2 antibody staining was satisfactory (Figure 3.10). This can be due to the different properties of saponin as a detergent or permeabilising molecule. Saponin acts mainly by solubilizing cholesterol to permeabilise the cell membrane without destroying it and leaves much of the membrane structure intact (Jacob et al 1991). The incubation time for saponin permeabilisation was optimized at 45min and therefore this protocol was used to simultaneously assess the levels of Mitosox-Red and SOD2 protein in HAC by confocal microscopy and flow cytometry.

While optimizing the saponin protocol, it was noticed that some HAC with higher SOD2 protein levels had lower Mitosox-Red levels and vice-versa. Therefore, to examine this further, HAC were isolated from seven different OA patients, stained with Mitosox-Red and anti-human SOD2 antibody and their fluorescence was assessed by flow cytometry (Figure 3.11). The result was inconclusive as five of the patients indicated a negative correlation between SOD2 and Mitosox Red, whereas two patients showed a positive correlation. Moreover, the correlation coefficients were very low, ranging from -0.22 to -0.35 for the five patients that showed a negative correlation, and 0.42 and 0.53 for the two patients with positive correlation. These results suggest that the expected negative correlation between $O_2^{\cdot-}$ and SOD2 levels possibly exists in HAC with some exceptions, but this observation is not consistent with the whole cell population. This can be due to the differences in SOD2 expression in cells from different zones of cartilage tissue (Scott et al 2010). However, as mentioned previously (section 3.4.3), Mitosox-Red is not readily retained in chondrocytes after trypsinisation, therefore these results might not be reliable in terms of the Mitosox-Red levels recorded.

3.5.4 SOD2 depletion causes a significant increase in superoxide levels in HAC mitochondria

Due to the nature of the FACS experiment, there was significant loss of HAC during the different incubations and washes. Also, the cells required trypsinisation prior to treatment with Mitosox-Red and this can also induce ROS as identified in other systems where trypsin induced ROS production in mouse lymphocytes and human lung fibroblasts (Lim et al 2006; Aoshiba et al 2001). Therefore, the assessment of the effect of SOD2 depletion on mitochondrial $O_2^{\cdot-}$ levels was performed on cells attached onto chamberslides (microscope slides) and cells were not treated with trypsin at any point. The fluorescence was then evaluated using a confocal microscope. HAC from cartilage of four different OA patients were transfected with SOD2 siRNA for 48hours and the effect on $O_2^{\cdot-}$ levels and SOD2 protein levels was assessed. In all four patients samples SOD2 siRNA depletion caused a significant decrease in SOD2 protein levels and a significant increase in mitochondrial $O_2^{\cdot-}$ levels as measured with Mitosox-Red (Figures 3.12 and 3.13). Therefore, SOD2 depletion can potentially have damaging effects to the cells due to oxidative damage caused by the increase in $O_2^{\cdot-}$ levels.

As described previously, SOD2 depletion is in homozygous mice has been associated with severe neurological and cardiac phenotypes possibly due to decreased Complex I and II activity, increased DNA damage and lipid peroxidation that have been linked with increased $O_2^{\cdot-}$ levels (Huang et al 2001; Li et al 1995; Lebovitz et al 1996; Melov et al 1999; Strassburger et al 2005). In OA, high levels of ROS have also been implicated with DNA damage (Chang et al 2005; Chen et al 2008), lipid peroxidation and activation of signalling pathways leading to increased collagenase expression and cartilage degradation (Tiku et al 2000; Shah et al 2005; Loeser et al 2002). Therefore, the increase in $O_2^{\cdot-}$ levels can lead to severe physiological phenotypes due to oxidative damage. As mentioned before, SOD2 depletion has been shown to have a chondroprotective effect in cartilage as it decreases IL-1 induced MMP-1 and MMP-13 expression possibly due to the reduced levels of H_2O_2 (Scott et al

2010). This is the first study that links the depletion of SOD2 in OA cartilage with an increase in $O_2^{\cdot-}$ in HAC *in vitro*.

3.5.5 SOD2 downregulation potentially induces lipid peroxidation in OA

As mentioned above, lipid peroxidation and DNA damage have been identified in OA, however, oxidative damage due to SOD2 depletion has only been reported in other systems. Also, the levels of lipid peroxidation in human OA and NOF cartilage have not been studied previously. To study this, a protocol for using the TBARS assay on cartilage homogenates was optimised (Figure 3.14). Three different amounts of cartilage were resuspended in the same volume of RIPA buffer and sonicated. A fixed volume of the resulting mixture was used in the assay. The amount measured from 50mg of cartilage was within the standard curve range and was considered optimum to measure MDA levels in NOF and OA cartilage samples. However, as mentioned in section 3.4.7, while transferring the supernatant of each sample after sonication, some cartilage homogenate was also transferred into the reaction mixture from the 50mg samples and a larger amount from the 100mg samples. This can explain the lower MDA levels in 100mg of cartilage compared to the MDA levels in 50mg as the presence of cartilage in the mixture can inhibit the reaction of TBA with MDA. Therefore, in order to avoid the presence of any cartilage in the samples, extra care was taken in order to transfer just the supernatant from the 50mg of OA and NOF cartilage samples that were examined. Eleven OA patient samples and eleven NOF patient samples were assayed. As expected, because of the absence of any cartilage in the reaction mixture, the MDA levels were significantly higher and well within the standard curve. OA cartilage samples were found to have significantly higher levels (although just 6.5% more) of MDA compared to NOF (Figure 3.15). This agreed with previous studies done *in vitro*, suggesting that lipid peroxidation is higher in OA (Tiku et al 2000; Shah et al 2005). It has been suggested that lipid peroxidation can lead to the oxidation and loss of collagen matrix (Tiku et al 2000; Tiku et al 2007). Also, Bonner *et al* demonstrated that lipids, especially polyunsaturated fatty acids, accumulate with normal ageing of human articular cartilage (Bonner et al 1975). Therefore, the higher levels of lipid peroxidation, can lead to the accumulation of oxidised collagen matrix and lead to matrix degradation and OA.

We hypothesized that the increase in MDA levels in OA cartilage is caused partially due to the decrease in SOD2 levels in OA. Previously it was suggested that low levels of SOD2 lead to higher MDA values in other systems (Strassburger et al 2005). To test this, SW1353 chondrosarcoma cells were treated with SOD2 siRNA and their MDA levels were compared to siControl using the TBARS assay protocol for cell cultures. SOD2 depletion led to a significant 2.5-fold increase in MDA levels in SW1353 cells suggesting that SOD2 downregulation contributes to the overall increase of lipid peroxidation in OA cartilage compared to NOF (Figure 3.16).

3.5.6 SOD2 downregulation can induce mtDNA strand breaks in SW1353 cells

Nuclear DNA and mtDNA damage, as mentioned above, has also been suggested to be higher in OA and in SOD2 knockout mice. mtDNA damage has been reported in livers of SOD2 heterozygous mice at 2–4 months of age (Williams et al 1998). However, the role of SOD2 downregulation in mtDNA strand break formation in chondrocytes has not been examined previously. SW1353 chondrosarcoma cells were treated with SOD2 siRNA and mtDNA strand break formation was evaluated and compared to the siControl treated cells. H_2O_2 treated cells were used as a positive control to make sure that the assay worked properly.

This assay was first described by Passos *et al* in 2007 (Passos et al 2007). In brief, a 11kb fragment of the major arc of the mtDNA was amplified using a long-range real-time PCR reaction. Any strand breaks in this region of the mtDNA prevent amplification of the full product by the Taq DNA polymerase and therefore a higher C_T value is recorded. This method can provide a quick indication of whether there are deletions present in the sample however it is not very helpful in terms of determining where the mutations are and whether they have a functional effect on mitochondrial respiration.

H_2O_2 induced a 42-fold mtDNA strand break formation compared to untreated control indicating that our assay worked (Figure 3.17). SOD2 depletion caused a significant 4.5-fold increase in mtDNA strand breaks, suggesting that SOD2 downregulation in chondrocytes contributes to oxidative mtDNA damage (Figure

3.17). The difference on the effect of H_2O_2 compared to the SOD2 RNAi treatment on mtDNA strand break formation could be due to the high concentration of H_2O_2 used in this assay although the duration of this treatment was much less compared to the RNAi treatment (one hour compared to 48 hours). The real-time PCR products were also screened for the presence of smaller fragments of mtDNA that could be formed from the repair of mtDNA molecules. Their presence could suggest the formation of large-scale mtDNA deletions, however no amplicons were observed. The presence of mtDNA deletions and strand breaks in OA cartilage, possibly caused by SOD2 downregulation in OA, was also assessed and it will be described in Chapter 4.

3.6 Conclusions

In summary, these results show that SOD2 depletion increases mitochondrial $O_2^{\cdot-}$ levels in HAC. As a result, the increase in $O_2^{\cdot-}$ levels induces higher levels of lipid peroxidation. Since, lipid peroxidation was higher in OA cartilage compared to NOF, these results suggest that SOD2 downregulation in OA can potentially induce lipid peroxidation in OA cartilage. Also, SOD2 depletion contributes to the formation of mtDNA strand breaks in SW1353 mitochondria however no large-scale deletions have been identified. When taken together, these results suggest that the SOD2 downregulation observed in OA cartilage compared to NOF can lead to oxidative damage in terms of lipid peroxidation and mtDNA damage that can potentially contribute to oxidation and loss of collagen and mitochondrial and cellular dysfunction, leading to cartilage degradation.

Chapter 4. Large-scale mtDNA deletions and mtDNA copy number in cartilage and other joint tissues

4.1 Hypothesis

Reduced expression of SOD2 causes long term accumulation of large-scale mtDNA deletions in cartilage due to increased ROS levels. This in turn may alter the mtDNA copy number in cartilage.

4.2 Introduction

In the previous chapter it was demonstrated that SOD2 downregulation resulted in increased levels of mitochondrial $O_2^{\cdot-}$. This downregulation also caused increased levels of lipid peroxidation in chondrocytes that was also apparent in OA cartilage, where SOD2 is reduced, compared to NOF (Scott et al 2010; Ruiz-Romero et al 2009; Aigner et al 2006). SOD2 depletion also caused mtDNA damage in the form of strand breaks in chondrocytes. As a result, mtDNA strand breaks might accumulate in OA cartilage compared to NOF. In addition, damage in mtDNA can be in the form of large-scale deletions, especially in post-mitotic tissue such as cartilage (Aigner et al 2001; Henrotin et al 2005). Also the mtDNA copy number could alter to compensate for the damage caused by SOD2 depletion.

mtDNA is close to the MRC machinery and the major free radical production sites (complex I and complex III) and therefore directly exposed to oxidative damage (Beckman, & Ames 1999). It has no histones and as a result the DNA is exposed and thus prone to damage from molecules such as ROS. Errors in mtDNA repair have been linked with the higher mutation rate in ageing tissues. Experiments on mice with an error-prone POLG, resulted in a 3-8 times higher number of somatic mtDNA mutations in most tissues compared to the wildtype. The mutant mice have deficiencies in the MRC, premature ageing features and reduced lifespan (Trifunovic et al 2004; Trifunovic et al 2005; Kujoth et al 2005). mtDNA damage was also reported in livers of SOD2 heterozygous mice (C57BL/6 background) at 2–4 months of age (Williams et al 1998).

Deletions are the primary cause of somatic mtDNA mutation in post-mitotic tissues, e.g. skeletal muscle, heart and brain, possibly due to the fact that these cells are non-dividing and therefore less exposed to purifying selection of mtDNA deletions (Cortopassi et al 1992). mtDNA deletions can be observed more often in aged post-mitotic tissues and individuals with neurodegenerative diseases such as Parkinson disease (Bender et al 2006; Kraytsberg et al 2006; Cortopassi et al 1992). As described in section 1.1.6, the mechanisms for mtDNA deletion generation include recombination (Mita et al 1990), slip-replication{Shoffner 1989), and double-strand break repair (Krishnan et al 2008) and these involve direct repeats, flanking the breakpoint, in mtDNA (Figure 1.5). Recently, a study has suggested that mtDNA deletions are not caused by direct repeats but by stable secondary structures that can form between distant segments of the mitochondrial genome (Guo et al 2010).

In OA, mtDNA deletions were reported in relation to the accumulation of the 4977bp (common deletion) (Chang et al 2005; Schon et al 1989; Shoffner et al 1989; Cortopassi et al 1992). The occurrence of this deletion was found to be higher in OA cartilage compared to healthy controls and was also higher in aged non-OA cartilage compared to young non-OA cartilage (Chang et al 2005). IL-1β and TNF-α have been shown to regulate apoptosis in OA chondrocytes by the induction of mtDNA damage and reduction in mitochondrial transcription and ATP production (Kim et al 2009). In the same study, NO and $O_2^{\cdot-}$ were also induced by IL-1β and TNF-α however NO was suggested as the main factor responsible for mtDNA damage accummulation after cytokine exposure. The authors also reported that OA chondrocyte mitochondria were more susceptible to mtDNA damage compared to NOF. It has been suggested that chondrocytes, especially OA chondrocytes, have reduced mtDNA repair capacity and cell viability following exposure to ROS (Grishko et al 2008). This evidence can support and can be supported by the hypothesis that mtDNA deletions in post-mitotic tissues, such as cartilage (Aigner et al 2001; Henrotin et al 2005), arise due to inefficient mtDNA repair (Krishnan et al 2008). However, the presence of other large-scale mtDNA deletions in cartilage and other joint tissue has not been studied extensively and any changes in mtDNA copy number in OA compared to healthy controls remain undefined.

4.3 Aims

- Evaluate the levels of mtDNA strand breaks in OA and NOF cartilage
- Determine changes in the functionality of the MRC potentially due to the mtDNA damage in chondrocyte mitochondria
- Identify and quantify mtDNA deletions and copy number in single isolated chondrocytes
- Evaluate mtDNA deletions in OA patient cartilage samples and other joint tissue and compare these with cartilage from healthy controls
- Quantify mtDNA copy number in OA patient cartilage samples and other joint tissue and compare these with cartilage from healthy controls

4.4 Results

4.4.1 mtDNA strand breaks in NOF and OA cartilage

As shown in Chapter 3 (section 3.4.8), SOD2 depletion in SW1353 cells leads to a 4.5 fold increase in mtDNA strand breaks (Figure 3.17). Therefore, mtDNA strand break accumulation in OA cartilage potentially due to SOD2 downregulation was evaluated. 12 NOF total DNA samples and 9 hipOA total DNA samples from cartilage were screened for mtDNA strand breaks using the same assay in order to determine whether SOD2 downregulation causes mtDNA damage in OA.

Total DNA was extracted from NOF and OA hip cartilage using the EZNA method as described in section 2.4.1. A fixed amount of total DNA was analysed by real-time PCR amplification of part of the major arc of the mtDNA. C_T values were normalized to the C_T values of MTND1 levels (which is not commonly deleted) to ensure evaluation of mtDNA strand breaks in equal number of mtDNA molecules in each patient sample.

OA cartilage had 8% higher levels of mtDNA strand breaks compared to NOF, however this difference was not statistically significant (Figure 4.1). To ensure that the assay can detect mtDNA damage efficiently, H_2O_2 treated and untreated SW1353 cells were also screened for mtDNA strand breaks as in section 3.4.8. H_2O_2 induced a 40-fold mtDNA strand break formation compared to untreated control indicating that the assay can detect mtDNA damage (data not shown).

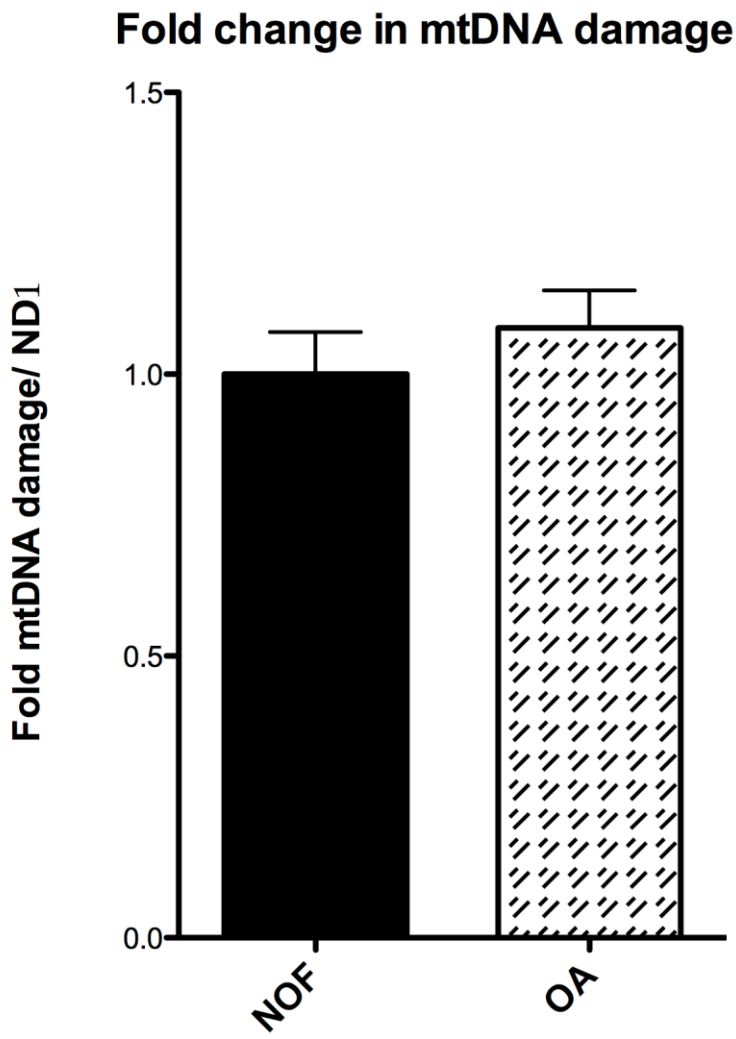

Figure 4.1 Strand break assay for NOF and OA mtDNA

Cartilage from OA and NOF femoral head replacement surgery was homogenised and total DNA was extracted using the EZNA kit following the manufacturer's protocol as in section 2.4.1. DNA was equalised to 10ng/µl and 50ng of DNA were used to assess the levels of mtDNA damage by real-time PCR as described in section 2.4.8. Mitochondrial gene MTND1 was used as normalisation reference. mtDNA amplification was normalised to the level of MTND1 using the calculation $2^{-\Delta C}{}_{T}$, were ΔC_T represents C_T (target gene) – C_T (MTND1).Figure represents the fold difference in mtDNA strand breaks in OA tissue compared to NOF. (NOF; n=12, median age = 79yrs OA; n=9, median age = 77yrs). No statistical difference was determined between NOF and OA samples (Mann Whitney U test).

4.4.2 Cytochrome c oxidase- Succinate Dehydrogenase (COX-SDH) reaction on cartilage sections and isolated chondrocytes

COX-SDH reaction indicates the presence of MRC dysfunction. COX is a mitochondrial complex (complex IV) with subunits encoded by both the mitochondrial and the nuclear genome, while SDH is a MRC complex (complex II) that is entirely encoded by the nuclear genome. 3,3'-diaminobenzidine (DAB) is added in the COX incubation medium as it is an effective electron donor and facilitates the reaction of COX (Seligman et al 1968). Nitroblue tetrazolium salt (NBT), an electron acceptor, is added in the SDH incubation media and facilitates the reaction of SDH (Old, & Johnson 1989; Cottrell et al 2001). Cells with functioning COX produce the brown reaction product associated with COX activity and saturate the cells. The presence of the brown, COX positive, reaction product suggests normal MRC activity and possibly no mitochondrial dysfunction (Old, & Johnson 1989; Johnson et al 1993). Cells with dysfunctional COX will not be saturated by the DAB product and therefore allow demonstration of SDH activity by the reduction of NBT, to a blue formazan product (Old, & Johnson 1989; Johnson et al 1993). Identification of COX-deficient cells is a useful indicator of mtDNA involvement in mitochondrial dysfunction.

COX-SDH reaction on cartilage sections

COX-SDH histochemistry was performed on cartilage sections in order to assess mitochondrial respiratory activity and determine whether mtDNA mutations are present in chondrocytes. However, the reaction did not work under any condition investigated. Multiple incubation times of each reagent were used as well as sections from different patient samples. This experiment was performed multiple times with the same negative result. This could be due to low permeability of cartilage to the COX-SDH incubation media or due to low expression of the MRC enzymes in those chondrocytes.

COX-SDH reaction on cultured HAC

Since it was not possible to investigate COX-SDH activity of cartilage chondrocytes directly on cartilage tissue sections, we decided to carry out the experiment on isolated HAC cultured in chamberslides as in section 2.6.2. The same COX-SDH histochemistry protocol was performed as on cartilage sections. COX positive cells produced a brown reaction product and COX deficient cells a blue reaction product (SDH reaction product).

On adherent cultured HAC, the SDH reaction worked well at 50 minutes but the COX reaction required 90 minutes to become visible (Figure 4.2). Sequential reaction was not successful possibly due to the lengthy COX-reaction. Cells were probably saturated with the very weak DAB reaction product that interferes with the binding and reduction of NBT in the SDH incubation media. Five patient samples were tested with identical results.

The COX reaction product was weak possibly due to the fact that HAC are considered mainly glycolytic cells and with low mitochondrial respiration (Stockwell 1983; Lee, & Urban 1997). Furthermore, the culture of HAC in high glucose media can favour glycolysis instead of mitochondrial respiration adding to the reason why COX activity is low and hard to detect (Gohil et al 2010).

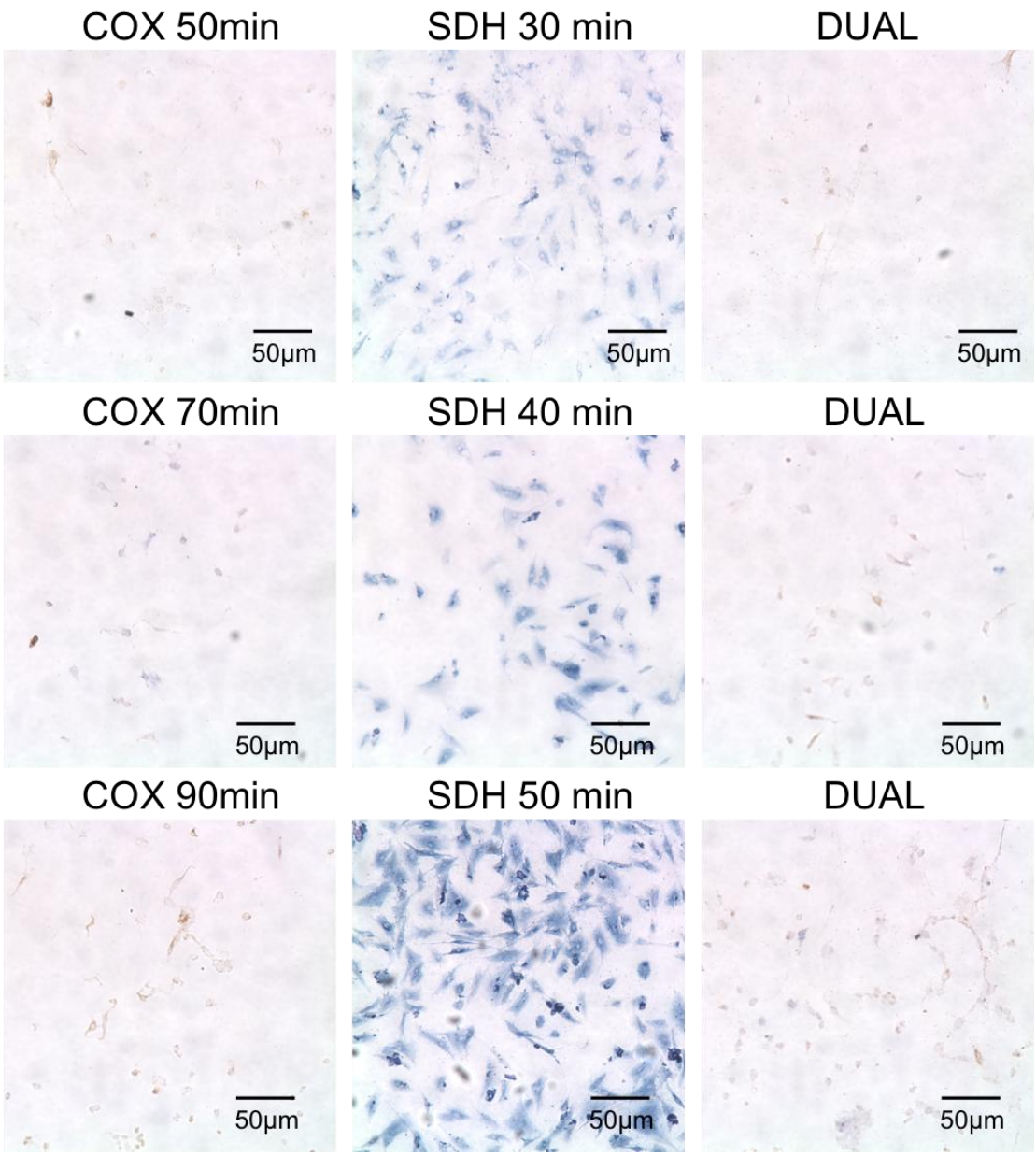

Figure 4.2 COX-SDH activity of adherent cultured HAC.

HAC were isolated from human knee cartilage and cultured for 10 days as described in section 2.3.1. Then cells were trypsinised, seeded in chamberslides and left to adhere for 24 hours. COX-SDH reaction was performed as in section 2.6.2. COX-positive cells produced a brown reaction product and COX-deficient cells produced a blue product. Cells were then visualised under a light microscope (x20 magnification).

COX-SDH reaction on freshly isolated HAC

Freshly extracted HAC were then cytospun directly after digestion from cartilage and COX-SDH activity was assessed in order to avoid any loss of activity due to mitochondrial dysfunction during culturing and the high glucose levels favouring glycolysis. On freshly extracted HAC, both reactions were performed efficiently (Figure 4.3). The COX reaction was optimised at a smaller incubation time (60 min) and the SDH reaction was best at 65min as described in section 2.6.2. The incubation times for chondrocytes were different to the incubation times optimised for a more mitochondrially active tissue such as muscle where the COX reaction has been optimised at 50mins and the SDH reaction at 45min (Krishnan et al 2010).

Cells reacted reasonably well for both COX and SDH activity. COX-deficient chondrocytes were found but their number was very low (≤1%) compared to the COX- positive cells. Cells were then isolated into sterile tubes, according to COX activity, using laser capture microdissection, and were screened for mtDNA deletions and mtDNA copy number levels.

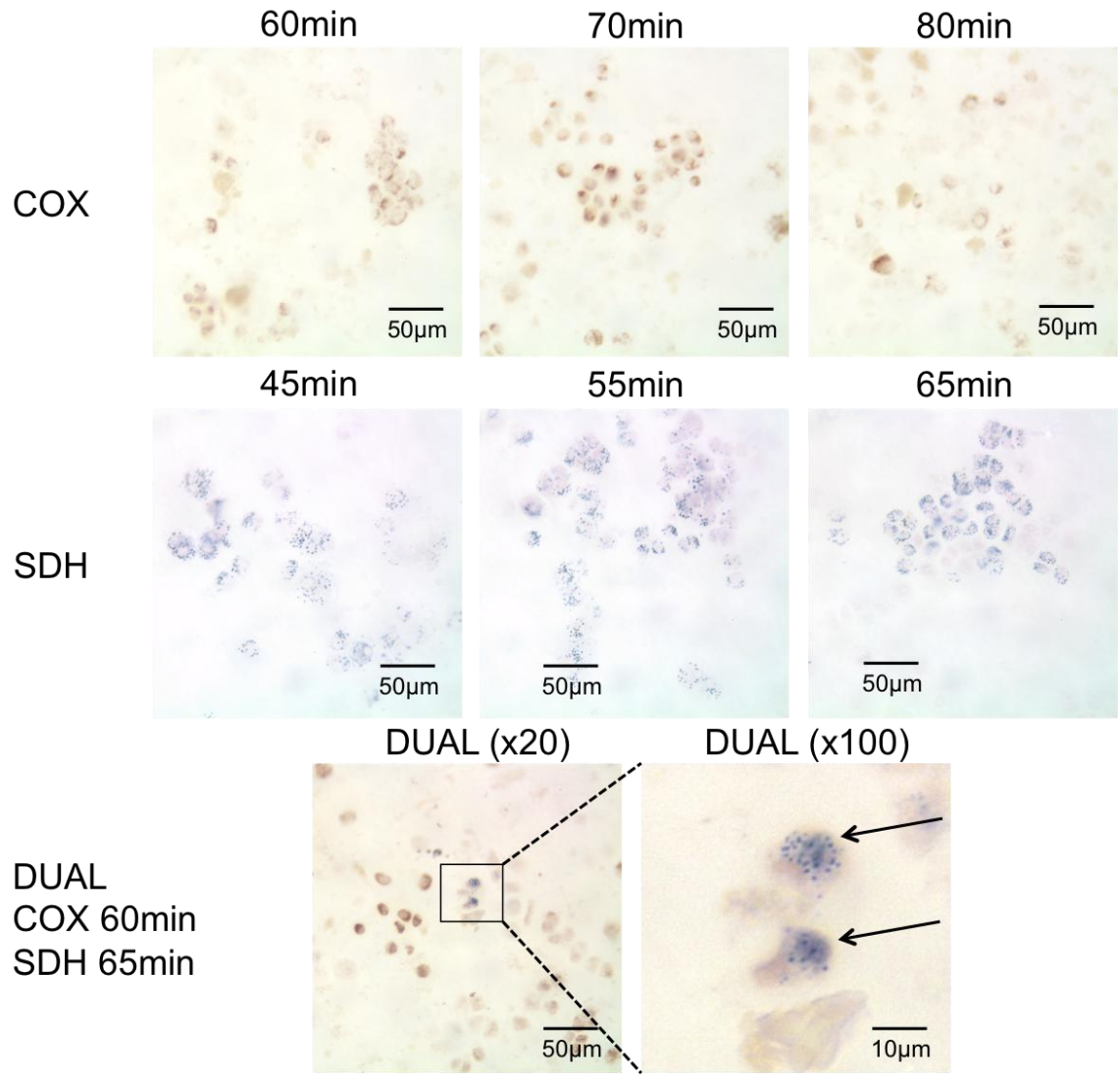

Figure 4.3 COX-SDH activity of freshly extracted cytospun HAC

HAC were isolated from human knee cartilage as in section 2.3.1 and then cytospun for 10mins at 800 x *g* onto 2µm polyethylene napthalate (PEN)-membrane slides. COX-SDH reactions were performed as in section 2.6.2. The optimum reaction conditions are shown in the dual reaction images. Cells were visualised under a light microscope. COX positive (brown) and COX-deficient cells (blue) were laser microdissected into sterile 0.2ml Eppendorf tubes. Figure shows staining from one patient sample and is representative of 5 separate successful experiments.

4.4.3 mtDNA copy number in COX positive and COX deficient chondrocytes.

Microdissected chondrocytes were pooled (50 cells) and lysed as in section 2.4.4 and the mtDNA copy number was assessed using real-time PCR amplification of MTND1. A standard curve of MTND1 copy number was used to quantify the mtDNA copy number (Figure 4.4). Table 4.1 shows the mtDNA copy number in COX-deficient and COX positive chondrocytes. Analysis of five patient samples suggested that there is no difference in the levels of mtDNA copies in COX positive and COX negative HAC. All the values were within the range of the standard curve. Three patients had more copies in the COX deficient cells (4550- 6800 copies per cell) compared to the COX-positive cells (3050-5800 copies per cell). Conversely, two patients had more copies in the COX positive cells (5400-6123) compared to the COX-deficient cells (940-3200). mtDNA copy number was attempted to be measure in single cells however the findings were very inconsistent and the *Ct* values very similar to the negative controls, therefore this experiment was not pursued further(data not shown).

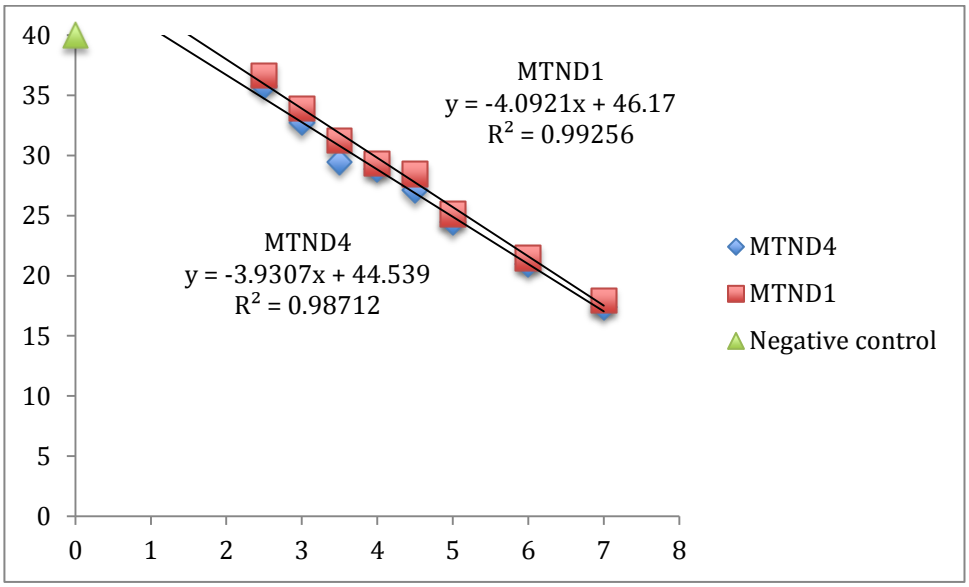

Figure 4.4 MTND1 and MTND4 standard curves

Real-time PCR reactions to determine standard curves for MTND1 and MTND4 levels were performed with every MTND1/MTND4 experiment as described in section 2.4.8. Negative controls were also used to ensure there was no contamination in the reaction mixture. Templates for both MTND1 and MTND4 were used to determine the standard curve in each real-time PCR reaction. The standard curves were used to calculate mtDNA copy number in HAC and to assess the presence of deletions.

	mtDNA copies/cell	
Patient ID	**COX- positive**	**COX- deficient**
N1946	5800 ± 1000	6800 ± 1400
N1950	4224 ± 800	4550 ± 1600
N1951	3050 ± 1200	5000 ± 2700
N2012	5400 ± 1600	3200 ± 500
N2024	6123 ± 2100	940 ± 45

Table 4.1 mtDNA copy number in COX positive and COX deficient HAC

Pools of 50 cells were isolated by laser microdissection and then lysed as in section 2.4.3. Cell lysates were used in a real time-PCR reaction as in section 2.4.8. mtDNA copy number was calculated using the MTND1 standard curves. Cells from 5 different patients were assessed and the reactions were performed in triplicate and the average number of mtDNA copies per cell and the standard deviation were calculated.

4.4.4 mtDNA deletions in single isolated chondrocytes

Single microdissected chondrocytes were lysed as in section 2.4.3 and screened for mtDNA deletions using real-time PCR amplification of the mitochondrial MTND1 and MTND4 regions. A standard curve of MTND1 and MTND4 copy number was used to quantify the levels of MTND1 and MTND4 copies in our samples (Figure). MTND1 is used as the control region since few deletions are found in this region of the mtDNA. Conversely, the majority of the mtDNA deletions (97% of those listed on MITOMAP) occur in the major arc of the mtDNA and remove part or all of MTND4, therefore it was used as a marker for mtDNA deletions ([NO STYLE for: Mitomap 2006]). The difference in the levels of MTND1 copies compared to MTND4 levels was determined as a percentage. A negative value suggests that more MTND1 copies have been detected compared to MTND4 copies suggesting the presence of mtDNA deletions in the MTND4 region. The results suggest that there is no significant difference between the level of deletions found in COX positive and COX-deficient chondrocytes (Figure 4.5). NOF patient 2030 had average heteroplasmy values of -51% in COX-deficient cell compared to -53% in COX-positive cells. OA patient 2042 had average heteroplasmy values of -40% in COX-deficient cells compared to -30% in COX-positive cells. These differences were not statistically significant.

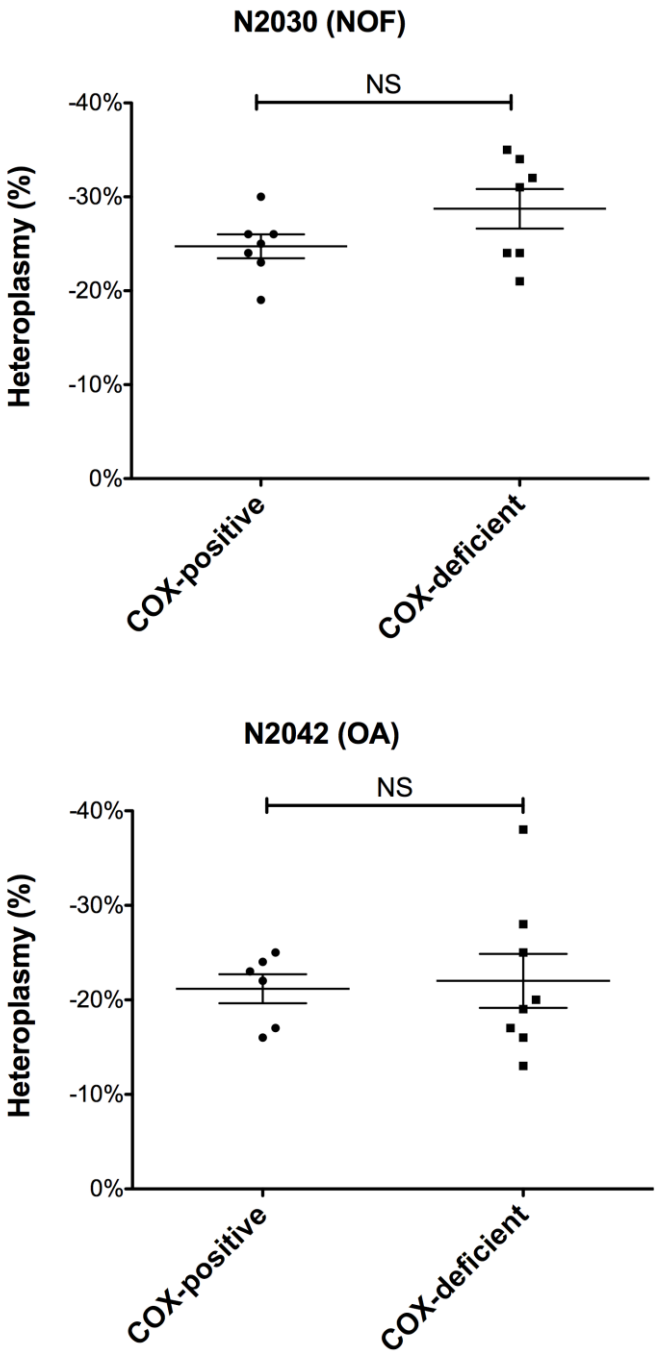

Figure 4.5 mtDNA deletions in single isolated HAC

Single HAC were isolated by laser capture microdissection and lysed as in section 2.4.3. Cell lysates were used in a multiplexed MTND1 and MTND4 real-time PCR reaction as in section 2.4.8. MTND1 and MTND4 copy values were calculated using the MTND1/MTND4 standard curves. mtDNA heteroplasmy values were calculated using the MTND1 and MTND4 copy values as described in section 2.4.8. Seven single cells from 2 different patients were assessed and the reactions were performed in triplicate. N2030 and N2042 indicate the patient number and COX-positive and COX-positive indicate the COX reactivity of the isolated cells. The scale on the y-axis indicates the average percentage heteroplasmy of each cell. Negative values indicate the presence of less MTND4 copies compared to MTND1. No statistical significance was determined between COX-positive and COX-deficient cells (Mann Whitney U test).

4.4.5 mtDNA large-scale deletions in cartilage tissue samples

Assessment of mtDNA damage based on the COX- activity in isolated chondrocytes produced inconsistent results. Therefore, we decided to screen for mtDNA deletions in DNA extracted from whole cartilage tissue. mtDNA of cartilage from OA knees, OA femoral heads and NOF was amplified using long amplification PCR reactions for a 9.9kb region spanning the D-loop of the mtDNA as described in section 2.4.8. PCR products were then separated by agarose gel electrophoresis (Figure 4.6), with fragments smaller than 9.9kb indicative of presence of deletions within the mtDNA. These fragments were isolated, cloned and further analysed by sequencing in order to characterise the mtDNA deletion breakpoint region. The results are summarized in Figure 4.7 and Table 4.2. Briefly, two mtDNA deletions were identified in the two OA hip patient samples and two deletions were identified in one OA knee patient sample. No mtDNA deletions were sequenced in NOF patient samples. Sequences were also analysed using BLAST analysis to identify whether there was any similarity at the breakpoints of the deletions ([NO STYLE for: BLAST 1990]). As shown in Table 4.2, only one mtDNA deletion in one patient was found to contain a direct repeat in the mtDNA sequence. The flanking regions of the deletions in the other two patients showed minor or no homology. Additionally, the intensity of the smaller amplicons was lower compared to the wildtype PCR amplicon indicating the presence of significantly reduced levels of mutated DNA (~1%) compared to wild type.

Also as shown in Figure 4.6, a 1.6kb amplification product was visible in PCR products of patient samples. Sequencing analysis of that amplicon has shown that it was an artifact of the PCR reaction as is showed no homology with any region of the mtDNA.

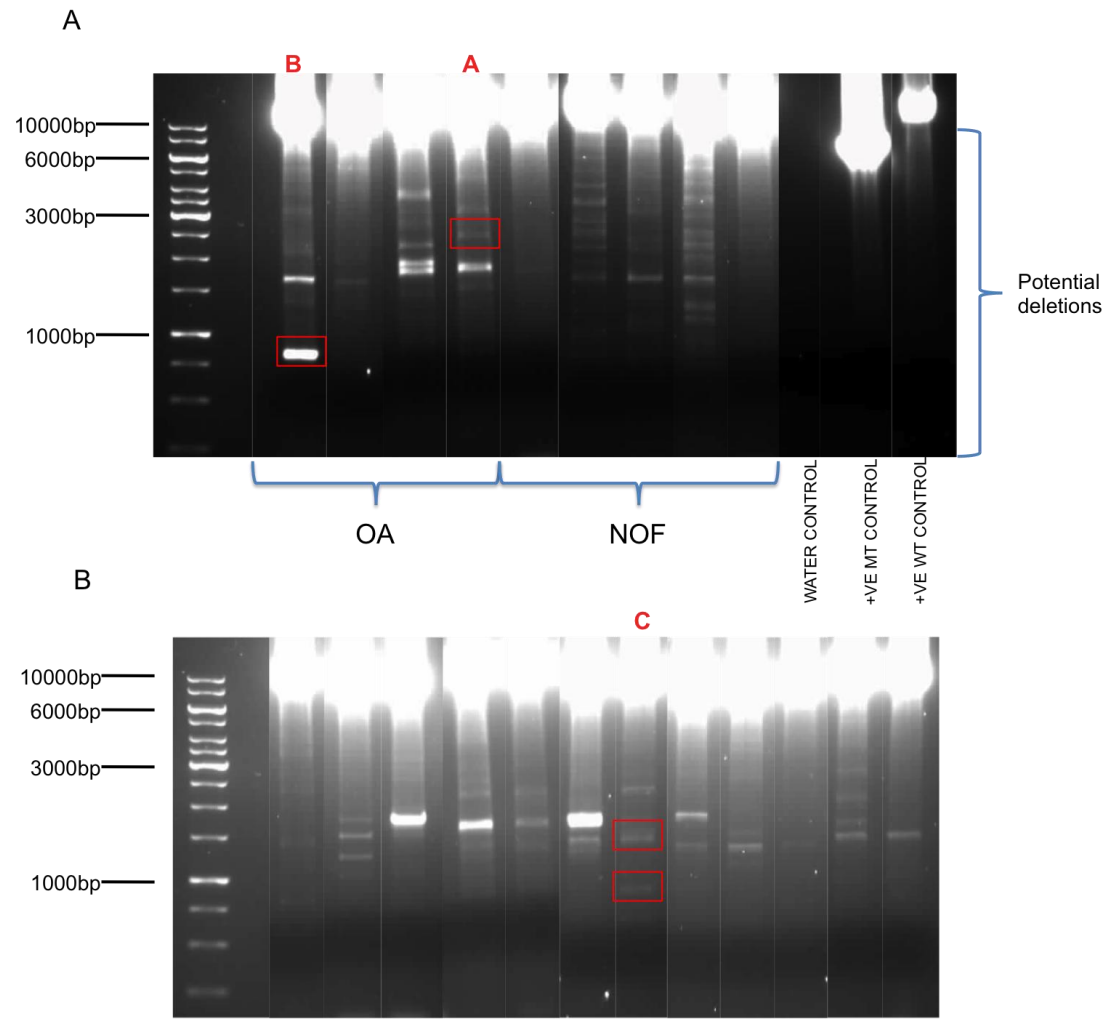

Figure 4.6 Long-amplification PCR reactions of whole tissue cartilage samples from OA and NOF patients

Cartilage from (A) OA (median age = 77yrs) and NOF (median age = 78yrs) femoral head and (B) OA knee (median age = 69yrs) replacement surgery was homogenised and total DNA was extracted using the EZNA kit following the manufacturer's protocol as described in section 2.4.1. DNA was equalised to 10ng/µl and 50ng of DNA were used in long-range amplification reactions of an approximately 10kb region of the mtDNA as in section 2.4.8. PCR products were separated by 0.8% agarose gel electrophoresis. Amplicons that were smaller than the wildtype 10kb amplicon suggest that deletions are present. Those amplicons were extracted, gel purified and analysed by sequencing as described in sections 2.4.9 and 2.4.10. Red boxes show the amplicons of samples where deletions have been identified and are shown in Figure 4.7.

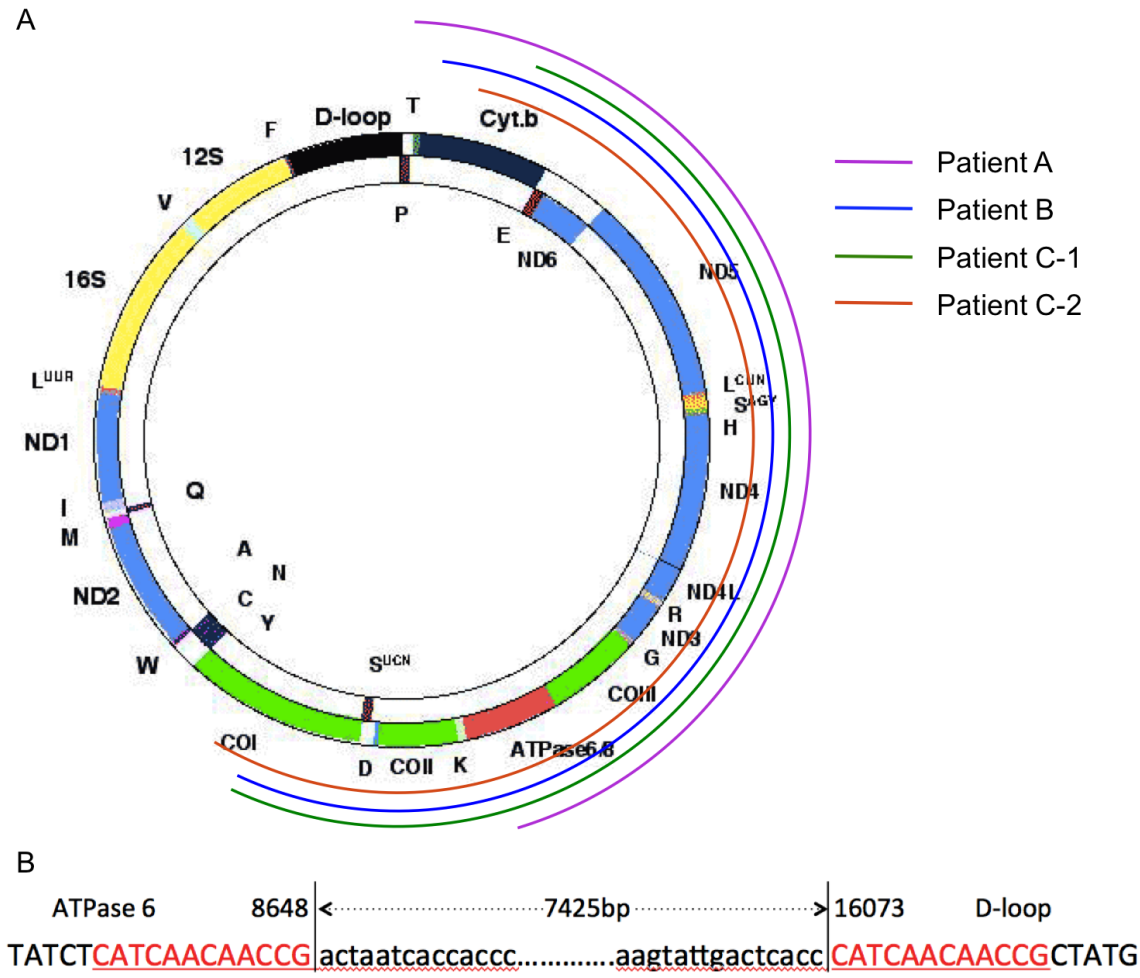

Figure 4.7 Summary diagram of mtDNA deletions identified in cartilage

Sequences were analysed using 4 Peaks sequence viewer and BLAST search. Deletions were confirmed by sequencing in both directions. (A) Curved lines are showing the position and the size of four deletions identified in cartilage from 3 OA patients. (B) The 7425bp deletion identified in Patient A. Vertical lines and numbers show the position of the breakpoint and within the lines the deleted region. The red and underlined nucleotides indicate the repeat sequences flanking the breakpoints.

Sample ID	Joint type	Tissue	Sex	Age	Break points	Size	Breakpoint homology/ repeats
Patient A	OA Hip	Cartilage	Male	85	8648-16073	7425	CATCAACAACCG
Patient B	OA hip	Cartilage	Female	76	6782-15880	9098	ATTT
Patient C-1	OA knee	Cartilage	Male	60	6783-15355	8572	TTT
Patient C-2	OA knee	Cartilage	Male	60	6364-15675	9311	None

Table 4.2 Summary patient information and mtDNA deletions identified in cartilage

Sequences were analysed for the presence of sequence repeats and homology between the breakpoints. Patient A had a 13bp repeat sequence identified between the breakpoints. Patients B and C had very minor homology. Patient C had one extra deletion identified that did not have any homology between the breakpoints.

4.4.6 mtDNA large-scale deletions in other joint tissue samples

Other joint tissue samples, such as cortical bone, cancellous bone, meniscus, synovium, ligament, osteophytes and fat pad from OA patients were also screened for large-scale mtDNA deletions. No healthy control samples for these tissues were available. As described above, total DNA was extracted from the tissues and mtDNA was amplified using long amplification PCR. The products were separated by agarose gel electrophoresis (Figure 4.8) and amplicons smaller than 9.9kb were isolated and analysed. The results are summarized in Figure 4.9 and Table 4.3. Briefly, three mtDNA deletions were identified in cortical bone samples from a single patient. Another deletion was identified in osteophyte samples from the same patient. A mtDNA deletion was identified in synovium samples from two different patients. These deletions were also analysed using BLAST for homology between the breakpoint regions. The flanking regions of the deletions in all three patients showed minor or no homology at all. As with cartilage samples there was amplification of a 1.6kb amplicon in the PCR reactions of some patient samples. Sequencing analysis of that amplicon has shown that it was a PCR amplification artifact in most of the cases due to the presence of sequences of no homology with any region of the mtDNA and also due to the absence of the primers used in the PCR reaction. Additionally, the intensity of the smaller amplicons was lower compared to the wildtype PCR amplicon indicating the presence of significantly reduced levels of mutated DNA (~1%) compared to wild type.

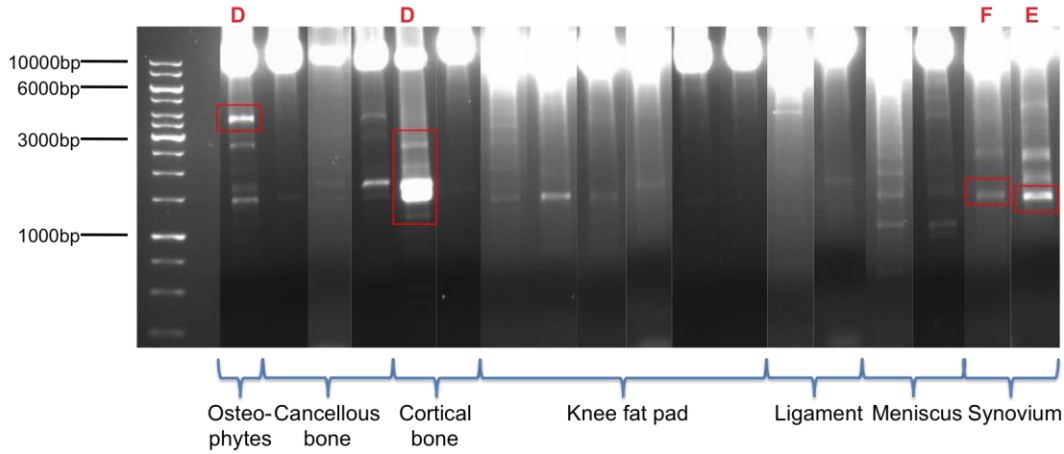

Figure 4.8 Long-amplification PCR reactions of other joint tissue samples from OA patients

Tissue from OA replacement surgery was homogenised and total DNA was extracted using the EZNA kit following the manufacturer's protocol. DNA was equalised to 10ng/µl and 50ng of DNA were used in long-range amplification reactions of an approximately 10kb region of the mtDNA as in section 2.4.8. PCR products were separated by 0.8% agarose gel electrophoresis. Amplicons that were smaller than the wildtype 10kb amplicon suggest that deletions are present. Those amplicons were extracted, gel purified and analysed by sequencing as described in section 2.4.9 and 2.4.10. Red boxes show the amplicons of samples where deletions have been identified and are shown in Figure 4.9.

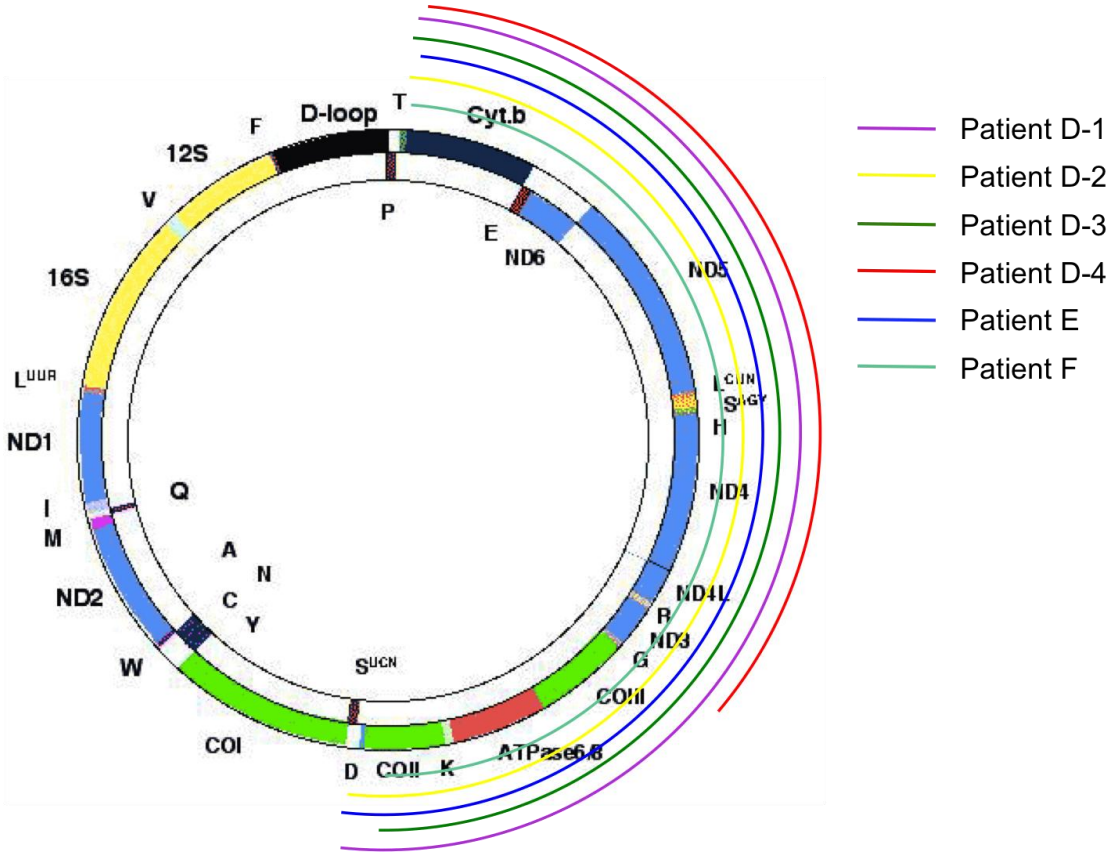

Figure 4.9 Summary diagram of mtDNA deletions identified in other OA joint tissues

Sequences were analysed using 4 Peaks sequence viewer and BLAST search. Deletions were confirmed by sequencing in both directions. Curved lines are showing the position and the size of 6 deletions identified in joint tissue from 3 OA patients.

Sample ID	Joint type	Tissue	Sex	Age	Break points	Size	Breakpoint homology/ repeat
Patient D	OA hip	Cortical bone	Male	85	7464-15906	8442	TTA
Patient D	OA hip	Cortical bone	Male	85	7547-15955	8408	TTTGT
Patient D	OA hip	Cortical bone	Male	85	7791-15888	8097	GGCAGG
Patient D	OA hip	Osteophytes	Male	85	10059-15922	5863	GTTTA
Patient E	OA knee	Synovium	Male	79	7449-15993	8544	CTTT
Patient F	OA Hip	Synovium	Male	60	7764-15916	8152	None

Table 4.3 Summary patient information and mtDNA deletions identified in other joint tissue

Sequences were analysed for the presence of sequence repeats and homology between the breakpoints. Patients D and E had very minor homology. Patient F did not have any homology between the breakpoints.

4.4.7 mtDNA copy number in cartilage and other OA joint tissue samples

mtDNA copy number quantification was performed in the same samples analysed above. Total DNA was used in two separate SYBR Green real-time PCR reactions amplifying the mitochondrial MTND1 gene and the nuclear β-2-microglobulin (b2m). MTND1 amplification values were normalized using the b2m amplification values from the same samples. As shown in Figure 4.10A, there were on average 2000 mtDNA copies/cell (1000 mtDNA copies per b2m copy) in NOF cartilage, 1500 mtDNA copies/cell (750 copies/b2m) in OA hip and 1700 mtDNA copies/cell (850 copies/b2m) in OA knee. There was no significant difference between these groups.

Other joint tissue samples showed a variable range of mtDNA copies ranging from 400 mtDNA copies/cell (200 mtDNA copies per b2m copy) in fat pad to 4200 mtDNA copies/cell (2100 copies/b2m) in cancellous bone (Figure 4.10B). No healthy controls of other tissue samples were available to perform statistical analysis.

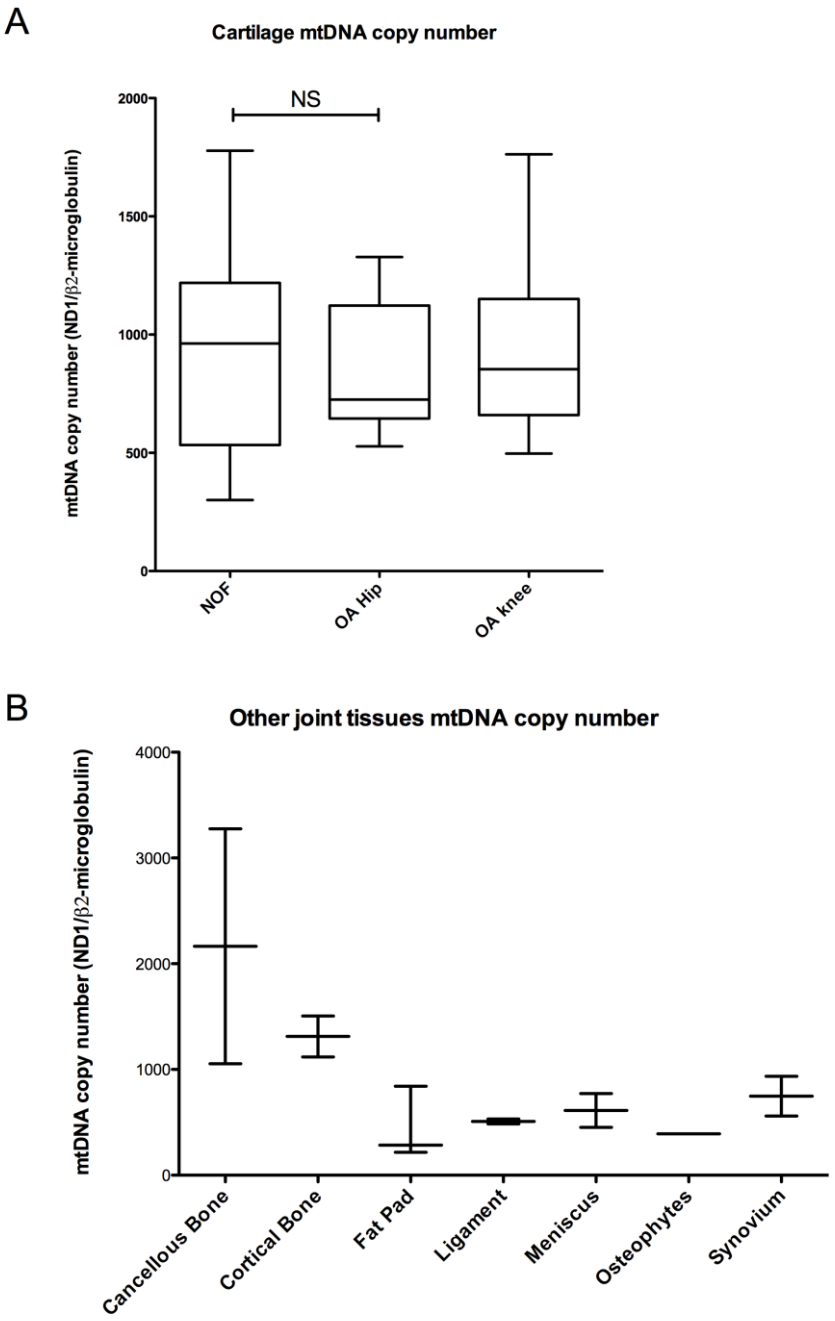

Figure 4.10 mtDNA copy number per β-2-microglobulin copy in cartilage and other joint tissue

(A) Cartilage and (B) other joint tissue from OA and NOF femoral head and OA knee replacement surgery was homogenised and total DNA was extracted using the EZNA kit as described in section 2.4.1. 10ng of DNA were analysed for mitochondrial gene MTND1 levels and normalised to B2M levels. (NOF; n=18, OA Hip; n=10, OA Knee; n=12, Cancellous Bone; n=3, Cortical Bone; n=2, Fat Pad; n=5, Ligament; n=3, Meniscus; n=2, Osteophytes; n=1, Synovium; n=2). Lines within the boxes represent the median, the boxes represent the 25th and 75th percentiles and the lines outside the boxes correspond to the minimum and maximum values.

4.5 Discussion

As described in Chapter 3, SOD2 downregulation in chondrocytes resulted in an increase in mitochondrial $O_2^{\cdot-}$ levels and oxidative damage in the form of high levels of lipid peroxidation and mtDNA strand breaks compared to control. Evidence of higher lipid peroxidation in OA tissue compared to NOF was also demonstrated.

SOD2 downregulation has been previously associated with DNA damage in in SOD2 knockout mice due to higher levels of mitochondrial $O_2^{\cdot-}$ (Melov et al 1999; Strassburger et al 2005). In OA, different studies have identified DNA damage in the form of total DNA base modifications (8-oxo-guanine) and strand breaks in total DNA however no study has associated DNA damage in OA to the reduced SOD2 expression compared to NOF (Chang et al 2005; Chen et al 2008; Kim et al 2009; Scott et al 2010).

In this chapter, different methods are employed to evaluate the levels of mtDNA damage in OA and NOF cartilage and other OA joint tissues, which are potentially acquired due to the decrease in SOD2 levels in OA and the increase of $O_2^{\cdot-}$ levels in chondrocytes.

mtDNA is localised in the mitochondrial matrix and is in close proximity to inner membrane where the main sites of $O_2^{\cdot-}$ production are found (complex I and complex III). As a result, it is very prone to oxidative damage from $O_2^{\cdot-}$ that can lead to mutation. mtDNA can undergo both point mutations and large-scale deletions but can also be exposed to strand breaks. In post-mitotic tissue, such as cartilage, deletions are primary cause of mtDNA mutation as described in studies performed on skeletal muscle, brain and heart (Cortopassi et al 1992). Moreover, mtDNA deletions were more common in aged post-mitotic tissue of patients with neurodegenerative disease (Bender et al 2006; Kraytsberg et al 2006; Cortopassi et al 1992). As OA, is a disease that affects cartilage, an aged post-mitotic tissue, we hypothesize that large-scale mitochondria DNA deletions would be found in OA cartilage.

4.5.1 There is no difference in the level of mtDNA strand breaks in OA and NOF cartilage

Firstly, since SOD2 downregulation in SW1353 chondrosarcoma cells induced mtDNA strand breaks (section 3.4.8), the levels of mtDNA strand breaks in cartilage tissue were assessed. The same assay was used as in (section 3.4.8).

Total DNA was extracted from OA and NOF cartilage and the levels of mtDNA strand breaks were assessed. OA cartilage had 8% higher level of mtDNA damage compared to NOF however this was not statistically significant (Figure 4.1). Therefore from this finding, we can conclude that there is very limited mtDNA damage in OA cartilage compared to NOF. However, using this assay we cannot determine the exact position of the deletions that might be present at low levels and whether they are found in chondrocytes at specific regions of cartilage. In a previous study (Chang et al 2005), although the 4977 bp mtDNA common deletion was identified in of OA and aged cartilage, the levels of other deletions compared to wildtype and the location of those deletions in cartilage were not evaluated.

4.5.2 COX-SDH activity cannot be detected on cartilage sections

To assess mitochondrial activity and dysfunction in cartilage, sequential histochemical reactions of cytochrome *c* oxidase (COX) and succinate dehydrogenase (SDH) activities were performed in cartilage sections. This technique is based on detecting cells that contain high levels of mtDNA mutation, which have clonally-expanded and may cause detectable MRC deficiency (Chinnery et al 2002). When the wild-type mtDNA copy number is at a level that is not sufficient to overcome the effect of the mutant mtDNA, functioning MRC proteins are less than the dysfunctional proteins encoded by the mutated mtDNA thus causing respiratory deficiencies. However, the exact mechanism of the how mtDNA mutations expand is currently unknown. One proposed mechanism suggests that mutant mtDNA has a replicative advantage over the wild-type mtDNA molecules and as a result mutant mtDNA is selected and replicated (Yoneda et al 1992). Another study suggested that random genetic drift is the main factor responsible for clonal expansion (Elson et al 2001). In post-mitotic cells such as chondrocytes and neurons, it is possible that

only a subpopulation of the mtDNA molecules are being replicated, as there is limited or no cell division. Therefore a mechanism that combines both mechanisms already described could be possible. Mutant molecules, which are selected due to their replicative advantage, expand due to random genetic drift since a lower number of replicative molecules can increase the speed of the genetic drift (Krishnan et al 2008).

The COX-SDH assay can be used to identify cells with respiratory deficiencies due to mtDNA involvement (Barron et al 2005). The COX complex subunits are encoded by both the mitochondrial and nuclear genome, whereas the subunits of the SDH complex are encoded entirely by the nuclear genome. Therefore, when the mtDNA mutation is at very low levels or absent, cells will have a functioning COX and they will react only for COX activity (brown product) and will not react for the blue SDH activity (blue product) (Old, & Johnson 1989; Johnson et al 1993). However, when the mtDNA mutation has exceeded the mutation threshold, cells will have a dysfunctional COX and therefore will not be saturated by the DAB product and allow demonstration of SDH activity by the reduction of NBT, to a blue formazan product (Old, & Johnson 1989; Johnson et al 1993).

Initially, the COX-SDH reaction was performed on cartilage sections. One advantage of performing this assay on cartilage tissue instead of isolated chondrocytes is that the location of the dysfunctional cells in the different regions of the cartilage can be determined. However, during incubation with the COX incubation medium, the sections detached from the microscope slide and therefore detection of SDH activity was not possible. This is possibly due to a chemical reaction of the cartilage section with the COX incubation medium that prevented the section to remain attached to the slide. Slides with a different coating were used and the problem was partially solved. However, optimisation of the COX-SDH reaction on cartilage sections was not possible as detection of neither COX nor SDH activity was achieved. The exact reasons are not clear, however it could be due to low permeability of cartilage to the COX-SDH incubation media, or due to low expression of the MRC enzymes in those chondrocytes. This problem was also encountered before by a previous member of our group however, COX immunohistochemistry on cartilage

sections has shown COX staining only in the superficial zones of cartilage and not in deeper zones (Dr Jenny Scott, unpublished data). One limitation of our experiment is that the reaction on cartilage sections with COX-SDH was not attempted using PEN-membrane slides instead of standard microscope slides as cartilage sections could possibly attach better on the membrane slides.

4.5.3 Cultured HAC react only for SDH activity but not for COX activity

To identify whether the COX-SDH reaction was not possible due to the very low expression of the mitochondrial respiratory enzymes in HAC, isolated HAC were cultured in chamberslides and the same COX-SDH reaction was performed. SDH reacted efficiently, however the COX reaction required long incubation times in order to produce a visible reaction product (Figure 4.2). As mentioned before, lengthy COX incubation interferes with the subsequent SDH reaction efficiency as DAB, found in the COX incubation media, can block reduction of NBT to produce the blue SDH reaction product. The COX reaction product was weak possibly due to the fact that HAC are mainly considered glycolytic cells with only low mitochondrial respiratory activity (Stockwell 1983; Lee, & Urban 1997). Additionally, the culture of cells (10 days) in high glucose media can favour glycolysis instead of mitochondrial respiration adding to the reason why COX activity is low and hard to detect (Gohil et al 2010).

4.5.4 COX-SDH activity can be detected in freshly isolated HAC

Freshly isolated HAC were cytospun on PEN-microscope slides and the COX-SDH reaction was performed in order to avoid any loss of mitochondrial activity as described above. Both reactions worked well and a COX-SDH protocol was optimised (Figure 4.3).

One advantage of the COX-SDH reaction is that single cells can be isolated by laser capture microdissection, their total DNA extracted and their mtDNA screened for copy number and deletions. Although the amount of COX-deficient chondrocytes identified was very low, both COX-positive and COX-deficient cells were identified and screened for mtDNA copy number and mtDNA deletions.

4.5.5 COX activity does not correlate with mtDNA copy number is HAC

mtDNA copy number was assessed using a real-time PCR reaction amplifying the mitochondrial *MTND1* gene and quantified using a standard curve of known MTND1 copies (Krishnan et al 2010). MTND1 was used to assess copy number because it is found in the minor arc of the mtDNA, which is less prone to mtDNA deletions compared to the major arc ([NO STYLE for: Mitomap 2006]). By analysing cells from 5 patients the results were inconclusive. In 3 patients COX-deficient cells had more mtDNA copies than COX- positive whereas in 2 patients the opposite was identified (Figure 4.4). Therefore no real correlation between the COX status and mtDNA copy number was identified in chondrocytes. Additionally due to the fact that pools of 50 cells were used for this analysis, differences in the mtDNA copy number in single cells might have been masked due to the high number of cells used.

4.5.6 COX activity does not correlate with the level of mtDNA deletions in HAC

The levels of mtDNA deletions were assessed using a multiplex real-time PCR reaction amplifying the MTND1 gene and the MTND4 gene (He et al 2002; Krishnan et al 2007). MTND4 is located in the major arc of the mtDNA. This assay relies on the assumption that deletions are more common in the major arc of the mtDNA and therefore if a deletion is present it will more likely delete MTND4 and not MTND1 and there will be a difference in real-time PCR amplification (He et al 2002). Therefore MTND1 has the role of the housekeeping marker in this assay. This assay does not allow identification of the type of mtDNA deletions however it can provide a good and fast indication of whether a deletion if present in the MTND4 region and further characterization of those samples can take place using different methods such as long amplification PCR (He et al 2002; Krishnan et al 2010).

In this thesis, COX-positive and COX-deficient were screened for deletions using this assay. The heteroplasmy values obtained from the chondrocytes analysed ranged from -20% to -30% indicating that some deletions might be present in the major arc of the mtDNA (Figure 4.5). However, since the mutation threshold required to suggest the presence of a biochemical defect is more than

60%, our results possibly suggest that although mtDNA deletions are present, there is no physiological effect in these chondrocytes (Chinnery et al 1997; Sciacco et al 1994). The studies suggesting the need of mtDNA mutation threshold to cause a biochemical defect were performed using muscle fibers, a post-mitotic tissue with much higher mitochondrial activity compared to chondrocytes (Chinnery et al 1997; Sciacco et al 1994; Blanco et al 2004). As a result, the mutation threshold in chondrocytes required to produce a biochemical effect might be smaller (less than 60%) due to the chondrocytes' low mitochondrial activity. In addition, as highlighted by Chinnery *et al*, a mean tissue mtDNA mutation threshold must exist for clinical expression of a disease therefore mtDNA from total cartilage has to be screened to determine the effect that mtDNA mutation load might have in OA (Chinnery et al 1997).

No significant difference in the levels of mtDNA deletions was detected between COX-deficient and COX-positive cells. In other systems, COX-deficient cells had higher levels of mtDNA deletions compared to COX-positive cells (Bender et al 2006; Taivassalo et al 2006). This finding might suggest that COX-deficiency in chondrocytes could be due to other reasons other than mtDNA deletions such as lower mitochondrial respiratory activity. Additionally, HAC from different zones of cartilage have different mitochondrial activity as reported previously and in our experiment cells were not isolated according to the different zones but from total cartilage (Blanco et al 2004). As a result cells from the deeper zones might have less COX activity but the same mtDNA as cells in superficial zones. This is a limitation of this thesis and since COX-SDH histochemistry on cartilage sections is important in establishing mitochondrial function and screening for mtDNA deletions in different cartilage zones in both OA and NOF tissue, optimisation of the COX-SDH assay on cartilage tissue will be a priority of future work.

4.5.7 mtDNA large-scale deletions are present at low levels in OA cartilage

Since using the mtDNA strand break assay the exact nature of the damage cannot be determined and also since the COX-SDH assay was not very consistent in terms of the correlation between the COX activity and the amount

of deletions present, the long–amplification (long-range/LA) PCR assay was performed on total DNA extracted from OA hip, OA knee and NOF cartilage samples as well as other OA joint tissues. Using this assay, small amounts of DNA can be screened for the presence of large-scale mtDNA deletions by amplifying a region within the major arc. The PCR products are then electrophoresed an agarose gel. PCR products smaller than the 9.9kb wildtype products indicate the presence of deletions and they can be gel extracted and sequenced. However, this is not a quantitative technique since PCR preferentially amplifies smaller amplicons, therefore the amount of mtDNA deletions might be exaggerated (Krishnan et al 2010).

Total DNA was extracted from cartilage and other joint tissues and a fixed amount was used in the LA-PCR reaction. The wildtype 9.9kb amplicons had a higher intensity than the smaller amplicons that indicate that deletions are present (Figure 4.6). This also suggests that the levels of deletions are very low in cartilage, similar to the results suggested from the strand break assay. Amplicons from NOF tissue had a lower intensity than the ones from OA suggesting that deletions might be present but at extremely low levels. The strength of amplicons from other OA joint tissues had a variable intensity. The smaller amplicons were then gel purified and sequenced.

Due to the nature of the agarose gel electrophoresis reaction performed in this experiment, amplicons larger than 7kb could not be isolated and analysed for deletions as the intensity of the wildtype amplicon restricted the identification of these products. A primer-shift PCR reaction approach could be performed to amplify these products at a position closer to the breakpoints. Also the agarose gel electrophoresis could be performed for longer to allow the larger amplicons to resolve.

Twenty OA (hip and knee) patient samples and fifteen NOF samples were screened for deletions. Two large-scale mtDNA deletions were identified in two OA hip samples (one in each patient) and two were identified in one OA knee sample (Figure 4.7). The 7425bp deletion identified in patient A is very similar to a deletion reported previously in other diseases including cardiomyopathies, cirrhotic liver in hepatic tumour, Pearson syndrome and skeletal muscle in

chronic fatigue (Hayakawa et al 1992; Rötig et al 1995; Yamamoto et al 1992; Zhang et al 1995). No amplicons were sequenced from NOF because the amplicons were very faint compared to the OA. Also in our experiments, there was amplification of a 1.6kb amplicon in most of the samples. Sequencing analysis of the amplicon suggested that is was an artifact of the PCR reaction, as the sequences from both primers had no homology to mtDNA.

None of the deletions identified were the 4977bp mtDNA common deletion identified by Chang *et al* in OA knee cartilage and aged non-OA cartilage (Chang et al 2005; Schon et al 1989; Shoffner et al 1989; Cortopassi et al 1992). In that study, the authors suggest that this deletion may contribute to the development of OA, however they did not find a correlation between the severity of OA and the incidence of the 4977bp mtDNA deletion. Similarly, in this thesis, due to the low levels of mtDNA deletions present compared to wild type mtDNA molecules, we predict that the deletions possibly have no physiological effect as the amount of mutated mtDNA is below the threshold required to cause a biochemical effect and respiratory dysfunction, although in chondrocytes the mutation threshold required to produce a biochemical effect might be smaller (less than 60%) due to the chondrocytes' low mitochondrial activity compared to other more mitochondrially active cells such as muscle fibers. This result can also support the small amount of cells that were COX-deficient. As in this experiment total cartilage was examined instead of single cells, the overall effect of the mtDNA deletion is possibly limited. The low levels of deletions identified in OA cartilage can also be due to the loss of cartilage tissue during disease progression and therefore the mutation levels are decreased.

4.5.8 Low levels of mtDNA large-scale deletions are present in other joint tissues

Other joint tissue samples, such as cortical bone, cancellous bone, meniscus, synovium, ligament, osteophytes and fat pad, from OA patients were screened for large-scale mtDNA deletions. One limitation of this experiment was that no healthy controls were available for analysis. In this case, three mtDNA deletions were identified in cortical bone samples from a single patient. Another deletion

was identified in osteophyte samples from the same patient. Two mtDNA deletions were identified in synovium samples from two different patients, one in each patient (Figure 4.8). The 7449bp breakpoint of the deletion identified in the synovium of patient E, has been reported previously in ocular myopathy, however the size of the deletion was different to the one identified in this thesis (Degoul et al 1991). The identification of a common breakpoint with another study performed using a different system, could suggest that the 7449bp breakpoint, which is within a tRNA encoding region, might be a mutation hotspot although no other large-scale deletions have been reported (Degoul et al 1991; [NO STYLE for: Mitomap 2006]). Similar to the cartilage experiment, there was amplification of the 1.6kb amplicon, which also in this case it was an artifact.

4.5.9 Most mtDNA deletions identified do not have direct repeats flanking the breakpoints

All of the sequences of the deletions identified were also analysed for the presence of repeat sequences. As described in the introduction, 85% of the mtDNA deletions created by slip-replication, recombination or double strand break repair, are flanked by direct repeats suggesting a role of the repeats in the generation of the deletions (Mita et al 1990; Shoffner et al 1989; Krishnan et al 2008). However, a recent study suggested that repeats do not cause deletions but deletions can be generated due to long and stable duplexes formed between distant segments of the mtDNA thus implying that different mechanism can be involved in mtDNA deletion generation (Guo et al 2010). In our analysis, only one OA hip sample (patient A) demonstrated a direct repeat flanking the deletion thus indicating that the repeat might have had a role in the generation of the deletion. This deletion is very similar to a deletion reported previously in other diseases (Hayakawa et al 1992; Rötig et al 1995; Yamamoto et al 1992; Zhang et al 1995). The only difference compared to the deletion identified in this thesis is that in these studies one of 12bp repeat-sequences flanking the deleted region is within the deleted fragments whereas in our study both repeat sequences were outside the deleted fragment (Figure 4.7B). The deletions identified in the rest of the cartilage and other joint tissue samples, were flanked by regions with minor or no homology between them, suggesting that, as in Guo *et al*, direct repeats do not have a role in deletion generation and

other mechanisms might also be involved such as by stable secondary structures that can form between distant segments of the mitochondrial genome (Guo et al 2010).

4.5.10 mtDNA copy number is not different in OA hip cartilage compared to NOF

mtDNA copy number was also assessed in the same cartilage and other OA joint tissue samples that were analysed for large-scale deletions. The levels of MTND1 were measured using a real-time PCR reaction and were normalized to the levels of β-2-microglobulin (B2M). The levels of the mtDNA copies in other OA joint tissues varied from approximately 4000 copies per cell in cancellous bone samples to 500 copies in fat pad samples. The mtDNA copy number of cartilage fat pad identified in this thesis is comparable to that determined in rat inguinal fat pads, suggesting that fat pad might not have requirement for high mitochondrial activity (Venhoff et al 2009). Cartilage samples did not show a significant difference in mtDNA copies per cell (Figure 4.10) although OA hip samples had less mtDNA copies compared to NOF (1500 and 2000 copies per cell respectively). Comparing the mtDNA copy number of cartilage with other tissues we can suggest that cartilage has similar numbers of mtDNA copies compared to skeletal muscle (another post-mitotic tissue) but also more than pancreatic islets (approximately 600 copies/cell) and less than mouse oocytes (more than 10 000 copies/cell) (Cree et al 2008; Menshikova et al 2006). Studies in other tissues identified that age is one of the factors that contributes to the decline in mtDNA copy number (Cree et al 2008; Menshikova et al 2006; Short et al 2005). Reductions in the mtDNA copy number have also been associated with mutations in both mitochondrial and nuclear genes in several diseases (Blakely et al 2008; Kim et al 2005; Pyle et al 2007).

4.6 Conclusions

In this chapter, the levels of mtDNA damage were assessed in OA and NOF cartilage and in HAC. No difference in the levels of mtDNA strands breaks between OA and NOF cartilage was identified however, low levels of mtDNA large-scale deletions are present in OA cartilage. Consequently, these deletions possibly have a negligible biological effect in chondrocytes. In addition, no

significant difference in the mtDNA copy number was identified between NOF and OA cartilage. Taken together, these results suggest that although SOD2 downregulation can cause mtDNA damage in chondrocytes, this damage does not accumulate in OA chondrocytes. However, the absence of mtDNA deletions can also be due to the loss of cartilage tissue during disease progression and therefore the total mutation levels are decreased.

Chapter 5. Mitochondria bioenergetics in OA

5.1 Hypothesis

SOD2 downregulation in OA causes mitochondrial respiratory dysfunction due to higher $O_2^{\cdot-}$ levels and lipid peroxidation

5.2 Introduction

In the previous two chapters it was demonstrated that SOD2 downregulation in chondrocytes resulted in increased $O_2^{\cdot-}$ levels, mtDNA strand breaks and lipid peroxidation. Higher levels of lipid peroxidation were also observed in OA cartilage, however as shown in the previous chapter the levels of mtDNA deletions in OA cartilage are very low and mtDNA copy number was not significantly different between OA and healthy controls. Despite the absence of changes in mtDNA in OA, the higher $O_2^{\cdot-}$ levels and lipid peroxidation observed could potentially affect the respiratory activity of mitochondria in chondrocytes.

The MRC is composed of five large multi-unit complexes, Complex I, II, III, IV. All the subunits of the complexes are encoded by both mitochondrial and nuclear encoded genes with the exception of complex II that is encoded entirely by the nucleus (Lister et al 2005). The MRC is the major site of ATP production in the cell, which takes place by the process of OXPHOS. OXPHOS is driven by transfer of electrons along electron carriers in the MRC to reduce molecular oxygen to water. This process is coupled to the transfer of protons into the mitochondrial intermembrane space thus creating a protonmotive force that drives ATP synthesis through the ATP synthase (Complex V). However, OXPHOS is not completely coupled to ATP synthesis since protons can leak across the membrane independently of ATP synthase, a process termed proton leak (Brand et al 1994). As described in section 1.1.7, previous studies suggested that increased proton leak can be a reaction to counteract the effects of increasing ROS levels (Brookes 2005) or even as a consequence of damaged membranes due to lipid peroxidation (Kokoszka et al 2001).

Chondrocytes produce approximately 25% of their total ATP production by OXPHOS and the remainder by glycolysis (Stockwell 1983; Lee, & Urban 1997). A decrease in complex II and III activity has been reported in OA chondrocytes as well as an increase in the mitochondrial mass, possibly as a mechanism to compensate for the decrease in respiratory chain activities. OA chondrocytes contain more depolarised mitochondria than normal, which could be due to the lower activity of the mitochondrial complex III (Maneiro et al 2003). Inhibition of complexes III and V of the MRC in human chondrocytes has resulted in an NF-κB mediated increase of cyclo-oxygenase 2 expression and prostaglandin E_2 (PGE2) production thus possibly playing a role in OA pathogenesis (Cillero-Pastor et al 2008).

5.3 Aims

- To compare the function of the MRC in chondrocytes from NOF and OA patients
- To assess the role of SOD2 in regulating the function of the MRC in chondrocytes
- To assess the role of SOD2 in maintaining the Δψm in chondrocytes

5.4 Results

5.4.1 HAC respiration is very low compared to SW1353 cells

Human Articular Chondrocytes (HAC) were isolated from patient cartilage samples by enzymatic digestion. Initially analysis of respiration was attempted at day 0, directly after the enzymatic digestion of cartilage to isolate HAC. However, no respiration was recorded (data not shown) possibly due to the physiological stresses that the cells were under after the long collagenase treatment. Therefore, cells were allowed to rest for 3 days after isolation, then trypsinised and resuspended in sodium pyruvate containing media and their respiration assessed as described in section 2.9.1.

The respiration of SW1353 cells was also assessed to compare with HAC respiration. SW1353 cells respiration was analysed in the same way as HAC (section 2.9.1, Figure 2.1).

HAC have very low respiration values compared to SW1353 cells as shown in Figure 5.1A. SW1353 cells had 6.7-fold higher basal respiration compared to HAC (Figure 5.1A). To assess the contribution of proton leak to basal respiration, ATP synthase was inhibited by oligomycin. The resulting non-oligomycin sensitive respiration is accounted to be due to proton-leak. The oligomycin sensitive respiration is considered to be due to ATP turnover. SW1353 cells had higher respiration (6.8-fold) after inhibition by oligomycin, higher uncoupled respiration (4.7-fold) after FCCP treatment and 3.4-fold higher non-mitochondrial respiration.

When assessing different parameters (section 2.9.1, Figure 2.1) of the MRC function (Figure 5.1B), HAC have 1.5-fold higher SRC and 1.8-fold higher RCR than SW1353 cells. ATP production is much higher (6.6-fold) in SW1353 cells compared to HAC suggesting that HAC do not produce as much ATP by OXPHOS as SW1353 cells.

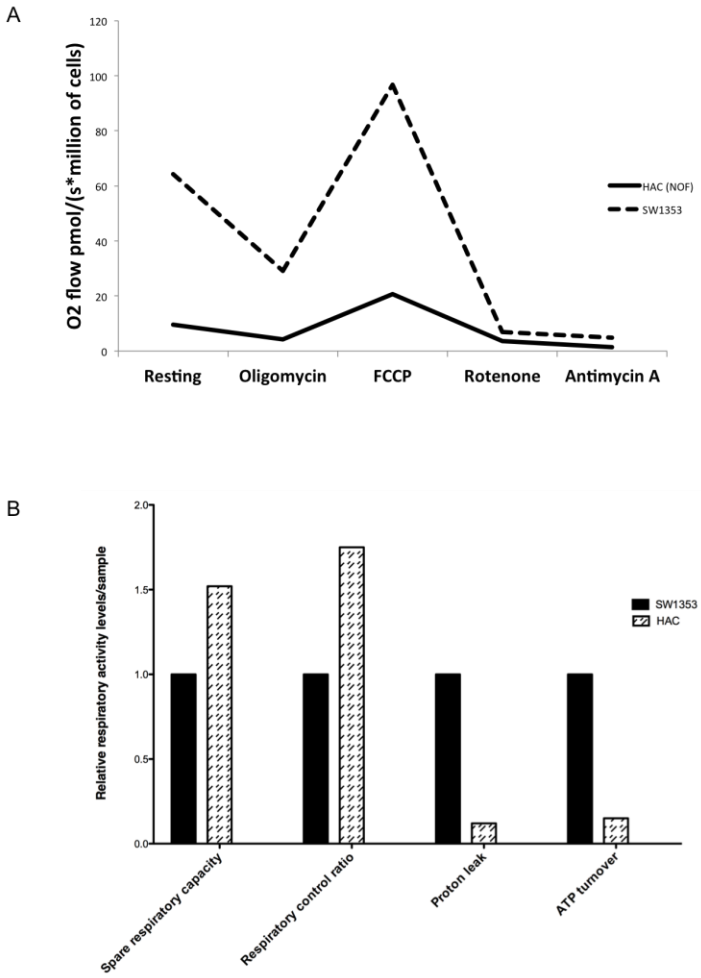

Figure 5.1 HAC and SW1353 respiration measured using the Oroboros Oxygraph respirometer

HAC were extracted from digested hip cartilage and cultured in 75cm^2 flasks for 3 days. Their respiration was compared to SW1353 chondrosarcoma cells. The respiration of both HAC and SW1353 cells was assessed using the same protocol. Cells were trypsinised and resuspended in sodium pyruvate containing media and then inserted in the Oroboros Oxygraph respirometer. Respiration was measured under resting conditions and after treatment with oligomycin (2.5µM, ATP synthase inhibitor), FCCP titration (Uncoupler), Rotenone (0.5µM, Complex I inhibitor) and Antimycin A (2.5µM, Complex III inhibitor) as in section 2.9.1. (A) shows average O_2 flow from SW1353 and HAC as measured using the Oroboros Oxygraph respirometer. O_2 consumption was allowed 10 mins to reach equilibrium after every treatment. Values shown in this graph represent equilibrated O_2 flow. This figure is representative of one experiment. No statistical analysis was performed. (B) shows respiratory parameters as calculated using the respiration values after different treatments as described in section 2.9.1. Spare respiratory capacity ratio, SRC, (where SRC= FCCP/Resting) and cell respiratory control ratio, RCR, (where RCR=(FCCP-Oligomycin)/Resting), Proton leak (Oligomycin) and ATP production (where = Resting-Oligomycin) were calculated using respiration values from SW1353 and HAC. Non-mitochondrial respiration (Antimycin A) was subtracted from all the values before calculating the parameters. This figure is representative of one experiment. No statistical analysis was performed.

5.4.2 OA chondrocytes respire more than NOF however they have higher proton leak and lower SRC and RCR

Both NOF and OA chondrocytes responded similarly to treatment with the different inhibitors as shown in Figure 5.2. OA chondrocytes had significantly higher basal respiration and higher respiration after oligomycin inhibition compared to NOF. Respiration after FCCP, rotenone and antimycin A treatment was not significantly different between NOF and OA cells.

Respiratory parameters were calculated as described in section 2.9.1. These parameters enable the thorough examination and identification of mitochondrial respiratory dysfunction (Brand, & Nicholls 2011). SRC, RCR, proton leak and ATP production were assessed. OA chondrocytes significantly showed 23% less SRC than NOF and they also had a 44% lower RCR as well as 93% higher proton leak. ATP production was also higher in OA but was not significantly different from NOF (Figure 5.3).

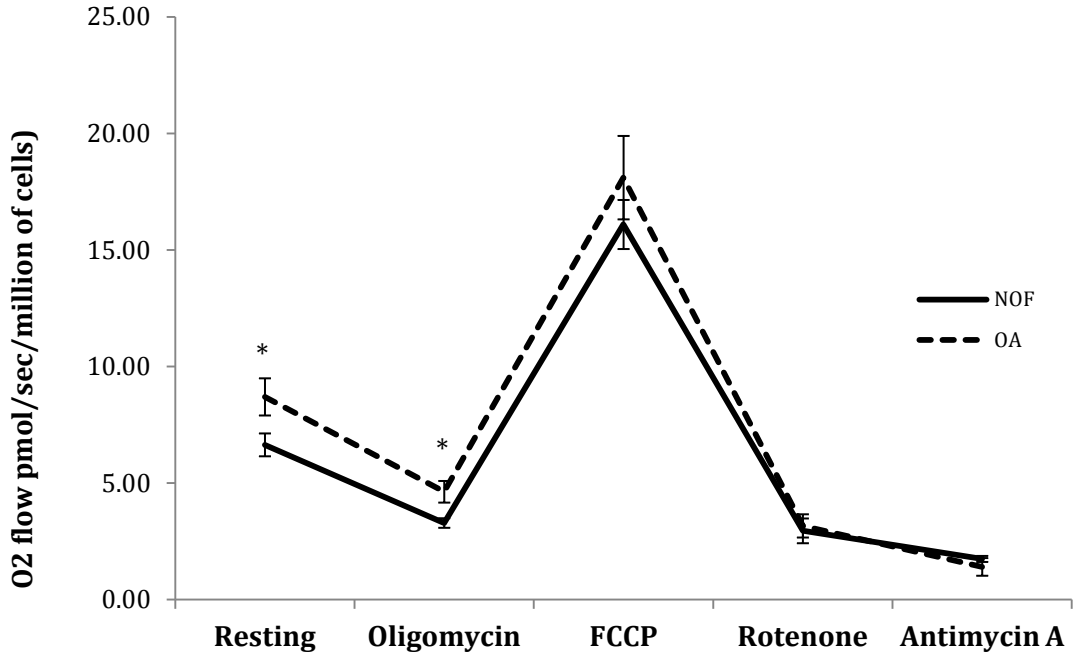

Figure 5.2 Average respiration values of NOF and OA chondrocytes measured with the Oroboros Oxygraph respirometer

Figure shows average O_2 flow (pmol per second per million cells) from NOF (n=8, median age = 75yrs) and OA (n=7, median age = 68yrs) hip chondrocytes as measured using the Oroboros Oxygraph respirometer. Respiration was measured under resting conditions and after treatment with oligomycin (2.5μM, ATP synthase inhibitor), FCCP titration (Uncoupler), Rotenone (0.5μM, Complex I inhibitor) and Antimycin A (2.5μM, Complex III inhibitor) as in section 2.9.1. *p≤0.05 OA compared to NOF (Mann Whitney U test).

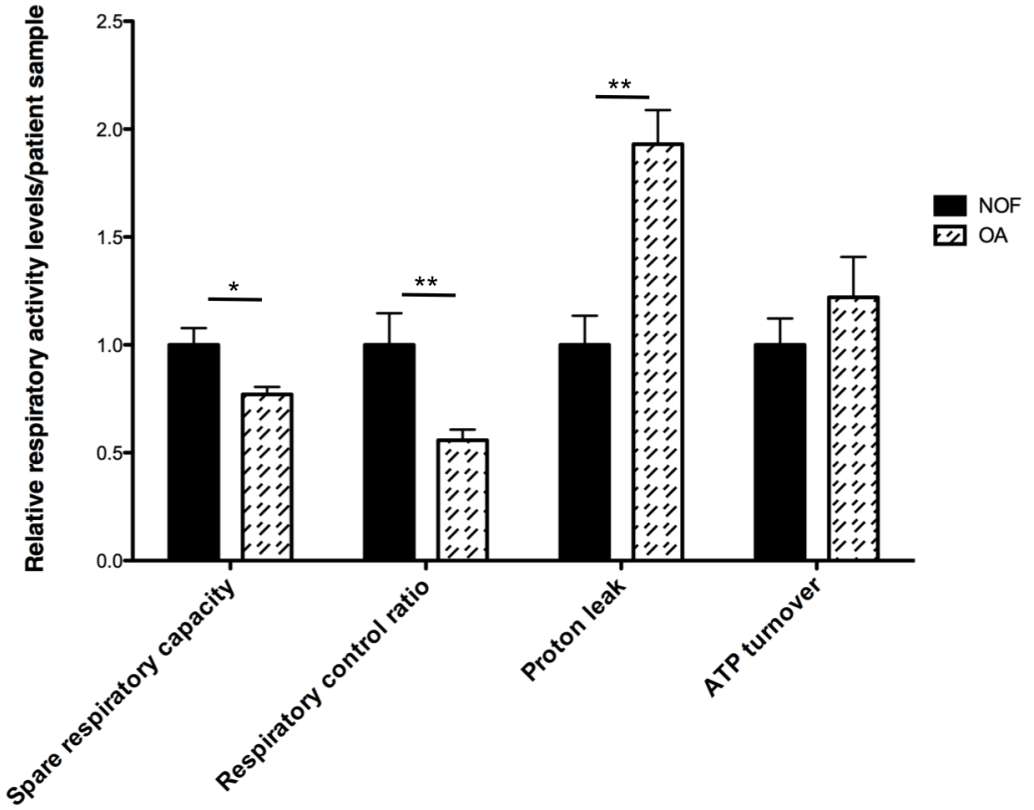

Figure 5.3 Relative respiratory activity parameters comparing NOF and OA mitochondrial respiration measured using the Oroboros Oxygraph respirometer

HAC isolated from hip cartilage were prepared for respiratory analysis as in section 2.9.1. Respiration values were determined as shown in Figure 5.1. Spare respiratory capacity ratio, SRC, (where SRC= FCCP/Resting) and cell respiratory control ratio, RCR, (where RCR=(FCCP-Oligomycin)/Resting), Proton leak (Oligomycin) and ATP production (where = Resting-Oligomycin) were calculated using respiration values from NOF (N=8) and OA (N=7) chondrocytes. Non-mitochondrial respiration (Antimycin A) was subtracted from all the values before calculating the parameters. Figure shows analysis of pooled data from all the NOF and OA experiments. *p≤0.05, **p≤0.01 OA compared to NOF (Mann Whitney U test).

5.4.3 Mitochondrial respiration in isolated chondrocytes measured using the Seahorse XF-24 extracellular flux analyser

Due to the fact that mitochondrial respiration in HAC is very low, the Seahorse XF-24 extracellular flux analyser was used to confirm the results identified using the Oroboros Oxygraph. The advantage of this system is that fewer cells are required and therefore multiple replicates per patient sample can be analysed. Also there is no requirement for the use of trypsin to harvest the cells for analysis since cells are cultured and analysed in the same culture plate. Trypsin has been reported to induce ROS production in mouse lymphocytes and human lung fibroblasts, therefore it can also potentially alter mitochondrial respiration (Lim et al 2006; Aoshiba et al 2001).

HAC were isolated from different patient samples and plated into Seahorse XF-24 plates. After 3 days their respiration was assessed as with the Oroboros Oxygraph.

Firstly, the amount of HAC required was determined by seeding cells at different densities, $1.75x10^4$, $3.5x10^4$ and $1.5x10^5$ cells/cm^2. The requirement was to cover the surface of the well completely but without the cells becoming too dense after culture. A density of $1.5x10^5$ cells per well was considered to be the most appropriate from this experiment as by day 3 the cells covered the plate surface fully (data not shown).

Both NOF and OA chondrocytes responded similarly to treatment with different inhibitors as shown in Figure 5.4. OA chondrocytes had significantly higher basal respiration and higher respiration after oligomycin inhibition and treatment with FCCP compared to NOF. There was no significant difference in the respiration between NOF and OA chondrocytes after rotenone and antimycin A treatment.

Cell respiratory control measurements were calculated analysing the SRC, RCR, proton leak andATP productionas described in section 2.9.1. OA chondrocytes have significantly 32% less SRC than NOF and they also have a significantly 35% lower RCR as well as 47% higher proton leak. ATP production

was also 65% significantly higher in OA compared to NOF (Figure 5.5 and Table 5.1).

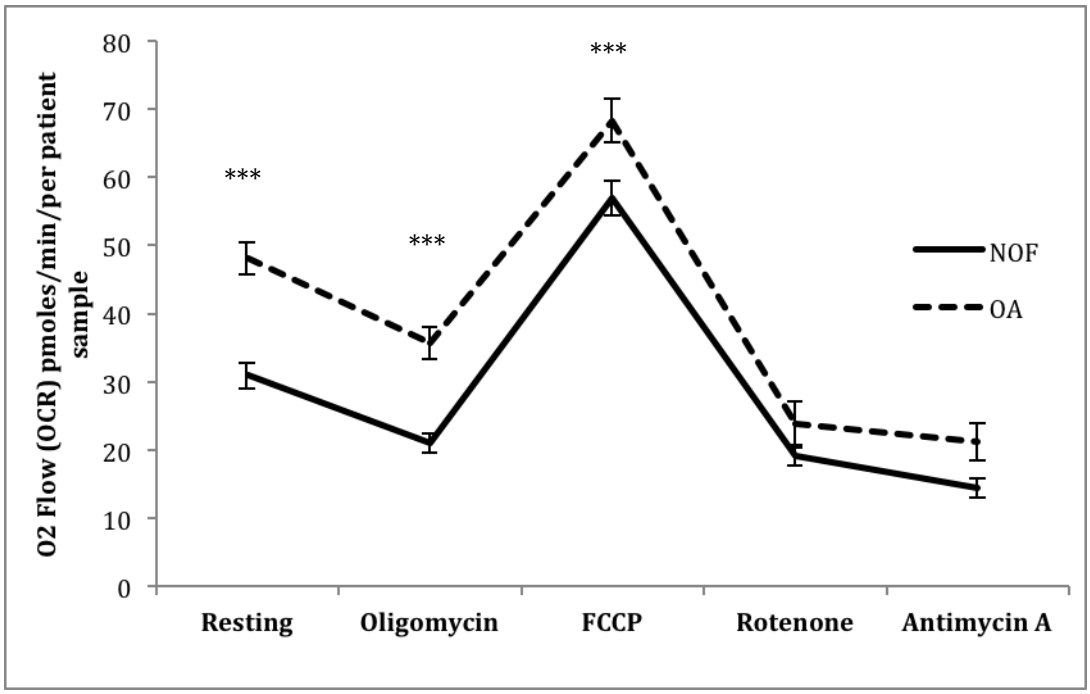

Figure 5.4 Average respiration values of NOF and OA chondrocytes measured with the Seahorse XF-24 respirometer

Figure shows average O2 flow/OCR (Oxygen Consumption Rate), pmol/min/well from NOF (n=3, median age = 77yrs) and OA (n=3, median age = 74yrs) hip chondrocytes as measured using the Seahorse XF-24 respirometer. Respiration was measured under resting conditions and after treatment with oligomycin (2.5µM, ATP synthase inhibitor), FCCP titration (1.5µM, Uncoupler), Rotenone (0.5µM, Complex I inhibitor) and Antimycin A (2.5µM, Complex III inhibitor) as in section 2.9.1. 5 technical repeats were performed for each measurement per patient sample. ***p≤0.001 OA compared to NOF (Mann Whitney U test).

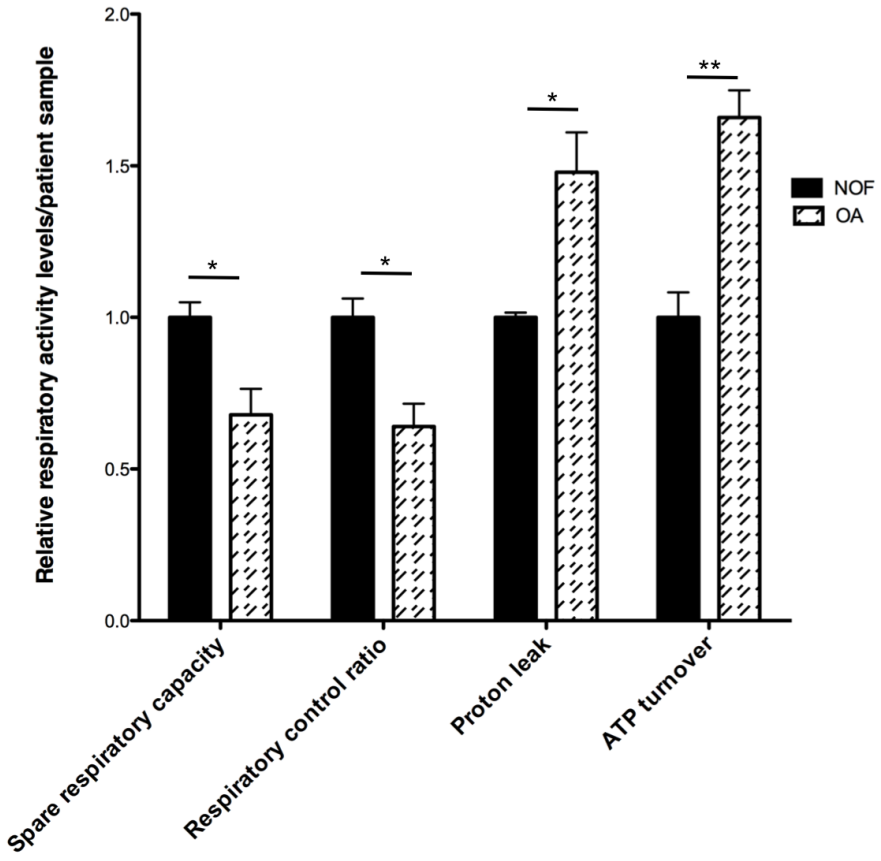

Figure 5.5 Relative respiratory activity parameters comparing NOF and OA mitochondrial respiration measured using the Seahorse XF-24 respirometer

HAC isolated from hip cartilage were prepared for respiratory analysis as in section 2.9.1. Respiration values were determined as shown in Figure 5.4. Spare respiratory capacity ratio, SRC, (where SRC= FCCP/Resting) and cell respiratory control ratio, RCR, (where RCR=(FCCP-Oligomycin)/Resting), Proton leak (Oligomycin) and ATP production (where = Resting-Oligomycin) were calculated using respiration values from NOF (N=3) and OA (N=3) chondrocytes. Non-mitochondrial respiration (Antimycin A) was subtracted from all the values before calculating the ratios. Figure shows analysis of pooled average data from all the NOF and OA experiments. Average respiration parameters of each experiment are shown at the table below. 5 technical repeats were performed for each measurement per patient sample. *p≤0.05, **p≤0.01 OA compared to NOF (Mann Whitney U test).

Sample ID	Spare respiratory capacity	Respiratory control ratio	Proton leak	
NOF1	3.29	6.67	7.75	7.00
NOF2	3.25	5.91	8.15	8.00
NOF3	2.81	5.38	7.80	6.00
NOF average	**3.12**	**5.99**	**7.90**	**7.00**
NOF st. deviation	0.26	0.64	0.21	1.00
OA1	1.61	3.52	10.50	11.50
OA2	2.22	4.72	13.75	12.75
OA3	2.52	3.26	10.80	10.60
OA average	**2.11**	**3.83**	**11.68**	**11.62**
OA st. deviation	0.46	0.77	1.79	1.08

Table 5.1 Average values of respiratory parameters comparing NOF and OA respiration using the Seahorse XF-24 extracellular flux analyser

HAC isolated from hip cartilage were prepared for respiratory analysis as in section 2.9.1. Respiration values were determined as shown in Figure 5.4. Spare respiratory capacity ratio, SRC, (where SRC= FCCP/Resting) and cell respiratory control ratio, RCR, (where RCR=(FCCP-Oligomycin)/Resting), Proton leak (Oligomycin) and ATP production (where = Resting-Oligomycin) were calculated using respiration values from NOF (N=3) and OA (N=3) chondrocytes. Non-mitochondrial respiration (Antimycin A) was subtracted from all the values before calculating the ratios. Table shows analysis of average respiration parameters of each patient sample, and the pooled average and standard deviation of the 3 OA and 3 NOF patients. 5 technical repeats were performed for each measurement per patient sample.

5.4.4 Extracellular acidification rate in HAC measured using the Seahorse XF-24 analyser

Another advantage of the Seahorse XF-24 system is that glycolytic and mitochondrial respiration can be assessed simultaneously. Extracellular Acidification rate (ECAR) is used as a measurement for glycolysis. Since mitochondrial respiration was low in chondrocytes, we decided to assess the levels of glycolysis in NOF and OA chondrocytes.

No difference was observed between NOF and OA, and ECAR did not change significantly upon addition of the different inhibitors (Figure 5.6A). By calculating the ratio of mitochondrial respiration (OCR) to glycolysis (ECAR) we observed resting OCR/ECAR values between 0.8 and 1.6 suggesting that chondrocytes depend almost as much on mitochondrial respiration as glycolysis under these experimental conditions (Figure 5.6B).

A

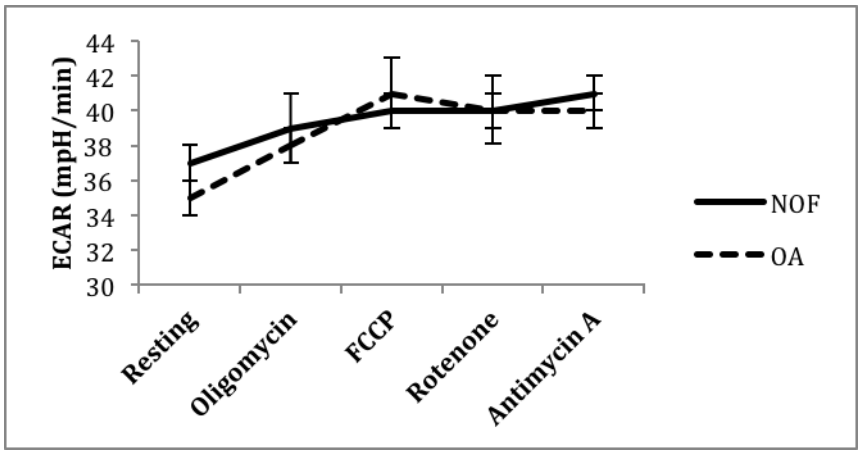

B

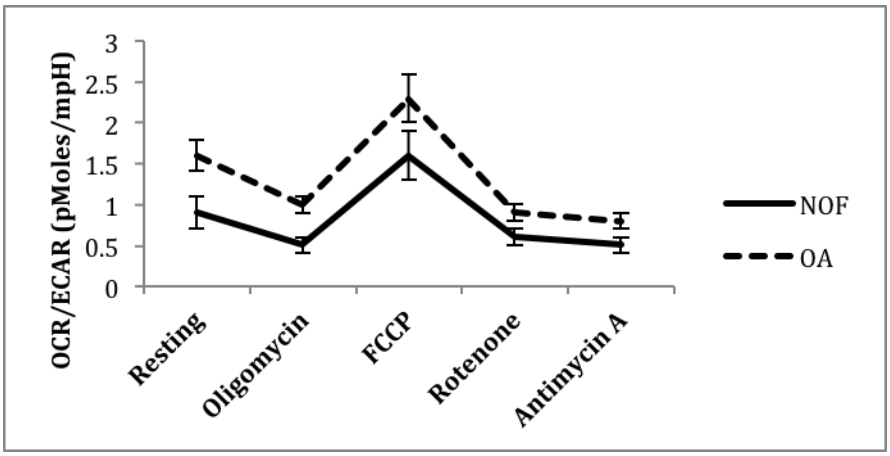

Figure 5.6 HAC Extracellular Acidification Rate (ECAR) and OCR/ECAR ratio measured using the Seahorse XF-24 respirometer

HAC isolated from hip cartilage were prepared for respiratory analysis as in section 2.9.1. ECAR was measured under resting conditions and after treatment with oligomycin (2.5μM, ATP synthase inhibitor), FCCP titration (1.5μM, Uncoupler), Rotenone (0.5μM, Complex I inhibitor) and Antimycin A (2.5μM, Complex III inhibitor) as in section 2.9.1. **(A)** shows rate of change in pH levels per patient sample (mpH/min) and **(B)** shows the ratio of OCR to ECAR in the same samples. Both figures are representative of three NOF and three OA experiment. 5 technical repeats were performed for each measurement per patient sample. No significant difference was determined between NOF and OA chondrocytes (Mann Whitney U test).

5.4.5 Effect of SOD2 downregulation on mitochondrial respiration in HAC measured using the Seahorse XF-24 extracellular flux analyser

In order to determine whether a reduction in the expression levels of SOD2 in OA affects mitochondrial respiration in human articular chondrocytes, HAC isolated from patient cartilage samples were transfected with siRNA targeted against SOD2 as in section 2.3.2. To confirm SOD2 depletion, cells were cultured in the Seahorse XF-24 plates, transfected with siRNA against SOD2 or non-targeting control for 48 hours and then cells were lysed and SOD2 mRNA levels were evaluated by real-time PCR (Figure 5.7). Transfection of 100nM concentration SOD2 targeted siRNA resulted in 90% reduction in mRNA levels in Seahorse XF-24 plates.

To assess respiration in SOD2 depleted cells, HAC were then analysed using the same method the same method as described above. Both SOD2 depleted chondrocytes and control control responded in a similar way to treatment but there was no significant difference in their difference in their respiration values (

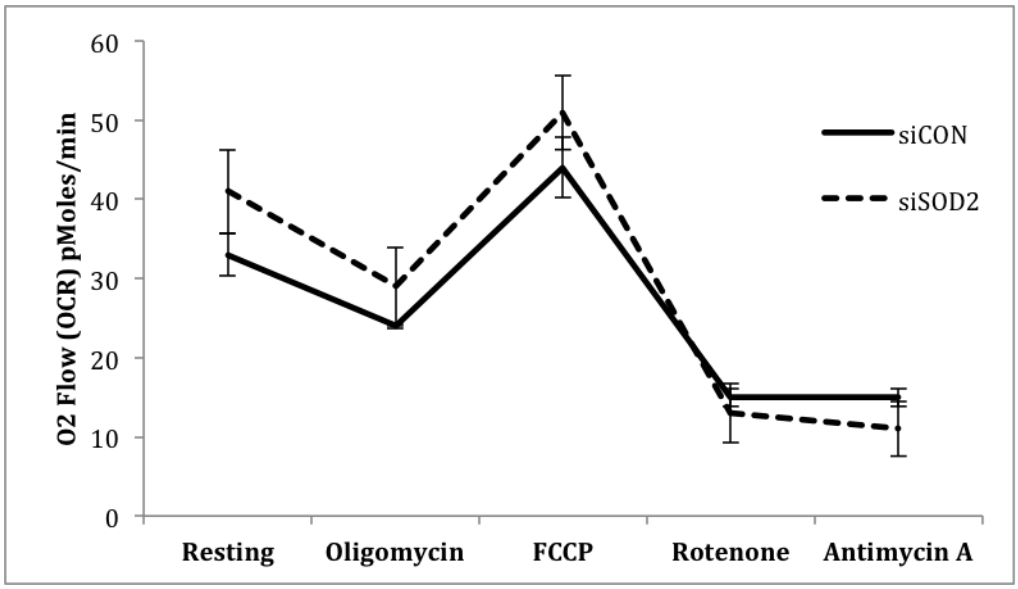

Figure 5.8). By analyzing the respiration parameters, RNAi depletion of SOD2 in chondrocytes resulted in 26% lower SRC and 16% higher proton leak compared to control, however, no difference was observed in other cell respiratory control measurements (Figure 5.9).

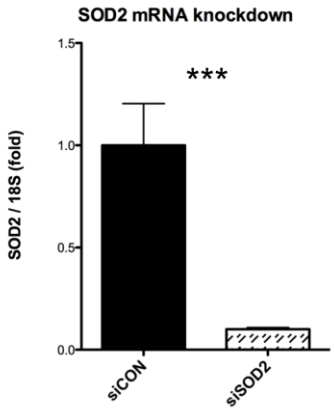

Figure 5.7 Assessment of SOD2 mRNA knockdown in Seahorse XF-24 plates

HAC isolated from knee cartilage were seeded in Seahorse XF-24 plates at a density of 3.5 x 10^4cells/well. After 24 hours cells were transfected with 100nM siRNA for 48 hours. Total RNA was extracted with Cells-to-cDNA lysis buffer as described in section 2.4.7, reverse transcribed to cDNA and subjected to real-time RT-PCR analysis of *SOD2* gene expression. Values were normalised to *18S* and plotted as mean fold induction over control ± SD (n=5). *** p≤0.001, compared to control. Figure is representative of two independent experiments.

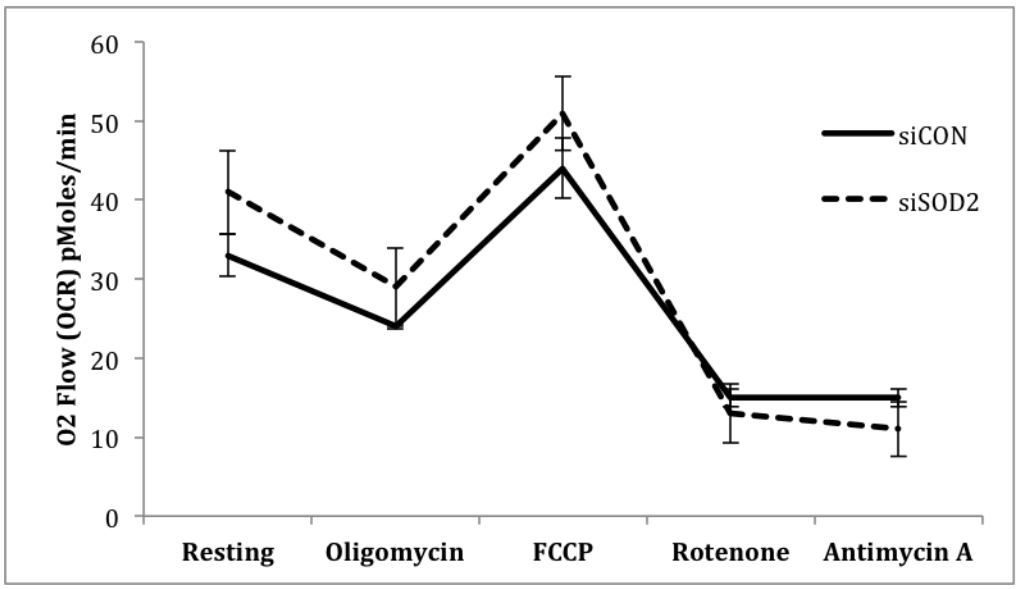

Figure 5.8 Average respiration values of siCON and siSOD2 transfected cells measured using the Seahorse XF-24 respirometer

Knee HAC were seeded in Seahorse XF-24 plates at a density of 3.5 x 10^4cells/well. After 24 hours cells were transfected with 100nM siRNA for 48 hours. Cells were washed in sodium pyruvate containing media and then inserted in Seahorse XF-24 respirometer. Respiration was measured under resting conditions and after treatment with oligomycin (2.5μM, ATP synthase inhibitor), FCCP titration (1.5μM, Uncoupler), Rotenone (0.5μM, Complex I inhibitor) and Antimycin A (2.5μM, Complex III inhibitor) as in section 2.9.1. Figure shows the average O2 flow/OCR (Oxygen Consumption Rate), pmol/min/well as calculated by pooling values of 4 independent experiments. 5 technical repeats were performed for each measurement. Statistical analysis was performed using the Mann-Whitney non-parametric test to test differences between siCON and siSOD2 treated cells. No statistical difference was determined.

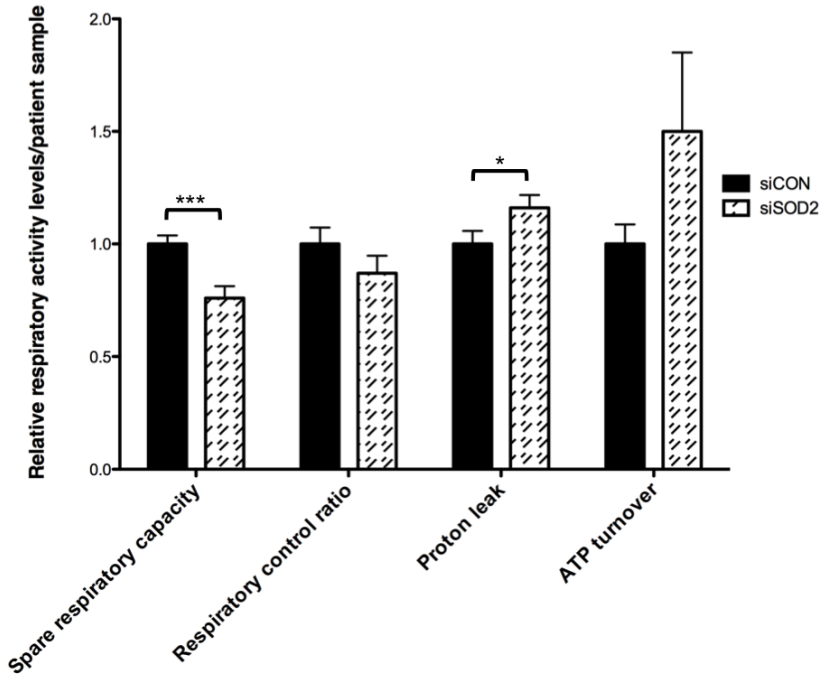

Figure 5.9 Relative respiratory activity parameters comparing mitochondrial respiration of siCON and siSOD2 treated cells measured using the Seahorse XF-24 respirometer

HAC isolated from knee cartilage were prepared for respiratory analysis as in section 2.9.1. Respiration values were determined as shown in

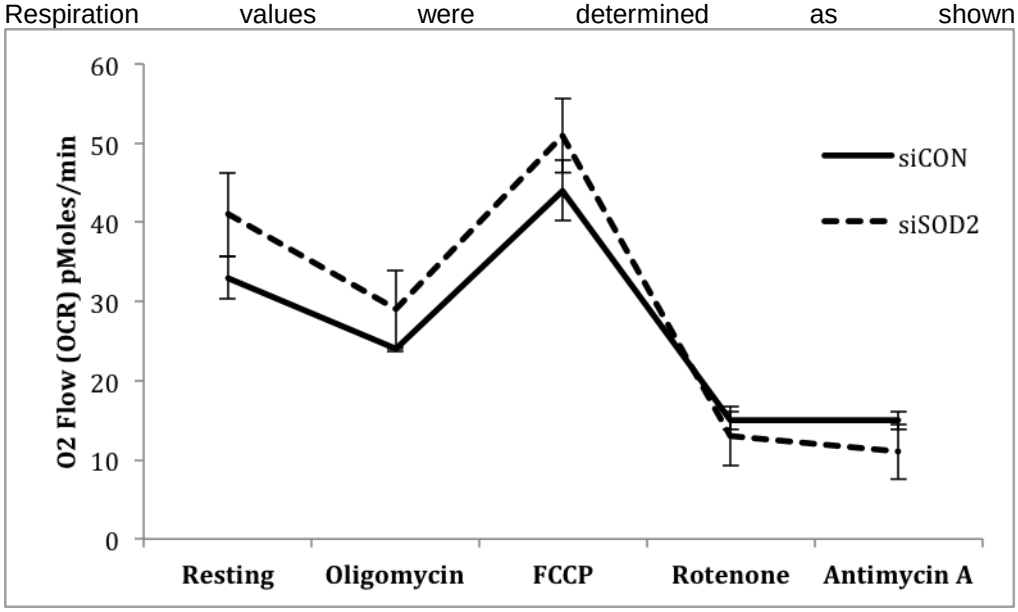

Figure 5.8. Spare respiratory capacity ratio, SRC, (where SRC= FCCP/Resting) and cell respiratory control ratio, RCR, (where RCR=(FCCP-Oligomycin)/Resting), Proton leak (Oligomycin) and ATP production (where = Resting-Oligomycin) were calculated using respiration values from siCON and siSOD2 transfected chondrocytes. Non-mitochondrial respiration (Antimycin A) was subtracted from all the values before calculating the ratios. 5 technical repeats were performed for each measurement. Figures show the fold change in SRC, RCR, Proton leak andATP productionbetween siCON and siSOD2 transfected cells in 4 independent experiments.

5.4.6 Effect of SOD2 downregulation on glycolysis in chondrocytes as measured using the Seahorse XF-24 analyser

ECAR was measured in cells depleted of SOD2 using siRNA transfection against SOD2. HAC isolated from patient cartilage samples were transfected with siRNA targeted against SOD2 as in section 2.3.2. Cells were treated and respiration was analysed in the same way as described above. RNAi targeted depletion of SOD2 in chondrocytes did not significantly effect glycolysis in any of our experiments (Figure 5.10).

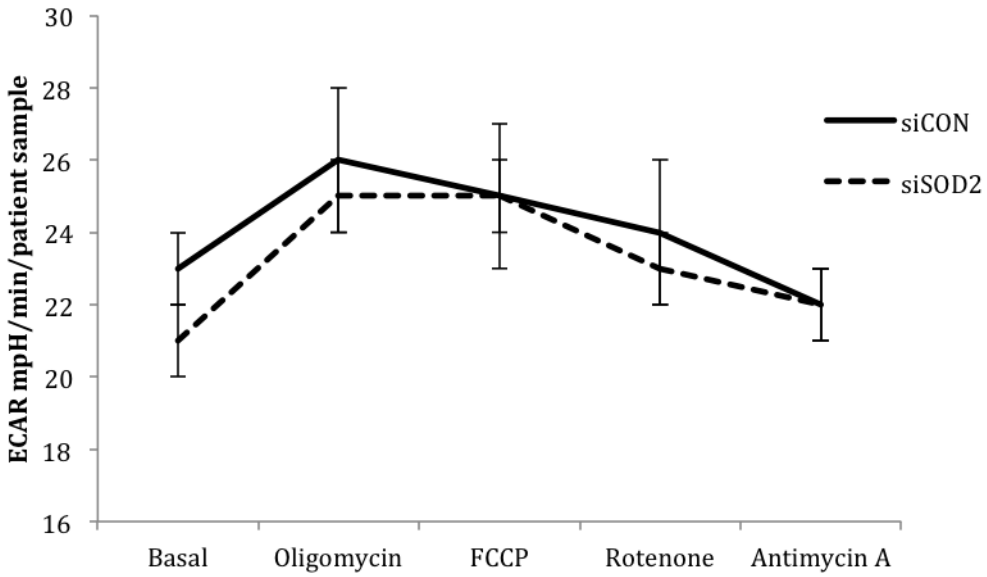

Figure 5.10 ECAR of siCON and siSOD2 transfected cells measured using the Seahorse XF-24 respirometer

HAC isolated from knee cartilage were seeded in Seahorse XF-24 plates at a density of 3.5 x 10^4cells/well. After 24 hours cells were transfected with 100nM siRNA for 48 hours. Cells were washed in sodium pyruvate containing media and then inserted in Seahorse XF-24 respirometer. Respiration and ECAR were measured under resting conditions and after treatment with oligomycin (2.5μM, ATP synthase inhibitor), FCCP titration (1.5μM, Uncoupler), Rotenone (0.5μM, Complex I inhibitor) and Antimycin A (2.5μM, Complex III inhibitor) as in section 2.9.1. Graph shows rate of change in pH levels per patient sample (mpH/min) per well and is representative of four experiments. 5 technical repeats were performed for each measurement. No statistical analysis was performed.

5.4.7 Effect of SOD2 depletion on Δψm in chondrocytes

As reported previously in Maneiro *et al*, OA chondrocytes are more depolarized compared to NOF (Maneiro et al 2003). SOD2 downregulation causes membrane potential depolarization in neurons possibly due to increase in proton leak and lipid peroxidation (Fukui, & Zhu 2010; Kokoszka et al 2001). In this thesis, we wanted to determine whether SOD2 regulates mitochondrial depolarization in chondrocytes. Two mitochondrial membrane potential dyes were assessed; JC-1 and TMRM.

Initially, JC-1 was used. In healthy cells, JC-1 stains the mitochondria red. Mitochondrial depolarization prevents JC-1 accumulation in the mitochondria and therefore it stays in the cytoplasm and possesses a green fluorescence. To assess the dye, mitochondria were depolarized by uncoupling respiration using FCCP. However, no change in the fluorescence pattern was noted (Figure 5.11).

TMRM was then assessed. TMRM is a cationic probe that is selectively localized in the mitochondrial matrix due to the presence of a net negative charge caused by the proton gradient. Any variations in the Δψm change the intensity but not the spectra of the probe. In healthy cells TMRM accumulates normally in the mitochondria as it is attracted by their negative charge and emits red fluorescence. Mitochondrial depolarization prevents TMRM accumulation in the mitochondria due to the collapse of the negative charge and therefore less TMRM enters the mitochondrial membrane and the some TMRM stays inactive in the cytoplasm. TMRM was more responsive compared to JC-1 and fluorescence changed in response to membrane potential changes in chondrocytes as membrane potential depolarization was evident after FCCP treatment since TMRM levels in the mitochondria were reduced (Figure 5.12).

RNAi SOD2 depleted cells and control cells were stained with 10nM TMRM (non-quench) and their fluorescence was assessed basally and after addition of oligomycin and FCCP. Addition of FCCP without oligomycin causes ATP synthase reversal and hydrolysis of ATP in order to restore the proton gradient. Therefore, oligomycin is added before FCCP to block this effect and allow measurement of the effect of FCCP on Δψm. Oligomycin normally causes Δψm

hyperpolarisation, which suggests normal respiratory function as it blocks ATP synthase from pumping protons back to the matrix during ATP synthesis. As a result there is a build up of protons and a net positive charge in the intermembrane space and a net negative charge in the matrix, which attracts more TMRM (Brand, & Nicholls 2011). If oligomycin causes Δψm depolarisation it suggests a dysfunctional respiratory activity (Brand, & Nicholls 2011). The mechanism of this process is currently unknown.

SOD2 depletion caused a Δψm depolarisation basally (Figure 5.13). Oligomycin also caused Δψm depolarisation in both SOD2 depleted HAC and controls. Mitochondria depolarised further after addition of FCCP but it is not clear whether it is due to the FCCP treatment or due to the prior oligomycin treatment and its depolarising effect on HAC mitochondria in this experiment.

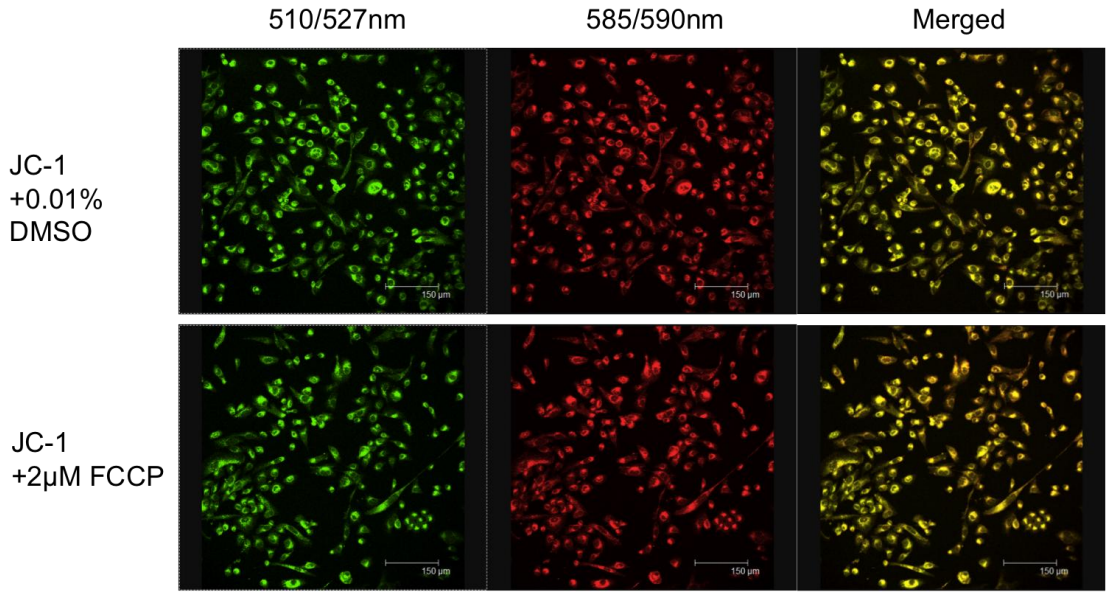

Figure 5.11 JC-1 Δψm staining in HAC

HAC isolated from knee cartilage were seeded in 6-well plates at a density of $3x10^5$ cells/well. After 24 hours cells were treated with 2μM FCCP (depolarisation) or 0.01% DMSO control for 10mins, to assess the colour changes in response to mitochondrial depolarisation (more green, less red). Cells were then treated with 50nM JC-1 for 15mins. Fluorescence was assessed with live cell confocal microscopy using the channels shown above. This figure is a representative of two independent experiments.

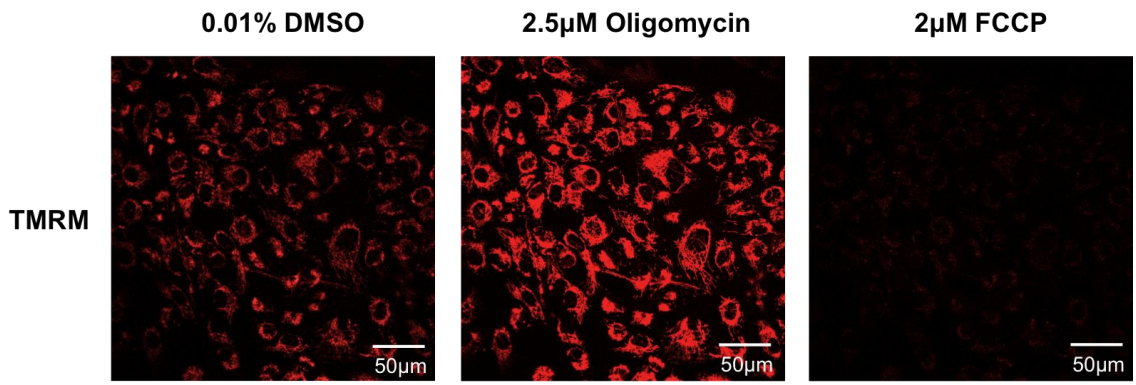

Figure 5.12 TMRM Δψm staining assessment

HAC isolated from knee cartilage were seeded in 6-well plates at a density of $3x10^5$ cells/well. After 24 hours cells were stained with 10nM TMRM (non-quench) for 30mins and TMRM fluorescent staining was measured in cells treated with 0.01% v/v DMSO (final concentration), 2.5µM oligomycin (final concentration) and 2µM FCCP (final concentration). Cells were visualised live using an inverted fluorescent microscope. Images were analysed using Image J.

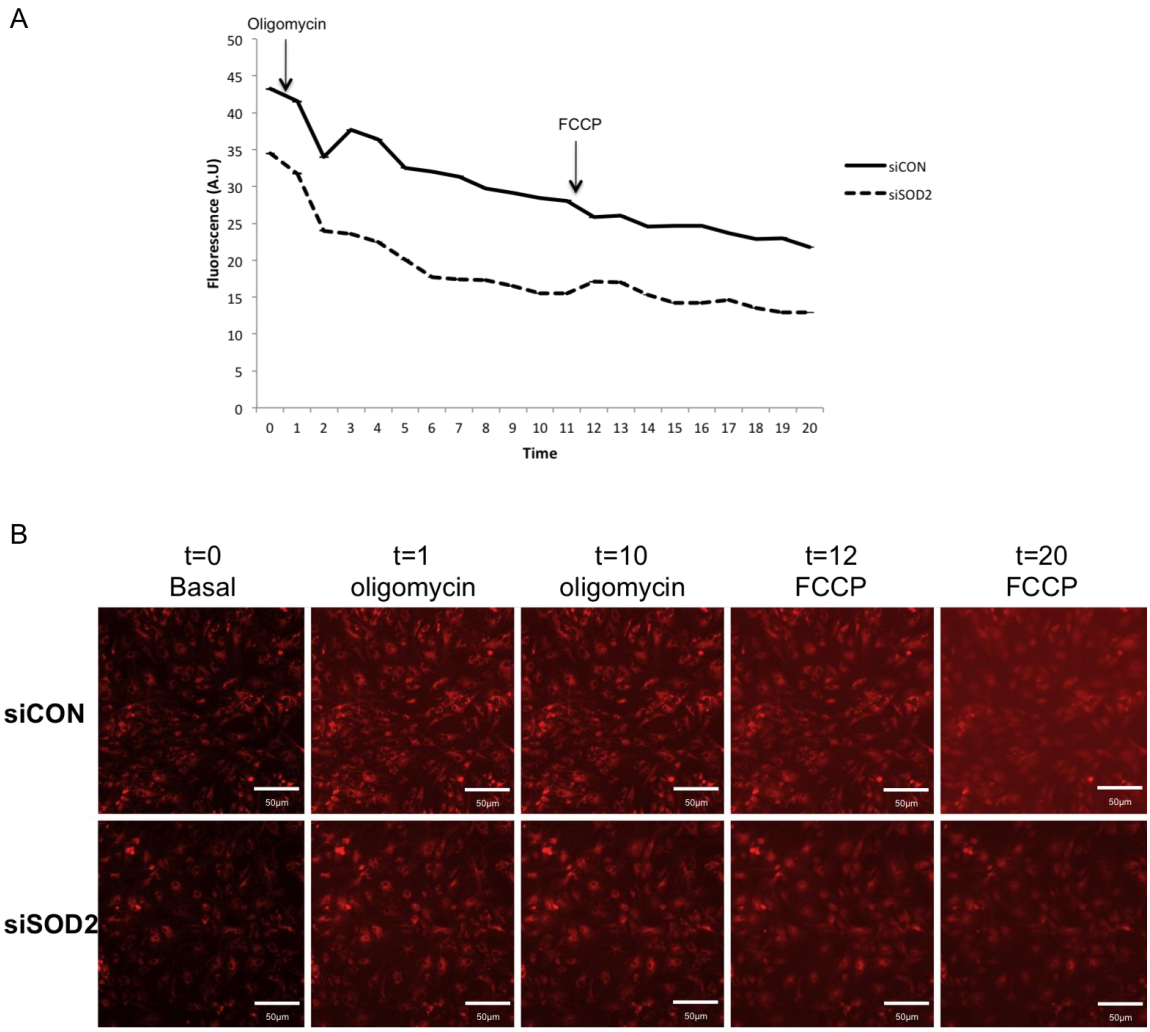

Figure 5.13 TMRM Δψm staining in HAC treated with siCON and siSOD2

HAC isolated from knee cartilage were seeded in chamberslides at a density of 1.5x 10^4 cells/well. After 24 hours they were transfected with 100nM siCON or siSOD2 for 48 hours. Then cells were stained with 10nM TMRM (non-quench) for 30mins and TMRM fluorescent staining was measured under basal conditions (time=0) and every one minute after treatment with 2.5µM Oligomycin (ATP synthase inhibitor, prevents ATP synthase reversal) at t=0 and 1.5µM FCCP (Uncoupled, induces mitochondrial depolarisation) at t=11. Cells were visualised live using an inverted fluorescent microscope. Images were analysed using Image J. (A) shows a graphical representation of TMRM levels in siCON and siSOD2 treated HAC. (B) shows TMRM levels at specific time points. Background fluorescence was measured and subtracted. This figure is representative of 2 independent experiments.

5.5 Discussion

Following the analysis of NOF and OA cartilage and HAC mtDNA for large-scale mtDNA deletions and mtDNA strand breaks in Chapter 4, the effect of SOD2 downregulation on mitochondrial respiration was examined. In particular, the downregulation of SOD2 in disease may have altered mitochondrial respiration compared to healthy controls. Respiration was therefore assessed in HAC from OA and NOF patient samples and the contribution of SOD2 examined by RNAi.

Previous reports highlight the role of glycolysis in articular chondrocytes, suggesting that approximately 25% of their total ATP is produced by OXPHOS (Stockwell 1983; Lee, & Urban 1997). However, mitochondrial respiration is not considered to be totally inactive as O_2 uptake increased upon treatment with protonophore DNP (2,4-dinitrophenol) (Lee, & Urban 1997). Johnson and colleagues also suggested that peroxynitrite and nitric oxide donors suppress respiration and ATP generation in chondrocytes (Johnson et al 2000). In addition, inhibition of the MRC with oligomycin (ATP synthase inhibitor) and antimycin (complex III inhibitor) reduced collagen and proteoglycan synthesis in the same cells (Johnson et al 2000). In OA chondrocytes, complex II and III activity has been shown to be decreased and mitochondrial mass increased compared to healthy controls (Maneiro et al 2003). More depolarized mitochondria were also identified in OA chondrocytes possibly due to the decrease in complex III activity (Maneiro et al 2003). Also, inhibition of complex III and IV in HAC resulted in an NF-κB mediated increase of cyclo-oxygenase 2 expression and prostaglandin E_2 (PGE2) production thus possibly playing a role in OA pathogenesis (Cillero-Pastor et al 2008).

As mentioned in chapter 3, SOD2 is one of the most important $O_2^{\cdot-}$ scavengers in the cell. SOD2 null mice, depending on their genetic background, experience embryonic (C57BL/6 J) or neonatal lethality (CD1, DBA/2 J, B6D2F1) associated with severe neurological and cardiac phonotypes and metabolic acidosis (Huang et al 2001; Li et al 1995; Lebovitz et al 1996). A reduction in the catalytic activity of complexes I and II of the MRC was also identified in SOD2 null mice (CD1 background) (Melov et al 1999).

These results suggest that the increase in ROS, $O_2^{\cdot-}$ in particular, due to the decrease of SOD2 levels in the mitochondria, can lead to a variety of biochemical defects. In this thesis, we have shown that SOD2 downregulation in OA can lead to an increase in $O_2^{\cdot-}$ levels in HAC and also higher levels of lipid peroxidation. The effect of SOD2 downregulation on mitochondrial respiration is therefore examined here.

5.5.1 Freshly isolated HAC do not respire by mitochondrial respiration

Initially, HAC respiration was assessed at day 0 after the enzymatic digestion of cartilage to avoid any loss of cells with dysfunctional respiration. However, when the respiration of those cells was measured using the Oroboros Oxygraph 2k respirometer, no respiration was recorded at all suggesting that the cells were dead (data not shown). This observation can probably be accounted to the fact that HAC were under extreme physiological stresses after the long collagenase treatment that could have affected their respiration. Therefore, it was decided to culture the cells for three days in normal culture media to allow them to rest and then they were trypsinised, resuspended in sodium pyruvate containing media to stimulate their mitochondrial respiration and respiration was assessed. However, the increase in respiration after culture of HAC can be attributed to a change in the mitochondrial properties of chondrocytes during culture as reported previously (Mignotte et al 1991). In this study, a 20-fold increase in the concentration of mitochondrial transcripts for cyt B, CO II and CO III has been reported in chondrocytes in culture compared to the levels in cartilage suggesting that the mitochondrial properties of chondrocytes change when transferred in an artificial culture environment.

5.5.2 HAC and SW1353 chondrosarcoma cells have different mitochondrial respiration patterns

Firstly, the respiration of HAC was compared to SW1353 chondrosarcoma cells respiration in terms of oxygen consumption/flow (O_2 flow) using the Oroboros Oxygraph 2k respirometer. This experiment was performed once in order to make sure that the respirometer works and therefore the results are only preliminary. SW1353 cells had approximately a 6.7-fold higher basal respiration

compared to HAC (Figure 5.1). SW1353 and HAC basal respiration was also compared to other cells based on data from other studies. SW1353 basal respiration was 1.5-fold higher, 2.4-fold higher and at similar levels compared to 2008-ovarian cancer cells, H460 lung cancer cells, MDA-MB468 breast cancerous cells (Verschoor et al 2010; Amoêdo et al 2011; Kristiansen et al 2011). HAC respiration is approximately 3-fold, 5-fold and 4-fold lower compared to mouse cortical synaptosomes, neonatal rat ventricular myocytes and RMS-13 myoblasts respectively (Flynn et al 2011; Hill et al 2009; Civitarese et al 2010).

Basal respiration is controlled mainly by ATP production and partly by proton-leak and substrate oxidation (Ainscow, & Brand 1999; Brown et al 1990). Therefore those parameters have to also be taken into consideration. In terms of substrate oxidation, all the cells were supplied with the same pyruvate and glucose containing media in order to keep this parameter constant between experiments. To assess the contribution of proton leak to basal respiration, ATP synthase was inhibited by oligomycin (Nobes et al 1990; Brand et al 1991). The resulting non-oligomycin sensitive respiration is accounted to be due to proton-leak (Nobes et al 1990; Brand et al 1991) with oligomycin sensitive respiration considered to be due to (Nobes et al 1990; Brand et al 1991). SW1353 cells had higher respiration (6.8-fold) after inhibition by oligomycin, higher uncoupled respiration (4.7-fold) after FCCP treatment and 3.4-fold higher non-mitochondrial respiration (Figure 5.1). Therefore, it have be concluded that SW1353 chondrosarcoma cells respire much more than HAC.

However, when assessing different parameters of the MRC function, HAC have 1.5-fold higher SRC and 1.8-fold higher RCR than SW1353 cells (Figure 5.3). This suggests that HAC can respond better to changes in energy demands compared to SW1353 cells and also they have a more efficient MRC as well (Brand, & Nicholls 2011; Choi et al 2009; Yadava, & Nicholls 2007). This can be due to the higher levels of proton leak found in SW1353 cells (8.4-fold) compared to HAC and therefore SW1353 cells utilize less of their available protons for ATP synthesis than HAC. However, due to the higher resting respiration in SW1353 cells, and therefore possibly higher ATP demand, ATP

production is much higher (6.6-fold) compared to HAC suggesting that HAC do not produce as much ATP by OXPHOS as SW1353 cells.

5.5.3 NOF and OA chondrocytes have different mitochondrial respiration patterns, as assessed by the Oroboros Oxygraph-2k

As mentioned above, a previous study reported that OA chondrocytes have lower complex II and complex III activities as well as more depolarized mitochondria and more mitochondrial mass (Maneiro et al 2003). However the respiratory activity of the cells has not been compared. In order to compare mitochondrial respiration between NOF and OA chondrocytes, HAC from both NOF and OA cartilage samples were extracted and analysed after three days in culture.

At first respiration was assessed using the Oroboros Oxygraph 2k respirometer. OA chondrocytes had a significantly higher basal and oligomycin insensitive respiration (Figure 5.2). They also had higher uncoupled respiration than NOF however this was not statistically significant. Non-mitochondrial respiration was almost identical in NOF and OA chondrocytes. The higher respiration in OA might be due to the higher mitochondrial mass reported in OA chondrocytes compared to NOF as an adaptive response to the lower complex II and complex III activities (Maneiro et al 2003). By assessing different parameters of respiratory function, OA chondrocytes had a significantly lower SRC, significantly lower RCR and significantly higher proton leak compared NOF (Figure 5.3). OA chondrocytes also had higher ATP production but it was not statistically significant. These parameters indicate that OA chondrocytes respire closer to their bioenergetics limit compared to NOF and therefore cannot respond as well to energy changes as NOF chondrocytes. In addition, OA HAC have a higher proton leak thus indicating that part of their basal respiration is not due to ATP production and also that they utilize less of the proton-gradient in the production of ATP compared to NOF. OA chondrocytes also have a lower RCR than NOF, which confirms the fact that OA chondrocytes have less SRC and more proton leak compared to NOF and suggests possible mitochondrial respiratory dysfunction.

Assessing mitochondrial respiration using the Oroboros system had some drawbacks. Firstly, the cells had to be trypsinised before assessing their respiration since the system requires the cells to be in a suspension. This could potentially alter the mitochondrial respiration as cells are lifted from their normal growth environment and exposed to a suspension environment. Another limitation of this system is the large number of cells required per experiment. At least 2 million chondrocytes were required in order to obtain sufficient respiration to compare between NOF and OA. Furthermore, the number of simultaneous technical repeats that can be performed are limited to two due to the presence of just two wells on the respirometer.

5.5.4 NOF and OA chondrocytes have different mitochondrial respiration patterns, as assessed by the Seahorse XF-24 analyser

A different respirometry system subsequently became available, the Seahorse XF-24 extracellular flux analyser. Using this system, cells must be able to adhere on the surface of the plates provided by Seahorse Inc. Therefore, HAC could be cultured directly after extraction in these plates and then examined for mitochondrial respiration directly in these plates without the need to use trypsin. Another advantage of this system is that twenty wells are available simultaneously for experimentation and therefore at least five technical repeats were performed per measurement. The number of cells required is significantly less compared to the Oroboros system, as 150,000 cells were required per well to perform the comparisons between NOF and OA chondrocytes.

Therefore, the Seahorse XF-24 system was used to confirm the results acquired using the Oroboros system. As with the experiments performed using the Oroboros system, OA chondrocytes respired significantly more than NOF chondrocytes at basal levels, after oligomycin inhibition and after FCCP uncoupling as they consumed more O_2 than NOF cells at these stages of the experiment (Figure 5.4). No significant difference was recorded in the non-mitochondria respiration measured after sequential rotenone and antimycin A treatment.

Analysis of respiration using the same parameters as with the Oroboros system produced similar results (Figure 5.5). OA chondrocytes had a significantly lower

SRC and significantly higher proton leak compared to NOF. As before, this suggests that OA HAC work closer to their bioenergetic limit compared to NOF and therefore have a lower SRC to respond to changes in energy demands. Also, they have a higher proton leak, which suggests that they have a larger amount of protons that is not utilized in ATP synthesis compared to NOF and this contributes to non-phosphorylating respiration. It also suggests that OA mitochondria are slightly uncoupled which can be due to changes in the proton conductance of the inner membrane and changes in the Δψm. OA chondrocytes have been reported to have more depolarized mitochondria compared to control, therefore this can partially explain the increase in proton leak (Maneiro et al 2003). The net effect is evident in the cell RCR values, which take into account both the capacity and proton leak of the cells. OA chondrocytes have a lower RCR compared to NOF, which suggests that their MRC is more dysfunctional due to the higher proton leak and lower SRC.ATP productionwas also significantly higher in OA chondrocytes as a result of the increasing respiration possibly due to the mild uncoupling of the MRC.

5.5.5 There is no difference in glycolysis between OA and NOF chondrocytes

Another advantage of the Seahorse XF-24 system is that it measures the level of glycolysis by measuring extracellular acidification rate (ECAR) at the same time as measuring the O_2 flow since it has two separate sensors. Therefore the glycolytic activity of NOF and OA chondrocytes was assessed. No significant difference was determined between the glycolytic activity of NOF and OA chondrocytes at any point of the experiment (Figure 5.6). An interesting observation is the fact that after inhibition of the ATP synthase by oligomycin, the glycolytic activity in both NOF and OA increased very slightly. ATP synthase inhibition normally induces ATP production by glycolysis (Brand, & Nicholls 2011). In other systems glycolysis after oligomycin inhibition accelerates approximately 10-fold in order to maintain ATP production (Brand, & Nicholls 2011). In this case, oligomycin induced only a non-statically significant 5% increase in both NOF and OA cells. This can due to the fact that oligomycin also causes a failure of glycolysis as well failure of fatty acid oxidation and catabolism and therefore causes a decrease in respiration or in this case a very

minor increase (Brown et al 1990; Nobes et al 1990). This observation could be explained by the fact that mitochondrial respiration is not highly active in chondrocytes, as suggested previously, and the cells rely massively on glycolysis (Lee, & Urban 1997; Stockwell 1983). Therefore, upon inhibition of the ATP synthase by oligomycin, glycolysis does not change, as the cells are already mainly glycolytic.

5.5.6 HAC have a low OXPHOS/Glycolysis ratio which confirms that they are mainly glycolytic as reported previously

It has been reported previously that only 25% of the chondrocytes' ATP is produced by OXPHOS and the remainder is by glycolysis (Stockwell 1983; Lee, & Urban 1997). By combining our data the ratio between mitochondrial and glycolysis was determined in order to assess how much the cells depend on OXPHOS in relation to glycolysis for ATP production (Figure 5.6). At basal levels, NOF chondrocytes depend more, or almost as much, on glycolysis as the OXPHOS/Glycolysis ratio was approximately 0.8 indicating that approximately 55% of the total respiration in NOF chondrocytes is due by glycolysis and 45% by OXPHOS. In OA chondrocytes the ratio was 1.5 possibly due to the higher activity and higher levels of identified in the previous experiments. This suggests that OA cells rely more on mitochondrial respiration as 60% of the respiration is due to OXPHOS and 40% by glycolysis. The comparison between NOF and OA chondrocytes was not statistically significant, however the general conclusion is that HAC rely almost as much on the MRC and OXPHOS for their ATP production as in glycolysis under the conditions examined as reported previously (Lee, & Urban 1997; Stockwell 1983).

Since in our study, total respiration was used in this calculation, and any mitochondrial respiration due to proton leakiness was not subtracted to calculate the respiration due to ATP production, the ratio calculated might be overestimated. Therefore, the ratio of OXPHOS dependent ATP production to glycolytic ATP production is possibly lower (approximately 33% ATP produced by OXPHOS and 67% by glycolysis assuming that the ECAR value is only due to ATP producing glycolysis) and therefore similar to the 25% ATP production by OXPHOS suggested previously (Stockwell 1983; Lee, & Urban 1997).

Additionally, the percentage of ATP produced by OXPHOS in chondrocytes as measured in this thesis might be exaggerated due to the use of sodium pyruvate to stimulate mitochondrial respiration.

5.5.7 SOD2 depletion causes similar changes in mitochondrial respiration pattern as in OA chondrocytes

The effect of SOD2 depletion on the mitochondrial respiration was also assessed. A recent study performed on SOD2 null mice, suggested that SOD2 depletion leads to a decrease in SRC in cortical synaptosomes due to increased levels of oxidative stress in the mitochondria (Flynn et al 2011).

Reduced SRC has been suggested as a consequence of mild uncoupling of the MRC in cerebellar granule neurons in order to reduce $O_2^{\cdot-}$ levels in the mitochondrial matrix (Johnson-Cadwell et al 2007). A study by the same group also suggested that an impaired SRC also regulates glutamate toxicity upon complex I inhibition (Yadava, & Nicholls 2007).

In this thesis, successful SOD2 downregulation was achieved by SOD2 RNAi transfection of HAC in the Seahorse XF-24 plates and HAC were analysed for their respiration using the Seahorse XF-24 system (Figure 5.7). SOD2 depleted HAC had higher (but not statistically significant) respiration compared to siCON transfected HAC (Figure 5.8). Subsequent analysis of the respiratory parameters showed SOD2 depleted HAC had significantly lower SRC and significantly higher proton leak compared to control, similar to the OA chondrocytes compared to NOF (Figure 5.9). RCR was lower and ATP production was higher in the SOD2 depleted HAC but the values did not reach statistical significance. Therefore, in HAC, SOD2 depletion causes SRC impairment as with the Flynn *et al* study, although the level of impairment was much lower in our study possibly due to the difference in respiratory requirements between HAC and cortical synaptosomes (Flynn et al 2011). Combined with the increase in proton-leak, these results suggest that SOD2 downregulation causes a mild uncoupling of the MRC, possibly to decrease $O_2^{\cdot-}$ levels in the mitochondrial matrix, however at the same time it caused impairment of the SRC which can potentially expose the cells to calcium

deregulation and glutamate-induced toxicity reported previously in OA models (Jean et al 2006; Johnson et al 2000).

5.5.8 SOD2 depleted HAC have more depolarised mitochondria compared to control

Another effect of SOD2 downregulation that has been reported in neurons is Δψm depolarization possibly due to increase in proton leak and lipid peroxidation (Fukui, & Zhu 2010; Kokoszka et al 2001). Similarly, it has been reported that OA chondrocytes have more depolarized mitochondria compared to healthy controls (Maneiro et al 2003). However, no link has been identified on the effect of SOD2 depletion in HAC and whether that resembles the disease phenotype. In this thesis, it was initially attempted to optimize the JC-1 Δψm stain in HAC, as it was used in Maneiro *et al* (Maneiro et al 2003). To assess the dye, HAC were treated with 0.01% (v/v) DMSO as a control and with 2μM FCCP to depolarize the mitochondria. JC-1 in cells with normal Δψm forms J-aggregates, which are complexes with red fluorescence (Maneiro et al 2003). In cells with depolarized mitochondria, JC-1 remains in its monomeric form that shows only green fluorescence (Maneiro et al 2003). Therefore, addition of FCCP should prevent formation of the red J-aggregates and JC-1 should remain in its green monomeric form. In our experiments however, FCCP did not induce any shift from red to green and therefore it was concluded that JC-1 was not appropriate to study Δψm changes (Figure 5.11). Additionally, JC-1 is prone to the formation of artifacts due to occasional red JC-1 speckles within individual mitochondria arising from localized J-aggregate formation (Keil et al 2011; Diaz et al 2000; Brand, & Nicholls 2011).

TMRM was then evaluated using the same protocol. TMRM is a cationic probe that is selectively localized in the mitochondrial matrix due to the presence of a net negatively change caused by the proton gradient. Any variations in the Δψm change the intensity but not the spectra of the probe. Addition of FCCP induced a decrease in the intensity of the TMRM dye, due to depolarization of the mitochondrial membrane (Figure 5.12). Addition of oligomycin also induced a mild hyperpolarization, in some cases, which was evident by the increase in TMRM intensity (Figure 5.12). TMRM was used at non-quench mode in order to

avoid aggregation and quenching in the mitochondrial matrix (Nicholls 2006; Brand, & Nicholls 2011). Additionally, non-quench mode enables comparison of populations of cells with a pre-existing difference in Δψm (Brand, & Nicholls 2011). Therefore, TMRM was used to assess possible changes in the Δψm due to SOD2 downregulation in chondrocytes.

HAC, transfected with siRNA against SOD2 or with a non-targeting siRNA, were stained with TMRM and their fluorescence was assessed at basal levels and after sequential oligomycin and FCCP treatment using a fluorescent microscope (Figure 5.13). HAC transfected with siRNA against SOD2 had a lower intensity compared to controls at basal levels and also after oligomycin and FCCP treatment. As TMRM is a slow-response probe, TMRM accumulation was allowed to equilibrate for 10mins after each treatment. Oligomycin treatment caused depolarization in both siSOD2 and siCON cells which possibly indicates a dysfunctional MRC (Brand, & Nicholls 2011). Mitochondria depolarised further after FCCP treatment however this effect could be due to the prior oligomycin treatment and its depolarising effect on HAC mitochondria in this experiment. Therefore, mitochondrial membrane depolarization in OA can potentially be due to SOD2 downregulation in HAC (Maneiro et al 2003). For more accurate measurement of Δψm, experiments could be performed in the simultaneous presence of a fluorescent cation, such as TMRM, and a fluorescence anion (PMPI, plasma membrane potential indicator) that enters the cytoplasm as the plasma membrane is depolarized (PMPI) (Nicholls 2006). This is required because accumulation of fluorescent membrane permeant cations, such as TMRM, is influenced by both plasma and mitochondrial membrane potentials and therefore measuring both can clear any ambiguity of what causes the accumulation of these cations (Nicholls 2006).

5.5.9 Summary

By combining the data shown in this chapter and data from chapter 3, it can be concluded that SOD2 downregulation increases $O_2^{\cdot-}$ levels in HAC mitochondria and this increase in $O_2^{\cdot-}$ induces oxidative damage and mitochondrial dysfunction. Higher ROS levels due to SOD2 downregulation can potentially induce higher levels of lipid peroxidation in chondrocytes and possibly in OA

cartilage. Increasing ROS levels can also cause mild uncoupling of mitochondrial respiration in the form of higher proton leak in order to decrease ROS production as shown in other systems (Korshunov et al 1997; Longo et al 1999; Skulachev 1996). In brief, by increasing the proton leak, the proton-motive force that drives ATP production is lower, and that can lead to a more oxidized ubiquinone pool and a lower concentration of ubisemiquinone. It can also increase oxygen consumption rate, as in the case of OA chondrocytes and SOD2 depleted chondrocytes, to lower the oxygen tension around the mitochondria. Since $O_2^{\cdot-}$ production depends on both ubisemiquinone and oxygen concentration, lowering the concentration of these two molecules leads to lower ROS production.

Membrane damage, in this case mitochondrial inner membrane damage, due to lipid peroxidation can also contribute to the increase in proton leak by increasing the proton conductance of the membrane and therefore allowing more protons to leak through the inner membrane into the matrix (Kokoszka et al 2001). Lipid peroxidation has also been associated with decreasing SRC. In a study on cardiomyocytes, induced lipid peroxidation depleted the SRC of the cells and induced protein damage and cell death (Hill et al 2009). A later study by the same group also showed that NO and H_2O_2 decreased the SRC in endothelial cells and caused cell death, suggesting that SRC is important in cell responses to oxidative stress (Dranka et al 2010).

Higher levels of proton leak can lead to mild uncoupling which can then lower the SRC of the cells as we see in OA chondrocytes and siSOD2 chondrocytes compared to their control. Proton leak can also depolarize the mitochondrial membrane and this was true in this thesis in SOD2 depleted cells as well as in Maneiro *et al*, where OA chondrocytes had more depolarized mitochondria compared to controls (Maneiro et al 2003).

These data suggest that there is mitochondrial dysfunction due to the downregulation of SOD2 in OA that can potentially lead to activation of apoptotic pathways and inflammatory pathways that can lead to cartilage degradation and osteoarthritis (López-Armada et al 2006; Lopezarmada et al 2006).

5.6 Conclusions

In this chapter mitochondrial and glycolysis was assessed in OA and NOF chondrocytes and the role of SOD2 in regulating respiration was evaluated. Mitochondrial respiration in HAC is low compared to SW1353 chondrosarcoma cells. OA chondrocytes have less SRC and more non-phosphorylating respiration, proton leak and ATP production compared to NOF. Also, HAC depend as much or even more on glycolysis for their ATP production than mitochondrial respiration. The role of SOD2 in mitochondrial respiratory regulation was also determined. SOD2 downregulation causes a decrease in SRC and increases proton-leak similar to OA however, SOD2 depletion does not affect glycolysis. In addition, SOD2 downregulation causes Δψm depolarisation similar to OA.

Taken together, these results suggest that there is mitochondrial respiratory dysfunction in OA, partially as consequence of SOD2 downregulation and higher $O_2^{\cdot-}$ levels. Although these changes may be a response to reduce the effect of higher $O_2^{\cdot-}$ levels, apoptotic pathways can also be potentially activated in chondrocytes and lead to cartilage degradation (Figure 5.14). Chondrocyte apoptosis has been linked to the reduced number of cells in OA cartilage and is considered to contribute to cartilage degradation (Blanco et al 1998; Hashimoto et al 1998; Stockwell 1967). However, a later study contradicted these findings and suggested that apoptosis does not play a role in OA as they identified very low levels of apoptotic chondrocytes (Aigner et al 2001). Inflammatory pathways can also be potentially activated in chondrocytes due to the increase in $O_2^{\cdot-}$ levels that can lead to collagenase activation and cartilage degradation (Figure 5.14).

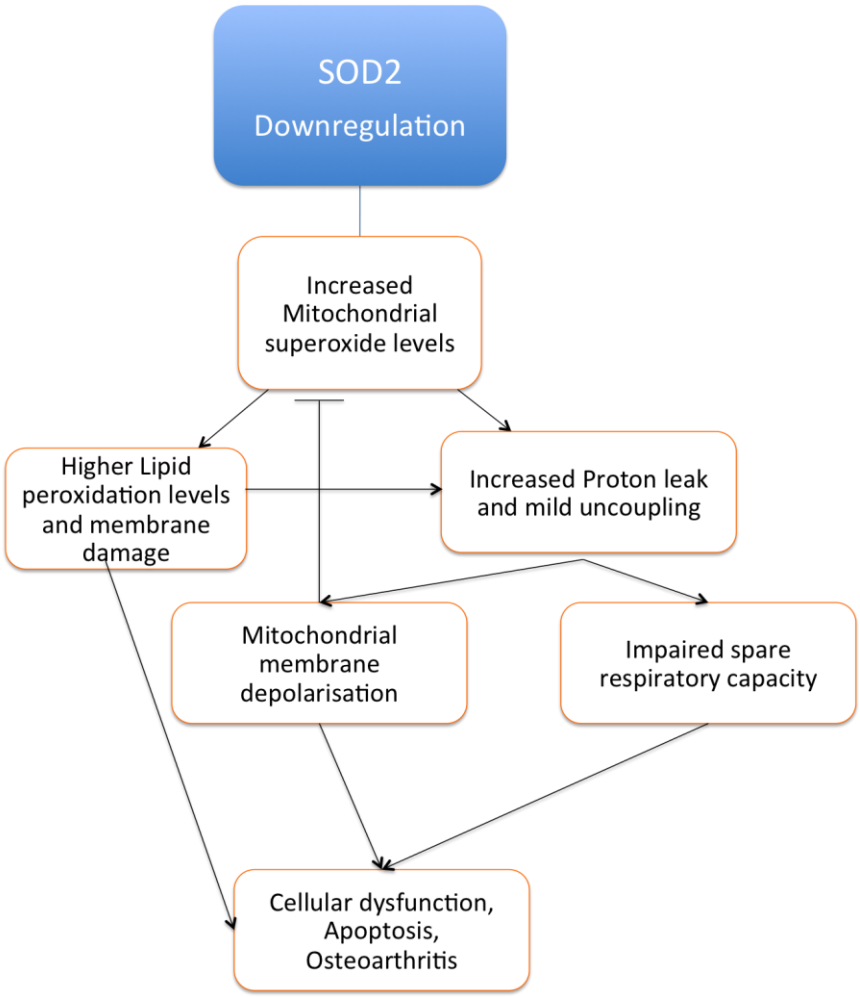

Figure 5.14 Potential effects of SOD2 downregulation and mitochondrial dysfunction in OA

Chapter 6. Mitochondria as an innate immunity signalling platform in OA

6.1 Hypothesis

Mitochondria act as a signalling platform for innate immunity, which could have a role in OA

6.2 Introduction

As discussed in more detail in sections 1.1.7 and 1.1.10, mitochondria have been considered to act as a signalling platform integrating signals that regulate different processes and signalling pathways including Ca^{2+} signalling and handling, ROS signalling, apoptosis and more recently innate immunity signalling.

Mitochondria maintain and dictate cytosolic Ca2+ concentrations through their ability to accumulate, buffer and release Ca2+ into and from the cytoplasm (Jouaville et al 1999; Landolfi et al 1998; Dumollard et al 2004).

Mitochondrial ROS (mtROS) have been reported to stimulate TNF-α mediated cell death and also inhibit the activity of different phosphatases including protein tyrosine phosphatase 1B, phosphatase & tensin homolog (PTEN) and MAPK phosphatases (Kamata et al 2005; Kwon et al 2004; Lee et al 1998; Levinthal, & Defranco 2005; Meng et al 2002). Studies have described the role of ROS as signalling molecules in both NLRP3-inflammasome dependent and independent pro-inflammatory cytokine release (IL-6, IL-1β and IL-18) and caspase activation (Bulua et al 2011; Nakahira et al 2011; Zhou et al 2011).

Mitochondria also play a major role in apoptosis. TNF-α, IL-1β release and NF-κB activation, facilitate the recruitment of members of the Bcl-2 family of pro-apoptotic proteins such as Bid and Bad which undergo conformational changes and translocate to the mitochondria to then facilitate the release of cytochrome *c* into the cytoplasm and trigger caspase 9 activation (Wachlin et al 2003; Kamata et al 2005).

In recent years, mitochondria have also been linked with regulation of innate immunity signalling. VISA has been identified to regulate IFNα and IFNβ production through the NF-κB, IRF3 and IRF7 pathways in response to viral dsRNA (Seth et al 2005; Kawai et al 2005; Meylan et al 2005; Xu et al 2005). dsRNA is sensed by TLR3, RIG-I and MDA5 (Kato et al 2005; Kato et al 2006; Gitlin et al 2006). VISA, found on the mitochondrial outer membrane, regulates both TLR3 and RLR dependent pathways by interacting with RIG-I (RLR dependent) as well as with downstream components of the TLR3 pathway, TRIF and TRAF6 (Kawai, & Akira 2006; Xu et al 2005).

Two independent studies have suggested that NLRX1 is also localized in the mitochondria and has a role in both negative (Moore et al 2008) and positive (Tattoli et al 2008) regulation of innate immunity signalling via two different modes of action. Firstly, it regulates immune signalling by negatively regulating the activity of VISA and thus downregulating the activation of the RLR dependent anti-viral response described above (Moore et al 2008). The same study suggested that NLRX1, like VISA, is localized at the mitochondrial outer membrane. Secondly, NLRX1 has also been identified to increase ROS production in response to TNF-α, *Shigella* infection and dsRNA treatment, resulting in amplified NF-κB and JUN dependent signalling pathways and therefore suggesting that NLRX1 is a positive regulator of the innate immunity response (Tattoli et al 2008). In 2009, the same group suggested that NLRX1 is localized in the mitochondrial matrix thus speculating that it does not interact with VISA to block signaling (Arnoult et al 2009). Another recent report, using NLRX1 knockout mice, has shown that NLRX1 deficiency does not alter VISA-dependent responses but identified a mitochondrial complex III subunit to be binding with NLRX1 thus suggesting that NLRX1 can regulate the activity of the MRC and alter ROS production (Rebsamen et al 2011).

As described previously in this thesis (section 1.3.2), SOD2 expression is reduced in OA both at the mRNA and protein level compared to NOF (Scott et al 2010; Ruiz-Romero et al 2009; Aigner et al 2006). In the previous chapters, the effects of SOD2 depletion were demonstrated in terms of oxidative damage, mtDNA deletions and changes in mitochondria bioenergetics. However, the

mechanisms of SOD2 regulation in chondrocytes and importantly OA have not been extremely investigated.

NF-κB has been identified as a positive regulator of *SOD2* activity in VA-13 human lung fibroblast cells upon stimulation with pro-inflammatory cytokines TNF-α and IL-1β (Xu et al 1999; Miao, & Clair 2009). The *SOD2* gene promoter has two NF-κB binding sites, one in the promoter region and a second located within an intronic (intron 2) enhancer (Xu et al 1999).

In a study performed by our laboratory, TLR3 expression has been shown to be significantly upregulated in OA cartilage compared to normal healthy cartilage (Zhang et al 2008). In the same study, TLR3 has been shown to upregulate NF-κB mediated *MMP-1* and *MMP-13* induction suggesting a role in matrix degradation. In a separate study from our laboratory (David A. Young, unpublished data) showed differential expression of both NLRX1 and TLR3 in OA and NOF cartilage suggesting a possible role of these proteins in OA progression (Figure 6.1).

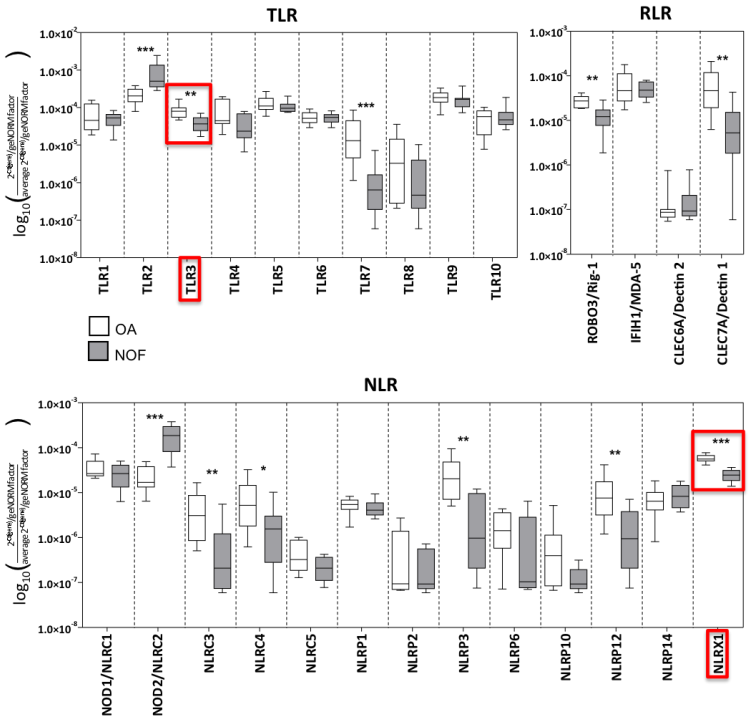

Figure 6.1 Real-time PCR data showing differential expression of *TLR3* and *NLRX1* in OA and NOF cartilage (by Dr David A. Young, unpublished data)

The gene expression levels of genes involved in innate immunity signalling in hip cartilage from patients with OA (open bars; n = 9, median age = 72yrs) or NOF (shaded bars; n = 10, median age = 76yrs) were and normalised *TNFRSF1A* and *IL6ST* expression levels calculated to be the most stable using genome analysis (Vandesompele et al 2002). Significant differences between the NOF and OA groups were determined using a two-sided Mann–Whitney U test, where *p≤0.05, **p≤0.01 and ***p≤0.001. Lines within the boxes represent the median, the boxes represent the 25th and 75th percentiles and the lines outside the boxes correspond to the minimum and maximum values.

Mitochondria appear of paramount importance in innate immunity signalling events. Therefore, we considered, since mitochondrial dysfunction may be important in OA, whether mitochondria regulate these signalling events in chondrocytes. Part of the work described in this chapter was performed in collaboration with Dr Marta Radwan.

6.3 Aims

- Determine the role of mitochondria in chondrocytes as an innate immunity signalling platform
- Identify the role of VISA and dsRNA in regulation of MMP-13 expression in chondrocytes

- Identify the role of NLRX1 and dsRNA in regulation of MMP-13 expression and NF-κB activation in chondrocytes
- Identify the role of NLRX1 and dsRNA in induction of reactive oxygen species in chondrocytes
- Determine the role of NLRX1 and dsRNA in SOD2 expression regulation in chondrocytes
- Cloning of SOD2 promoter region to identify changes that differentially regulate its expression in OA and NOF

6.4 Results

6.4.1 siRNA targeted depletion of NLRX1 and VISA

RNAi-mediated depletion of NLRX1 mRNA and protein levels was used to study the role of NLRX1 in the regulation of *MMP-13* expression and the activation of ROS in chondrocytes. The optimal transfection procedure and duration of siRNA incubation are described in section 2.3.2. Transfection of NLRX1 targeted siRNA resulted in 75% reduction in basal mRNA levels in HAC (Figure 6.2A). A pronounced decrease in intensity of basal protein levels was identified in HAC targeted with siRNA against NLRX1 (Figure 6.2B). In SW1353 cells, similar levels of NLRX1 protein and mRNA downregulation were achieved (data not shown).

RNAi-mediated depletion of VISA mRNA and protein levels was used to study the role of VISA in the regulation of *MMP-13* expression. The optimal transfection procedure and duration of siRNA incubation are described in section 2.3.2. Transfection of VISA targeted siRNA resulted in 80% reduction in basal mRNA levels (Figure 6.2A). A pronounced decrease in intensity of basal protein levels was identified in HAC targeted with siRNA against VISA (Figure 6.2C).

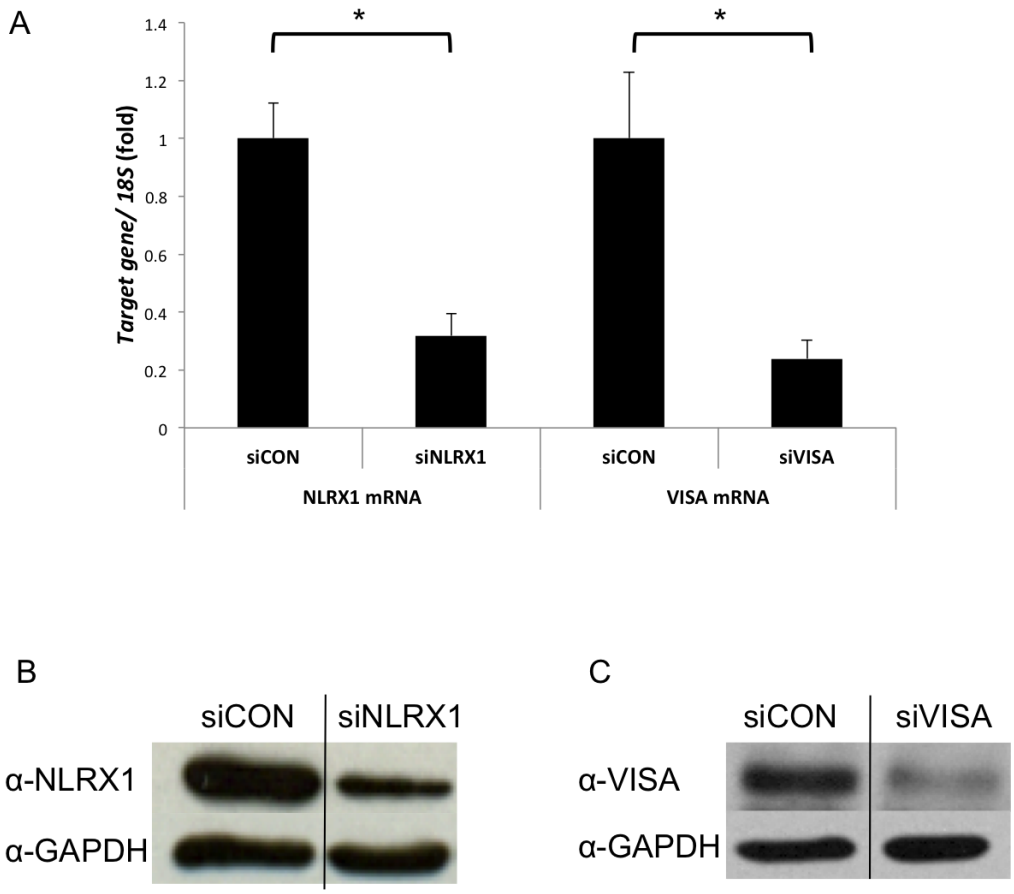

Figure 6.2 Effect of NLRX1 and VISA siRNA knockdown on mRNA and protein levels of NLRX1 and VISA respectively (performed together with Dr Radwan)

(A) HAC isolated from knee cartilage were transfected with 50nM of NLRX1, VISA or control siRNA for 48 hours. Cells were then serum starved for 24 hours. Total RNA was extracted with Cells-to-cDNA lysis buffer as described in section 2.4.7, reverse transcribed to cDNA and subjected to real-time qRT-PCR analysis of *NLRX1* or *VISA* gene expression. Values were normalised to *18S* and plotted as mean fold induction over control ± SEM (n=5). (B and C) HAC were transfected as above. Cells were then serum starved for 24 hours. Total protein was extracted, resolved by SDS-PAGE and immunoblotted as in section 2.5.3 with the (B) NLRX1, (C) VISA and (B and C) GAPDH antibodies. * p≤0.05, compared to control. Figures are representative of two independent experiments.

6.4.2 Effect of poly(I:C) on MMP-13 levels in SW1353 cells

Stimulation with extracellular dsRNA mimic poly(I:C) has been shown to activate TLR3, whereas transfected poly(I:C) bypasses TLR3 activation and activates RIG-I or MDA5 (Kato et al 2005; Kato et al 2006; Gitlin et al 2006). Also TLR3 and MDA5 preferentially bind to high molecular weight (HMW) poly(I:C) (long dsRNA) whereas RIG-I binds to low molecular weight (LMW) poly(I:C) (short dsRNA) as long dsRNA stimulates IFN-β production in an MDA5 dependent manner and short dsRNA stimulates IFN-β production in a RIG-I dependent manner (Kato et al 2008). In the same study, RIG-I has been shown to recognise dsRNA without 5'- triphosphates however other studies suggested the requirement of 5'- triphosphates for dsRNA recognition by RIG-I (Hornung et al 2006; Schmidt et al 2009).

In this experiment, the MMP-13 mRNA expression levels were assessed in response to extracellular and transfected poly(I:C) stimulation in SW1353 cells (Figure 6.3). Extracellular and transfected HMW poly(I:C) stimulation caused similar high levels of MMP-13 mRNA upregulation compared to unstimulated controls. Transfected LMW poly(I:C) stimulation also resulted in highly up-regulated MMP-13 mRNA levels, however extracellular LMW poly(I:C) stimulation only marginally increased *MMP-13* expression. Poly(I:C) transfection of HAC was not as reproducible but provided similar pattern of *MMP-13* expression as to that observed by SW1353 cells.

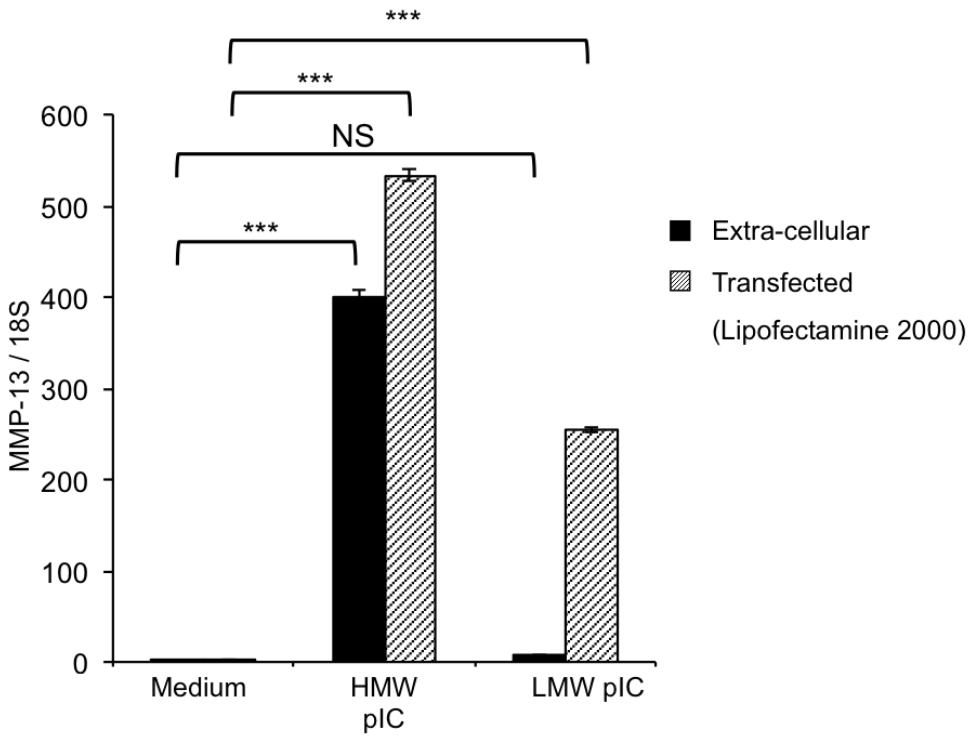

Figure 6.3 Effect of poly(I:C) stimulation (extracellular and transfection) on MMP-13 mRNA levels in SW1353 cells (performed by Dr Radwan)

SW1353 cells were stimulated with 0.5µg/ml HMW or 0.5µg/ml LMW Poly(I:C) for 24 hours. Total RNA was extracted with Cells-to-cDNA lysis buffer as described in section 2.4.7, reverse transcribed to cDNA and subjected to real-time qRT-PCR analysis of *MMP-13* gene expression. Values were normalised to *18S* and plotted as mean fold induction over control ± SEM (n=6). Figure is representative of two independent experiments. Values were normalised to *18S* and plotted as mean fold induction over control ± SEM. ***p≤0.001 and NS= not statistically significant compared to control siRNA (siCON).

6.4.3 Effect of VISA depletion on MMP-13 mRNA levels in SW1353 cells and HAC.

VISA has been identified by several studies to regulate IFNα and IFNβ production as a response to viral dsRNA (Seth et al 2005; Kawai et al 2005; Meylan et al 2005; Xu et al 2005). Therefore, due to its localisation in the mitochondria, proposed function in innate immunity signalling and due to its suggested interaction with NLRX1, the function of VISA in *MMP-13* regulation in chondrocytes was assessed in both SW1353 cells and HAC.

In HAC, VISA depletion significantly decreased basal *MMP-13* expression only in one set of experiments (Figure 6.4B) whereas in the other two, basal *MMP-13* mRNA levels did not alter significantly. RNAi depletion of VISA in SW1353 cells significantly reduced basal *MMP-13* levels in all of our experiments (Figure 6.5). Poly(I:C) induced *MMP-13* expression did not alter significantly after VISA depletion in either HAC (Figure 6.4) or SW1353 cells (Figure 6.5).

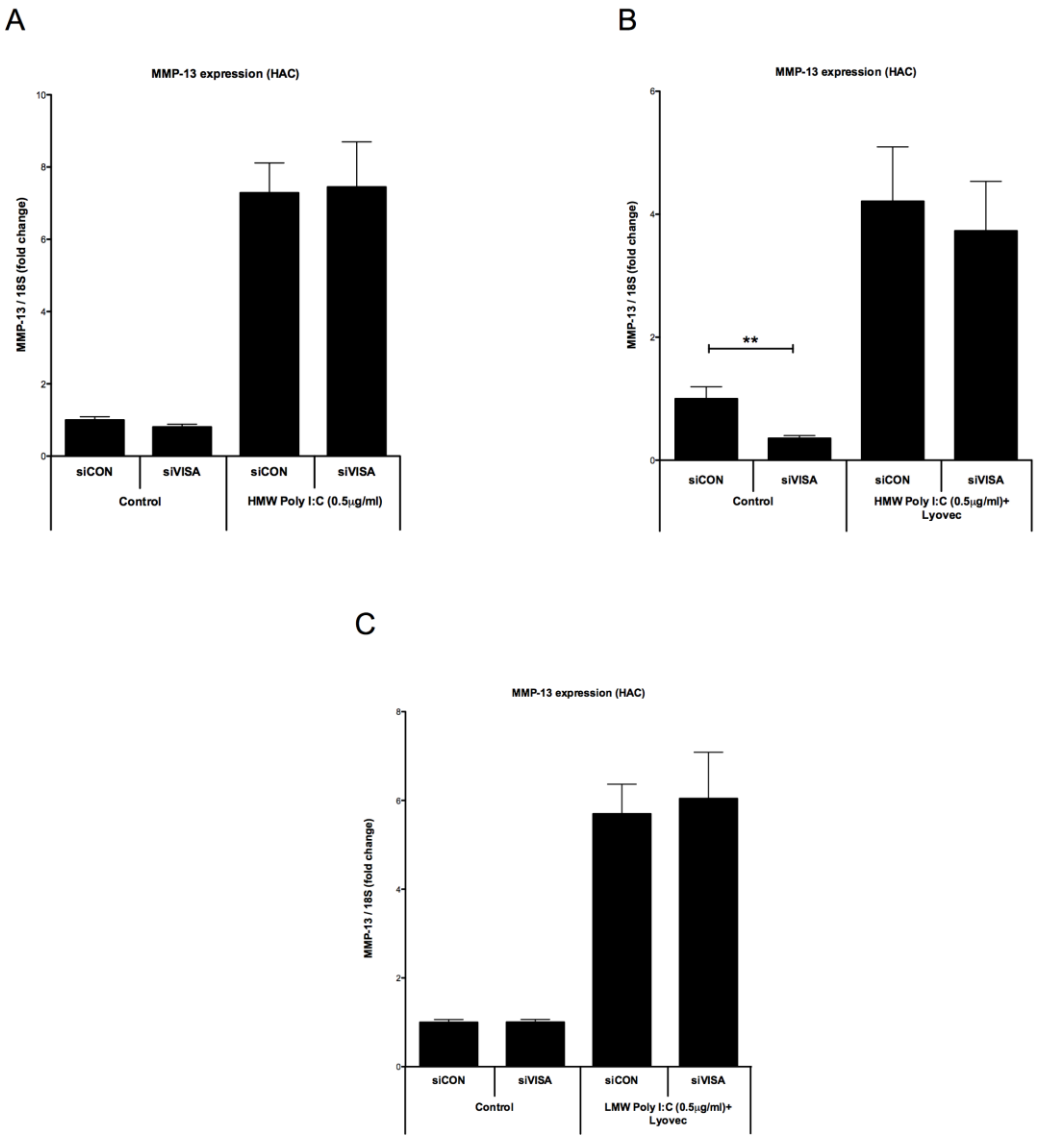

Figure 6.4 Effect of VISA siRNA knockdown and stimulation with poly(I:C) on *MMP-13* expression levels in HAC (performed together with Dr Radwan)

HAC isolated from knee cartilage were transfected with 50nM of VISA or control siRNA for 48 hours. Cells were then serum starved for 24 hours and then (A) stimulated with 0.5μg/ml naked HMW poly(I:C), (B) transfected with 0.5μg/ml HMW poly(I:C) using ready to use transfection complex poly(I:C) with lyovec or (C) 0.5μg/ml LMW poly(I:C) using lyovec, for 24 hours. Total RNA was extracted with Cells-to-cDNA lysis buffer as described in section 2.4.7, reverse transcribed to cDNA and subjected to real-time qRT-PCR analysis of *MMP-13* gene expression. Values were normalised to *18S* and plotted as mean fold induction over control ± SEM. Figures are representative of pooled results from 5 independent experiments. **p≤0.01 compared to control siRNA (siCON).

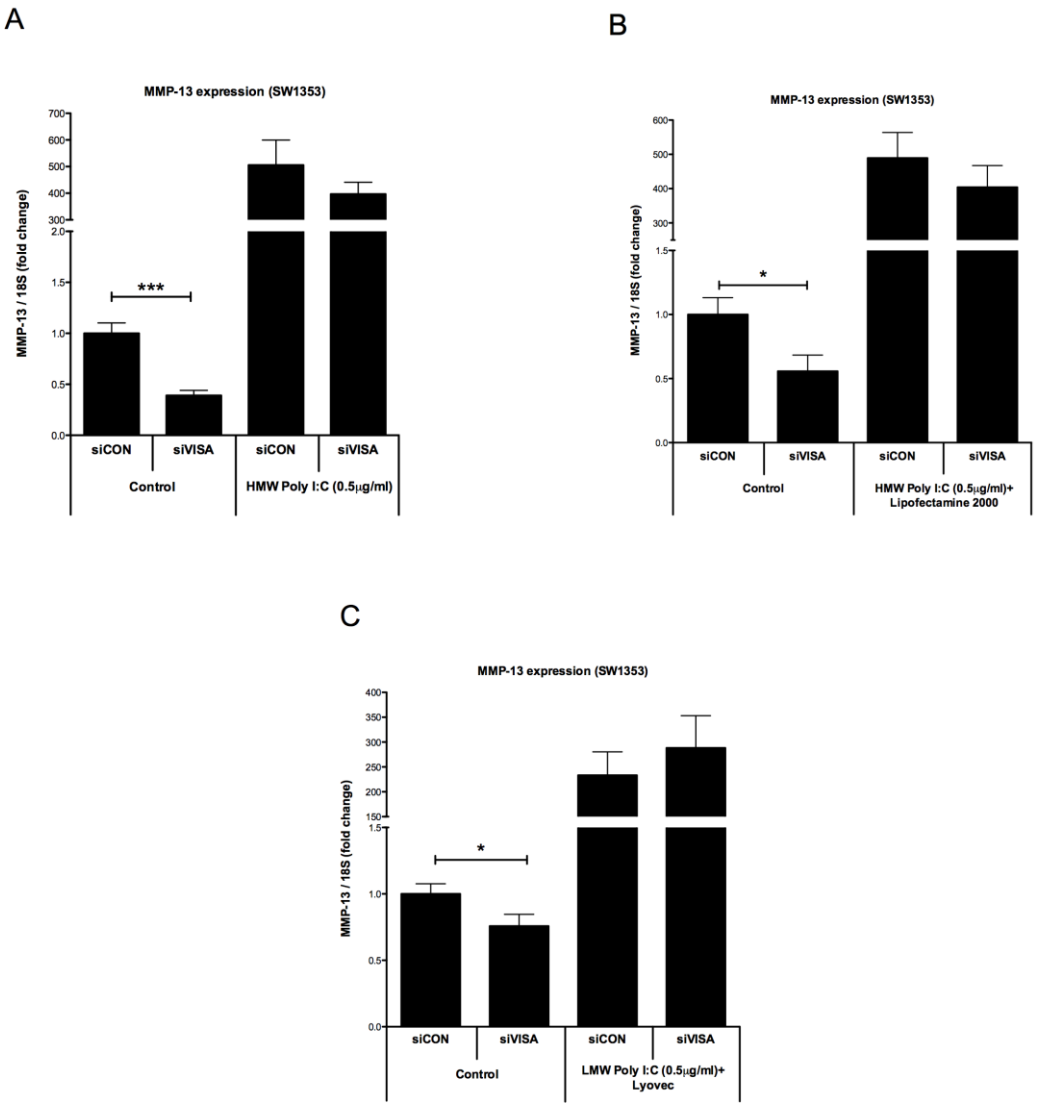

Figure 6.5 Effect of VISA siRNA knockdown and stimulation or transfection with poly(I:C) on *MMP-13* expression levels in SW1353 chondrosarcoma cells (performed together with Dr Radwan)

SW1353 cells were transfected with 50nM of VISA or control siRNA for 48 hours. Cells were then serum starved for 24 hours and then (A) stimulated with 0.5μg/ml HMW, (B) transfected with 0.5μg/ml HMW poly(I:C) using lipofectamine 2000 or (C) 0.5μg/ml LMW poly(I:C) using lyovec, for 24 hours. Total RNA was extracted with Cells-to-cDNA lysis buffer as described in section 2.4.7, reverse transcribed to cDNA and subjected to real-time qRT-PCR analysis of *MMP-13* gene expression. Values were normalised to *18S* and plotted as mean fold induction over control ± SEM. Figures are representative of pooled results from 5 independent experiments. *p≤0.05, ***p≤0.001 compared to control siRNA (siCON).

6.4.4 Effect of NLRX1 downregulation on MMP-13 mRNA levels in SW1353 cells and HAC.

As mentioned above, NLRX1 has been identified to negatively and positively regulate innate immunity signalling. Firstly, it was identified as an inhibitor of VISA (Moore et al 2008) although some studies have suggested that NLRX1 and VISA do not interact (Arnoult et al 2009; Rebsamen et al 2011). Secondly, NLRX1 has been shown to increase ROS production and amplified NF-κB and JNK dependent pathways in HeLa and human embryonic kidney 293 (HEK293) cells upon stimulation with TNF-α, Shigella infection and poly(I:C) (Tattoli et al 2008). Since NLRX1 mRNA is upregulated in OA cartilage compared to NOF, its function in chondrocytes was examined in terms of MMP-13 and SOD2 mRNA as well as ROS regulation.

In NLRX1-depleted HAC the MMP-13 mRNA levels were upregulated significantly under basal conditions (Figure 6.6A, B and C). However NLRX1 depletion followed by stimulation with poly(I:C) did not significantly change *MMP-13* expression (Figure 6.6A, B and C).

The role of NLRX1 depletion in regulating MMP-13 mRNA levels in SW1353 cells was also examined. As in HAC, NLRX1 depletion resulted in significant upregulation of MMP-13 mRNA levels under basal conditions (Figure 6.7A, B and C). However NLRX1 depletion followed by stimulation with poly(I:C) did not significantly change *MMP-13* expression (Figure 6.7A, B and C).

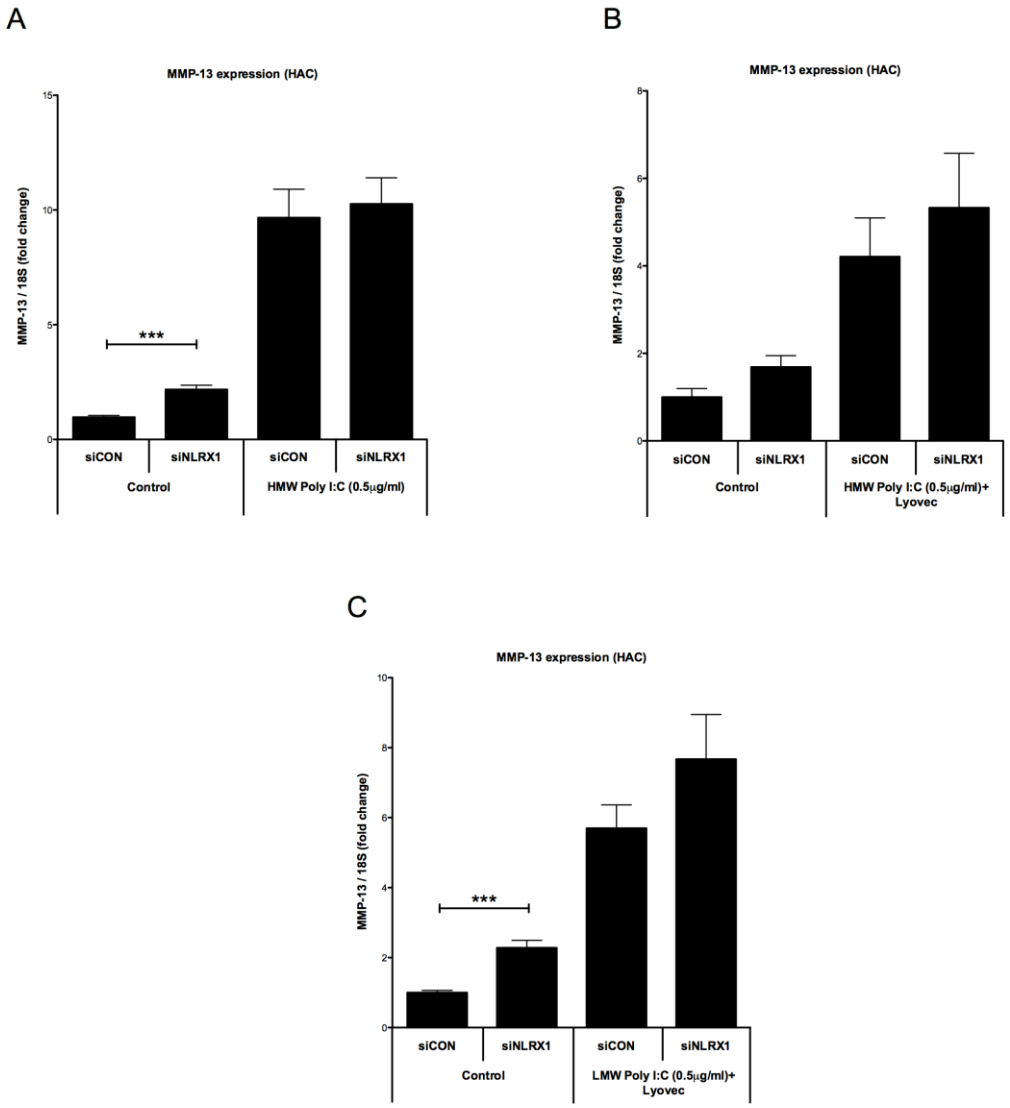

Figure 6.6 Effect of NLRX1 siRNA knockdown and stimulation or transfection with poly(I:C) on MMP-13 mRNA expression levels in HAC (performed together with Dr Radwan)

HAC isolated from knee cartilage were transfected with 50nM of NLRX1 or control siRNA for 48 hours. Cells were then serum starved for 24 hours and then (A) stimulated with 0.5μg/ml HMW poly(I:C), (B) transfected with 0.5μg/ml HMW poly(I:C) using lyovec or (C) 0.5μg/ml LMW poly(I:C) using lyovec, for 24 hours. Total RNA was extracted with Cells-to-cDNA lysis buffer as described in section 2.4.7, reverse transcribed to cDNA and subjected to real-time qRT-PCR analysis of *MMP-13* gene expression. Values were normalised to *18S* and plotted as mean fold induction over control ± SEM. Figures are representative of pooled results from 5 independent experiments. ***p≤0.001 compared to control siRNA (siCON).

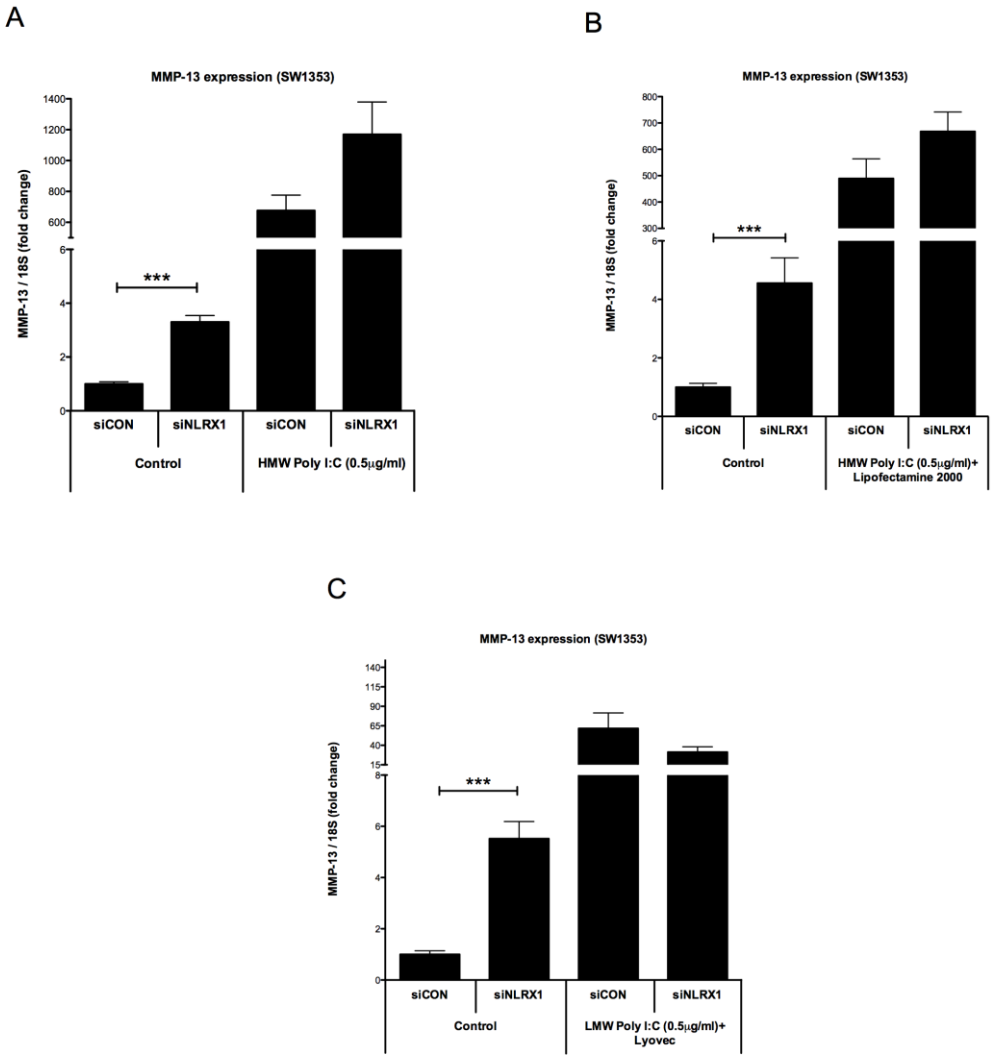

Figure 6.7 Effect of NLRX1 siRNA knockdown and stimulation or transfection with poly(I:C) on MMP-13 mRNA expression levels in SW1353 cells (performed together with Dr Radwan)

SW1353 cells were transfected with 50nM of NLRX1 or control siRNA for 48 hours. Cells were then serum starved for 24 hours and then (A) stimulated with 0.5μg/ml HMW poly(I:C), (B) transfected with 0.5μg/ml HMW poly(I:C) using lipofectamine 2000 or (C) 0.5μg/ml LMW poly(I:C) using lyovec, for 24 hours. Total RNA was extracted with Cells-to-cDNA lysis buffer as described in section 2.4.7, reverse transcribed to cDNA and subjected to real-time qRT-PCR analysis of *MMP-13* gene expression. Values were normalised to *18S* and plotted as mean fold induction over control ± SEM. Figures are representative of pooled results from 5 independent experiments. ***p≤0.001 compared to control siRNA (siCON).

6.4.5 Effect of NLRX1 overexpression and poly(I:C) and IL-1β stimulation on Nf-κb- activation in chondrocytes

MMP-13 regulation is well recognized as being NF-κB dependent and NLRX1 has been linked to NF-κB regulation (Schmucker et al 2012). Therefore, we examined the effect of NLRX1 and poly(I:C) stimulation on NF-κB promoter driven luciferase expression with transient co-transfection of NLRX1 expression constructs in SW1353 chondrosarcoma cells. The effect of poly(I:C) and IL-1β stimulation on NF-κB activation was also assessed. NLRX1 overexpression increased NF-κB -luciferase levels significantly by 2.5 fold under basal conditions (Figure 6.8). A 6-hour poly(I:C) stimulation induced NF-κB luciferase levels by 2.5-fold (Figure 6.8A) whereas IL-1β stimulation for the same time period induced a 17-fold increase in NF-κB luciferase levels (Figure 6.8B). However, NLRX1 overexpression did not significantly alter poly(I:C) or IL-1β induced luciferase expression.

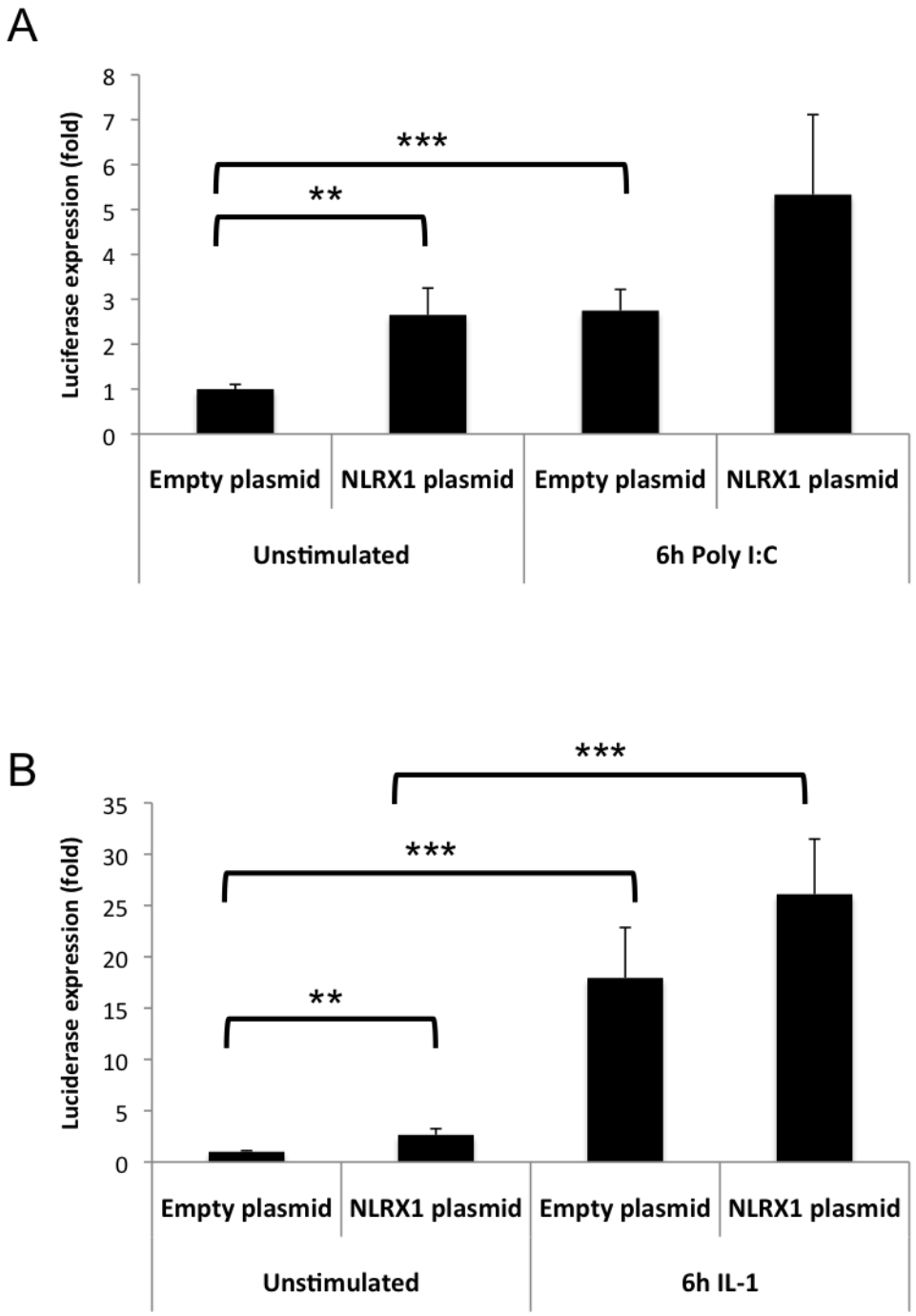

Figure 6.8 Effect of NLRX1 overexpression on NF-κB activity (performed together with Dr Radwan)

SW1353 cells were transfected with the *NLRX1* promoter constructs or empty pcDNA 3.1 vector for 24 hours as detailed in section 2.3.2. Cells were then stimulated with (A) 0.5μg/ml poly(I:C) and (B) 0.5ng/ml IL-1. Total protein was extracted with reporter lysis buffer and assayed for luciferase expression as detailed in section 2.3.3. Values were plotted as fold change in light units ±SEM. Figures are representative of pooled results from 5 independent experiments. **p≤0.01, *** p≤0.001, compared to control.

6.4.6 Effect of NLRX1 downregulation on ROS levels in HAC

Previous studies have suggested that NLRX1 regulates innate immunity signalling by increasing ROS levels upon infection{Tattoli 2008; Rebsamen 2011).

In order to determine whether NLRX1 regulates the ROS levels in HAC, HAC isolated from patient cartilage samples were transfected with siRNA targeted against NLRX1 as in section 2.3.2. The effect of dsRNA infection on ROS levels in HAC was also assessed by stimulating cells with 0.5ng/ml poly(I:C) for 6 hours. Cells were then stained with DHR, an uncharged and nonfluorescent ROS indicator that can passively diffuse across membranes where it is oxidized by cellular H_2O_2 and and hydroxyl radicals to cationic rhodamine 123, which localizes in the mitochondria and exhibits green fluorescence. Cells were visualized using a confocal microscope and images were analysed using Image J.

NLRX1 depletion using RNAi did not change the levels of ROS in HAC. However, stimulation with poly(I:C) increased ROS levels by 15%. This increase in ROS was diminished to approximately the basal levels when NLRX1 was depleted (Figure 6.9).

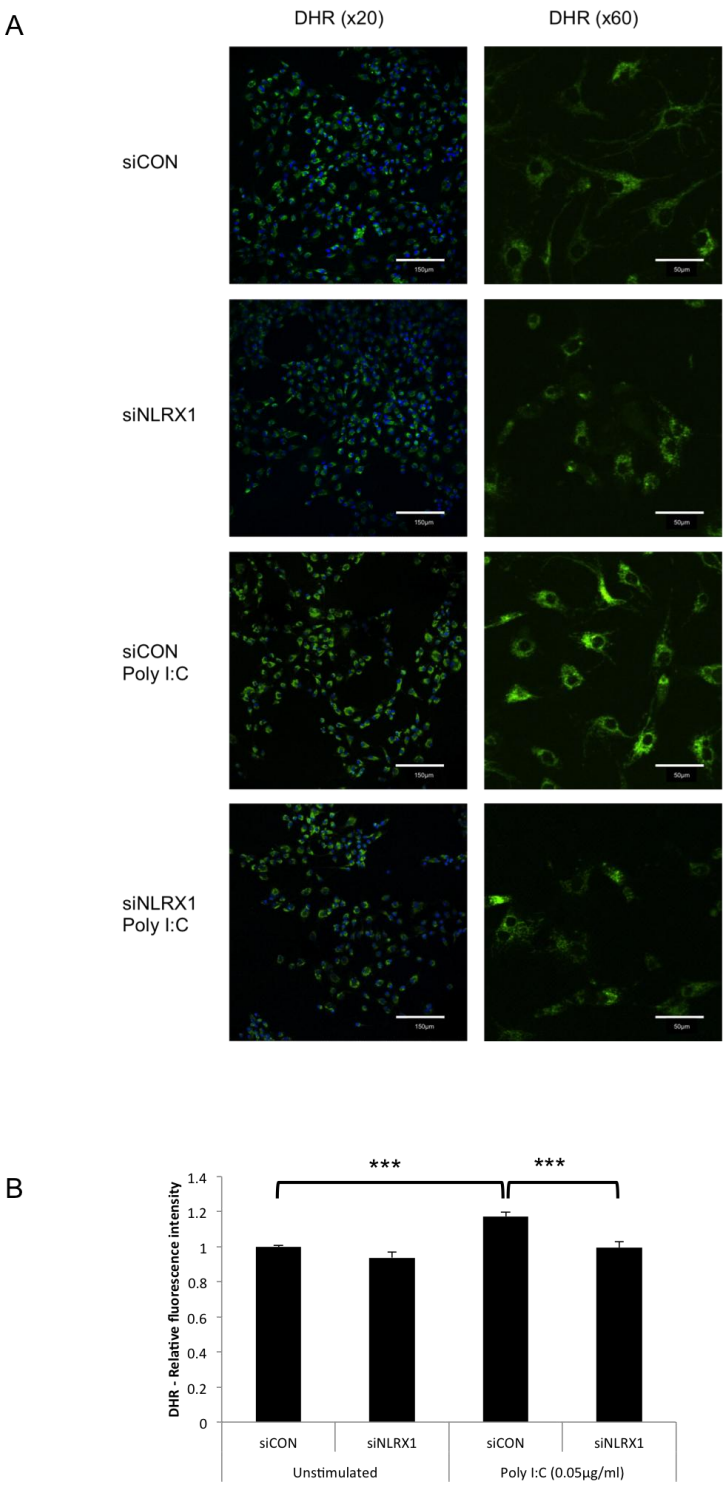

Figure 6.9 Effect of NLRX1 downregulation and poly(I:C) stimulation on DHR levels in HAC

HAC isolated from knee cartilage were transfected with 50nM of NLRX1 or control siRNA for 48 hours. Cells were then serum starved for 24 hours and then stimulated with 0.5µg/ml HMW poly(I:C) for 6 hours. Cells were then stained with 75µM DHR-123 for 30 mins and then washed with media. Fluorescence was assessed using confocal microscopy and the images were analysed using Image J. Figure A is representative of three experiments. Figure B is pooled data analysis of three independent experiments using three different patient samples. *** $p \leq 0.001$, compared to control. DAPI is shown in blue and DHR shown in green.

6.4.7 Effect of NLRX1 downregulation and poly(I:C) stimulation on SOD2 mRNA expression in chondrocytes

Since NLRX1 regulates poly(I:C) stimulated ROS production in HAC, the mechanism of ROS regulation by NLRX1 was evaluated by assessing its role in *SOD2* regulation in HAC and SW1353 cells. Cells were transfected for 48 hours with 50nM siRNA targeted against NLRX1 and subsequently stimulated or transfected with 0.5ng/ml poly(I:C) for 24hours. HAC stimulation with poly(I:C) stimulated a 2.5 fold increase in the SOD2 mRNA levels (Figure 6.10). However, transfection of HAC with poly(I:C) did not alter *SOD2* expression at all. Additionally, HAC transfection with siRNA against NLRX1 did not alter either basal or poly(I:C) stimulated SOD2 mRNA levels. Stimulation and transfection of SW1353 cells with poly(I:C) stimulated a respective 25-fold and 7-fold increase in *SOD2* expression (Figure 6.11) however, the level of *SOD2* induction by poly(I:C) is much lower compared to the *MMP-13* induction described in section 6.4.2. As with HAC, transfection with siRNA against NLRX1 did not significantly alter *SOD2* expression.

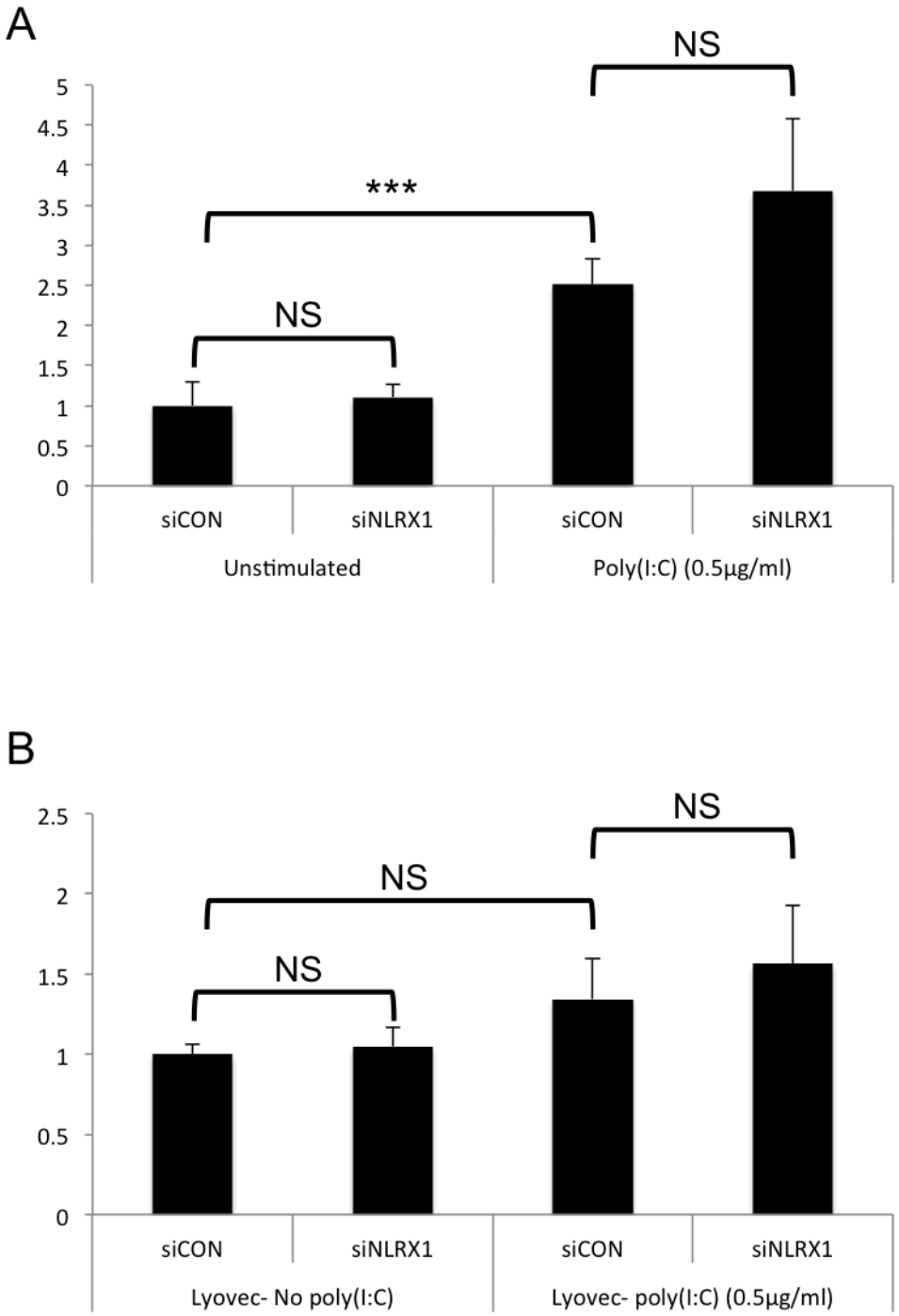

Figure 6.10 Effect of NLRX1 downregulation and poly(I:C) on SOD2 mRNA expression in HAC

HAC isolated from knee cartilage were transfected with 50nM of NLRX1 or control siRNA for 48 hours. Cells were then serum starved for 24 hours and then (A) stimulated or (B) transfected with 0.5µg/ml HMW poly(I:C) for 24 hours. Total RNA was extracted with Cells-to-cDNA lysis buffer as described in section 2.4.7, reverse transcribed to cDNA and subjected to real-time qRT-PCR analysis of SOD2 gene expression. Values were normalised to *18S* and plotted as mean fold induction over control ± SEM. Figures are representative of pooled results from 2 independent experiments. ** p≤0.01, *** p≤0.001, NS= not significant, compared to control.

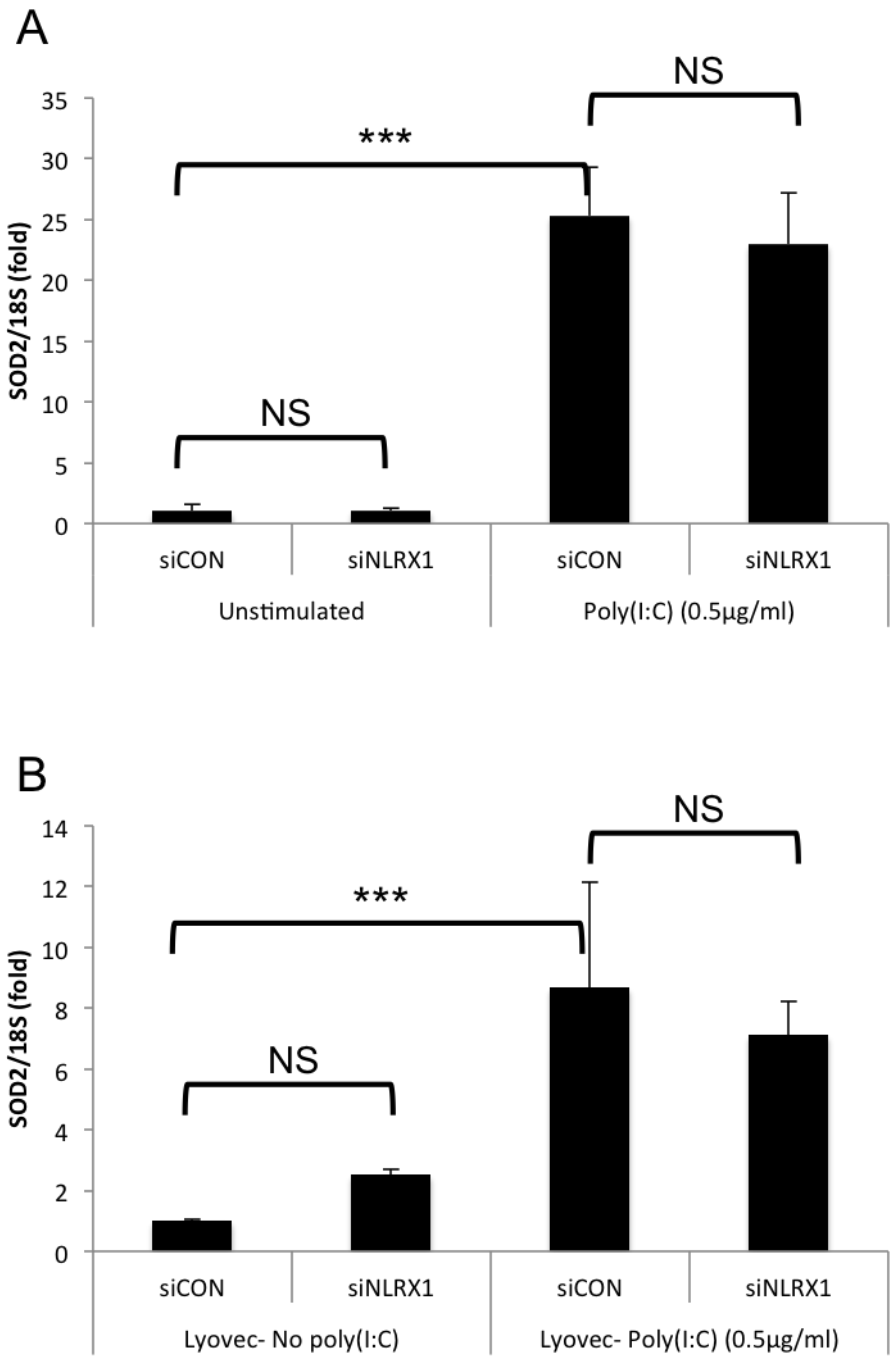

Figure 6.11 Effect of NLRX1 downregulation and poly(I:C) on SOD2 mRNA expression in SW1353 cells

SW1353 cells were transfected with 50nM of NLRX1 or control siRNA for 48 hours. Cells were then serum starved for 24 hours and then (A) stimulated or (B) transfected with 0.5µg/ml HMW poly(I:C) for 24 hours. Total RNA was extracted with Cells-to-cDNA lysis buffer as described in section 2.4.7, reverse transcribed to cDNA and subjected to real-time qRT-PCR analysis of SOD2 gene expression. Values were normalised to *18S* and plotted as mean fold induction over control ± SEM. Figures are representative of 2 independent experiments. *** p≤0.001, NS= not significant, compared to control.

6.4.8 Cloning of human SOD2 promoter and intronic enhancer

SOD2 is differentially expressed in OA and NOF (Scott et al 2010; Ruiz-Romero et al 2009; Aigner et al 2006). In order to identify changes in signalling pathways that are responsible for the differential expression of SOD2 in OA and NOF, we attempted to construct a luciferase vector driven by the SOD2 promoter and enhancer. Firstly, the promoter and the intronic enhancer of human SOD2 were attempted to be amplified and isolated.

Initially isolation of the complete promoter and enhancer regions from a BAC containing the complete SOD2 gene was attempted. However, complete amplification of the entire promoter region into one amplicon was never achieved (data not shown). Therefore, the promoter region was sub-divided into seven parts in order to be amplified separately. As shown in Figure 6.12B, six out of seven sections of the promoter amplified using conventional PCR techniques as well as the intronic (intron 2) enhancer (Figure 6.12C). However, the seventh section of the promoter did not amplify. By analysing the sequence of that sector it was obvious that the region had a very high GC content, which can inhibit the PCR reaction (Xu et al 2007). Therefore, PCR for GC rich regions was performed and the majority of that section was amplified (Figure 6.12D) and analysed by sequencing. However, approximately 70-100bp of 95% GC-content were deleted as shown in Figure 6.13. To complete and accurate amplification of this region without the deletion has not been successful using any PCR-based technique.

Recently, SOD2 promoter constructs were kindly donated to our laboratory by Dr Harry S. Nick (University of Florida) and isolation of the full promoter region was performed by Dr Catherine Bui however to date, the sub-cloning into a luciferase vector has not been performed.

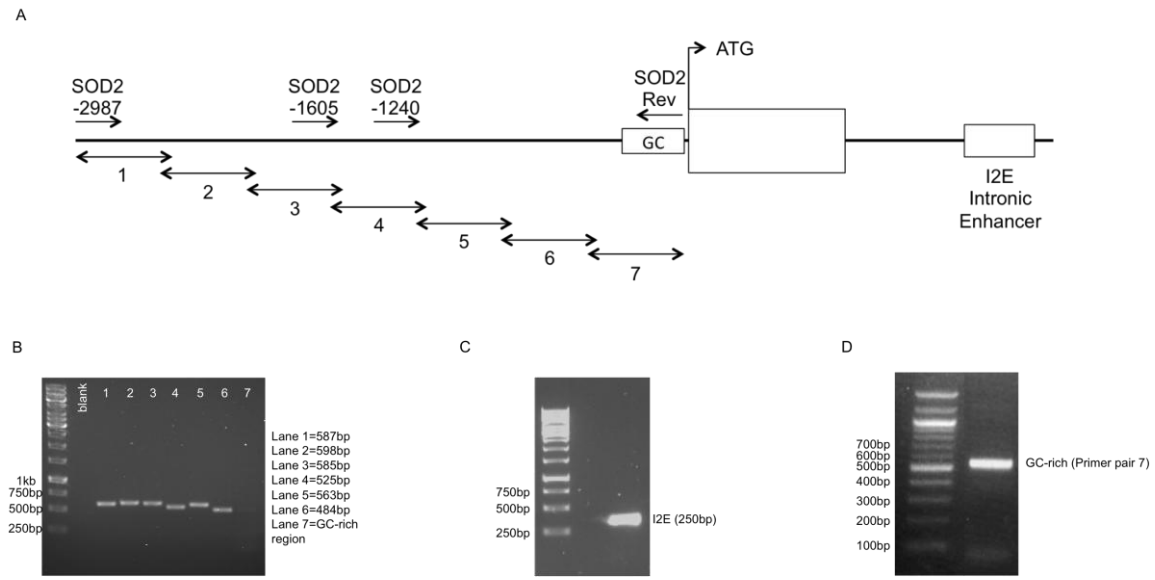

Figure 6.12 sod2 promoter and intronic enhancer amplification

(A) Primer pairs for amplification of SOD2 promoter region based on Table 2.2. (B) SOD2 promoter region (Figure 1.9) was amplified using conventional PCR. Amplicons show 7 different sections of the SOD2 promoter. (C) SOD2 Intronic enhancer amplification using conventional PCR. (D) SOD2 GC-rich region was amplified using GC-rich taq polymerase with the addition of 10% betaine. PCR products were separated by 1% (v/v) agarose gel electrophoresis. Size suggests that there is no deletion but sequencing analysis has shown 70-100bp deletions. Figures (B), (C) and (D) are representative of 2, 5 and 2 independent experiments respectively.

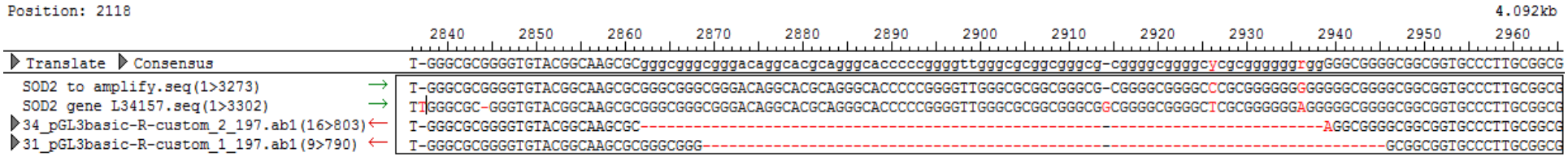

Figure 6.13 Representation of deleted GC-region in the SOD2 promoter as shown by SeqMan software

Figure shows a representation of the deleted 70 to 100bp GC-rich region of the SOD2 promoter (in red dash lines) indicating the high GC content of this section of the promoter sequence. Figure is an example of sequences from two independent bacterial clones of region 7 (primer pair 7) of the SOD2 (-300nt-+40nt) gene.

6.5 Discussion

As discussed previously in this thesis (section 1.1.10), mitochondria have been proposed as a signalling platform intergrading different pathways related to Ca2+ and ROS signalling, apoptosis and innate immunity signalling (Bulua et al 2011; Nakahira et al 2011; Zhou et al 2011; Dröge 2002; Valko et al 2007; Landolfi et al 1998; Dumollard et al 2004; Wachlin et al 2003; Kamata et al 2005; Tattoli et al 2008; Moore et al 2008; Meylan et al 2005). Two recent studies from our laboratory indicate the importance of innate immunity signalling pathways in chondrocytes. In the first study, TLR3 expression was found to be upregulated in OA compared to NOF and also increase NF-κB mediated MMP-1 and dramatically MMP-13 induction (Zhang et al 2008). In the second study, the mitochondrially localized gene NLRX1 was also identified to be upregulated in OA compared to NOF (David A. Young, unpublished data, Figure 6.1). NLRX1 has been suggested to inhibit innate immune responses by regulating NF-κB activation via inhibition of VISA and the VISA-RIG-I interaction as well as by interacting with TRAF6 and IκB kinase (Moore et al 2008; Xia et al 2011; Allen et al 2011). However, NLRX1 was also reported as a positive regulator of innate immune responses by stimulating ROS production and amplification of NF-κB and JNK dependent pathways (Tattoli et al 2008).

In the previous three chapters, the functional effect of SOD2 downregulation in OA was studied in terms of changes in ROS production, lipid peroxidation, mtDNA damage and mitochondrial dysfunction in chondrocytes. A general observation is that SOD2 downregulation can cause oxidative damage and mitochondrial dysfunction thus leading to cellular damage. However, as pointed out in Scott *et al*, SOD2 depletion leads to a reduction in MMP-1 and MMP-13 mRNA levels possibly due to the decreased levels of H_2O_2 (Scott et al 2010). Therefore, SOD2 depletion can have both a “chondro-protective” and a “chondro-damaging” effect. Interestingly, pathways such as NF-κB and MAPK, that regulate MMP expression in chondrocytes, can also regulate SOD2 expression (Karin 1995; Liacini et al 2002; Liacini et al 2003; Xu et al 1999; Xu et al 2007; Zhu et al 2001). Furthermore, p50, another member of the NF-κB family, has been reported to negatively regulate SOD2 expression (Dhar et al 2007).

As mitochondria appear to have a central role in regulation of these signalling events, the functional role of NLRX1 and partly VISA was examined, in terms of regulation of *MMP-13* and *SOD2* expression as well as ROS production in chondrocytes.

6.5.1 SOD2 promoter amplification by PCR results into deletions due to GC-rich regions in the promoter

In order to address the changes in signalling pathways in OA and NOF chondrocytes, construction of a luciferase vector driven by the SOD2 promoter and enhancer was attempted (Figure 6.12). This vector would then be transfected in OA and NOF chondrocytes in order to screen for differential SOD2 expression at the transcriptional level. Subsequently, the activity of different pathways would be assessed in order to determine the mechanism of SOD2 downregulation in OA.

Isolation of the complete promoter region was not successful whereas, the enhancer region was successfully amplified. Analysis of the region that did not amplify by conventional PCR techniques revealed that this region had a high GC content, which can potentially inhibit the reaction. A previous study identified a single stranded nucleotide loop within that GC rich region of the promoter that prevents accurate amplification of the sod2 promoter and deletion within this region significantly decreases promoter activity (Xu et al 2007). Therefore, different PCR reactions specific for GC rich regions were performed however 70-100bp of 95% GC-content were consistently deleted from this region (Figure 6.13). Since this region is essential for efficient promoter activity, the cloning of the complete promoter into a luciferase vector was not performed (Xu et al 2007).

6.5.2 Poly(I:C) stimulates MMP-13 expression in SW1353 cells

Poly(I:C) has been reported previously to regulate MMP-13 expression in chondrocytes (Zhang et al 2008). LMW and HMW poly(I:C) were used to assess their effect on *MMP-13* expression. As mentioned before, stimulation with extracellular (naked) poly(I:C) has been shown to activate TLR3, whereas transfected poly(I:C) bypasses TLR3 activation and activates RIG-I or MDA5 in

a cell-type specific manner and signal via the mitochondria (VISA) (Kato et al 2005; Kato et al 2006; Gitlin et al 2006). Also MDA5 preferentially binds to long, HMW poly(I:C), whereas RIG-I binds to LMW poly(I:C) with and without a 5'-triphosphate end (Kato et al 2008; Hornung et al 2006; Schmidt et al 2009). 5'-triphosphate ends are incorporated when RNA polymerase initiates transcription (Bieger, & Nierlich 1989). In this thesis, we examined whether poly(I:C), which signals via the RLRs and the mitochondria (VISA and NLRX1), can regulate *MMP-13* expression and therefore determine whether mitochondrial potentially have a role in controlling MMP-13 expression and therefore cartilage destruction.

Therefore, the effect of both extracellular and transfected poly(I:C) on MMP-13 mRNA regulation was also assessed (Figure 6.3). When LMW poly(I:C) was added extracellularly there was no significant induction of *MMP-13* expression, therefore it possibly does not activate TLR3, MDA5 or RIG-I in chondrocytes. Both extracellular and transfected (intracellular) HMW poly(I:C) stimulated *MMP-13* expression whereas only transfected LMW poly(I:C) stimulated *MMP-13* expression levels. These results suggest that HMW poly(I:C) can potentially activate TLR3 and RLR dependent signalling whereas LMW poly(I:C) can potentially activate only RLR dependent signalling in chondrocytes. Consequently, stimulation of extracellular and transfected HMW poly(I:C) and transfected LMW poly(I:C) was used to determine whether NLRX1 and VISA regulate MMP-13 expression.

A separate study performed in our laboratory, identified that TLR3, RIG-I and MDA5 depletion suppresses poly(I:C) stimulated *MMP-13* expression in chondrocytes (Marta Radwan, unpublished data). However, in the same study, *MMP-13* expression was also reduced in TLR3-depleted cells transfected with HMW and LMW poly(I:C), suggesting that transfected poly(I:C) does not entirely bypass TLR3 activation in chondrocytes as suggested in the literature (Kato et al 2005; Kato et al 2006; Gitlin et al 2006). Interestingly, this study has also shown that *MMP-13* induction by naked poly(I:C) is also dependent on RIG-I and MDA5 (Marta Radwan, unpublished data). A limitation of stimulation with transfected poly(I:C) is that not all of the poly(I:C) might be taken up by the liposomes of the transfection reagent and therefore some poly(I:C) might act

extracellularly. Additionally, liposomal transfection utilises the endosomes therefore transfected poly(I:C) can also activate TLR3 in the endosomes.

Collectively these findings suggest that induction of *MMP-13* expression by poly(I:C) in chondrocytes depends on both TLR3 and RLR signalling regardless of the cytosolic or extracellular delivery of poly(I:C) in chondrocytes. Therefore, induction of *MMP-13* expression in chondrocytes poly(I:C) might be regulated by TLR3 dependent signalling, RLR dependent signalling or both, or via a common pathway involving both TLR3 and RLR receptors, which could also potentially signal via the mitochondria. Additionally, poly(I:C) could bind both TLR3 and RLRs by binding first to high-mobility group box (HMGB) proteins, HMGB1 and HMGB2, which have been reported to be required for subsequent recognition of poly(I:C) from PAMPs, in order to activate innate immune responses (Yanai et al 2009).

6.5.3 VISA regulates basal MMP-13 expression only in SW1353 cells

siRNA depletion of VISA in both SW1353 and HAC did not alter poly(I:C) induced MMP-13 mRNA expression levels (Figure 6.4 and 6.5). In HAC, VISA depletion did not consistently affect basal *MMP-13* expression. However, in SW1353 cells, VISA depletion consistently and significantly decreased basal MMP-13 mRNA expression (Figure 6.5). This suggests that VISA is not essential for poly(I:C)-induced MMP-13 expression in chondrocytes. However it may be important for maintaining the basal level of MMP-13.

6.5.4 NLRX1 regulates basal MMP-13 expression in both HAC and SW1353 cells

As mentioned previously, NLRX1 has been identified to regulate the NF-κB pathway via inhibition of VISA but also via the regulation of ROS production (Moore et al 2008; Tattoli et al 2008). Since NLRX1 mRNA levels have been shown to be upregulated in OA (Figure 6.1) and due to its mitochondrial localisation, its role in regulating MMP-13 levels and ROS production in chondrocytes was assessed in this thesis.

Under basal conditions, NLRX1 depletion increased MMP-13 mRNA expression in HAC and SW1353 cells although it did not significantly alter poly(I:C) induced MMP-13 mRNA expression in HAC or SW1353 cells (Figure 6.6 and 6.7). As with VISA, NLRX1 appears to have a role in regulating basal MMP-13 mRNA levels however, our data suggests that NLRX1 does not regulate poly(I:C) mediated induction of MMP-13 in chondrocytes. A recent report suggested that NLRX1 regulates basal NF-κB activation by interacting with TRAF-6 in a TLR-dependent fashion (Xia et al 2011; Allen et al 2011).

6.5.5 NLRX1 regulates basal NF-κB activation in SW1353 cells

To begin to address how NLRX1 was regulating basal MMP-13 we examined whether NLRX1 regulates NF-κB activation. As mentioned previously, NLRX1 has been shown to activate NF-κB by regulation of VISA as well as by regulating ROS production (Moore et al 2008; Tattoli et al 2008). In chondrocytes, NF-κB transcription factors have been shown to regulate TNF-α and IL-1 induced *MMP-13* expression as inhibition of the NF-κB by curcumin, antioxidant pyrrolidine dithiocarbamate, Bay-11-7085 (which prevents phosphorylation of the NF-κB inhibitor IκB), and inhibitors of the ubiquitin–proteasome pathway (which prevent the ubiquitin-dependent degradation of the NF-κB inhibitor IκB), resulted in suppression of the IL-1 and TNF-α induced *MMP-13* expression (Liacini et al 2002; Liacini et al 2003; Zhang et al 2008). NLRX1 was overexpressed in SW1353 cells and NF-κB activation was assessed using NF-κB promoter-driven luciferase activation. The results are in agreement with our previous findings on MMP-13. NLRX1 can regulate basal NF-κB activity levels but does not regulate poly(I:C) mediated NF-κB induction in SW1353 cells (Figure 6.8).

Firstly, these findings can be partly explained by the fact that VISA does not regulate poly(I:C) induced *MMP-13* expression in chondrocytes. Therefore, inhibition of VISA and subsequently NF-κB by NLRX1, as suggested by Moore *et al* (Moore et al 2008), will not affect poly(I:C) induced *MMP-13* expression in chondrocytes. Moreover, a separate study suggested that NLRX1 does not interact with VISA at all and therefore it doesn't regulate NF-κB activation via inhibition of VISA (Rebsamen et al 2011). Furthermore, a recent study by Allen

et al, suggested that NLRX1 attenuates IFN-I and NF-κB, through separate pathways in a cell type- and pathogen-specific manner (Allen 2011). Consequently, the regulation of MMP-13 by NLRX1 might be affected by the cell type-specific regulation of innate immunity signalling by NLRX1.

6.5.6 NLRX1 regulates poly(I:C) induced ROS levels in HAC

In order to investigate the role of NLRX1 in ROS regulation, the ROS levels in HAC were assessed after NLRX1 depletion and extracellular poly(I:C) stimulation. NLRX1 depletion did not affect basal ROS levels in HAC. Poly(I:C), however, significantly stimulated ROS levels. Depletion of NLRX1 significantly reduced poly(I:C) induced ROS levels suggesting that NLRX1 is a positive regulator of poly(I:C) mediated ROS production in HAC as reported previously in other systems (Tattoli et al 2008; Abdul-Sater et al 2010), although we were unable to demonstrate an alteration in the expression of poly(I:C) sensitive genes, such as *MMP-13* (Figure 6.9).

Previous studies reported that NLRX1 regulated ROS production via interaction with the mitochondrial UQCRC2 (Arnoult et al 2009; Rebsamen et al 2011). In this thesis, the regulation of ROS production by NLRX1 was evaluated by assessing its role in SOD2 regulation in HAC and SW1353 cells. NLRX1 depletion did not alter poly(I:C) mediated SOD2 induction (Figure 6.10 and 6.11). SOD2 mRNA expression is induced by only extracellular poly(I:C) in HAC possibly because HAC are difficult to transfect although it can also suggest that poly(I:C)-induced SOD2 expression is possibly TLR3 dependent. Additionally, SOD2 mRNA expression is induced by both extracellular and transfected poly(I:C) in SW1353 cells. Therefore, from these results we can conclude that poly(I:C) stimulates SOD2 mRNA expression however this is not regulated by NLRX1 in either HAC or SW1353 cells. Consequently, NLRX1 does not regulate ROS production in chondrocytes by altering SOD2 expression. The exact mechanism of ROS regulation by NLRX1 in HAC has to be investigated further and it will be interesting to determine whether ROS are regulated via interaction with the mitochondrial UQCRC2 as suggested by other groups (Arnoult et al 2009; Rebsamen et al 2011).

6.6 Conclusions

Taken together, these findings suggest that mitochondria in chondrocytes might not function as innate immunity signalling platforms to regulate MMP-13 expression. *MMP-13* expression in chondrocytes is regulated by the activation of innate immunity signalling by dsRNA (in this case poly(I:C)). VISA is a positive regulator of basal *MMP-13* expression in SW1353 cells and possibly in HAC, however it does not regulate poly(I:C) induced *MMP-13* expression. NLRX1 is a negative regulator of basal *MMP-13* expression in both HAC and SW1353 cells however, similarly to VISA, it does not regulate poly(I:C) induced *MMP-13* expression. Interestingly, NLRX1 is a positive regulator of poly(I:C) induced ROS production in HAC but the mechanism of ROS regulation does not act via regulation of SOD2 expression. Further work can potentially uncover the exact mechanism of ROS regulation by NLRX1 in HAC as well as its role in basal MMP-13 regulation and also identify more pathways involved in the regulation of SOD2 expression in osteoarthritic and healthy cartilage.

Chapter 7. General Discussion

Mitochondria are considered the powerhouse of the cells, being the major site of ATP production via OXPHOS. In addition, they are also involved in Δψm regulation, Ca^{2+} handling and apoptosis and in the regulation of cell toxicity by mainly regulating ROS production as well as inhibition (Landolfi et al 1998; Newmeyer et al 1994; Mitchell, & Moyle 1969; Turrens, & Boveris 1980; Cadenas et al 1977). SOD2 is localized in the mitochondrial matrix and dismutases $O_2^{\cdot-}$ to H_2O_2. SOD2 deficiency increases mitochondrial superoxide levels in mice and leads to prenatal or neonatal lethality (Melov et al 1999; Li et al 1995). This phenotype is associated with severe neurological and cardiac phenotypes and linked to decreased Complex I and II activity as well as mitochondrial aconitase deficiencies, lipid peroxidation and oxidative gDNA damage in brain, heart, skeletal muscle and liver (Morten et al 2006; Huang et al 2001; Li et al 1995; Lebovitz et al 1996; Melov et al 1999).

OA is a degenerative joint disease mainly characterised by cartilage degradation due to changes in the molecular structure of the sole cell in cartilage, the chondrocyte and the composition of the extracellular matrix (Brandt et al 2006). The involvement of mitochondria in the pathogenesis of OA has been considered. Their direct role in ROS regulation, ATP production and apoptosis has been linked to cartilage degeneration. A decrease in complex II and III activity has been observed in OA chondrocytes as well as mitochondrial depolarisation (Maneiro et al 2003). The 4977bp mtDNA deletion has been identified in OA and mtDNA repair capacity as well as mtDNA integrity being reduced in OA chondrocytes (Chang et al 2005; Grishko et al 2008). SOD2 expression is also downregulated in OA cartilage compared to control both at the mRNA and protein level (Scott et al 2010; Ruiz-Romero et al 2009; Aigner et al 2006).

A more comprehensive understanding of mitochondrial function and dysfunction in OA and NOF chondrocytes and the functional role of SOD2 in chondrocytes would contribute to research into the pathology of OA and other diseases. Accordingly, the aim of this thesis was to compare the levels of oxidative

damage and mitochondrial function in OA and NOF chondrocytes and assess the role of SOD2 downregulation to these events.

7.1 Mitochondria as an innate signalling platform

Mitochondria have been considered to act as a signalling platform regulating processes and signalling pathways including Ca^{2+} signalling and handling (Jouaville et al 1999; Landolfi et al 1998; Dumollard et al 2004), ROS signalling (Kamata et al 2005; Kwon et al 2004; Lee et al 1998; Levinthal, & Defranco 2005; Meng et al 2002) and apoptosis (Wachlin et al 2003; Kamata et al 2005). More recently their contribution to innane immunity signalling was also suggested as two mitochondrially localised proteins, NLRX1 and VISA, were identified to regulate TLR3 and RLR innate immune responses (Xu et al 2005; Kawai, & Akira 2006; Moore et al 2008; Tattoli et al 2008; Xia et al 2011). TLR3 and NLRX1 expression were found to be upregulated in OA suggesting a possible role of these proteins in OA progression (Zhang et al 2008)(David Young, unpublished data, Figure 6.1). TLR3 has been shown to upregulate NF-κB mediated MMP-1 and MMP-13 induction suggesting a role in matrix degradation (Zhang et al 2008). In this thesis the role of NLRX1 in MMP-13 expression, ROS induction as well as SOD2 expression was assessed.

NLRX1 has been suggested to inhibit innate immune responses via inhibition of VISA and the VISA-RIG-I interaction as well as by interacting with TRAF6 and IκB kinase (Moore et al 2008; Xia et al 2011; Allen et al 2011). However, NLRX1 was also reported as a positive regulator of innate immune responses by stimulating ROS production and amplification of NF-κB and JNK dependent pathways (Tattoli et al 2008). In NLRX1-depleted HAC and SW1353 cells the MMP-13 mRNA levels were upregulated significantly under basal conditions (section 6.4.4, Figure 6.6, Figure 6.7). However NLRX1 depletion followed by stimulation with poly(I:C) did not significantly change MMP-13 expression (section 6.4.4, Figure 6.6, Figure 6.7). NLRX1 appears to have a role in regulating basal MMP-13 mRNA levels however, our data suggests that NLRX1 does not regulate poly(I:C) mediated induction of MMP-13 in chondrocytes. Also NLRX1 can regulate basal NF-κB activity levels but does not regulate poly(I:C) mediated NF-κB induction in SW1353 cells (section 6.4.5, Figure 6.8).

SW1353 chondrosarcoma cells are considered a substitute for a chondrocytic experimental system. However, a study comparing the gene expression profile of SW1353 cells and HAC reported that SW1353 cells have very limited similarities in gene expression compared to HAC (Gebauer et al 2005). The authors suggested that SW1353 cells could be used to study the induction of MMPs however their potential to mimic HAC function is limited. The results acquired in this thesis using SW1353 chondrosarcoma cells as a model system for chondrocytes have to be interpreted carefully in terms of their relevance to mimic the function in HAC and the use of these cells in some experiments is a limitation of this thesis.

Previous studies reported that NLRX1 regulated ROS production via interaction with the mitochondrial UQCRC2 (Arnoult et al 2009; Rebsamen et al 2011). Depletion of NLRX1 reduced poly(I:C) induced ROS levels (section 6.4.6, Figure 6.9) suggesting that NLRX1 is a positive regulator of poly(I:C) mediated ROS production in HAC as reported previously in other systems (Tattoli et al 2008; Abdul-Sater et al 2010). The role of NLRX1 in SOD2 regulation in HAC and SW1353 cells was also evaluated. NLRX1 depletion did not alter poly(I:C) mediated SOD2 induction in chondrocytes (section 6.4.7, Figure 6.10, Figure 6.11) suggesting that NLRX1 does not regulate ROS production in chondrocytes by altering SOD2 expression and poly(I:C) induced SOD2 expression is possibly TLR3 dependent.

These findings suggest that mitochondria in chondrocytes might not function as innate immunity signalling platforms to regulate MMP-13 expression. However, NLRX1 is a positive regulator of poly(I:C) induced ROS production in HAC but the mechanism of ROS regulation does not act via regulation of SOD2 expression suggesting a different mechanism of ROS regulation by NLRX1.

Conversely, inhibition of complexes III and V of the mitochondrial respiratory chain in HAC induces the production of other proinflammatory stimuli, including IL-1, IL-6 and IL-18, prostaglandin E2 (PGE2) as well as MMP-1, MMP-3 and MMP-13 (Lopez-Armada et al 2006). These results can partially explain the role of mitochondria in some inflammatory pathways implicated in OA pathogenesis.

In order to address the changes in signalling pathways in OA and NOF chondrocytes, construction of a luciferase vector driven by the SOD2 promoter and enhancer was attempted however, isolation of the complete promoter region was not successful due to the presence of deletions within a highly GC-rich region of the SOD2 promoter. This was possibly due to a single stranded nucleotide loop within that GC-rich region of the promoter that prevents accurate amplification of the SOD2 promoter and deletion within this region significantly decreases promoter activity (Xu et al 2007). Since this region is essential for efficient promoter activity, the cloning of the complete promoter into a luciferase vector was not performed (Xu et al 2007).

7.2 Oxidative stress and mtDNA damage in OA

As mentioned previously (section 1.1.9), SOD2 is essential for cell viability and normal mitochondrial activity and regulation of oxidative damage in the cell (Huang et al 2001; Li et al 1995; Lebovitz et al 1996; Melov et al 1999; Morten et al 2006). The expression of all three SODs (SOD1, SOD2 and SOD3) is downregulated in OA cartilage compared to NOF (Scott et al 2010; Ruiz-Romero et al 2009; Aigner et al 2006). High levels of $O_2^{\cdot-}$ and nitrogen oxide (NO) have been reported in OA, which lead to higher levels of H_2O_2 and $ONOO^-$ (Hiran et al 1997; Loeser et al 2002; Tiku et al 1998). Additionally, ROS have been implicated in matrix degradation and have been shown to lead to the cleavage of collagen and hyaluronan (Gao et al 2008; Petersen et al 2004; Henrotin et al 2005). Consequently, firstly in this thesis, the effect of SOD2 downregulation on $O_2^{\cdot-}$ levels in HAC was established. The results demonstrated that, similar to other systems, SOD2 downregulation in HAC leads to an increase in the mitochondrial $O_2^{\cdot-}$ levels (section 3.4.6, Figure 3.12, Figure 3.13).

Previous *in vitro* studies suggested that lipid peroxidation is higher in OA and can contribute to the oxidation and loss of collagen matrix (Tiku et al 2000; Shah et al 2005; Tiku et al 2007). High levels of $O_2^{\cdot-}$ and nitrogen oxide (NO) have been reported in OA and have been implicated in matrix degradation and have been shown to lead to the cleavage of collagen and hyaluronan (Hiran et al 1997; Loeser et al 2002; Tiku et al 1998; Gao et al 2008; Petersen et al 2004;

Henrotin et al 2005). Bonner *et al* demonstrated that lipids, especially polyunsaturated fatty acids, accumulate with normal ageing of human articular cartilage (Bonner et al 1975). Therefore, the higher levels of lipid peroxidation, can lead to the accumulation of oxidised collagen matrix and lead to matrix degradation and OA. In this thesis, lipid peroxidation was measured in OA cartilage and compared to NOF. In agreement with the *in vitro* studies, OA cartilage had higher levels of lipid peroxidation compared to NOF (section 3.4.7, Figure 3.15). Also, SOD2 depletion increased the levels of lipid peroxidation in SW1353 cells (section 3.4.7, Figure 3.16) suggesting that SOD2 downregulation can potentially contribute to the overall increase of lipid peroxidation in OA cartilage compared to NOF.

Both nuclear and mitochondrial DNA damage, as mentioned above, has also been suggested to be higher in OA and in SOD2 knockout mice (Hiran et al 1997; Loeser et al 2002; Tiku et al 1998; Chang et al 2005; Chen et al 2008; Kim et al 2009; Melov et al 1999). mtDNA damage has been reported in livers of SOD2 heterozygous mice at 2–4 months of age (Williams et al 1998). Although this was a good model to study mtDNA damage due to ROS, the young age of the mice make it difficult to relate to our model, that includes samples from old individuals. Also in human cartilage SOD2 levels are decreasing with ageing (Scott et al 2010) thus comparison with a SOD2 heterozygous mouse model is not appropriate. However, until recently, there were no reports of examination of cartilage in SOD2 heterozygous mice. In a recent study, the effect of exercise on cartilage in heterozygote SOD2-deficient mice was assessed (Baur et al 2011). Elevated levels of 15-F2t-isoprostane and nitrotyrosine were detected in articular cartilage of SOD2 +/- mice compared to wild type possibly due the increased $O_2^{\cdot-}$ levels in SOD2 +/- mice. The levels of these molecules in articular cartilage were increased in both SOD2 +/+ and SOD2 +/- after aerobic running exercise due to the fact that ROS levels were possibly induced by electron leakage from the MRC (Baur et al 2011). However, these changes had no effect on cartilage morphology, structure and function and SOD2 +/- mice did not show any features of OA suggesting that SOD2 downregulation might not have a direct effect on OA progression and might be a secondary effect of changes in cell signalling in mice.

In Chapter 3 of this thesis, the role of SOD2 downregulation in mtDNA damage in chondrocytes has been examined. SOD2 depletion caused a significant increase in mtDNA strand breaks (section 3.4.8, Figure 3.17), suggesting that SOD2 downregulation in chondrocytes contributes to oxidative mtDNA damage as reported in other systems previously (Hiran et al 1997; Loeser et al 2002; Tiku et al 1998; Chang et al 2005; Chen et al 2008; Kim et al 2009; Melov et al 1999). This suggests that SOD2 downregulation is chondrocytes can potentially lead to accumulation of mtDNA damage in OA cartilage. Then in Chapter 4, accumulation of mtDNA damage in the form of large-scale deletions was evaluated in OA and NOF cartilage and chondrocytes.

OA and NOF cartilage were screened for mtDNA strand breaks in the same assay used to screen SOD2 depleted cells. No significant difference in mtDNA strand breaks was identified between NOF and OA cartilage samples (section 4.4.1, Figure 4.1). Then cartilage sections and chondrocytes were screened for MRC dysfunction using the COX-SDH assay. Identification of COX-deficient cells is a useful indicator of mtDNA involvement in mitochondrial dysfunction (Old, & Johnson 1989; Johnson et al 1993). COX-SDH histochemistry was firstly performed on cartilage sections although the reaction was weak (section 4.5.2). This could be due to low permeability of cartilage to the COX-SDH incubation media or due to low expression of the MRC enzymes in those chondrocytes. COX-SDH histochemistry on cartilage sections is important in establishing mitochondrial function and screening for mtDNA deletions in different cartilage zones in both OA and NOF tissue and this thesis is weaker without such analysis. A priority of future work would be to establish a working assay on cartilage tissue in order to be able to examine mitochondrial function in different zones of OA and NOF cartilage.

COX-SDH activity was then assessed in freshly extracted HAC. COX-deficient chondrocytes were found but their number was very low (≤1%) compared to the COX- positive cells (section 4.5.4, Figure 4.3Figure 4.4Figure 4.5. Analysis of the mtDNA of isolated chondrocytes revealed no correlation of mtDNA copy number abnormality or mtDNA deletions with COX activity in HAC (sections 4.4.3 and 4.4.4, Figure 4.4, Figure 4.5, Table 4.1).

Since by using the mtDNA strand break assay the exact nature of the damage cannot be determined and also because the COX-SDH assay was inconsistent in terms of the correlation between the COX activity and the deletions present, mtDNA from OA and NOF cartilage was also screened for mtDNA deletions using a long amplification PCR assay (section 4.4.5, Figure 4.6). Low levels of two large-scale mtDNA deletions were identified in two OA hip samples (one in each patient) and two were identified in one OA knee sample (section 4.4.5, Figure 4.7, Table 4.2). No amplicons were sequenced from NOF because the intensity of the amplicons was very weak compared to the OA. None of the deletions identified included the 4977bp mtDNA common deletion identified by Chang *et al* in OA knee cartilage and aged non-OA cartilage (Chang et al 2005; Schon et al 1989; Shoffner et al 1989; Cortopassi et al 1992). Additionally, one of the deletions identified from patient C (OA knee cartilage) had a similar 5' breakpoint to the deletion identified from patient B (OA hip cartilage) at nucleotides 6783 and 6782 for the OA knee and OA hip respectively.

All of the sequences of the deletions identified were also analysed for the presence of repeat sequences (section 4.4.5, Table 4.2). Majority of the mtDNA deletions created by slip-replication, recombination or double strand break repair, are flanked by direct repeats suggesting a role of the repeats in the generation of the deletions (Mita et al 1990; Shoffner et al 1989; Krishnan et al 2008). However, a recent study suggested that repeats do not cause deletions but deletions can be generated due to long and stable duplexes formed between distant segments of the mtDNA (Guo et al 2010). The 7425bp deletion identified in patient A (Table 4.2, Figure 4.7) is very similar to a deletion reported previously in other diseases including cardiomyopathies, cirrhotic liver in hepatic tumour, Pearson syndrome and skeletal muscle in chronic fatigue (Hayakawa et al 1992; Rötig et al 1995; Yamamoto et al 1992; Zhang et al 1995). The only difference compared to the deletion identified in this thesis is that in these studies one of 12bp repeat-sequences flanking the deleted region is located within the deleted fragments whereas in our study both repeat sequences were outside the deleted fragment (section 4.4.5, Table 4.2). Since in our analysis, only one OA hip sample demonstrated a direct repeat flanking the deletion, it implies that in cartilage, as in Guo *et al* 2010, direct repeats

possibly do not have a significant role in deletion generation and other mechanisms might be involved (Guo et al 2010).

In this thesis, due to the low levels of mtDNA deletions present compared to wild type mtDNA molecules, we predict that the deletions possibly have no biochemical effect as the amount of mutated mtDNA is below the threshold required to cause a biochemical defect and respiratory dysfunction (Chinnery et al 1997; Sciacco et al 1994). mtDNA copy number was also assessed in the same samples and no significant difference was identified between OA hip cartilage and NOF (section 4.4.7, Figure 4.10).

Taken together, these results suggest that the SOD2 downregulation observed in OA cartilage compared to NOF can lead to an increase in mitochondrial $O_2^{\cdot-}$ in chondrocytes and potentially contribute to the higher levels of lipid peroxidation in OA cartilage. Although SOD2 downregulation can cause mtDNA deletions in chondrocytes, this damage does not accumulate in OA chondrocytes. However, the absence of mtDNA deletions can also be due to the loss of cartilage tissue during disease progression and therefore the total mutation levels identified are reduced. Other factors such as mtDNA haplogrous have been linked to the risk of developing OA. Haplogroup J has been demonstrated to protect against knee and hip OA whereas carriers with haplogroups H and U have an increased risk of developing OA (Rego-Perez et al 2008; Rego et al 2009; Rego-Perez et al 2010; Rego-Perez et al 2011). Therefore although mtDNA oxidative damage might not contribute to the OA phenotype, the mtDNA haplogroup might contribute to increased risk of developing OA.

7.3 Mitochondrial respiratory activity and membrane potential in OA

OXPHOS is driven by transfer of electrons along electron carriers in the MRC to reduce molecular oxygen to water and it is coupled to the transfer of protons into the mitochondrial intermembrane space thus creating a protonmotive force that drives ATP synthesis through the ATP synthase (Complex V). However, protons can leak across the membrane independently of ATP synthase (Brand et al 1994). Previous studies suggested that increased proton leak can be a reaction to counteract the effects of increasing ROS levels (Brookes 2005) or

even as a consequence of damaged membranes due to lipid peroxidation (Kokoszka et al 2001).

Chondrocytes produce approximately 25% of their total ATP production by OXPHOS and the remaining by glycolysis (Stockwell 1983; Lee, & Urban 1997). A decrease in complex II and III activity has been observed in OA chondrocytes as well as an increase in the mitochondrial mass (Maneiro et al 2003). OA chondrocytes contained more depolarised mitochondria than normal and this could be due to the lower activity of the mitochondrial complex III (Maneiro et al 2003). Despite the absence of mtDNA deletions in OA, the higher $O_2^{\cdot-}$ levels and lipid peroxidation observed in OA can potentially affect the respiratory activity of mitochondria in chondrocytes. Consequently the mitochondrial respiratory activity was evaluated in OA chondrocytes and compared to NOF chondrocytes. The potential effect of SOD2 downregulation on mitochondrial respiration and membrane potential was also examined.

HAC respiration was compared to the respiration of SW1353 cells (section 5.4.1, Figure 5.1). Although this experiment was performed once, it suggested that SW1353 cell respiration is higher compared to HAC. However, HAC have higher SRC, higher respiratory control ratio and lower proton leak than SW1353 cells suggesting that HAC can respond better to changes in energy demands compared to SW1353 cells and also they have a more efficient MRC as well (section 5.4.1, Figure 5.1) (Brand, & Nicholls 2011; Choi et al 2009; Yadava, & Nicholls 2007). These findings highlight another difference between HAC and SW1353 and demonstrate that results acquired by SW1353 cells have to be interpreted carefully in terms of their relevance to mimic the function in HAC (Gebauer et al 2005). However, these results are weaker without analysis of repeat experiments and therefore more experimental repeats will be performed in the future. HAC and SW1353 basal respiration was also compared to other cells based on data from other studies. HAC respiration was compared to other post-mitotic cells and was approximately 3-fold, 5-fold and 4-fold lower compared to mouse cortical synaptosomes, neonatal rat ventricular myocytes and RMS-13 myoblasts respectively (Flynn et al 2011; Hill et al 2009; Civitarese et al 2010). SW1353 basal respiration was compared to other cancer cell lines and was approximately 1.5-fold higher, 2.4-fold higher and at similar levels

compared to 2008-ovarian cancer cells, H460 lung cancer cells, MDA-MB468 breast cancerous cells (Verschoor et al 2010; Amoêdo et al 2011; Kristiansen et al 2011). Direct comparison of HAC and SW1353 with other post-mitotic and cancer cell lines respectively is not feasible due to the different experimental conditions and models (some are mouse cells) that have been followed. Although this comparison can provide us with an indication of the respiration of HAC compared to other cells, no definite conclusions can be drawn.

NOF respiration was then compared to OA respiration using two different respirometers, which produced very similar results (sections 5.4.2 and 5.4.3). OA chondrocytes respired significantly more than NOF chondrocytes at basal levels, after oligomycin inhibition and after FCCP uncoupling as they used more O_2 than NOF cells at these stages of the experiment (Figure 5.2, Figure 5.4). Analysis of respiration using respiratory parameters (Figure 5.3, Figure 5.5) suggested firstly that OA chondrocytes have a significantly lower SRC compared to NOF, therefore OA HAC possibly work closer to their bioenergetic limit compared to NOF and have a lower capacity to respond to changes in energy demands (Choi et al 2009). OA HAC also have a significantly higher proton leak compared to NOF. This suggests that OA mitochondria are slightly uncoupled which can be due to changes in the proton conductance of the inner membrane and changes in the $\Delta\psi m$ (Yadava, & Nicholls 2007). OA chondrocytes have been reported to have more depolarized mitochondria compared to healthy controls; therefore this can partially explain the increase in proton leak (Maneiro et al 2003; Fukui, & Zhu 2010; Kokoszka et al 2001). The cell respiratory control ratio values, which take into account both the capacity and proton leak of the cells, showed that OA chondrocytes have a lower respiratory control ratio compared to NOF, which suggests that their MRC is more dysfunctional due to the higher proton leak and lower SRC (Brand, & Nicholls 2011).

Nitric oxide can also potentially affect mitochondrial respiration although this hypothesis was not tested in this thesis. iNOS (inducible NO synthase) is up-regulated in OA, resulting in production of NO (Amin et al 1995). NO has been demonstrated to inhibit the activity of the complex IV in human articular chondrocytes and to contribute to the depolarization of the $\Delta\psi m$ (Maneiro et al

2005). Addtionally, a gradual 2-fold increase in NO levels in guinea pig chondrocytes has resulted in a 50% decrease in the levels of ATP produced (Johnson et al 2004). In the same study, to confirm that the cause of ATP depletion was mitochondrial dysfunction, they found an increase in the lactate: pyruvate ratio, a compensation reaction to mitochondrial dysfunction. Cillero Pastor *et al* also demonstrated that NO induced mitochondrial depolarization and cell death in human OA synoviocytes (Cillero-Pastor et al 2011). NO treatment also reduced mitochondrial mass and ATP turnover and decreased Bcl-2, Mcl-1 and pro-caspase-3 protein expression in the same cells (Cillero-Pastor et al 2011).

Glycolysis was also analysed in NOF and OA HAC (section 5.4.4, Figure 5.6). Although there was no difference in glycolysis between NOF and OA HAC, general comparison of mitochondrial to glycolysis suggested that HAC rely almost as much on the MRC and OXPHOS for their ATP production as in glycolysis. When only ATP producing mitochondrial respiration is taken into account, the ratio of OXPHOS dependent ATP production to glycolytic ATP production is possibly lower (approximately 33% ATP produced by OXPHOS and 67% by glycolysis) and therefore similar to the 25% ATP production by OXPHOS suggested previously (Stockwell 1983; Lee, & Urban 1997).

One limitation of this experiment is the requirement to culture HAC for three days prior to respiratory analysis for the reason that freshly isolated HAC did not respire possibly due to the physiological stresses that the cells were under after the long collagenase treatment. A 20-fold increase in the concentration of mitochondrial transcripts for cyt B, CO II and CO III has been reported in chondrocytes in culture compared to the levels in cartilage suggesting that the mitochondrial properties of chondrocytes change when transferred in an artificial culture environment (Mignotte et al 1991). Therefore the findings of this experiment might have been affected by the prior culture of HAC.

The effect of SOD2 downregulation on respiratory activity was also assessed in HAC (sections 5.4.5 and 5.4.6). A recent study performed on SOD2 null mice, suggested that SOD2 depletion leads to a decrease in SRC in cortical synaptosomes due to increased levels of oxidative stress in the mitochondria

(Flynn et al 2011). Reduced SRC has been suggested as a consequence of mild uncoupling of the MRC in cerebellar granule neurons in order to reduce $O_2^{\cdot-}$ levels in the mitochondrial matrix (Johnson-Cadwell et al 2007). A study by the same group also suggested that an impaired SRC also regulates glutamate toxicity upon complex I inhibition (Yadava, & Nicholls 2007). In this thesis, SOD2 downregulation in HAC increases (not significantly) respiration compared to control (Figure 5.8). SOD2 depleted HAC have significantly lower SRC compared to controls (Figure 5.9), however the levels of impairment was much lower in our study compared to the study by Flynn *et al* possibly due to the approximately 3-fold higher level of respiration of in cortical synaptosomes compared to HAC (Flynn et al 2011). SOD2 downregulation also increased proton leak in HAC (Figure 5.9). Combined with the lower SRC, these results suggest that SOD2 downregulation causes a mild uncoupling of the MRC, possibly to decrease $O_2^{\cdot-}$ levels in the mitochondrial matrix, however at the same time it caused impairment of the SRC which can potentially expose the cells to calcium deregulation and glutamate-induced toxicity reported previously in OA models (Jean et al 2006; Johnson et al 2000).

Previous studies reported that SOD2 downregulation in neurons causes Δψm depolarization possibly due to increase in proton leak and lipid peroxidation (Fukui, & Zhu 2010; Kokoszka et al 2001). Similarly, it has been reported that OA chondrocytes have more depolarized mitochondria compared to healthy controls (Maneiro et al 2003). In this thesis Δψm was measured by TMRM under basal conditions and after oligomycin and FCCP treatments (section 5.4.7, Figure 5.13). HAC transfected with siRNA against SOD2 had a lower intensity compared to controls at basal levels and also after oligomycin and FCCP treatment. Oligomycin treatment caused depolarization in both siSOD2 and siCON cells which possibly indicates a dysfunctional MRC (Brand, & Nicholls 2011). Mitochondria depolarised further after FCCP treatment however this effect could be due to the prior oligomycin treatment and its depolarising effect on HAC mitochondria in this experiment. Therefore, mitochondrial membrane depolarization in OA can potentially be due to SOD2 downregulation in HAC (Maneiro et al 2003).

It also has to be emphasised that these experiments were performed under normal O_2 conditions in order to stimulate the respiratory activity of the cells, therefore if oxygen levels similar to the cartilage (hypoxia) were used the results could differ. This thesis is weaker without such analysis and a priority of future work would be to determine mitochondrial respiratory activity in HAC under anoxic conditions. Previous work has shown that bovine articular chondrocytes and cartilage consume oxygen at a rate of 10nmoles/hour/million cells under high oxygen tensions (5%-21%) compared to the rate of 2.4nmoles/hour/million cells measured in this thesis (Zhou et al 2004). Lower oxygen tension (<5%) resulted in lower oxygen consumption (Zhou et al 2004).

Another important factor that has been reported to have a role in regulating mitochondrial function and ROS in chondrocytes is NO. It has been suggested that NO induces apoptosis in chondrocytes by decreasing the activity of Complex IV and decreasing the mitochondrial Δψm (Maneiro et al 2005; Johnson et al 2000). NO also has additional effects on mitochondria by inducing ROS and mtDNA damage, which have roles in cell death (Blanco et al 2011). Therefore, the effect of NO induction together with SOD2 downregulation in OA can potentially induce mitochondrial dysfunction in HAC and contribute to the development of OA.

In summary, these findings show that OA chondrocytes have a dysfunctional respiratory activity due to the lower spare respiratory capacity and higher proton leak partially as a consequence of SOD2 downregulation and higher superoxide levels. Although these changes may be a response to reduce the effect of higher $O_2^{\cdot-}$ levels, inflammatory and apoptotic pathways can also be potentially activated in chondrocytes that can lead to collagenase activation and cartilage degradation.

7.4 Future directions

The results and discussion presented in this thesis have furthered the understanding of mitochondrial dysfunction and oxidative damage in OA. However, a number of questions remain outstanding:

- Does mechanical stress or joint injury contribute to oxidative stress and mitochondrial dysfunction? Cartilage from DMM (Destabilization of Medial meniscus) OA mouse models (Glasson et al 2007) could be used to evaluate SOD2 expression and the levels of ROS and lipid peroxidation and as well as the possible accumulation of mtDNA damage and mitochondrial respiratory dysfunction.

- Does SOD2 downregulation cause mitochondrial dysfunction and oxidative damage in cartilage and potentially OA and does it contribute to further OA progression? SOD2 +/- or cartilage specific (COL2A1-CRE-SOD2 null) DMM mouse models could be used to further assess the contribution of SOD2 downregulation to OA progression and assess the levels of oxidative damage, mtDNA damage and mitochondrial dysfunction in cartilage.

- Does diminished mtDNA repair capacity affect OA progression? POLG mutator DMM or POLG mutator normal ageing mouse models could be used to assess the role of mtDNA repair in OA progression.

- Are the levels of mtDNA damage different in the different zones of cartilage? The COX-SDH protocol would be optimised to detect reactivity on cartilage sections. Chondrocytes would be isolated from the different zones according to COX activity and screened for mtDNA damage.

- Does mitochondrial respiratory activity in isolated NOF and OA chondrocytes differ under anoxic conditions? Isolated HAC would be cultured under anoxic conditions to simulate the oxygen levels in cartilage and mitochondrial respiratory activity would be assessed and compared to the activity under normoxic conditions.

- What changes in cell signalling regulate differential SOD2 expression in NOF and OA? SOD2 promoter constructs, kindly donated by Dr Nick Harry, would be sub-cloned into a luciferase vector and then transfected into NOF and OA HAC to compare the expression levels. Then different signalling pathways known to be altered in OA would be stimulated or inhibited and assess the effect on SOD2 expression.

- Is SOD2 expression regulated by differential H3K27 acetylation in OA and NOF? H3K27 acetylation a marker of active transcription regions and enhancers. Chromatin immunoprecipitation (ChIP) with antibody against H3K27 acetylation will be performed on OA and NOF chondrocytes. Then PCR will be performed to the SOD2 locus in order to identify differences in SOD2 transcriptional activity between NOF and OA. Previously ChIP was difficult to perform without vast numbers of cells, however newer techniques allow the use of less cells and therefore it is suitable for analyzing HAC (Collas 2010).

7.5 Summary

The findings of the thesis were the following. SOD2 downregulation increased mitochondrial $O_2^{\cdot-}$ levels in HAC. Measurement of lipid peroxidation levels in OA and NOF cartilage showed that OA cartilage has higher levels of lipid peroxidation compared to NOF possibly as a consequence of SOD2 downregulation and higher $O_2^{\cdot-}$ levels. Additionally, SOD2 depletion led to a significant increase in mtDNA strand breaks in SW1353 cells although there was no difference detected in OA compared to NOF mtDNA. However, large-scale mtDNA deletions were identified in OA cartilage and other OA joint tissues but the low levels of mutated mtDNA observed were not considered to be pathologically relevant. OA chondrocytes showed less spare respiratory capacity, higher non-phosphorylating respiration and higher proton leak compared to NOF, possibly as a consequence of SOD2 downregulation. Indeed, SOD2-depleted HAC also showed a lower spare respiratory capacity and higher proton leak as well as mitochondrial depolarisation. HAC demonstrated a very low mitochondrial/glycolysis ratio, suggesting that HAC are highly glycolytic cells. NLRX1 was also identified to regulate basal levels of (MMP-13) and ds RNA- induced ROS levels in chondrocytes.

Taken together, these findings suggest that SOD2 depletion in chondrocytes leads to oxidative damage and mitochondrial dysfunction caused by increasing ROS levels. As a consequence, these effects can potentially lead towards alterations in cell signalling pathways, cellular dysfunction and cartilage degradation.

Together with the findings on the role of NO and other inflammatory mediators on mitochondrial function and mtDNA, as well as with the identification of mtDNA haplogroups with increased or lower risk in developing OA, the findings of this thesis will contribute to research focused on understanding how mitochondrial function and ROS regulate chondrocyte function and homeostasis. The development of animal models that mimic the effects identified in human cartilage and chondrocytes is also essential to be able to identify potential therapies for OA. In particular, with the significant role of mitochondria and ROS in disease, identification of the effects of oxidative stress and mitochondrial dysfunction in OA will aid understanding of the disease pathology and contribute to the identification of potential targets for the treatment and prevention of OA.

Chapter 8. References

Abdul-Sater, A.A., Said-Sadier, N., Lam, V.M., Singh, B., Pettengill, M.A., Soares, F., Tattoli, I., Lipinski, S., Girardin, S.E., Rosenstiel, P. & Ojcius, D.M., 2010, Enhancement of reactive oxygen species production and chlamydial infection by the mitochondrial Nod-like family member, NLRX1, *The Journal of biological chemistry*.

Abrahams, J.P., Leslie, A.G., Lutter, R. & Walker, J.E., 1994, Structure at 2.8 A resolution of F1-ATPase from bovine heart mitochondria, *Nature*, 370(6491), pp. 621-8.

Ackrell, B.A., Kearney, E.B. & Edmondson, D., 1975, Mechanism of the reductive activation of succinate dehydrogenase, *The Journal of biological chemistry*, 250(18), pp. 7114-9.

Afonso, V., Champy, R., Mitrovic, D., Collin, P. & Lomri, A., 2007, Reactive oxygen species and superoxide dismutases: Role in joint diseases, *Joint, bone, spine : revue du rhumatisme*, 74(4), pp. 324-9.

Ahmad, R., Sylvester, J., Ahmad, M. & Zafarullah, M., 2011, Involvement of H-Ras and reactive oxygen species in proinflammatory cytokine-induced matrix metalloproteinase-13 expression in human articular chondrocytes, *Archives of biochemistry and biophysics*, 507(2), pp. 350-5.

Aigner, T., Fundel, K., Saas, J., Gebhard, P.M., Haag, J., Weiss, T., Zien, A., Obermayr, F., Zimmer, R. & Bartnik, E., 2006, Large-scale gene expression profiling reveals major pathogenetic pathways of cartilage degeneration in osteoarthritis, *Arthritis and rheumatism*, 54(11), pp. 3533-44.

Aigner, T., Hemmel, M., Neureiter, D., Gebhard, P.M., Zeiler, G., Kirchner, T. & McKenna, L., 2001, Apoptotic cell death is not a widespread phenomenon in normal aging and osteoarthritis human articular knee cartilage: a study of proliferation, programmed cell death (apoptosis), and viability of chondrocytes in normal and osteoarthritic human knee cartilage, *Arthritis and rheumatism*, 44(6), pp. 1304-12.

Aigner, T., Vornehm, S. & Zeiler, G., 1997, Suppression of cartilage matrix gene expression in upper zone chondrocytes of osteoarthritic cartilage, *Arthritis & Rheumatism*,44(3), pp. 562-69.

Ainscow, E.K. & Brand, M.D., 1999, Top-down control analysis of ATP turnover, glycolysis and oxidative phosphorylation in rat hepatocytes, *European journal of biochemistry / FEBS*, 263(3), pp. 671-85.

Alexander, C., Votruba, M., Pesch, U.E., Thiselton, D.L., Mayer, S., Moore, A., Rodriguez, M., Kellner, U., Leo-Kottler, B., Auburger, G., Bhattacharya, S.S. & Wissinger, B., 2000, OPA1, encoding a dynamin-related GTPase, is mutated in autosomal dominant optic atrophy linked to chromosome 3q28, *Nature genetics*, 26(2), pp. 211-5.

Allen, I.C., Moore, C.B., Schneider, M., Lei, Y., Davis, B.K., Scull, M.A., Gris, D., Roney, K.E., Zimmermann, A.G., Bowzard, J.B., Ranjan, P., Monroe, K.M., Pickles, R.J., Sambhara, S. & Ting, J.P.Y., 2011, NLRX1 protein attenuates inflammatory responses to infection by interfering with the RIG-I-MAVS and TRAF6-NF-κB signaling pathways, *Immunity*, 34(6), pp. 854-65.

Amin, A.R., Cesare, P.E.D., Vyas, P., Attur, M., Tzeng, E., Billiar, T.R., Stuchin, S.A. & Abramson, S.B., 1995, The expression and regulation of nitric oxide synthase in human osteoarthritis-affected chondrocytes: evidence for up-regulated neuronal nitric oxide synthase, *The Journal of experimental medicine*, 182(6), pp. 2097-102.

Amoêdo, N.D., Rodrigues, M.F., Pezzuto, P., Galina, A., da Costa, R.M., de Almeida, F.C., El-Bacha, T. & Rumjanek, F.D., 2011, Energy metabolism in H460 lung cancer cells: effects of histone deacetylase inhibitors, *PLoS ONE*, 6(7), p. e22264.

Anderson, S., Bankier, A.T., Barrell, B.G., de Bruijn, M.H., Coulson, A.R., Drouin, J., Eperon, I.C., Nierlich, D.P., Roe, B.A., Sanger, F., Schreier, P.H., Smith, A.J., Staden, R. & Young, I.G., 1981, Sequence and organization of the human mitochondrial genome, *Nature*, 290(5806), pp. 457-65.

Andrews, R.M., Kubacka, I., Chinnery, P.F., Lightowlers, R.N., Turnbull, D.M. & Howell, N., 1999, Reanalysis and revision of the Cambridge reference sequence for human mitochondrial DNA, *Nature genetics*, 23(2), p. 147.

Aoshiba, K., Yasuda, K., Yasui, S., Tamaoki, J. & Nagai, A., 2001, Serine proteases increase oxidative stress in lung cells, *Am J Physiol Lung Cell Mol Physiol*, 281(3), pp. L556-64.

Arnoult, D., Soares, F., Tattoli, I., Castanier, C., Philpott, D.J. & Girardin, S.E., 2009, An N-terminal addressing sequence targets NLRX1 to the mitochondrial matrix, *Journal of cell science*, 122(Pt 17), pp. 3161-8.

Aruoma, O.I., Halliwell, B., Hoey, B.M. & Butler, J., 1989, The antioxidant action of N-acetylcysteine: its reaction with hydrogen peroxide, hydroxyl radical, superoxide, and hypochlorous acid, *Free radical biology & medicine*, 6(6), pp. 593-7.

Badley, R.A., Woods, A., Carruthers, L. & Rees, D.A., 1980, Cytoskeleton changes in fibroblast adhesion and detachment, *Journal of cell science*, 43, pp. 379-90.

Baker, A.H., Edwards, D.R. & Murphy, G., 2002, Metalloproteinase inhibitors: biological actions and therapeutic opportunities, *Journal of cell science*, 115(Pt 19), pp. 3719-27.

Balaban, R.S., Nemoto, S. & Finkel, T., 2005, Mitochondria, oxidants, and aging, *Cell*, 120(4), pp. 483-95.

Barja, G. & Herrero, A., 1998, Localization at complex I and mechanism of the higher free radical production of brain nonsynaptic mitochondria in the short-lived rat than in the longevous pigeon, *Journal of bioenergetics and biomembranes*, 30(3), pp. 235-43.

Barreiro, E., Sánchez, D., Gáldiz, J.B., Hussain, S.N.A., Gea, J. & project, E.I.C., 2005, N-acetylcysteine increases manganese superoxide dismutase activity in septic rat diaphragms, *The European respiratory journal : official*

journal of the European Society for Clinical Respiratory Physiology, 26(6), pp. 1032-9.

Barrell, B.G., Bankier, A.T. & Drouin, J., 1979, A different genetic code in human mitochondria, *Nature*, 282(5735), pp. 189-94.

Barron, M.J., Chinnery, P.F., Howel, D., Blakely, E.L., Schaefer, A.M., Taylor, R.W. & Turnbull, D.M., 2005, Cytochrome c oxidase deficient muscle fibres: substantial variation in their proportions within skeletal muscles from patients with mitochondrial myopathy, *Neuromuscular disorders : NMD*, 15(11), pp. 768-74.

Basbaum, C.B. & Werb, Z., 1996, Focalized proteolysis: spatial and temporal regulation of extracellular matrix degradation at the cell surface, *Current opinion in cell biology*, 8(5), pp. 731-8.

Bates, E.J., Johnson, C.C. & Lowther, D.A., 1985a, Inhibition of proteoglycan synthesis by hydrogen peroxide in cultured bovine articular cartilage, *Biochimica et biophysica acta*, 838(2), pp. 221-8.

Bates, E.J., Lowther, D.A. & Johnson, C.C., 1985b, Hyaluronic acid synthesis in articular cartilage: an inhibition by hydrogen peroxide, *Biochemical and biophysical research communications*, 132(2), pp. 714-20.

Baur, A., Henkel, J., Bloch, W., Treiber, N., Scharffetter-Kochanek, K., Ggemann, G.-P.B. & Niehoff, A., 2011, Effect of exercise on bone and articular cartilage in heterozygous manganese superoxide dismutase (SOD2) deficient mice, *Free radical research*, 45(5), pp 550-8.

Beckman, K.B. & Ames, B.N., 1999, Endogenous oxidative damage of mtDNA, *Mutation research*, 424(1-2), pp. 51-8.

Beesk, F., Dizdaroglu, M., Schulte-Frohlinde, D. & von Sonntag, C., 1979, Radiation-induced DNA strand breaks in deoxygenated aqueous solutions. The formation of altered sugars as end groups, *Int J Radiat Biol Relat Stud Phys Chem Med*, 36(6), pp. 565-76.

Behar, D.M., Villems, R., Soodyall, H., Blue-Smith, J., Pereira, L., Metspalu, E., Scozzari, R., Makkan, H., Tzur, S., Comas, D., Bertranpetit, J., Quintana-Murci, L., Tyler-Smith, C., Wells, R.S., Rosset, S. & Consortium, G., 2008, The dawn of human matrilineal diversity, *American journal of human genetics*, 82(5), pp. 1130-40.

Bender, A., Krishnan, K.J., Morris, C.M., Taylor, G.A., Reeve, A.K., Perry, R.H., Jaros, E., Hersheson, J.S., Betts, J., Klopstock, T., Taylor, R.W. & Turnbull, D.M., 2006, High levels of mitochondrial DNA deletions in substantia nigra neurons in aging and Parkinson disease, *Nature genetics*, 38(5), pp. 515-7.

Benedictis, G.D., Carrieri, G., Varcasia, O., Bonafè, M. & Franceschi, C., 2000, Inherited variability of the mitochondrial genome and successful aging in humans, *Annals of the New York Academy of Sciences*, 908, pp. 208-18.

Bereiter-Hahn, J., 1994, Dynamics of mitochondria in living cells: shape changes, dislocations, fusion, and fission of mitochondria, *Microscopy research and technique*, 27(3), pp. 198-219.

Berry, E.A., Guergova-Kuras, M., Huang, L.S. & Crofts, A.R., 2000, Structure and function of cytochrome bc complexes, *Annu Rev Biochem*, 69, pp. 1005-75.

Bieger, C.D. & Nierlich, D.P., 1989, Distribution of 5'-triphosphate termini on the mRNA of Escherichia coli, *Journal of bacteriology*, 171(1), pp. 141-7.

Billinghurst, R., Dahlberg, L. & Ionescu, M., 1997, Enhanced cleavage of type II collagen by collagenases in osteoarthritic articular cartilage, *Journal of Clinical Investigation*, 99(7), pp. 1534-45.

Blakely, E., He, L., Gardner, J.L., Hudson, G., Walter, J., Hughes, I., Turnbull, D.M. & Taylor, R.W., 2008, Novel mutations in the TK2 gene associated with fatal mitochondrial DNA depletion myopathy, *Neuromuscular disorders : NMD*, 18(7), pp. 557-60.

Blanco, F., Lopezarmada, M. & Maneiro, E., 2004, Mitochondrial dysfunction in osteoarthritis, *Mitochondrion*, 4(5-6), pp. 715-28.

Blanco, F.J., Guitian, R., Vázquez-Martul, E., de Toro, F.J. & Galdo, F., 1998, Osteoarthritis chondrocytes die by apoptosis. A possible pathway for osteoarthritis pathology, *Arthritis and rheumatism*, 41(2), pp. 284-9.

Blanco, F.J., Rego, I. & Ruiz-Romero, C., 2011, The role of mitochondria in osteoarthritis, *Nat Rev Rheumatol*, 7(3), pp. 161-9.

Blaney Davidson, E.N., van der Kraan, P.M. & van den Berg, W.B., 2007, TGF-beta and osteoarthritis, *Osteoarthritis and cartilage / OARS, Osteoarthritis Research Society*, 15(6), pp. 597-604.

BLAST 1990, Basic Local Alignment Search Tool, *BLAST.* from http://blast.ncbi.nlm.nih.gov/Blast.cgi

Bonner, W.M., Jonsson, H., Malanos, C. & Bryant, M., 1975, Changes in the lipids of human articular cartilage with age, *Arthritis and rheumatism*, 18(5), pp. 461-73.

Borgstahl, G.E., Parge, H.E., Hickey, M.J., Beyer, W.F., Hallewell, R.A. & Tainer, J.A., 1992, The structure of human mitochondrial manganese superoxide dismutase reveals a novel tetrameric interface of two 4-helix bundles, *Cell*, 71(1), pp. 107-18.

Boyer, P., 1975, A model for conformational coupling of membrane potential and proton translocation to ATP synthesis and to active transport, *FEBS letters*, 58(1), pp. 1-6.

Boyer, P.D., Cross, R.L. & Momsen, W., 1973, A new concept for energy coupling in oxidative phosphorylation based on a molecular explanation of the oxygen exchange reactions, *Proc Natl Acad Sci USA*, 70(10), pp. 2837-9.

Brand, M.D. & Nicholls, D.G., 2011, Assessing mitochondrial dysfunction in cells, *The Biochemical journal*, 435(2), pp. 297-312.

Brand, M.D., Chien, L.F., Ainscow, E.K., Rolfe, D.F. & Porter, R.K., 1994, The causes and functions of mitochondrial proton leak, *Biochimica et biophysica acta*, 1187(2), pp. 132-9.

Brand, M.D., Couture, P., Else, P.L., Withers, K.W. & Hulbert, A.J., 1991, Evolution of energy metabolism. Proton permeability of the inner membrane of liver mitochondria is greater in a mammal than in a reptile, *The Biochemical journal*, 275 (Pt 1), pp. 81-6.

Brand, M.D., Pakay, J.L., Ocloo, A., Kokoszka, J., Wallace, D.C., Brookes, P.S. & Cornwall, E.J., 2005, The basal proton conductance of mitochondria depends on adenine nucleotide translocase content, *The Biochemical journal*, 392(Pt 2), pp. 353-62.

Brandt, K.D., Radin, E.L., Dieppe, P.A. & de Putte, L.V., 2006, Yet more evidence that osteoarthritis is not a cartilage disease, *Annals of the rheumatic diseases*, 65(10), pp. 1261-4.

Brookes, P.S., 2005, Mitochondrial H(+) leak and ROS generation: an odd couple, *Free radical biology & medicine*, 38(1), pp. 12-23.

Brookes, P.S., Buckingham, J.A., Tenreiro, A.M., Hulbert, A.J. & Brand, M.D., 1998, The proton permeability of the inner membrane of liver mitochondria from ectothermic and endothermic vertebrates and from obese rats: correlations with standard metabolic rate and phospholipid fatty acid composition, *Comparative biochemistry and physiology. Part B, Biochemistry & molecular biology*, 119(2), pp. 325-34.

Brown, G.C., Lakin-Thomas, P.L. & Brand, M.D., 1990, Control of respiration and oxidative phosphorylation in isolated rat liver cells, *European journal of biochemistry / FEBS*, 192(2), pp. 355-62.

Buckwalter, J. & MANKIN, H., 1997, Instructional Course Lectures, The American Academy of Orthopaedic Surgeons - Articular Cartilage. Part II: Degeneration and Osteoarthrosis, Repair, Regeneration, and Transplantation, *The Journal of Bone and Joint Surgery*, 79(4), pp 612-32.

Bulua, A.C., Simon, A., Maddipati, R., Pelletier, M., Park, H., Kim, K.Y., Sack, M.N., Kastner, D.L. & Siegel, R.M., 2011, Mitochondrial reactive oxygen species promote production of proinflammatory cytokines and are elevated in TNFR1-

associated periodic syndrome (TRAPS), *The Journal of experimental medicine*, 208(3), pp. 519-33.

Burgunder, J.M., Varriale, A. & Lauterburg, B.H., 1989, Effect of N-acetylcysteine on plasma cysteine and glutathione following paracetamol administration, *Eur J Clin Pharmacol*, 36(2), pp. 127-31.

Butler, G.S., Butler, M.J., Atkinson, S.J., Will, H., Tamura, T., Schade van Westrum, S., Crabbe, T., Clements, J., d'Ortho, M.P. & Murphy, G., 1998, The TIMP2 membrane type 1 metalloproteinase "receptor" regulates the concentration and efficient activation of progelatinase A. A kinetic study, *The Journal of biological chemistry*, 273(2), pp. 871-80.

Cadenas, E., Boveris, A., Ragan, C.I. & Stoppani, A.O., 1977, Production of superoxide radicals and hydrogen peroxide by NADH-ubiquinone reductase and ubiquinol-cytochrome c reductase from beef-heart mitochondria, *Archives of biochemistry and biophysics*, 180(2), pp. 248-57.

Caramés, B., Hasegawa, A., Taniguchi, N., Miyaki, S., Blanco, F.J. & Lotz, M., 2011, Autophagy activation by rapamycin reduces severity of experimental osteoarthritis, *Annals of the rheumatic diseases*.

Carbajo, R.J., Kellas, F.A., Runswick, M.J., Montgomery, M.G., Walker, J.E. & Neuhaus, D., 2005, Structure of the F1-binding domain of the stator of bovine F1Fo-ATPase and how it binds an alpha-subunit, *Journal of molecular biology*, 351(4), pp. 824-38.

Carlo, M.D. & Loeser, R.F., 2003, Increased oxidative stress with aging reduces chondrocyte survival: correlation with intracellular glutathione levels, *Arthritis and rheumatism*, 48(12), pp. 3419-30.

Caterson, B., Flannery, C.R., Hughes, C.E. & Little, C.B., 2000, Mechanisms involved in cartilage proteoglycan catabolism, *Matrix biology : journal of the International Society for Matrix Biology*, 19(4), pp. 333-44.

Catterall, J.B., Carrère, S., Koshy, P.J., Degnan, B.A., Shingleton, W.D., Brinckerhoff, C.E., Rutter, J., Cawston, T.E. & Rowan, A.D., 2001, Synergistic

induction of matrix metalloproteinase 1 by interleukin-1alpha and oncostatin M in human chondrocytes involves signal transducer and activator of transcription and activator protein 1 transcription factors via a novel mechanism, *Arthritis and rheumatism*, 44(10), pp. 2296-310.

Cecchini, G., 2003, Function and structure of complex II of the respiratory chain, *Annu Rev Biochem*, 72, pp. 77-109.

Chakraborti, S., Mandal, M., Das, S. & Mandal, A., 2003, Regulation of matrix metalloproteinases: An overview, *Molecular and Cellular Biochemistry*, 253(1-2), pp. 269-85.

Chang, D., 1984, Precise identification of individual promoters for transcription of each strand of human mitochondrial DNA, *Cell*, 36(3), pp. 635-43.

Chang, D.T.W., Honick, A.S. & Reynolds, I.J., 2006, Mitochondrial trafficking to synapses in cultured primary cortical neurons, *The Journal of neuroscience : the official journal of the Society for Neuroscience*, 26(26), pp. 7035-45.

Chang, M., Hung, S., Chen, W., Chen, T., Lee, C., Lee, H., Wang, K., Chiou, C. & Wei, Y., 2005, Accumulation of mitochondrial DNA with 4977-bp deletion in knee cartilage -- an association with idiopathic osteoarthritis, *Osteoarthritis and Cartilage*, 13(11), pp. 1004-11.

Chen, A.F., Davies, C.M., Lin, M.D. & Fermor, B., 2008, Oxidative DNA damage in osteoarthritic porcine articular cartilage, *J. Cell. Physiol.*, 217(3), pp. 828-33.

Chen, H. & Chan, D.C., 2005, Emerging functions of mammalian mitochondrial fusion and fission, *Human molecular genetics*, 14 Spec No. 2, pp. R283-9.

Chen, H., Detmer, S.A., Ewald, A.J., Griffin, E.E., Fraser, S.E. & Chan, D.C., 2003, Mitofusins Mfn1 and Mfn2 coordinately regulate mitochondrial fusion and are essential for embryonic development, *J Cell Biol*, 160(2), pp. 189-200.

Chen, H., Vermulst, M., Wang, Y.E., Chomyn, A., Prolla, T.A., McCaffery, J.M. & Chan, D.C., 2010, Mitochondrial fusion is required for mtDNA stability in skeletal muscle and tolerance of mtDNA mutations, *Cell*, 141(2), pp. 280-9.

Chen, Q., Vazquez, E.J., Moghaddas, S., Hoppel, C.L. & Lesnefsky, E.J., 2003, Production of reactive oxygen species by mitochondria: central role of complex III, *The Journal of biological chemistry*, 278(38), pp. 36027-31.

Chinnery, P.F., Howell, N., Lightowlers, R.N. & Turnbull, D.M., 1997, Molecular pathology of MELAS and MERRF. The relationship between mutation load and clinical phenotypes, *Brain : a journal of neurology*, 120 (Pt 10), pp. 1713-21.

Chinnery, P.F., Samuels, D.C., Elson, J. & Turnbull, D.M., 2002, Accumulation of mitochondrial DNA mutations in ageing, cancer, and mitochondrial disease: is there a common mechanism? *Lancet*, 360(9342), pp. 1323-5.

Choi, S.W., Gerencser, A.A. & Nicholls, D.G., 2009, Bioenergetic analysis of isolated cerebrocortical nerve terminals on a microgram scale: spare respiratory capacity and stochastic mitochondrial failure, *Journal of neurochemistry*, 109(4), pp. 1179-91.

Chung, L., Dinakarpandian, D., Yoshida, N., Lauer-Fields, J.L., Fields, G.B., Visse, R. & Nagase, H., 2004, Collagenase unwinds triple-helical collagen prior to peptide bond hydrolysis, *EMBO J*, 23(15), pp. 3020-30.

Cillero-Pastor, B., Caramés, B., Lires-Deán, M., Vaamonde-Garc\'\ia, C., Blanco, F.J. & López-Armada, M.J., 2008, Mitochondrial dysfunction activates cyclooxygenase 2 expression in cultured normal human chondrocytes, *Arthritis and rheumatism*, 58(8), pp. 2409-19.

Cillero-Pastor, B., Martin, M.A., Arenas, J., López-Armada, M.J. & Blanco, F.J., 2011, Effect of nitric oxide on mitochondrial activity of human synovial cells, *BMC musculoskeletal disorders*, 12, pp. 42.

Civitarese, A.E., MacLean, P.S., Carling, S., Kerr-Bayles, L., McMillan, R.P., Pierce, A., Becker, T.C., Moro, C., Finlayson, J., Lefort, N., Newgard, C.B., Mandarino, L., Cefalu, W., Walder, K., Collier, G.R., Hulver, M.W., Smith, S.R. & Ravussin, E., 2010, Regulation of skeletal muscle oxidative capacity and insulin signaling by the mitochondrial rhomboid protease PARL, *Cell metabolism*, 11(5), pp. 412-26.

Clayton, D.A., 1982, Replication of animal mitochondrial DNA, *Cell*, 28(4), pp. 693-705.

Clerk, A., Michael, A. & Sugden, P.H., 1998, Stimulation of multiple mitogen-activated protein kinase sub-families by oxidative stress and phosphorylation of the small heat shock protein, HSP25/27, in neonatal ventricular myocytes, *The Biochemical journal*, 333 (Pt 3), pp. 581-9.

Collas, P., 2010, The current state of chromatin immunoprecipitation, *Molecular biotechnology*, 45(1), pp. 87-100.

Coller, H.A., Khrapko, K., Bodyak, N.D., Nekhaeva, E., Herrero-Jimenez, P. & Thilly, W.G., 2001, High frequency of homoplasmic mitochondrial DNA mutations in human tumors can be explained without selection, *Nature genetics*, 28(2), pp. 147-50.

Collinson, I.R., Raaij, M.J.V., Runswick, M.J., Fearnley, I.M., Skehel, J.M., Orriss, G.L., Miroux, B. & Walker, J.E., 1994a, ATP synthase from bovine heart mitochondria. In vitro assembly of a stalk complex in the presence of F1-ATPase and in its absence, *Journal of molecular biology*, 242(4), pp. 408-21.

Collinson, I.R., Runswick, M.J., Buchanan, S.K., Fearnley, I.M., Skehel, J.M., Raaij, M.J.V., Griffiths, D.E. & Walker, J.E., 1994b, Fo membrane domain of ATP synthase from bovine heart mitochondria: purification, subunit composition, and reconstitution with F1-ATPase, *Biochemistry*, 33(25), pp. 7971-8.

Colombini, M., 1979, A candidate for the permeability pathway of the outer mitochondrial membrane, *Nature*, 279(5714), pp. 643-5.

Cooke, M.S., Evans, M.D., Dizdaroglu, M. & Lunec, J., 2003, Oxidative DNA damage: mechanisms, mutation, and disease, *The FASEB journal : official publication of the Federation of American Societies for Experimental Biology*, 17(10), pp. 1195-214.

Cortopassi, G.A., Shibata, D., Soong, N.W. & Arnheim, N., 1992, A pattern of accumulation of a somatic deletion of mitochondrial DNA in aging human tissues, *Proc Natl Acad Sci USA*, 89(16), pp. 7370-4.

Cottrell, D.A., Blakely, E.L., Johnson, M.A., Ince, P.G., Borthwick, G.M. & Turnbull, D.M., 2001, Cytochrome c oxidase deficient cells accumulate in the hippocampus and choroid plexus with age, *Neurobiology of aging*, 22(2), pp. 265-72.

Cree, L.M., Samuels, D.C., de Lopes, S.C.S., Rajasimha, H.K., Wonnapinij, P., Mann, J.R., Dahl, H.-H.M. & Chinnery, P.F., 2008, A reduction of mitochondrial DNA molecules during embryogenesis explains the rapid segregation of genotypes, *Nature genetics*, 40(2), pp. 249-54.

D'Lima, D.D., Hashimoto, S., Chen, P.C., Colwell, C.W. & Lotz, M.K., 2001, Human chondrocyte apoptosis in response to mechanical injury, *Osteoarthr Cartil*, 9(8), pp. 712-9.

Daems, W., 1966, Shape and attachment of the cristae mitochondriales in mouse hepatic cell mitochondria, *Journal of ultrastructure research*, 26(2), pp. 207-10

Dasgupta, J., Kar, S., Liu, R., Joseph, J., Kalyanaraman, B., Remington, S.J., Chen, C. & Melendez, J.A., 2010, Reactive oxygen species control senescence-associated matrix metalloproteinase-1 through c-Jun-N-terminal kinase, *Journal of cellular physiology*, 225(1), pp. 52-62.

Dasgupta, J., Kar, S., Remmen, H.V. & Melendez, J.A., 2009, Age-dependent increases in interstitial collagenase and MAP Kinase levels are exacerbated by superoxide dismutase deficiencies, *Experimental gerontology*, 44(8), pp. 503-10.

Degoul, F., Nelson, I., Amselem, S., Romero, N., Obermaier-Kusser, B., Ponsot, G., Marsac, C. & Lestienne, P., 1991, Different mechanisms inferred from sequences of human mitochondrial DNA deletions in ocular myopathies, *Nucleic acids research*, 19(3), pp. 493-6.

Delettre, C., Lenaers, G., Griffoin, J.M., Gigarel, N., Lorenzo, C., Belenguer, P., Pelloquin, L., Grosgeorge, J., Turc-Carel, C., Perret, E., Astarie-Dequeker, C., Lasquellec, L., Arnaud, B., Ducommun, B., Kaplan, J. & Hamel, C.P., 2000,

Nuclear gene OPA1, encoding a mitochondrial dynamin-related protein, is mutated in dominant optic atrophy, *Nature genetics*, 26(2), pp. 207-10.

Desagher, S., Osen-Sand, A., Nichols, A., Eskes, R., Montessuit, S., Lauper, S., Maundrell, K., Antonsson, B. & Martinou, J.C., 1999, Bid-induced conformational change of Bax is responsible for mitochondrial cytochrome c release during apoptosis, *J Cell Biol*, 144(5), pp. 891-901.

Dhar, S.K., Xu, Y., Noel, T. & St Clair, D.K., 2007, Chronic exposure to 12-O-tetradecanoylphorbol-13-acetate represses sod2 induction in vivo: the negative role of p50, *Carcinogenesis*, 28(12), pp. 2605-13.

Diaz, G., Falchi, A.M., Gremo, F., Isola, R. & Diana, A., 2000, Homogeneous longitudinal profiles and synchronous fluctuations of mitochondrial transmembrane potential, *FEBS letters*, 475(3), pp. 218-24.

Dickson, V.K., Silvester, J.A., Fearnley, I.M., Leslie, A.G.W. & Walker, J.E., 2006, On the structure of the stator of the mitochondrial ATP synthase, *EMBO J*, 25(12), pp. 2911-8.

Dizdaroglu, M., Gajewski, E., Reddy, P. & Margolis, S.A., 1989, Structure of a hydroxyl radical induced DNA-protein cross-link involving thymine and tyrosine in nucleohistone, *Biochemistry*, 28(8), pp. 3625-8.

Dizdaroglu, M., Jaruga, P., Birincioglu, M. & Rodriguez, H., 2002, Free radical-induced damage to DNA: mechanisms and measurement, *Free radical biology & medicine*, 32(11), pp. 1102-15.

Dlasková, A., Clarke, K.J. & Porter, R.K., 2010, The role of UCP 1 in production of reactive oxygen species by mitochondria isolated from brown adipose tissue, *Biochimica et biophysica acta*, 1797(8), pp. 1470-6.

Doege, K.J., Sasaki, M., Kimura, T. & Yamada, Y., 1991, Complete coding sequence and deduced primary structure of the human cartilage large aggregating proteoglycan, aggrecan. Human-specific repeats, and additional alternatively spliced forms, *The Journal of biological chemistry*, 266(2), pp. 894-902.

Dranka, B.P., Hill, B.G. & Darley-Usmar, V.M., 2010, Mitochondrial reserve capacity in endothelial cells: The impact of nitric oxide and reactive oxygen species, *Free radical biology & medicine*, 48(7), pp. 905-14.

Dröge, W., 2002, Free radicals in the physiological control of cell function, *Physiol Rev*, 82(1), pp. 47-95.

Dumollard, R., Marangos, P., Fitzharris, G., Swann, K., Duchen, M. & Carroll, J., 2004, Sperm-triggered [Ca2+] oscillations and Ca2+ homeostasis in the mouse egg have an absolute requirement for mitochondrial ATP production, *Development*, 131(13), pp. 3057-67.

Eeckhout, Y. & Vaes, G., 1977, Further studies on the activation of procollagenase, the latent precursor of bone collagenase. Effects of lysosomal cathepsin B, plasmin and kallikrein, and spontaneous activation, *The Biochemical journal*, 166(1), pp. 21-31.

Efremov, R.G., Baradaran, R. & Sazanov, L.A., 2010, The architecture of respiratory complex I, *Nature*, 465(7297), pp. 441-5.

Elson, J.L., Samuels, D.C., Turnbull, D.M. & Chinnery, P.F., 2001, Random intracellular drift explains the clonal expansion of mitochondrial DNA mutations with age, *American journal of human genetics*, 68(3), pp. 802-6.

Eskes, R., Desagher, S., Antonsson, B. & Martinou, J.C., 2000, Bid induces the oligomerization and insertion of Bax into the outer mitochondrial membrane, *Molecular and cellular biology*, 20(3), pp. 929-35.

Falchuk, K.H., Goetzl, E.J. & Kulka, J.P., 1970, Respiratory gases of synovial fluids:: An approach to synovial tissue circulatory-metabolic imbalance in rheumatoid arthritis, *The American journal of medicine*, 49(2), pp. 223-31.

Falkenberg, M., Gaspari, M., Rantanen, A., Trifunovic, A., Larsson, N.-G. & Gustafsson, C.M., 2002, Mitochondrial transcription factors B1 and B2 activate transcription of human mtDNA, *Nature genetics*, 31(3), pp. 289-94.

Fay, J., Varoga, D., Wruck, C.J., Kurz, B., Goldring, M.B. & Pufe, T., 2006, Reactive oxygen species induce expression of vascular endothelial growth

factor in chondrocytes and human articular cartilage explants, *Arthritis research & therapy*, 8(6), pp. 189.

Fedtke, N., Boucheron, J.A., Walker, V.E. & Swenberg, J.A., 1990, Vinyl chloride-induced DNA adducts. II: Formation and persistence of 7-(2'-oxoethyl)guanine and N2,3-ethenoguanine in rat tissue DNA, *Carcinogenesis*, 11(8), pp. 1287-92.

Feldmann, M., Andreakos, E., Smith, C., Bondeson, J., Yoshimura, S., Kiriakidis, S., Monaco, C., Gasparini, C., Sacre, S., Lundberg, A., Paleolog, E., Horwood, N.J., Brennan, F.M. & Foxwell, B.M.J., 2002, Is NF-kappaB a useful therapeutic target in rheumatoid arthritis? *Annals of the rheumatic diseases*, 61 Suppl 2, pp. ii13-8.

Feng, L., Precht, P., Balakir, R. & Horton, W.E., 1998, Evidence of a direct role for Bcl-2 in the regulation of articular chondrocyte apoptosis under the conditions of serum withdrawal and retinoic acid treatment, *Journal of cellular biochemistry*, 71(2), pp. 302-9.

Fernandez-Silva, P., Martinez-Azorin, F., Micol, V. & Attardi, G., 1997, The human mitochondrial transcription termination factor (mTERF) is a multizipper protein but binds to DNA as a monomer, with evidence pointing to intramolecular leucine zipper interactions, *EMBO J*, 16(5), pp. 1066-79.

Filippin, L.I., Vercelino, R., Marroni, N.P. & Xavier, R.M., 2008, Redox signalling and the inflammatory response in rheumatoid arthritis, *Clinical and experimental immunology*, 152(3), pp. 415-22.

Fisher, G.J., Quan, T., Purohit, T., Shao, Y., Cho, M.K., He, T., Varani, J., Kang, S. & Voorhees, J.J., 2009, Collagen fragmentation promotes oxidative stress and elevates matrix metalloproteinase-1 in fibroblasts in aged human skin, *The American journal of pathology*, 174(1), pp. 101-14.

Fisher, R.P., Topper, J.N. & Clayton, D.A., 1987, Promoter selection in human mitochondria involves binding of a transcription factor to orientation-independent upstream regulatory elements, *Cell*, 50(2), pp. 247-58.

Fitzgerald, J.B., Jin, M., Dean, D., Wood, D.J., Zheng, M.H. & Grodzinsky, A.J., 2004, Mechanical compression of cartilage explants induces multiple time-dependent gene expression patterns and involves intracellular calcium and cyclic AMP, *The Journal of biological chemistry*, 279(19), pp. 19502-11.

Flynn, J.M., Choi, S.W., Day, N.U., Gerencser, A.A., Hubbard, A. & Melov, S., 2011, Impaired spare respiratory capacity in cortical synaptosomes from Sod2 null mice, *Free radical biology & medicine*, 50(7), pp. 866-73.

Fosang, A.J., Last, K. & Maciewicz, R.A., 1996, Aggrecan is degraded by matrix metalloproteinases in human arthritis. Evidence that matrix metalloproteinase and aggrecanase activities can be independent, *The Journal of clinical investigation*, 98(10), pp. 2292-9.

Frey, T.G. & Mannella, C.A., 2000, The internal structure of mitochondria, *Trends Biochem Sci*, 25(7), pp. 319-24.

Fukui, M. & Zhu, B.T., 2010, Mitochondrial superoxide dismutase SOD2, but not cytosolic SOD1, plays a critical role in protection against glutamate-induced oxidative stress and cell death in HT22 neuronal cells, *Free radical biology & medicine*, 48(6), pp. 821-30.

Gao, F., Koenitzer, J.R., Tobolewski, J.M., Jiang, D., Liang, J., Noble, P.W. & Oury, T.D., 2008, Extracellular superoxide dismutase inhibits inflammation by preventing oxidative fragmentation of hyaluronan, *The Journal of biological chemistry*, 283(10), pp. 6058-66.

Gao, P., Zhang, H., Dinavahi, R., Li, F., Xiang, Y., Raman, V., Bhujwalla, Z.M., Felsher, D.W., Cheng, L., Pevsner, J., Lee, L.A., Semenza, G.L. & Dang, C.V., 2007, HIF-dependent antitumorigenic effect of antioxidants in vivo, *Cancer Cell*, 12(3), pp. 230-8.

Gebauer, M., Saas, J., Sohler, F., Haag, J., Söder, S., Pieper, M., Bartnik, E., Beninga, J., Zimmer, R. & Aigner, T., 2005, Comparison of the chondrosarcoma cell line SW1353 with primary human adult articular chondrocytes with regard to their gene expression profile and reactivity to IL-1beta, *Osteoarthritis and cartilage / OARS, Osteoarthritis Research Society*, 13(8), pp. 697-708.

Gitlin, L., Barchet, W., Gilfillan, S., Cella, M., Beutler, B., Flavell, R.A., Diamond, M.S. & Colonna, M., 2006, Essential role of mda-5 in type I IFN responses to polyriboinosinic:polyribocytidylic acid and encephalomyocarditis picornavirus, *Proc Natl Acad Sci USA*, 103(22), pp. 8459-64.

Glasson, S.S., Askew, R., Sheppard, B., Carito, B., Blanchet, T., Ma, H.-L., Flannery, C.R., Peluso, D., Kanki, K., Yang, Z., Majumdar, M.K. & Morris, E.A., 2005, Deletion of active ADAMTS5 prevents cartilage degradation in a murine model of osteoarthritis, *Nature*, 434(7033), pp. 644-8.

Glasson, S.S., Blanchet, T.J. & Morris, E.A., 2007, The surgical destabilization of the medial meniscus (DMM) model of osteoarthritis in the 129/SvEv mouse, *Osteoarthritis and cartilage / OARS, Osteoarthritis Research Society*, 15(9), pp. 1061-9.

Gohil, V.M., Sheth, S.A., Nilsson, R., Wojtovich, A.P., Lee, J.H., Perocchi, F., Chen, W., Clish, C.B., Ayata, C., Brookes, P.S. & Mootha, V.K., 2010, Nutrient-sensitized screening for drugs that shift energy metabolism from mitochondrial respiration to glycolysis, *Nature Biotechnology*, 28(3), p. 249.

Golden, T. & Melov, S., 2001, Mitochondrial DNA mutations, oxidative stress, and aging, *Mechanisms of ageing and development*, 26(2), pp. 207-10

Goldring, M.B. & Goldring, S.R., 2007, Osteoarthritis, *J. Cell. Physiol.*, 213(3), pp. 626-34.

Goto, Y., Koga, Y., Horai, S. & Nonaka, I., 1990, Chronic progressive external ophthalmoplegia: a correlative study of mitochondrial DNA deletions and their phenotypic expression in muscle biopsies, *Journal of the neurological sciences*, 100(1-2), pp. 63-9.

Greenwald, A.S. & Haynes, D.W., 1969, A pathway for nutrients from the medullary cavity to the articular cartilage of the human femoral head, *The Journal of bone and joint surgery British volume*, 51(4), pp. 747-53.

Griffiths, G.J., Dubrez, L., Morgan, C.P., Jones, N.A., Whitehouse, J., Corfe, B.M., Dive, C. & Hickman, J.A., 1999, Cell damage-induced conformational

changes of the pro-apoptotic protein Bak in vivo precede the onset of apoptosis, *J Cell Biol*, 144(5), pp. 903-14.

Grimshaw, M.J. & Mason, R.M., 2000, Bovine articular chondrocyte function in vitro depends upon oxygen tension, *Osteoarthr Cartil*, 8(5), pp. 386-92.

Grishko, V., Ho, R., Wilson, G. & Pearsall, A., 2008, Diminished mitochondrial DNA integrity and repair capacity in OA chondrocytes, *Osteoarthritis and Cartilage*, 26(2), pp. 207-10

Grohmann, K., Amairic, F., Crews, S. & Attardi, G., 1978, Failure to detect "cap" structures in mitochondrial DNA-coded poly(A)-containing RNA from HeLa cells, *Nucleic acids research*, 5(3), pp. 637-51.

Guo, X., Popadin, K.Y., Markuzon, N., Orlov, Y.L., Kraytsberg, Y., Krishnan, K.J., Zsurka, G., Turnbull, D.M., Kunz, W.S. & Khrapko, K., 2010, Repeats, longevity and the sources of mtDNA deletions: evidence from 'deletional spectra', *Trends in genetics : TIG*, 26(8), pp. 340-3.

Hafner, R.P., Nobes, C.D., McGown, A.D. & Brand, M.D., 1988, Altered relationship between protonmotive force and respiration rate in non-phosphorylating liver mitochondria isolated from rats of different thyroid hormone status, *European journal of biochemistry / FEBS*, 178(2), pp. 511-8.

Han, Z., Boyle, D.L., Chang, L., Bennett, B., Karin, M., Yang, L., Manning, A.M. & Firestein, G.S., 2001, c-Jun N-terminal kinase is required for metalloproteinase expression and joint destruction in inflammatory arthritis, *The Journal of clinical investigation*, 108(1), pp. 73-81.

Handschin, C. & Spiegelman, B.M., 2006, Peroxisome proliferator-activated receptor gamma coactivator 1 coactivators, energy homeostasis, and metabolism, *Endocrine reviews*, 27(7), pp. 728-35.

Hansen, A.B., Griner, N.B., Anderson, J.P., Kujoth, G.C., Prolla, T.A., Loeb, L.A. & Glick, E., 2006, Mitochondrial DNA integrity is not dependent on DNA polymerase-beta activity, *DNA repair*, 5(1), pp. 71-9.

Hansford, R.G., Hogue, B.A. & Mildaziene, V., 1997, Dependence of H2O2 formation by rat heart mitochondria on substrate availability and donor age, *Journal of bioenergetics and biomembranes*, 29(1), pp. 89-95.

Hashimoto, S., Ochs, R.L., Komiya, S. & Lotz, M., 1998, Linkage of chondrocyte apoptosis and cartilage degradation in human osteoarthritis, *Arthritis and rheumatism*, 41(9), pp. 1632-8.

Hayakawa, M., Hattori, K., Sugiyama, S. & Ozawa, T., 1992, Age-associated oxygen damage and mutations in mitochondrial DNA in human hearts, *Biochemical and biophysical research communications*, 189(2), pp. 979-85.

He, L., Chinnery, P.F., Durham, S.E., Blakely, E.L., Wardell, T.M., Borthwick, G.M., Taylor, R.W. & Turnbull, D.M., 2002, Detection and quantification of mitochondrial DNA deletions in individual cells by real-time PCR, *Nucleic acids research*, 30(14), p. e68.

Heiden, M.G.V., Chandel, N.S., Li, X.X., Schumacker, P.T., Colombini, M. & Thompson, C.B., 2000, Outer mitochondrial membrane permeability can regulate coupled respiration and cell survival, *Proc Natl Acad Sci USA*, 97(9), pp. 4666-71.

Heinrich, P.C., Behrmann, I., Haan, S., Hermanns, H.M., Müller-Newen, G. & Schaper, F., 2003, Principles of interleukin (IL)-6-type cytokine signalling and its regulation, *The Biochemical journal*, 374(Pt 1), pp. 1-20.

Heinrich, P.C., Behrmann, I., Müller-Newen, G., Schaper, F. & Graeve, L., 1998, Interleukin-6-type cytokine signalling through the gp130/Jak/STAT pathway, *The Biochemical journal*, 334 (Pt 2), pp. 297-314.

Henrotin, Y., Kurz, B. & Aigner, T., 2005, Oxygen and reactive oxygen species in cartilage degradation: friends or foes? *Osteoarthritis and Cartilage*, 13(8), pp. 643-54.

Hill, B.G., Dranka, B.P., Zou, L., Chatham, J.C. & Darley-Usmar, V.M., 2009, Importance of the bioenergetic reserve capacity in response to cardiomyocyte

stress induced by 4-hydroxynonenal, *The Biochemical journal*, 424(1), pp. 99-107.

Hiran, T.S., Moulton, P.J. & Hancock, J.T., 1997, Detection of superoxide and NADPH oxidase in porcine articular chondrocytes, *Free radical biology & medicine*, 23(5), pp. 736-43.

Hisabori, T., Kondoh, A. & Yoshida, M., 1999, The gamma subunit in chloroplast F(1)-ATPase can rotate in a unidirectional and counter-clockwise manner, *FEBS letters*, 463(1-2), pp. 35-8.

Holt, I.J., 2009, Mitochondrial DNA replication and repair: all a flap, *Trends Biochem Sci*, 34(7), pp. 358-65.

Holt, I.J., Lorimer, H.E. & Jacobs, H.T., 2000, Coupled leading- and lagging-strand synthesis of mammalian mitochondrial DNA, *Cell*, 100(5), pp. 515-24.

Hornung, V., Ellegast, J., Kim, S., Brzózka, K., Jung, A., Kato, H., Poeck, H., Akira, S., Conzelmann, K.K. & Schlee, M., 2006, 5'-Triphosphate RNA is the ligand for RIG-I, *Science*, 314(5801), p. 994.

Huang, T.T., Carlson, E.J., Kozy, H.M., Mantha, S., Goodman, S.I., Ursell, P.C. & Epstein, C.J., 2001, Genetic modification of prenatal lethality and dilated cardiomyopathy in Mn superoxide dismutase mutant mice, *Free radical biology & medicine*, 31(9), pp. 1101-10.

Hudson, G. & Chinnery, P.F., 2006, Mitochondrial DNA polymerase-gamma and human disease, *Human molecular genetics*, 15 Spec No 2, pp. R244-52.

Hui, W., Barksby, H.E., Young, D.A., Cawston, T.E., McKie, N. & Rowan, A.D., 2005, Oncostatin M in combination with tumour necrosis factor alpha induces a chondrocyte membrane associated aggrecanase that is distinct from ADAMTS aggrecanase-1 or -2, *Annals of the rheumatic diseases*, 64(11), pp. 1624-32.

Hui, W., Rowan, A.D., Richards, C.D. & Cawston, T.E., 2003, Oncostatin M in combination with tumor necrosis factor alpha induces cartilage damage and matrix metalloproteinase expression in vitro and in vivo, *Arthritis and rheumatism*, 48(12), pp. 3404-18.

Hunter, D.J. & Felson, D.T., 2006, Osteoarthritis, *BMJ (Clinical research ed.)*, 332(7542), pp. 639-42.

Huser, C.A.M., Peacock, M. & Davies, M.E., 2006, Inhibition of caspase-9 reduces chondrocyte apoptosis and proteoglycan loss following mechanical trauma, *Osteoarthr Cartil*, 14(10), pp. 1002-10.

Ishihara, N., Nomura, M., Jofuku, A., Kato, H., Suzuki, S.O., Masuda, K., Otera, H., Nakanishi, Y., Nonaka, I., Goto, Y.-I., Taguchi, N., Morinaga, H., Maeda, M., Takayanagi, R., Yokota, S. & Mihara, K., 2009, Mitochondrial fission factor Drp1 is essential for embryonic development and synapse formation in mice, *Nature Cell Biology*, 11(8), pp. 958-66.

Ishikawa, K., Takenaga, K., Akimoto, M., Koshikawa, N., Yamaguchi, A., Imanishi, H., Nakada, K., Honma, Y. & Hayashi, J.-I., 2008, ROS-generating mitochondrial DNA mutations can regulate tumor cell metastasis, *Science*, 320(5876), pp. 661-4.

Itoh, Y. & Seiki, M., 2006, MT1-MMP: a potent modifier of pericellular microenvironment, *Journal of cellular physiology*, 206(1), pp. 1-8.

Ivashkiv, L., 2003, The JAK/STAT pathway in rheumatoid arthritis: Pathogenic or protective? *Arthritis and rheumatism*, 29(1), pp. 89-95.

Iwata, S., Ostermeier, C., Ludwig, B. & Michel, H., 1995, Structure at 2.8 A resolution of cytochrome c oxidase from Paracoccus denitrificans, *Nature*, 376(6542), pp. 660-9.

Jacob, M.C., Favre, M. & Bensa, J.C., 1991, Membrane cell permeabilization with saponin and multiparametric analysis by flow cytometry, *Cytometry*, 12(6), pp. 550-8.

Jean, Y.-H., Wen, Z.-H., Chang, Y.-C., Lee, H.-S., Hsieh, S.-P., Wu, C.-T., Yeh, C.-C. & Wong, C.-S., 2006, Hyaluronic acid attenuates osteoarthritis development in the anterior cruciate ligament-transected knee: Association with excitatory amino acid release in the joint dialysate, *Journal of orthopaedic*

research : official publication of the Orthopaedic Research Society, 24(5), pp. 1052-61.

Johnson, K., Jung, A., Murphy, A., Andreyev, A., Dykens, J. & Terkeltaub, R., 2000, Mitochondrial oxidative phosphorylation is a downstream regulator of nitric oxide effects on chondrocyte matrix synthesis and mineralization, *Arthritis and rheumatism*, 43(7), pp. 1560-70.

Johnson, K., Svensson, C.I., Etten, D.V., Ghosh, S.S., Murphy, A.N., Powell, H.C. & Terkeltaub, R., 2004, Mediation of spontaneous knee osteoarthritis by progressive chondrocyte ATP depletion in Hartley guinea pigs, *Arthritis and rheumatism*, 50(4), pp. 1216-25.

Johnson, M.A., Bindoff, L.A. & Turnbull, D.M., 1993, Cytochrome c oxidase activity in single muscle fibers: assay techniques and diagnostic applications, *Annals of neurology*, 33(1), pp. 28-35.

Johnson-Cadwell, L.I., Jekabsons, M.B., Wang, A., Polster, B.M. & Nicholls, D.G., 2007, 'Mild Uncoupling' does not decrease mitochondrial superoxide levels in cultured cerebellar granule neurons but decreases spare respiratory capacity and increases toxicity to glutamate and oxidative stress, *Journal of neurochemistry*, 101(6), pp. 1619-31.

Jouaville, L.S., Pinton, P., Bastianutto, C., Rutter, G.A. & Rizzuto, R., 1999, Regulation of mitochondrial ATP synthesis by calcium: evidence for a long-term metabolic priming, *Proc Natl Acad Sci USA*, 96(24), pp. 13807-12.

Kamata, H., Honda, S.-I., Maeda, S., Chang, L., Hirata, H. & Karin, M., 2005, Reactive oxygen species promote TNFalpha-induced death and sustained JNK activation by inhibiting MAP kinase phosphatases, *Cell*, 120(5), pp. 649-61.

Karin, M., 1995, The regulation of AP-1 activity by mitogen-activated protein kinases, *Journal of Biological Chemistry*, 29(1), pp. 89-95.

Kashiwagi, M., Tortorella, M., Nagase, H. & Brew, K., 2001, TIMP-3 is a potent inhibitor of aggrecanase 1 (ADAM-TS4) and aggrecanase 2 (ADAM-TS5), *The Journal of biological chemistry*, 276(16), pp. 12501-4.

Kato, H., Sato, S., Yoneyama, M., Yamamoto, M., Uematsu, S., Matsui, K., Tsujimura, T., Takeda, K., Fujita, T., Takeuchi, O. & Akira, S., 2005, Cell type-specific involvement of RIG-I in antiviral response, *Immunity*, 23(1), pp. 19-28.

Kato, H., Takeuchi, O., Mikamo-Satoh, E., Hirai, R., Kawai, T., Matsushita, K., Hiiragi, A., Dermody, T.S., Fujita, T. & Akira, S., 2008, Length-dependent recognition of double-stranded ribonucleic acids by retinoic acid-inducible gene-I and melanoma differentiation-associated gene 5, *The Journal of experimental medicine*, 205(7), pp. 1601-10.

Kato, H., Takeuchi, O., Sato, S., Yoneyama, M., Yamamoto, M., Matsui, K., Uematsu, S., Jung, A., Kawai, T., Ishii, K.J., Yamaguchi, O., Otsu, K., Tsujimura, T., Koh, C.-S., Sousa, C.R.E., Matsuura, Y., Fujita, T. & Akira, S., 2006, Differential roles of MDA5 and RIG-I helicases in the recognition of RNA viruses, *Nature*, 441(7089), pp. 101-5.

Kato-Yamada, Y., Noji, H., Yasuda, R., Kinosita, K. & Yoshida, M., 1998, Direct observation of the rotation of epsilon subunit in F1-ATPase, *The Journal of biological chemistry*, 273(31), pp. 19375-7.

Kawai, T. & Akira, S., 2006, Innate immune recognition of viral infection, *Nature immunology*, 7(2), pp. 131-7.

Kawai, T., Takahashi, K., Sato, S., Coban, C., Kumar, H., Kato, H., Ishii, K.J., Takeuchi, O. & Akira, S., 2005, IPS-1, an adaptor triggering RIG-I- and Mda5-mediated type I interferon induction, *Nature immunology*, 6(10), pp. 981-8.

Keil, V.C., Funke, F., Zeug, A., Schild, D. & Müller, M., 2011, Ratiometric high-resolution imaging of JC-1 fluorescence reveals the subcellular heterogeneity of astrocytic mitochondria, *Pflügers Archiv: European journal of physiology*, 462(5), pp. 693-708.

Kevorkian, L., Young, D.A., Darrah, C., Donell, S.T., Shepstone, L., Porter, S., Brockbank, S.M.V., Edwards, D.R., Parker, A.E. & Clark, I.M., 2004, Expression profiling of metalloproteinases and their inhibitors in cartilage, *Arthritis and rheumatism*, 50(1), pp. 131-41.

Kim, H.A., Lee, Y.J., Seong, S.C., Choe, K.W. & Song, Y.W., 2000, Apoptotic chondrocyte death in human osteoarthritis, *The Journal of rheumatology*, 27(2), pp. 455-62.

Kim, J., Xu, M., Xo, R., Mates, A., Wilson, G., Pearsall, A. & Grishko, V., 2009, Mitochondrial DNA damage is involved in apoptosis caused by pro-inflammatory cytokines in human OA chondrocytes, *Osteoarthr Cartil*. 29(1), pp. 89-95.

Kim, J.Y., Hwang, J.-M., Ko, H.S., Seong, M.-W., Park, B.-J. & Park, S.S., 2005, Mitochondrial DNA content is decreased in autosomal dominant optic atrophy, *Neurology*, 64(6), pp. 966-72.

Klug, D., Rabani, J. & Fridovich, I., 1972, A direct demonstration of the catalytic action of superoxide dismutase through the use of pulse radiolysis, *The Journal of biological chemistry*, 247(15), pp. 4839-42.

Knäuper, V., Will, H., López-Otin, C., Smith, B., Atkinson, S.J., Stanton, H., Hembry, R.M. & Murphy, G., 1996, Cellular mechanisms for human procollagenase-3 (MMP-13) activation. Evidence that MT1-MMP (MMP-14) and gelatinase a (MMP-2) are able to generate active enzyme, *The Journal of biological chemistry*, 271(29), pp. 17124-31.

Koehler, C.M., Jarosch, E., Tokatlidis, K., Schmid, K., Schweyen, R.J. & Schatz, G., 1998, Import of mitochondrial carriers mediated by essential proteins of the intermembrane space, *Science*, 279(5349), pp. 369-73.

Kokoszka, J.E., Coskun, P., Esposito, L.A. & Wallace, D.C., 2001, Increased mitochondrial oxidative stress in the Sod2 (+/-) mouse results in the age-related decline of mitochondrial function culminating in increased apoptosis, *Proc Natl Acad Sci USA*, 98(5), pp. 2278-83.

Koncz, P., Szanda, G., Fülöp, L., Rajki, A. & Spät, A., 2009, Mitochondrial Ca2+ uptake is inhibited by a concerted action of p38 MAPK and protein kinase D, *Cell Calcium*, 46(2), pp. 122-9.

Kops, G.J.P.L., Dansen, T.B., Polderman, P.E., Saarloos, I., Wirtz, K.W.A., Coffer, P.J., Huang, T.-T., Bos, J.L., Medema, R.H. & Burgering, B.M.T., 2002,

Forkhead transcription factor FOXO3a protects quiescent cells from oxidative stress, *Nature*, 419(6904), pp. 316-21.

Korhonen, J.A., Gaspari, M. & Falkenberg, M., 2003, TWINKLE Has 5' -> 3' DNA helicase activity and is specifically stimulated by mitochondrial single-stranded DNA-binding protein, *The Journal of biological chemistry*, 278(49), pp. 48627-32.

Korhonen, J.A., Pham, X.H., Pellegrini, M. & Falkenberg, M., 2004, Reconstitution of a minimal mtDNA replisome in vitro, *EMBO J*, 23(12), pp. 2423-9.

Korshunov, S.S., Skulachev, V.P. & Starkov, A.A., 1997, High protonic potential actuates a mechanism of production of reactive oxygen species in mitochondria, *FEBS letters*, 416(1), pp. 15-8.

Koshy, P.J., Henderson, N., Logan, C., Life, P.F., Cawston, T.E. & Rowan, A.D., 2002, Interleukin 17 induces cartilage collagen breakdown: novel synergistic effects in combination with proinflammatory cytokines, *Annals of the rheumatic diseases*, 61(8), pp. 704-13.

Kostal, V. & Arriaga, E.A., 2011, Capillary Electrophoretic Analysis Reveals Subcellular Binding between Individual Mitochondria and Cytoskeleton, *Analytical chemistry*.

Kraytsberg, Y., Kudryavtseva, E., McKee, A.C., Geula, C., Kowall, N.W. & Khrapko, K., 2006, Mitochondrial DNA deletions are abundant and cause functional impairment in aged human substantia nigra neurons, *Nature genetics*, 38(5), pp. 518-20.

Krebs, H.A. & Eggleston, L.V., 1940, The oxidation of pyruvate in pigeon breast muscle, *The Biochemical journal*, 34(3), pp. 442-59.

Krishnan, K.J., Bender, A., Taylor, R.W. & Turnbull, D.M., 2007, A multiplex real-time PCR method to detect and quantify mitochondrial DNA deletions in individual cells, *Analytical biochemistry*, 370(1), pp. 127-9.

Krishnan, K.J., Blackwood, J.K., Reeve, A.K., Turnbull, D.M. & Taylor, R.W., 2010, Detection of mitochondrial DNA variation in human cells, *Methods in molecular biology (Clifton, N.J.)*, 628, pp. 227-57.

Krishnan, K.J., Reeve, A.K., Samuels, D.C., Chinnery, P.F., Blackwood, J.K., Taylor, R.W., Wanrooij, S., Spelbrink, J.N., Lightowlers, R.N. & Turnbull, D.M., 2008, What causes mitochondrial DNA deletions in human cells? *Nature genetics*, 40(3), pp. 275-9.

Kristiansen, G., Hu, J., Wichmann, D., Stiehl, D.P., Rose, M., Gerhardt, J., Bohnert, A., Ten Haaf, A., Moch, H., Raleigh, J., Varia, M.A., Subarsky, P., Scandurra, F.M., Gnaiger, E., Gleixner, E., Bicker, A., Gassmann, M., Hankeln, T., Dahl, E. & Gorr, T.A., 2011, Endogenous Myoglobin in Breast Cancer Is Hypoxia-inducible by Alternative Transcription and Functions to Impair Mitochondrial Activity: A ROLE IN TUMOR SUPPRESSION? *The Journal of biological chemistry*, 286(50), pp. 43417-28.

Kruse, B., Narasimhan, N. & Attardi, G., 1989, Termination of transcription in human mitochondria: identification and purification of a DNA binding protein factor that promotes termination, *Cell*, 58(2), pp. 391-7.

Kujoth, G.C., Hiona, A., Pugh, T.D., Someya, S., Panzer, K., Wohlgemuth, S.E., Hofer, T., Seo, A.Y., Sullivan, R., Jobling, W.A., Morrow, J.D., Remmen, H.V., Sedivy, J.M., Yamasoba, T., Tanokura, M., Weindruch, R., Leeuwenburgh, C. & Prolla, T.A., 2005, Mitochondrial DNA mutations, oxidative stress, and apoptosis in mammalian aging, *Science*, 309(5733), pp. 481-4.

Kurz, B., Lemke, A., Fay, J., Pufe, T. & Grodzinsky, A., 2005, Pathomechanisms of cartilage destruction by mechanical injury, *Annals of Anatomy*, 29(1), pp. 89-95.

Kwon, J., Lee, S.-R., Yang, K.-S., Ahn, Y., Kim, Y.J., Stadtman, E.R. & Rhee, S.G., 2004, Reversible oxidation and inactivation of the tumor suppressor PTEN in cells stimulated with peptide growth factors, *Proc Natl Acad Sci USA*, 101(47), pp. 16419-24.

Landolfi, B., Curci, S., Debellis, L., Pozzan, T. & Hofer, A.M., 1998, Ca2+ homeostasis in the agonist-sensitive internal store: functional interactions between mitochondria and the ER measured In situ in intact cells, *J Cell Biol*, 142(5), pp. 1235-43.

Lane, L.B., Villacin, A. & Bullough, P.G., 1977, The vascularity and remodelling of subchondrial bone and calcified cartilage in adult human femoral and humeral heads. An age-and stress-related phenomenon, *Journal of Bone and Joint Surgery-British Volume*, 59(3), p. 272.

Lauterburg, B.H., Corcoran, G.B. & Mitchell, J.R., 1983, Mechanism of action of N-acetylcysteine in the protection against the hepatotoxicity of acetaminophen in rats in vivo, *The Journal of clinical investigation*, 71(4), pp. 980-91.

Lebovitz, R.M., Zhang, H., Vogel, H., Cartwright, J., Dionne, L., Lu, N., Huang, S. & Matzuk, M.M., 1996, Neurodegeneration, myocardial injury, and perinatal death in mitochondrial superoxide dismutase-deficient mice, *Proc Natl Acad Sci USA*, 93(18), pp. 9782-7.

Lee, R.B. & Urban, J.P., 1997, Evidence for a negative Pasteur effect in articular cartilage, *The Biochemical journal*, 321 (Pt 1), pp. 95-102.

Lee, S.R., Kwon, K.S., Kim, S.R. & Rhee, S.G., 1998, Reversible inactivation of protein-tyrosine phosphatase 1B in A431 cells stimulated with epidermal growth factor, *The Journal of biological chemistry*, 273(25), pp. 15366-72.

Legendre, F., Bogdanowicz, P., Boumediene, K. & Pujol, J.P., 2005, Role of interleukin 6 (IL-6)/IL-6R-induced signal tranducers and activators of transcription and mitogen-activated protein kinase/extracellular, *The Journal of rheumatology*, 32(7), pp. 1307-16.

Lemarie, A., Huc, L., Pazarentzos, E., Mahul-Mellier, A.-L. & Grimm, S., 2011, Specific disintegration of complex II succinate:ubiquinone oxidoreductase links pH changes to oxidative stress for apoptosis induction, *Cell death and differentiation*, 18(2), pp. 338-49.

Lestienne, P. & Ponsot, G., 1988, Kearns-Sayre syndrome with muscle mitochondrial DNA deletion, *Lancet*, 1(8590), p. 885.

Levinthal, D.J. & Defranco, D.B., 2005, Reversible oxidation of ERK-directed protein phosphatases drives oxidative toxicity in neurons, *The Journal of biological chemistry*, 280(7), pp. 5875-83.

Li, N., Ragheb, K., Lawler, G., Sturgis, J., Rajwa, B., Melendez, J.A. & Robinson, J.P., 2003, Mitochondrial complex I inhibitor rotenone induces apoptosis through enhancing mitochondrial reactive oxygen species production, *The Journal of biological chemistry*, 278(10), pp. 8516-25.

Li, W.Q., Dehnade, F. & Zafarullah, M., 2001, Oncostatin M-induced matrix metalloproteinase and tissue inhibitor of metalloproteinase-3 genes expression in chondrocytes requires Janus kinase/STAT signaling pathway, *Journal of immunology (Baltimore, Md : 1950)*, 166(5), pp. 3491-8.

Li, Y., Huang, T.T., Carlson, E.J., Melov, S., Ursell, P.C., Olson, J.L., Noble, L.J., Yoshimura, M.P., Berger, C., Chan, P.H., Wallace, D.C. & Epstein, C.J., 1995, Dilated cardiomyopathy and neonatal lethality in mutant mice lacking manganese superoxide dismutase, *Nature genetics*, 11(4), pp. 376-81.

Liacini, A., Sylvester, J., Li, W.Q. & Zafarullah, M., 2002, Inhibition of interleukin-1-stimulated MAP kinases, activating protein-1 (AP-1) and nuclear factor kappa B (NF-kappa B) transcription factors down-regulates matrix metalloproteinase gene expression in articular chondrocytes, *Matrix biology : journal of the International Society for Matrix Biology*, 21(3), pp. 251-62.

Liacini, A., Sylvester, J., Li, W.Q., Huang, W., Dehnade, F., Ahmad, M. & Zafarullah, M., 2003, Induction of matrix metalloproteinase-13 gene expression by TNF-alpha is mediated by MAP kinases, AP-1, and NF-kappaB transcription factors in articular chondrocytes, *Experimental cell research*, 288(1), pp. 208-17.

Liesa, M., Palac\'\in, M. & Zorzano, A., 2009, Mitochondrial dynamics in mammalian health and disease, *Physiol Rev*, 89(3), pp. 799-845.

Lightowlers, R., Chinnery, P., Turnbull, D. & Howell, N., 1997, Mammalian mitochondrial genetics: heredity, heteroplasmy and disease, *Trends in Genetics*, 13(11):450-5

Ligon, L. & Oswald, S., 2000, Role of microtubules and actin filaments in the movement of mitochondria in the axons and dendrites of cultured hippocampal neurons, *The Journal of comparative neurology*, 16(1), pp. 15-8.

Lim, S.Y., Tennant, G.M., Kennedy, S., Wainwright, C.L. & Kane, K.A., 2006, Activation of mouse protease-activated receptor-2 induces lymphocyte adhesion and generation of reactive oxygen species, *British Journal of Pharmacology*, 149(5), p. 591.

Lires-Dean, M., Caramés, B., Cillero-Pastor, B., Galdo, F., López-Armada, M.J. & Blanco, F.J., 2008, Anti-apoptotic effect of transforming growth factor-beta1 on human articular chondrocytes: role of protein phosphatase 2A, *Osteoarthr Cartil*, 16(11), pp. 1370-8.

Lister, R., Hulett, J., Lithgow, T. & Whelan, J., 2005, Protein import into mitochondria: origins and functions today (Review), *Molecular membrane biology*.

Little, C.B., Barai, A., Burkhardt, D., Smith, S.M., Fosang, A.J., Werb, Z., Shah, M. & Thompson, E.W., 2009, Matrix metalloproteinase 13-deficient mice are resistant to osteoarthritic cartilage erosion but not chondrocyte hypertrophy or osteophyte development, *Arthritis and rheumatism*, 60(12), pp. 3723-33.

Little, C.B., Hughes, C.E., Curtis, C.L., Janusz, M.J., Bohne, R., Wang-Weigand, S., Taiwo, Y.O., Mitchell, P.G., Otterness, I.G., Flannery, C.R. & Caterson, B., 2002, Matrix metalloproteinases are involved in C-terminal and interglobular domain processing of cartilage aggrecan in late stage cartilage degradation, *Matrix biology : journal of the International Society for Matrix Biology*, 21(3), pp. 271-88.

Little, C.B., Meeker, C.T., Golub, S.B., Lawlor, K.E., Farmer, P.J., Smith, S.M. & Fosang, A.J., 2007, Blocking aggrecanase cleavage in the aggrecan

interglobular domain abrogates cartilage erosion and promotes cartilage repair, *The Journal of clinical investigation*, 117(6), pp. 1627-36.

Liu, X., Kim, C.N., Yang, J., Jemmerson, R. & Wang, X., 1996, Induction of apoptotic program in cell-free extracts: requirement for dATP and cytochrome c, *Cell*, 86(1), pp. 147-57.

Loeser, R.F., 2006, Molecular mechanisms of cartilage destruction: mechanics, inflammatory mediators, and aging collide, *Arthritis and rheumatism*, 54(5), pp. 1357-60.

Loeser, R.F., Carlson, C.S., Carlo, M.D. & Cole, A., 2002, Detection of nitrotyrosine in aging and osteoarthritic cartilage: Correlation of oxidative damage with the presence of interleukin-1? and with chondrocyte resistance to insulin-like growth factor 1, *Arthritis & Rheumatism*, 46(9), pp. 2349-57.

Longo, V.D., Liou, L.L., Valentine, J.S. & Gralla, E.B., 1999, Mitochondrial superoxide decreases yeast survival in stationary phase, *Archives of biochemistry and biophysics*, 365(1), pp. 131-42.

Lopezarmada, M., Carames, B., Martin, M., Cilleropastor, B., Liresdean, M., Fuentesboquete, I., Arenas, J. & Blanco, F., 2006, Mitochondrial activity is modulated by TNFα and IL-1β in normal human chondrocyte cells, *Osteoarthritis and Cartilage*, 14(10), pp. 1011-22.

López-Armada, M.J., Caramés, B., Lires-Deán, M., Cillero-Pastor, B., Ruiz-Romero, C., Galdo, F. & Blanco, F.J., 2006, Cytokines, tumor necrosis factor-alpha and interleukin-1beta, differentially regulate apoptosis in osteoarthritis cultured human chondrocytes, *Osteoarthr Cartil*, 14(7), pp. 660-9.

Lu, C.Y., Lee, H.C., Fahn, H.J. & Wei, Y.H., 1999, Oxidative damage elicited by imbalance of free radical scavenging enzymes is associated with large-scale mtDNA deletions in aging human skin, *Mutation research*, 423(1-2), pp. 11-21.

Ma, Q., Cavallin, L.E., Yan, B., Zhu, S., Duran, E.M., Wang, H., Hale, L.P., Dong, C., Cesarman, E., Mesri, E.A. & Goldschmidt-Clermont, P.J., 2009,

Antitumorigenesis of antioxidants in a transgenic Rac1 model of Kaposi's sarcoma, *Proc Natl Acad Sci USA*, 106(21), pp. 8683-8.

Malemud, C., 2004, Protein kinases in chondrocyte signaling and osteoarthritis, *Clinical orthopaedics and related research*, 6(1), pp. 15-8.

Maneiro, E., Lopez-Armada, M. & de Andres, M., 2005, Effect of nitric oxide on mitochondrial respiratory activity of human articular chondrocytes, *Annals of the rheumatic diseases*, 64(3), pp. 388-95.

Maneiro, E., Martín, M.A., de Andres, M.C., López-Armada, M.J., Fernández-Sueiro, J.L., del Hoyo, P., Galdo, F., Arenas, J. & Blanco, F.J., 2003, Mitochondrial respiratory activity is altered in osteoarthritic human articular chondrocytes, *Arthritis and rheumatism*, 48(3), pp. 700-8.

Manicourt, D.H., Poilvache, P., Egeren, A.V., Devogelaer, J.P., Lenz, M.E. & Thonar, E.J., 2000, Synovial fluid levels of tumor necrosis factor alpha and oncostatin M correlate with levels of markers of the degradation of crosslinked collagen and cartilage aggrecan in rheumatoid arthritis but not in osteoarthritis, *Arthritis and rheumatism*, 43(2), pp. 281-8.

Marcus, R.E., 1973, The effect of low oxygen concentration on growth, glycolysis, and sulfate incorporation by articular chondrocytes in monolayer culture, *Arthritis and rheumatism*, 16(5), pp. 646-56.

Margolis, S.A., Coxon, B., Gajewski, E. & Dizdaroglu, M., 1988, Structure of a hydroxyl radical induced cross-link of thymine and tyrosine, *Biochemistry*, 27(17), pp. 6353-9.

Marnett, L.J., 1999, Lipid peroxidation-DNA damage by malondialdehyde, *Mutation research*, 424(1-2), pp. 83-95.

Martin, J. & Buckwalter, J., 2002, Aging, articular cartilage chondrocyte senescence and osteoarthritis, *Biogerontology*, 3(5):257-64.

Martin, J.A. & Buckwalter, J.A., 2003, The role of chondrocyte senescence in the pathogenesis of osteoarthritis and in limiting cartilage repair, *The Journal of bone and joint surgery American volume*, 85-A Suppl 2, pp. 106-10.

Martin, J.A., Brown, T.D., Heiner, A.D. & Buckwalter, J.A., 2004, Chondrocyte senescence, joint loading and osteoarthritis, *Clinical orthopaedics and related research*(427 Suppl), pp. S96-103.

Martinon, F., Burns, K. & Tschopp, J., 2002, The inflammasome: a molecular platform triggering activation of inflammatory caspases and processing of proIL-beta, *Molecular cell*, 10(2), pp. 417-26.

Mathy-Hartert, M., Hogge, L., Sanchez, C., Deby-Dupont, G., Crielaard, J.M. & Henrotin, Y., 2008, Interleukin-1beta and interleukin-6 disturb the antioxidant enzyme system in bovine chondrocytes: a possible explanation for oxidative stress generation, *Osteoarthr Cartil*, 16(7), pp. 756-63.

Matthes, M., Weisbeek, P.J. & Denhardt, D.T., 1982, Mechanism of replication of bacteriophage phi X174 XIX. Initiation of phi X174 viral strand DNA synthesis at internal sites on the genome, *Journal of virology*, 42(1), pp. 301-5.

Mauck, R.L., Hung, C.T. & Ateshian, G.A., 2003, Modeling of neutral solute transport in a dynamically loaded porous permeable gel: implications for articular cartilage biosynthesis and tissue engineering, *J Biomech Eng*, 125(5), pp. 602-14.

McShane, M.A., Hammans, S.R., Sweeney, M., Holt, I.J., Beattie, T.J., Brett, E.M. & Harding, A.E., 1991, Pearson syndrome and mitochondrial encephalomyopathy in a patient with a deletion of mtDNA, *American journal of human genetics*, 48(1), pp. 39-42.

Melov, S., Coskun, P., Patel, M., Tuinstra, R., Cottrell, B., Jun, A.S., Zastawny, T.H., Dizdaroglu, M., Goodman, S.I., Huang, T.T., Miziorko, H., Epstein, C.J. & Wallace, D.C., 1999, Mitochondrial disease in superoxide dismutase 2 mutant mice, *Proc Natl Acad Sci USA*, 96(3), pp. 846-51.

Melov, S., Doctrow, S.R., Schneider, J.A., Haberson, J., Patel, M., Coskun, P.E., Huffman, K., Wallace, D.C. & Malfroy, B., 2001, Lifespan extension and rescue of spongiform encephalopathy in superoxide dismutase 2 nullizygous mice treated with superoxide dismutase-catalase mimetics, *The Journal of*

neuroscience : the official journal of the Society for Neuroscience, 21(21), pp. 8348-53.

Melov, S., Schneider, J.A., Day, B.J., Hinerfeld, D., Coskun, P., Mirra, S.S., Crapo, J.D. & Wallace, D.C., 1998, A novel neurological phenotype in mice lacking mitochondrial manganese superoxide dismutase, *Nature genetics*, 18(2), pp. 159-63.

Meng, T.-C., Fukada, T. & Tonks, N.K., 2002, Reversible oxidation and inactivation of protein tyrosine phosphatases in vivo, *Molecular cell*, 9(2), pp. 387-99.

Menshikova, E.V., Ritov, V.B., Fairfull, L., Ferrell, R.E., Kelley, D.E. & Goodpaster, B.H., 2006, Effects of exercise on mitochondrial content and function in aging human skeletal muscle, *The journals of gerontology. Series A, Biological sciences and medical sciences*, 61(6), pp. 534-40.

Meylan, E., Curran, J., Hofmann, K., Moradpour, D., Binder, M., Bartenschlager, R. & Tschopp, J., 2005, Cardif is an adaptor protein in the RIG-I antiviral pathway and is targeted by hepatitis C virus, *Nature*, 437(7062), pp. 1167-72.

Miao, L. & Clair, D.K.S., 2009, Regulation of superoxide dismutase genes: implications in disease, *Free radical biology & medicine*, 47(4), pp. 344-56.

Mignotte, F., Champagne, A.M., Froger-Gaillard, B., Benel, L., Gueride, M., Adolphe, M. & Mounolou, J.C., 1991, Mitochondrial biogenesis in rabbit articular chondrocytes transferred to culture, *Biology of the cell / under the auspices of the European Cell Biology Organization*, 71(1-2), pp. 67-72.

Mihara, K., Blobel, G. & Sato, R., 1982, In vitro synthesis and integration into mitochondria of porin, a major protein of the outer mitochondrial membrane of Saccharomyces cerevisiae, *Proc Natl Acad Sci USA*, 79(23), pp. 7102-6.

Miller, E.J., Harris, E.D., Chung, E., Finch, J.E., McCroskery, P.A. & Butler, W.T., 1976, Cleavage of Type II and III collagens with mammalian collagenase: site of cleavage and primary structure at the NH2-terminal portion of the smaller fragment released from both collagens, *Biochemistry*, 15(4), pp. 787-92.

Mita, S., Rizzuto, R., Moraes, C.T., Shanske, S., Arnaudo, E., Fabrizi, G.M., Koga, Y., DiMauro, S. & Schon, E.A., 1990, Recombination via flanking direct repeats is a major cause of large-scale deletions of human mitochondrial DNA, *Nucleic acids research*, 18(3), pp. 561-7.

Mita, S., Schmidt, B., Schon, E.A., DiMauro, S. & Bonilla, E., 1989, Detection of "deleted" mitochondrial genomes in cytochrome-c oxidase-deficient muscle fibers of a patient with Kearns-Sayre syndrome, *Proc Natl Acad Sci USA*, 86(23), pp. 9509-13.

Mitchell, P. & Moyle, J., 1967, Chemiosmotic hypothesis of oxidative phosphorylation, *Nature*, 213(5072):137-9.

Mitchell, P. & Moyle, J., 1969, Estimation of membrane potential and pH difference across the cristae membrane of rat liver mitochondria, *European journal of biochemistry / FEBS*, 7(4), pp. 471-84.

Mitchell, P., 1961, Coupling of phosphorylation to electron and hydrogen transfer by a chemi-osmotic type of mechanism, *Nature*, 191, pp. 144-8.

Mitchell, P., 1976, Possible molecular mechanisms of the protonmotive function of cytochrome systems, *J Theor Biol*, 62(2):327-67.

Mitchell, P.G., Magna, H.A., Reeves, L.M., Lopresti-Morrow, L.L., Yocum, S.A., Rosner, P.J., Geoghegan, K.F. & Hambor, J.E., 1996, Cloning, expression, and type II collagenolytic activity of matrix metalloproteinase-13 from human osteoarthritic cartilage, *The Journal of clinical investigation*, 97(3), pp. 761-8.

Mitomap 2006, Mitomap database, *MITOMAP [online]. Centre for Molecular Medicine, Emory University, Atlanta, GA.* from http://www.mitomap.org/

Monboisse, J.C., Gardès-Albert, M., Randoux, A., Borel, J.P. & Ferradini, C., 1988, Collagen degradation by superoxide anion in pulse and gamma radiolysis, *Biochimica et biophysica acta*, 965(1), pp. 29-35.

Montoya, J., Christianson, T., Levens, D., Rabinowitz, M. & Attardi, G., 1982, Identification of initiation sites for heavy-strand and light-strand transcription in human mitochondrial DNA, *Proc Natl Acad Sci USA*, 79(23), pp. 7195-9.

Montoya, J., Ojala, D. & Attardi, G., 1981, Distinctive features of the 5'-terminal sequences of the human mitochondrial mRNAs, *Nature*, 290(5806), pp. 465-70.

Moodley, D., Mody, G., Patel, N. & Chuturgoon, A., 2008, Mitochondrial depolarisation and oxidative stress in rheumatoid arthritis patients, *Clinical biochemistry*, p. 6.

Moore, C.B., Bergstralh, D.T., Duncan, J.A., Lei, Y., Morrison, T.E., Zimmermann, A.G., Accavitti-Loper, M.A., Madden, V.J., Sun, L., Ye, Z., Lich, J.D., Heise, M.T., Chen, Z. & Ting, J.P.-Y., 2008, NLRX1 is a regulator of mitochondrial antiviral immunity, *Nature*, 451(7178), pp. 573-7.

Morris, R.L. & Hollenbeck, P.J., 1995, Axonal transport of mitochondria along microtubules and F-actin in living vertebrate neurons, *J Cell Biol*, 131(5), pp. 1315-26.

Morten, K.J., Ackrell, B.A.C. & Melov, S., 2006, Mitochondrial reactive oxygen species in mice lacking superoxide dismutase 2: attenuation via antioxidant treatment, *The Journal of biological chemistry*, 281(6), pp. 3354-9.

Moser, C.C., Keske, J.M., Warncke, K., Farid, R.S. & Dutton, P.L., 1992, Nature of biological electron transfer, *Nature*, 355(6363), pp. 796-802.

Muramoto, K., Hirata, K., Shinzawa-Itoh, K., Yoko-o, S., Yamashita, E., Aoyama, H., Tsukihara, T. & Yoshikawa, S., 2007, A histidine residue acting as a controlling site for dioxygen reduction and proton pumping by cytochrome c oxidase, *Proceedings of the National Academy of Sciences of the United States of America*, 104(19), pp. 7881-6.

Murphy, G., Knäuper, V., Atkinson, S., Butler, G., English, W., Hutton, M., Stracke, J. & Clark, I., 2002, Matrix metalloproteinases in arthritic disease, *Arthritis research*, 4 Suppl 3, pp. S39-49.

Murphy, M.P., 2009, How mitochondria produce reactive oxygen species, *The Biochemical journal*, 417(1), pp. 1-13.

Nagase, H. & Fushimi, K., 2008, Elucidating the function of non catalytic domains of collagenases and aggrecanases, *Connective tissue research*, 49(3), pp. 169-74.

Nakagawa, S., Arai, Y., Mazda, O., Kishida, T., Takahashi, K.A., Sakao, K., Saito, M., Honjo, K., Imanishi, J. & Kubo, T., 2010, N-acetylcysteine prevents nitric oxide-induced chondrocyte apoptosis and cartilage degeneration in an experimental model of osteoarthritis, *Journal of orthopaedic research : official publication of the Orthopaedic Research Society*, 28(2), pp. 156-63.

Nakahira, K., Haspel, J.A., Rathinam, V.A.K., Lee, S.-J., Dolinay, T., Lam, H.C., Englert, J.A., Rabinovitch, M., Cernadas, M., Kim, H.P., Fitzgerald, K.A., Ryter, S.W. & Choi, A.M.K., 2011, Autophagy proteins regulate innate immune responses by inhibiting the release of mitochondrial DNA mediated by the NALP3 inflammasome, *Nature immunology*, 12(3), pp. 222-30.

Nelson, K. & Melendez, J., 2004, Mitochondrial redox control of matrix metalloproteinases, *Free Radical Biology and Medicine*. 281(20):14100-10.

Newmeyer, D.D., Farschon, D.M. & Reed, J.C., 1994, Cell-free apoptosis in Xenopus egg extracts: inhibition by Bcl-2 and requirement for an organelle fraction enriched in mitochondria, *Cell*, 79(2), pp. 353-64.

Nicholls, D.G., 2005, Mitochondria and calcium signaling, *Cell Calcium*, 38(3-4), pp. 311-7.

Nicholls, D.G., 2006, Simultaneous monitoring of ionophore- and inhibitor-mediated plasma and mitochondrial membrane potential changes in cultured neurons, *The Journal of biological chemistry*, 281(21), pp. 14864-74.

Niwa, Y., Ishimoto, K. & Kanoh, T., 1990, Induction of superoxide dismutase in leukocytes by paraquat: correlation with age and possible predictor of longevity, *Blood*, 76(4), pp. 835-41.

Nobes, C.D., Brown, G.C., Olive, P.N. & Brand, M.D., 1990, Non-ohmic proton conductance of the mitochondrial inner membrane in hepatocytes, *The Journal of biological chemistry*, 265(22), pp. 12903-9.

Noji, H., Yasuda, R., Yoshida, M. & Kinosita, K., 1997, Direct observation of the rotation of F1-ATPase, *Nature*, 386(6622), pp. 299-302.

O'Hara, B.P., Urban, J.P. & Maroudas, A., 1990, Influence of cyclic loading on the nutrition of articular cartilage, *Annals of the rheumatic diseases*, 49(7), pp. 536-9.

Oelkrug, R., Kutschke, M., Meyer, C.W., Heldmaier, G. & Jastroch, M., 2010, Uncoupling protein 1 decreases superoxide production in brown adipose tissue mitochondria, *The Journal of biological chemistry*, 285(29), pp. 21961-8.

Ohnishi, T. & Salerno, J.C., 1976, Thermodynamic and EPR characteristics of two ferredoxin-type iron-sulfur centers in the succinate-ubiquinone reductase segment of the respiratory chain, *The Journal of biological chemistry*, 251(7), pp. 2094-104.

Ojala, D., Montoya, J. & Attardi, G., 1981, tRNA punctuation model of RNA processing in human mitochondria, *Nature*, 290(5806), pp. 470-4.

Old, S.L. & Johnson, M.A., 1989, Methods of microphotometric assay of succinate dehydrogenase and cytochrome c oxidase activities for use on human skeletal muscle, *Histochem J*, 21(9-10), pp. 545-55.

Olinski, R., Nackerdien, Z. & Dizdaroglu, M., 1992, DNA-protein cross-linking between thymine and tyrosine in chromatin of gamma-irradiated or H2O2-treated cultured human cells, *Archives of biochemistry and biophysics*, 297(1), pp. 139-43.

Olmos, Y., Valle, I., Borniquel, S., Tierrez, A., Soria, E., Lamas, S. & Monsalve, M., 2009, Mutual dependence of Foxo3a and PGC-1alpha in the induction of oxidative stress genes, *The Journal of biological chemistry*, 284(21), pp. 14476-84.

Ott, M., Gogvadze, V., Orrenius, S. & Zhivotovsky, B., 2007, Mitochondria, oxidative stress and cell death, *Apoptosis : an international journal on programmed cell death*, 12(5), pp. 913-22.

Oven, M.V. & Kayser, M., 2009, Updated comprehensive phylogenetic tree of global human mitochondrial DNA variation, *Human mutation*, 30(2), pp. E386-94.

Palmer, C.S., Osellame, L.D., Stojanovski, D. & Ryan, M.T., 2011, The regulation of mitochondrial morphology: intricate mechanisms and dynamic machinery, *Cellular signalling*, 23(10), pp. 1534-45.

Parisi, M.A. & Clayton, D.A., 1991, Similarity of human mitochondrial transcription factor 1 to high mobility group proteins, *Science*, 252(5008), p. 965.

Park, C.B., Asin-Cayuela, J., Cámara, Y., Shi, Y., Pellegrini, M., Gaspari, M., Wibom, R., Hultenby, K., Erdjument-Bromage, H., Tempst, P., Falkenberg, M., Gustafsson, C.M. & Larsson, N.-G., 2007, MTERF3 is a negative regulator of mammalian mtDNA transcription, *Cell*, 130(2), pp. 273-85.

Parker, N., Vidal-Puig, A. & Brand, M.D., 2008, Stimulation of mitochondrial proton conductance by hydroxynonenal requires a high membrane potential, *Biosci Rep*, 28(2), pp. 83-8.

Passos, J.F., Saretzki, G., Ahmed, S., Nelson, G., Richter, T., Peters, H., Wappler, I., Birket, M.J., Harold, G., Schaeuble, K., Birch-Machin, M.A., Kirkwood, T.B.L. & Zglinicki, T.V., 2007, Mitochondrial dysfunction accounts for the stochastic heterogeneity in telomere-dependent senescence, *PLoS biology*, 5(5), p. e110.

Pelletier, J., Martel-Pelletier, J. & Abramson, S., 2001, Osteoarthritis, an inflammatory disease, *Arthritis and rheumatism*.

Perry, J.J.P., Shin, D.S., Getzoff, E.D. & Tainer, J.A., 2010, The structural biochemistry of the superoxide dismutases, *Biochimica et biophysica acta*, 1804(2), pp. 245-62.

Petersen, S.V., Oury, T.D., Ostergaard, L., Valnickova, Z., Wegrzyn, J., Thøgersen, I.B., Jacobsen, C., Bowler, R.P., Fattman, C.L., Crapo, J.D. & Enghild, J.J., 2004, Extracellular superoxide dismutase (EC-SOD) binds to type

i collagen and protects against oxidative fragmentation, *The Journal of biological chemistry*, 279(14), pp. 13705-10.

Phylotree 2009, Phylotree, from http://www.phylotree.org

Porter, S., Clark, I., Kevorkian, L. & Edwards, D., 2005, The ADAMTS metalloproteinases, *Biochemical Journal*, 386(Pt 1):15-27.

Poyton, R.O., Ball, K.A. & Castello, P.R., 2009, Mitochondrial generation of free radicals and hypoxic signaling, *Trends Endocrinol Metab*, 20(7), pp. 332-40.

Price, J.S., Waters, J.G., Darrah, C., Pennington, C., Edwards, D.R., Donell, S.T. & Clark, I.M., 2002, The role of chondrocyte senescence in osteoarthritis, *Aging cell*, 1(1), pp. 57-65.

Pyle, A., Taylor, R., Durham, Deschauer, Schaefer, Samuels & Chinnery, 2007, Depletion of mitochondrial DNA in leucocytes harbouring the 3243A→ G mtDNA mutation, *Journal of medical genetics,* 44(1):69-74.

Qadri, I., Iwahashi, M., Capasso, J.M., Hopken, M.W., Flores, S., Schaack, J. & Simon, F.R., 2004, Induced oxidative stress and activated expression of manganese superoxide dismutase during hepatitis C virus replication: role of JNK, p38 MAPK and AP-1, *The Biochemical journal*, 378(Pt 3), pp. 919-28.

Rachek, L.I., Grishko, V.I., Alexeyev, M.F., Pastukh, V.V., LeDoux, S.P. & Wilson, G.L., 2004, Endonuclease III and endonuclease VIII conditionally targeted into mitochondria enhance mitochondrial DNA repair and cell survival following oxidative stress, *Nucleic acids research*, 32(10), pp. 3240-7.

Rachek, L.I., Grishko, V.I., Musiyenko, S.I., Kelley, M.R., LeDoux, S.P. & Wilson, G.L., 2002, Conditional targeting of the DNA repair enzyme hOGG1 into mitochondria, *The Journal of biological chemistry*, 277(47), pp. 44932-7.

Ragan, C.I. & Racker, E., 1973a, Partial resolution of the enzymes catalyzing oxidative phosphorylation. 28. The reconstitution of the first site of energy conservation, *The Journal of biological chemistry*, 248(7), pp. 2563-9.

Ragan, C.I. & Racker, E., 1973b, Resolution and reconstitution of the mitochondrial electron transport system. IV. The reconstitution of rotenone-sensitive reduced nicotinamide adenine dinucleotide-ubiquinone reductase from reduced nicotinamide adenine dinucleotide dehydrogenase and phospholipids, *The Journal of biological chemistry*, 248(19), pp. 6876-84.

Rajasekhar, L., Liou, L.B., Chan, C.Y., Tsai, W.P. & Cheng, C.Y., 2004, Matrix metalloproteinase-8 in sera and from polymorphonuclear leucocytes in rheumatoid arthritis: in vitro characterization and correlation with disease activity, *Clinical and experimental rheumatology*, 22(5), pp. 597-602.

Ranganathan, A.C., Nelson, K.K., Rodriguez, A.M., Kim, K.H., Tower, G.B., Rutter, J.L., Brinckerhoff, C.E., Huang, T.T., Epstein, C.J., Jeffrey, J.J. & Melendez, J.A., 2001, Manganese superoxide dismutase signals matrix metalloproteinase expression via H2O2-dependent ERK1/2 activation, *The Journal of biological chemistry*, 276(17), pp. 14264-70.

Rebsamen, M., Vazquez, J., Tardivel, A., Guarda, G., Curran, J. & Tschopp, J., 2011, NLRX1/NOD5 deficiency does not affect MAVS signalling, *Cell death and differentiation*, 18(8):1387.

Rees, D.M., Leslie, A.G.W. & Walker, J.E., 2009, The structure of the membrane extrinsic region of bovine ATP synthase, *Proc Natl Acad Sci USA*, 106(51), pp. 21597-601.

Regan, E., Flannelly, J., Bowler, R., Tran, K., Nicks, M., Carbone, B.D., Glueck, D., Heijnen, H., Mason, R. & Crapo, J., 2005, Extracellular superoxide dismutase and oxidant damage in osteoarthritis, *Arthritis and rheumatism*, 52(11), pp. 3479-91.

Regan, E.A., Bowler, R.P. & Crapo, J.D., 2008, Joint fluid antioxidants are decreased in osteoarthritic joints compared to joints with macroscopically intact cartilage and subacute injury, *Osteoarthr Cartil*, 16(4), pp. 515-21.

Rego, I., Fernández-Moreno, M., Fernández-López, C., Gómez-Reino, J., González, A., Arenas, J. & Blanco, F., 2009, The role of European mtDNA

haplogroups in the prevalence of hip osteoarthritis in Galicia (Northern Spain), *Annals of the rheumatic diseases*, 69(1):210-3.

Rego-Perez, I., Fernández-Moreno, M., Deberg, M., Pértega, S., Fenández-López, C., Oreiro, N., Henrotin, Y. & Blanco, F.J., 2010, Mitochondrial DNA haplogroups modulate the serum levels of biomarkers in patients with osteoarthritis, *Annals of the rheumatic diseases*, 69(5), pp. 910-7.

Rego-Perez, I., Fernández-Moreno, M., Deberg, M., Pértega, S., Fernández-López, C., Oreiro, N., Henrotin, Y. & Blanco, F.J., 2011, Mitochondrial DNA haplogroups and serum levels of proteolytic enzymes in patients with osteoarthritis, *Annals of the rheumatic diseases*, 70(4), pp. 646-52.

Rego-Perez, I., Fernández-Moreno, M., Fernández-López, C., Arenas, J. & Blanco, F.J., 2008, Mitochondrial DNA haplogroups: Role in the prevalence and severity of knee osteoarthritis, *Arthritis and rheumatism*, 58(8), pp. 2387-96.

Rich, P.R. & Maréchal, A., 2010, The mitochondrial respiratory chain, *Essays Biochem*, 47, pp. 1-23.

Roach, H.I., Aigner, T. & Kouri, J.B., 2004, Chondroptosis: a variant of apoptotic cell death in chondrocytes? *Apoptosis : an international journal on programmed cell death*, 9(3), pp. 265-77.

Robberson, D.L. & Clayton, D.A., 1972, Replication of mitochondrial DNA in mouse L cells and their thymidine kinase - derivatives: displacement replication on a covalently-closed circular template, *Proc Natl Acad Sci USA*, 69(12), pp. 3810-4.

Robinson, K.M., Janes, M.S. & Beckman, J.S., 2008, The selective detection of mitochondrial superoxide by live cell imaging, *Nature protocols*, 3(6), pp. 941-7.

Robinson, K.M., Janes, M.S., Pehar, M., Monette, J.S., Ross, M.F., Hagen, T.M., Murphy, M.P. & Beckman, J.S., 2006, Selective fluorescent imaging of superoxide in vivo using ethidium-based probes, *Proc Natl Acad Sci USA*, 103(41), pp. 15038-43.

Rodriguez-Manzaneque, J.C., Westling, J., Thai, S.N.-M., Luque, A., Knauper, V., Murphy, G., Sandy, J.D. & Iruela-Arispe, M.L., 2002, ADAMTS1 cleaves aggrecan at multiple sites and is differentially inhibited by metalloproteinase inhibitors, *Biochemical and biophysical research communications*, 293(1), pp. 501-8.

Rotilio, G., Bray, R.C. & Fielden, E.M., 1972, A pulse radiolysis study of superoxide dismutase, *Biochimica et biophysica acta*, 268(2), pp. 605-9.

Roughley, P.J., 2001, Articular cartilage and changes in arthritis: noncollagenous proteins and proteoglycans in the extracellular matrix of cartilage, *Arthritis research*, 3(6), pp. 342-7.

Rowan, A. & Young, D., 2007, Collagenase gene regulation by pro-inflammatory cytokines in cartilage, *Frontiers in bioscience : a journal and virtual library*, 12:536-50.

Rötig, A., Bourgeron, T., Chretien, D., Rustin, P. & Munnich, A., 1995, Spectrum of mitochondrial DNA rearrangements in the Pearson marrow-pancreas syndrome, *Human molecular genetics*, 4(8), pp. 1327-30.

Rötig, A., Cormier, V., Blanche, S., Bonnefont, J.P., Ledeist, F., Romero, N., Schmitz, J., Rustin, P., Fischer, A. & Saudubray, J.M., 1990, Pearson's marrow-pancreas syndrome. A multisystem mitochondrial disorder in infancy, *The Journal of clinical investigation*, 86(5), pp. 1601-8.

Ruiz-Romero, C., Calamia, V., Mateos, J., Carreira, V., Mart\'\inez-Gomariz, M., Fernández, M. & Blanco, F., 2009, Mitochondrial Dysregulation of Osteoarthritic Human Articular Chondrocytes Analyzed by Proteomics: A Decrease in Mitochondrial Superoxide Dismutase Points to a Redox Imbalance, *Molecular & cellular proteomics : MCP*, 8(1), pp. 172-89.

Sasaki, H., Takayama, K., Matsushita, T., Ishida, K., Kubo, S., Matsumoto, T., Fujita, N., Oka, S., Kurosaka, M. & Kuroda, R., 2011, Autophagy modulates osteoarthritis-related gene expressions in human chondrocytes, *Arthritis and rheumatism*, 64(6):1920-8.

Sazanov, L.A. & Hinchliffe, P., 2006, Structure of the hydrophilic domain of respiratory complex I from Thermus thermophilus, *Science*, 311(5766), p. 1430.

Schleyer, M. & Neupert, W., 1985, Transport of proteins into mitochondria: translocational intermediates spanning contact sites between outer and inner membranes, *Cell*, 43(1), pp. 339-50.

Schmidt, A., Schwerd, T., Hamm, W., Hellmuth, J.C., Cui, S., Wenzel, M., Hoffmann, F.S., Michallet, M.-C., Besch, R., Hopfner, K.-P., Endres, S. & Rothenfusser, S., 2009, 5'-triphosphate RNA requires base-paired structures to activate antiviral signaling via RIG-I, *Proc Natl Acad Sci USA*, 106(29), pp. 12067-72.

Schmucker, A.C., Wright, J.B., Cole, M.D. & Brinckerhoff, C.E., 2012, Distal Interleukin-1β (IL-1β) Response Element of Human Matrix Metalloproteinase-13 (MMP-13) Binds Activator Protein 1 (AP-1) Transcription Factors and Regulates Gene Expression, *The Journal of biological chemistry*, 287(2), pp. 1189-97.

Schon, E.A., Rizzuto, R., Moraes, C.T., Nakase, H., Zeviani, M. & DiMauro, S., 1989, A direct repeat is a hotspot for large-scale deletion of human mitochondrial DNA, *Science*, 244(4902), pp. 346-9.

Schroder, K. & Tschopp, J., 2010, The inflammasomes, *Cell*, 140(6), pp. 821-32.

Schuessler, H. & Schilling, K., 1984, Oxygen effect in the radiolysis of proteins. Part 2. Bovine serum albumin, *Int J Radiat Biol Relat Stud Phys Chem Med*, 45(3), pp. 267-81.

Schultz, B.E. & Chan, S.I., 2001, Structures and proton-pumping strategies of mitochondrial respiratory enzymes, *Annu Rev Biophys Biomol Struct*, 30, pp. 23-65.

Schwartz, M. & Vissing, J., 2002, Paternal Inheritance of Mitochondrial DNA, *New England Journal of Medicine*, 347(8):576-80.

Sciacco, M., Bonilla, E., Schon, E.A., DiMauro, S. & Moraes, C.T., 1994, Distribution of wild-type and common deletion forms of mtDNA in normal and

respiration-deficient muscle fibers from patients with mitochondrial myopathy, *Human molecular genetics*, 3(1), pp. 13-9.

Scott, J.L., Gabrielides, C., Davidson, R.K., Swingler, T.E., Clark, I.M., Wallis, G.A., Boot-Handford, R.P., Kirkwood, T.B.L., Talyor, R.W. & Young, D.A., 2010, Superoxide dismutase downregulation in osteoarthritis progression and end-stage disease, *Annals of the rheumatic diseases*, 69(8):1502-10.

Seligman, A.M., Karnovsky, M.J., Wasserkrug, H.L. & Hanker, J.S., 1968, Nondroplet ultrastructural demonstration of cytochrome oxidase activity with a polymerizing osmiophilic reagent, diaminobenzidine (DAB), *J Cell Biol*, 38(1), pp. 1-14.

Seth, R.B., Sun, L., Ea, C.-K. & Chen, Z.J., 2005, Identification and characterization of MAVS, a mitochondrial antiviral signaling protein that activates NF-kappaB and IRF 3, *Cell*, 122(5), pp. 669-82.

Shah, R., Raska, K. & Tiku, M.L., 2005, The presence of molecular markers of in vivo lipid peroxidation in osteoarthritic cartilage: a pathogenic role in osteoarthritis, *Arthritis and rheumatism*, 52(9), pp. 2799-807.

Shoffner, J.M., Lott, M.T., Voljavec, A.S., Soueidan, S.A., Costigan, D.A. & Wallace, D.C., 1989, Spontaneous Kearns-Sayre/chronic external ophthalmoplegia plus syndrome associated with a mitochondrial DNA deletion: a slip-replication model and metabolic therapy, *Proc Natl Acad Sci USA*, 86(20), pp. 7952-6.

Short, K.R., Bigelow, M.L., Kahl, J., Singh, R., Coenen-Schimke, J., Raghavakaimal, S. & Nair, K.S., 2005, Decline in skeletal muscle mitochondrial function with aging in humans, *Proc Natl Acad Sci USA*, 102(15), pp. 5618-23.

Siems, W.G., Grune, T. & Esterbauer, H., 1995, 4-Hydroxynonenal formation during ischemia and reperfusion of rat small intestine, *Life sciences*, 57(8), pp. 785-9.

Skulachev, V., 1996, Role of uncoupled and non-coupled oxidations in maintenance of safely low levels of oxygen and its one-electron reductants, *Quarterly reviews of biophysics*, 29(2):169-202.

Smirnova, E., Griparic, L., Shurland, D.L. & Bliek, A.M.V.D., 2001, Dynamin-related protein Drp1 is required for mitochondrial division in mammalian cells, *Molecular biology of the cell*, 12(8), pp. 2245-56.

Sprong, R.C., Winkelhuyzen-Janssen, A.M., Aarsman, C.J., Oirschot, J.F.V., Bruggen, T.V.D. & Asbeck, B.S.V., 1998, Low-dose N-acetylcysteine protects rats against endotoxin-mediated oxidative stress, but high-dose increases mortality, *American journal of respiratory and critical care medicine*, 157(4 Pt 1), pp. 1283-93.

Stanton, H., Rogerson, F.M., East, C.J., Golub, S.B., Lawlor, K.E., Meeker, C.T., Little, C.B., Last, K., Farmer, P.J., Campbell, I.K., Fourie, A.M. & Fosang, A.J., 2005, ADAMTS5 is the major aggrecanase in mouse cartilage in vivo and in vitro, *Nature*, 434(7033), pp. 648-52.

Steenken, S., 1987, Addition--elimination paths in electron-transfer reactions between radicals and molecules. Oxidation of organic molecules by the OH radical, *J. Chem. Soc,* 83, pp. 113-24.

Steuerwald, N., Barritt, J.A., Adler, R., Malter, H., Schimmel, T., Cohen, J. & Brenner, C.A., 2000, Quantification of mtDNA in single oocytes, polar bodies and subcellular components by real-time rapid cycle fluorescence monitored PCR, *Zygote (Cambridge, England)*, 8(3), pp. 209-15.

Stewart, J.B., Freyer, C., Elson, J.L. & Larsson, N.-G., 2008a, Purifying selection of mtDNA and its implications for understanding evolution and mitochondrial disease, *Nature Reviews Genetics*, 9(9), pp. 657-62.

Stewart, J.B., Freyer, C., Elson, J.L., Wredenberg, A., Cansu, Z., Trifunovic, A. & Larsson, N.-G., 2008b, Strong purifying selection in transmission of mammalian mitochondrial DNA, *PLoS biology*, 6(1), p. e10.

Stock, D., Gibbons, C., Arechaga, I., Leslie, A.G. & Walker, J.E., 2000, The rotary mechanism of ATP synthase, *Current opinion in structural biology*, 10(6), pp. 672-9.

Stockwell, R.A., 1967, The cell density of human articular and costal cartilage, *J Anat*, 101(Pt 4), pp. 753-63.

Stockwell, R.A., 1983, *Cartilage-Structure, function and biochemistry (Hall, B. K.,ed),* Academic Press, New York .

Strassburger, M., Bloch, W., Sulyok, S., Schüller, J., Keist, A.F., Schmidt, A., Wenk, J., Peters, T., Wlaschek, M., Lenart, J., Krieg, T., Hafner, M., Kümin, A., Werner, S., Müller, W. & Scharffetter-Kochanek, K., 2005, Heterozygous deficiency of manganese superoxide dismutase results in severe lipid peroxidation and spontaneous apoptosis in murine myocardium in vivo, *Free radical biology & medicine*, 38(11), pp. 1458-70.

Struglics, A., Larsson, S., Pratta, M.A., Kumar, S., Lark, M.W. & Lohmander, L.S., 2006, Human osteoarthritis synovial fluid and joint cartilage contain both aggrecanase- and matrix metalloproteinase-generated aggrecan fragments, *Osteoarthr Cartil*, 14(2), pp. 101-13.

Sun, F., Huo, X., Zhai, Y., Wang, A., Xu, J., Su, D., Bartlam, M. & Rao, Z., 2005, Crystal structure of mitochondrial respiratory membrane protein complex II, *Cell*, 121(7), pp. 1043-57.

Susin, S.A., Lorenzo, H.K., Zamzami, N., Marzo, I., Brenner, C., Larochette, N., Prévost, M.C., Alzari, P.M. & Kroemer, G., 1999, Mitochondrial release of caspase-2 and -9 during the apoptotic process, *The Journal of experimental medicine*, 189(2), pp. 381-94.

Sylva, T.R.D., Connor, A., Mburu, Y., Keystone, E. & Wu, G.E., 2005, Somatic mutations in the mitochondria of rheumatoid arthritis synoviocytes, *Arthritis research & therapy*, 7(4), p. R844.

Szanda, G., Koncz, P., Rajki, A. & Spät, A., 2008, Participation of p38 MAPK and a novel-type protein kinase C in the control of mitochondrial Ca2+ uptake, *Cell Calcium*, 43(3), pp. 250-9.

Taivassalo, T., Gardner, J.L., Taylor, R.W., Schaefer, A.M., Newman, J., Barron, M.J., Haller, R.G. & Turnbull, D.M., 2006, Endurance training and detraining in mitochondrial myopathies due to single large-scale mtDNA deletions, *Brain : a journal of neurology*, 129(Pt 12), pp. 3391-401.

Tanaka, A., Cleland, M.M., Xu, S., Narendra, D.P., Suen, D.-F., Karbowski, M. & Youle, R.J., 2010, Proteasome and p97 mediate mitophagy and degradation of mitofusins induced by Parkin, *J Cell Biol*, 191(7), pp. 1367-80.

Taskiran, D., Stefanovic-Racic, M., Georgescu, H. & Evans, C., 1994, Nitric oxide mediates suppression of cartilage proteoglycan synthesis by interleukin-1, *Biochemical and biophysical research communications*, 200(1), pp. 142-8.

Tattoli, I., Carneiro, L.A., J|[Eacute]|Hanno, M., Magalhaes, J.G., Shu, Y., Philpott, D.J., Arnoult, D. & Girardin, S.E., 2008, NLRX1 is a mitochondrial NOD-like receptor that amplifies NF-|[kappa]|B and JNK pathways by inducing reactive oxygen species production, *EMBO reports*, 9(3), p. 293.

Taylor, R.W., Barron, M.J., Borthwick, G.M., Gospel, A., Chinnery, P.F., Samuels, D.C., Taylor, G.A., Plusa, S.M., Needham, S.J., Greaves, L.C., Kirkwood, T.B.L. & Turnbull, D.M., 2003, Mitochondrial DNA mutations in human colonic crypt stem cells, *The Journal of clinical investigation*, 112(9), pp. 1351-60.

Temperley, R., Richter, R., Dennerlein, S., Lightowlers, R.N. & Chrzanowska-Lightowlers, Z.M., 2010, Hungry codons promote frameshifting in human mitochondrial ribosomes, *Science*, 327(5963), p. 301.

Tetlow, L.C., Adlam, D.J. & Woolley, D.E., 2001, Matrix metalloproteinase and proinflammatory cytokine production by chondrocytes of human osteoarthritic cartilage: associations with degenerative changes, *Arthritis and rheumatism*, 44(3), pp. 585-94.

Thannickal, V.J. & Fanburg, B.L., 2000, Reactive oxygen species in cell signaling, *Am J Physiol Lung Cell Mol Physiol*, 279(6), pp. L1005-28.

Thonar, E.J., Buckwalter, J.A. & Kuettner, K.E., 1986, Maturation-related differences in the structure and composition of proteoglycans synthesized by chondrocytes from bovine articular cartilage, *The Journal of biological chemistry*, 261(5), pp. 2467-74.

Thorneley, R.N., 1974, A convenient electrochemical preparation of reduced methyl viologen and a kinetic study of the reaction with oxygen using an anaerobic stopped-flow apparatus, *Biochimica et biophysica acta*, 333(3), pp. 487-96.

Tiku, M.L., Narla, H., Jain, M. & Yalamanchili, P., 2007, Glucosamine prevents in vitro collagen degradation in chondrocytes by inhibiting advanced lipoxidation reactions and protein oxidation, *Arthritis research & therapy*, 9(4), p. R76.

Tiku, M.L., Shah, R. & Allison, G.T., 2000, Evidence linking chondrocyte lipid peroxidation to cartilage matrix protein degradation. Possible role in cartilage aging and the pathogenesis of osteoarthritis, *The Journal of biological chemistry*, 275(26), pp. 20069-76.

Tiku, M.L., Yan, Y.P. & Chen, K.Y., 1998, Hydroxyl radical formation in chondrocytes and cartilage as detected by electron paramagnetic resonance spectroscopy using spin trapping reagents, *Free radical research*, 29(3), pp. 177-87.

Toime, L.J. & Brand, M.D., 2010, Uncoupling protein-3 lowers reactive oxygen species production in isolated mitochondria, *Free radical biology & medicine*, 49(4), pp. 606-11.

Torroni, A., Petrozzi, M., D'Urbano, L., Sellitto, D., Zeviani, M., Carrara, F., Carducci, C., Leuzzi, V., Carelli, V., Barboni, P., Negri, A.D. & Scozzari, R., 1997, Haplotype and phylogenetic analyses suggest that one European-specific mtDNA background plays a role in the expression of Leber hereditary optic neuropathy by increasing the penetrance of the primary mutations 11778 and 14484, *American journal of human genetics*, 60(5), pp. 1107-21.

Toussaint, O., Medrano, E.E. & Zglinicki, T.V., 2000, Cellular and molecular mechanisms of stress-induced premature senescence (SIPS) of human diploid fibroblasts and melanocytes, *Experimental gerontology*, 35(8), pp. 927-45.

Trifunovic, A., Hansson, A., Wredenberg, A., Rovio, A.T., Dufour, E., Khvorostov, I., Spelbrink, J.N., Wibom, R., Jacobs, H.T. & Larsson, N.-G., 2005, Somatic mtDNA mutations cause aging phenotypes without affecting reactive oxygen species production, *Proc Natl Acad Sci USA*, 102(50), pp. 17993-8.

Trifunovic, A., Wredenberg, A., Falkenberg, M., Spelbrink, J.N., Rovio, A.T., Bruder, C.E., Bohlooly-Y, M., Gidlöf, S., Oldfors, A., Wibom, R., Törnell, J., Jacobs, H.T. & Larsson, N.-G., 2004, Premature ageing in mice expressing defective mitochondrial DNA polymerase, *Nature*, 429(6990), pp. 417-23.

Turrens, J.F. & Boveris, A., 1980, Generation of superoxide anion by the NADH dehydrogenase of bovine heart mitochondria, *The Biochemical journal*, 191(2), pp. 421-7.

Turrens, J.F., 2003, Mitochondrial formation of reactive oxygen species, *J Physiol (Lond)*, 552(Pt 2), pp. 335-44.

Valko, M., Leibfritz, D., Moncol, J., Cronin, M.T.D., Mazur, M. & Telser, J., 2007, Free radicals and antioxidants in normal physiological functions and human disease, *Int J Biochem Cell Biol*, 39(1), pp. 44-84.

Vandesompele, J., De Preter, K., Pattyn, F., Poppe, B., Van Roy, N., De Paepe, A. & Speleman, F., 2002, Accurate normalization of real-time quantitative RT-PCR data by geometric averaging of multiple internal control genes, *Genome biology*, 3(7), pp. 34.

Venhoff, A.C., Lebrecht, D., Reuss, F.U., Heckl-Ostreicher, B., Wehr, R., Walker, U.A. & Venhoff, N., 2009, Mitochondrial DNA depletion in rat liver induced by fosalvudine tidoxil, a novel nucleoside reverse transcriptase inhibitor prodrug, *Antimicrobial agents and chemotherapy*, 53(7), pp. 2748-51.

Verschoor, M.L., Wilson, L.A., Verschoor, C.P. & Singh, G., 2010, Ets-1 regulates energy metabolism in cancer cells, *PLoS ONE*, 5(10), p. e13565.

Verzijl, N., DeGroot, J., Thorpe, S.R., Bank, R.A., Shaw, J.N., Lyons, T.J., Bijlsma, J.W., Lafeber, F.P., Baynes, J.W. & TeKoppele, J.M., 2000, Effect of collagen turnover on the accumulation of advanced glycation end products, *The Journal of biological chemistry*, 275(50), pp. 39027-31.

Vincenti, M.P. & Brinckerhoff, C.E., 2002, Transcriptional regulation of collagenase (MMP-1, MMP-13) genes in arthritis: integration of complex signaling pathways for the recruitment of gene-specific transcription factors, *Arthritis research*, 4(3), pp. 157-64.

Vogel, R.O., Smeitink, J.A.M. & Nijtmans, L.G.J., 2007, Human mitochondrial complex I assembly: a dynamic and versatile process, *Biochimica et biophysica acta*, 1767(10), pp. 1215-27.

Voos, W., Martin, H., Krimmer, T. & Pfanner, N., 1999, Mechanisms of protein translocation into mitochondria, *Biochimica et biophysica acta*, 1422(3), pp. 235-54.

Votyakova, T.V. & Reynolds, I.J., 2001, DeltaPsi(m)-Dependent and -independent production of reactive oxygen species by rat brain mitochondria, *Journal of neurochemistry*, 79(2), pp. 266-77.

Wachlin, G., Augstein, P., Schröder, D., Kuttler, B., Klöting, I., Heinke, P. & Schmidt, S., 2003, IL-1beta, IFN-gamma and TNF-alpha increase vulnerability of pancreatic beta cells to autoimmune destruction, *J Autoimmun*, 20(4), pp. 303-12.

Wang, M., Dhingra, K., Hittelman, W.N., Liehr, J.G., de Andrade, M. & Li, D., 1996, Lipid peroxidation-induced putative malondialdehyde-DNA adducts in human breast tissues, *Cancer Epidemiol Biomarkers Prev*, 5(9), pp. 705-10.

Wang, Z., Juttermann, R. & Soloway, P.D., 2000, TIMP-2 is required for efficient activation of proMMP-2 in vivo, *The Journal of biological chemistry*, 275(34), pp. 26411-5.

Westermann, B., 2010, Mitochondrial fusion and fission in cell life and death, *Nat Rev Mol Cell Biol*, 11(12), pp. 872-84.

Wikstrom, J.D., Twig, G. & Shirihai, O.S., 2009, What can mitochondrial heterogeneity tell us about mitochondrial dynamics and autophagy? *Int J Biochem Cell Biol*, 41(10), pp. 1914-27.

Wikstrom, M., 1977, Proton pump coupled to cytochrome c oxidase in mitochondria, *Nature*, 266(5599):271-3.

Williams, M.D., Remmen, H.V., Conrad, C.C., Huang, T.T., Epstein, C.J. & Richardson, A., 1998, Increased oxidative damage is correlated to altered mitochondrial function in heterozygous manganese superoxide dismutase knockout mice, *The Journal of biological chemistry*, 273(43), pp. 28510-5.

Worley, J.R., Thompkins, P.B., Lee, M.H., Hutton, M., Soloway, P., Edwards, D.R., Murphy, G. & Knäuper, V., 2003, Sequence motifs of tissue inhibitor of metalloproteinases 2 (TIMP-2) determining progelatinase A (proMMP-2) binding and activation by membrane-type metalloproteinase 1 (MT1-MMP), *The Biochemical journal*, 372(Pt 3), pp. 799-809.

Xia, X., Cui, J., Wang, H.Y., Zhu, L., Matsueda, S., Wang, Q., Yang, X., Hong, J., Songyang, Z., Chen, Z.J. & Wang, R.-F., 2011, NLRX1 negatively regulates TLR-induced NF-κB signaling by targeting TRAF6 and IKK, *Immunity*, 34(6), pp. 843-53.

Xu, L.-G., Wang, Y.-Y., Han, K.-J., Li, L.-Y., Zhai, Z. & Shu, H.-B., 2005, VISA is an adapter protein required for virus-triggered IFN-beta signaling, *Molecular cell*, 19(6), pp. 727-40.

Xu, Y., Fang, F., Dhar, S., Clair, W.S., Kasarskis, E. & Clair, D.S., 2007, The Role of a Single-stranded Nucleotide Loop in Transcriptional Regulation of the Human sod2 Gene, *Journal of Biological Chemistry*, 282(22), p. 15981.

Xu, Y., Kiningham, K.K., Devalaraja, M.N., Yeh, C.C., Majima, H., Kasarskis, E.J. & Clair, D.K.S., 1999, An intronic NF-kappaB element is essential for induction of the human manganese superoxide dismutase gene by tumor necrosis factor-alpha and interleukin-1beta, *DNA and cell biology*, 18(9), pp. 709-22.

Yadava, N. & Nicholls, D.G., 2007, Spare respiratory capacity rather than oxidative stress regulates glutamate excitotoxicity after partial respiratory inhibition of mitochondrial complex I with rotenone, *The Journal of neuroscience : the official journal of the Society for Neuroscience*, 27(27), pp. 7310-7.

Yamamoto, H., Tanaka, M., Katayama, M., Obayashi, T., Nimura, Y. & Ozawa, T., 1992, Significant existence of deleted mitochondrial DNA in cirrhotic liver surrounding hepatic tumor, *Biochemical and biophysical research communications*, 182(2), pp. 913-20.

Yamamoto, T. & Gay, C.V., 1988, Ultrastructural analysis of cytochrome oxidase in chick epiphyseal growth plate cartilage, *The journal of histochemistry and cytochemistry : official journal of the Histochemistry Society*, 36(9), pp. 1161-6.

Yanai, H., Ban, T., Wang, Z., Choi, M.K., Kawamura, T., Negishi, H., Nakasato, M., Lu, Y., Hangai, S., Koshiba, R., Savitsky, D., Ronfani, L., Akira, S., Bianchi, M.E., Honda, K., Tamura, T., Kodama, T. & Taniguchi, T., 2009, HMGB proteins function as universal sentinels for nucleic-acid-mediated innate immune responses, *Nature*, 462(7269), pp. 99-103.

Yasukawa, T., Reyes, A., Cluett, T.J., Yang, M.-Y., Bowmaker, M., Jacobs, H.T. & Holt, I.J., 2006, Replication of vertebrate mitochondrial DNA entails transient ribonucleotide incorporation throughout the lagging strand, *EMBO J*, 25(22), pp. 5358-71.

Yoneda, M., Chomyn, A., Martinuzzi, A., Hurko, O. & Attardi, G., 1992, Marked replicative advantage of human mtDNA carrying a point mutation that causes the MELAS encephalomyopathy, *Proc Natl Acad Sci USA*, 89(23), pp. 11164-8.

Yoshida, M., Muneyuki, E. & Hisabori, T., 2001, ATP synthase--a marvellous rotary engine of the cell, *Nat Rev Mol Cell Biol*, 2(9), pp. 669-77.

Yudoh, K., Nguyen, T., Nakamura, H., Hongo-Masuko, K., Kato, T. & Nishioka, K., 2005, Potential involvement of oxidative stress in cartilage senescence and development of osteoarthritis: oxidative stress induces chondrocyte telomere

instability and downregulation of chondrocyte function, *Arthritis research & therapy*, 7(2), pp. R380-91.

Zelko, I.N., Mariani, T.J. & Folz, R.J., 2002, Superoxide dismutase multigene family: a comparison of the CuZn-SOD (SOD1), Mn-SOD (SOD2), and EC-SOD (SOD3) gene structures, evolution, and expression, *Free radical biology & medicine*, 33(3), pp. 337-49.

Zhang, C., Baumer, A., Mackay, I.R., Linnane, A.W. & Nagley, P., 1995, Unusual pattern of mitochondrial DNA deletions in skeletal muscle of an adult human with chronic fatigue syndrome, *Human molecular genetics*, 4(4), pp. 751-4.

Zhang, J., Khvorostov, I., Hong, J.S., Oktay, Y., Vergnes, L., Nuebel, E., Wahjudi, P.N., Setoguchi, K., Wang, G., Do, A., Jung, H.J., McCaffery, J.M., Kurland, I.J., Reue, K., Lee, W.N., Koehler, C.M. & Teitell, M.A., 2011, UCP2 regulates energy metabolism and differentiation potential of human pluripotent stem cells, *EMBO J*, 30(24), pp. 4860-73.

Zhang, L., Yu, L. & Yu, C.A., 1998, Generation of superoxide anion by succinate-cytochrome c reductase from bovine heart mitochondria, *The Journal of biological chemistry*, 273(51), pp. 33972-6.

Zhang, Q., Hui, W., Litherland, G.J., Barter, M.J., Davidson, R., Darrah, C., Donell, S.T., Clark, I.M., Cawston, T.E., Robinson, J.H., Rowan, A.D. & Young, D.A., 2008, Differential Toll-like receptor-dependent collagenase expression in chondrocytes, *Annals of the rheumatic diseases*, 67(11), pp. 1633-41.

Zhou, R., Yazdi, A.S., Menu, P. & Tschopp, J., 2011, A role for mitochondria in NLRP3 inflammasome activation, *Nature*, 469(7329), pp. 221-5.

Zhou, S., Cui, Z. & Urban, J.P.G., 2004, Factors influencing the oxygen concentration gradient from the synovial surface of articular cartilage to the cartilage-bone interface: a modeling study, *Arthritis and rheumatism*, 50(12), pp. 3915-24.

Zhu, C.H., Huang, Y., Oberley, L.W. & Domann, F.E., 2001, A family of AP-2 proteins down-regulate manganese superoxide dismutase expression, *The Journal of biological chemistry*, 276(17), pp. 14407-13.

Appendix I. Patient data

Patient ID	Age	Gender	Joint type	Tissue	Experiments
DTOS 1599	72	MALE	OA KNEE	CARTILAGE	Innate Immunity
DTOS 1759	67	MALE	OA KNEE	CARTILAGE	Innate Immunity
DTOS 1876	81	FEMALE	OA KNEE	CARTILAGE	Innate Immunity
DTOS 1891	74	FEMALE	OA KNEE	CARTILAGE	Innate Immunity
DTOS 2123	70	FEMALE	OA KNEE	CARTILAGE	Innate Immunity
T002	73	MALE	NOF	CARTILAGE	Mitochondrial respiration
T004	83	MALE	NOF	CARTILAGE	Mitochondrial respiration
T005	69	MALE	NOF	CARTILAGE	Mitochondrial respiration
T010	86	MALE	NOF	CARTILAGE	Mitochondrial respiration
T015	78	MALE	NOF	CARTILAGE	Mitochondrial respiration
T032	82	FEMALE	NOF	CARTILAGE	Mitochondrial respiration
T042	91	FEMALE	NOF	CARTILAGE	Mitochondrial respiration
T045	78	MALE	NOF	CARTILAGE	Mitochondrial respiration
T046	79	MALE	NOF	CARTILAGE	Mitochondrial respiration
DTOS 1744	50	MALE	OA KNEE	CARTILAGE	Mitochondrial respiration, ROS
DTOS 1773	62	MALE	OA KNEE	CARTILAGE	Mitochondrial respiration, ROS
DTOS 1779	83	MALE	OA HIP	CARTILAGE	Mitochondrial respiration, ROS
DTOS 1791	58	MALE	OA HIP	CARTILAGE	Mitochondrial respiration, ROS
DTOS 1840	76	MALE	OA HIP	CARTILAGE	Mitochondrial respiration, ROS
DTOS 2035	68	FEMALE	OA HIP	CARTILAGE	Mitochondrial respiration, ROS
DTOS 2098	75	FEMALE	OA HIP	CARTILAGE	Mitochondrial respiration, ROS
39833	69	MALE	OA KNEE	CANC BONE	mtDNA deletions, mtDNA copy number
234515	58	MALE	OA KNEE	FAT PAD	mtDNA deletions, mtDNA copy number
234515	58	MALE	OA KNEE	LIGAMENT	mtDNA deletions, mtDNA copy number
333031	75	MALE	OA KNEE	CARTILAGE	mtDNA deletions, mtDNA copy number
333031	75	MALE	OA KNEE	MENISCUS	mtDNA deletions,

					mtDNA copy number
333031	75	MALE	OA KNEE	MENISCUS	mtDNA deletions, mtDNA copy number
333031	75	MALE	OA KNEE	MENISCUS	mtDNA deletions, mtDNA copy number
333031	75	MALE	OA KNEE	FAT PAD	mtDNA deletions, mtDNA copy number
957390	60	MALE	OA HIP	SYNOVIUM	mtDNA deletions, mtDNA copy number
1284908	82	FEMALE	OA KNEE	CARTILAGE	mtDNA deletions, mtDNA copy number
8011503	54	FEMALE	OA HIP	LIGAMENT	mtDNA deletions, mtDNA copy number
8048367	85	MALE	OA HIP	CANC BONE	mtDNA deletions, mtDNA copy number
8048367	85	MALE	OA HIP	CANC BONE	mtDNA deletions, mtDNA copy number
8048367	85	MALE	OA HIP	CORT BONE	mtDNA deletions, mtDNA copy number
8048367	85	MALE	OA HIP	CORT BONE	mtDNA deletions, mtDNA copy number
8048367	85	MALE	OA HIP	CORT BONE	mtDNA deletions, mtDNA copy number
8048367	85	MALE	OA HIP	CORT BONE	mtDNA deletions, mtDNA copy number
8048367	85	MALE	OA HIP	CORT BONE	mtDNA deletions, mtDNA copy number
8048367	85	MALE	OA HIP	OSTEOPHYTES	mtDNA deletions, mtDNA copy number
8048367	85	MALE	OA HIP	OSTEOPHYTES	mtDNA deletions, mtDNA copy number
8048367	85	MALE	OA HIP	OSTEOPHYTES	mtDNA deletions, mtDNA copy number
8048367	85	MALE	OA HIP	OSTEOPHYTES	mtDNA deletions, mtDNA copy number
8098004	72	FEMALE	OA HIP	CORT BONE	mtDNA deletions, mtDNA copy number
8098004	72	FEMALE	OA HIP	CANC BONE	mtDNA deletions, mtDNA copy number
8117954	62	MALE	OA KNEE	FAT PAD	mtDNA deletions, mtDNA copy number
8157410	82	FEMALE	OA KNEE	FAT PAD	mtDNA deletions, mtDNA copy number
8157410	82	FEMALE	OA KNEE	MENISCUS	mtDNA deletions, mtDNA copy number
DTOS 1718	72	FEMALE	OA KNEE	CARTILAGE	mtDNA deletions, mtDNA copy number
DTOS 1724	74	MALE	OA KNEE	CARTILAGE	mtDNA deletions, mtDNA copy number
DTOS 1744	50	MALE	OA KNEE	CARTILAGE	mtDNA deletions, mtDNA copy number
DTOS 1744	50	MALE	OA KNEE	CARTILAGE	mtDNA deletions, mtDNA copy number
DTOS 1757	58	FEMALE	OA KNEE	CARTILAGE	mtDNA deletions, mtDNA copy number
DTOS 1762	80	FEMALE	OA HIP	CARTILAGE	mtDNA deletions, mtDNA copy number
DTOS 1782	79	MALE	OA KNEE	CARTILAGE	mtDNA deletions, mtDNA copy number
DTOS 1814	53	MALE	OA KNEE	CARTILAGE	mtDNA deletions,

					mtDNA copy number
DTOS 1818	60	MALE	OA KNEE	CARTILAGE	mtDNA deletions, mtDNA copy number
DTOS 1819	67	MALE	OA KNEE	CARTILAGE	mtDNA deletions, mtDNA copy number
DTOS 1820	76	FEMALE	OA HIP	CARTILAGE	mtDNA deletions, mtDNA copy number
DTOS 1820	76	FEMALE	OA HIP	CARTILAGE	mtDNA deletions, mtDNA copy number
DTOS 1820	76	FEMALE	OA HIP	CARTILAGE	mtDNA deletions, mtDNA copy number
DTOS 1820	76	FEMALE	OA HIP	CARTILAGE	mtDNA deletions, mtDNA copy number
DTOS 1820	76	FEMALE	OA HIP	CARTILAGE	mtDNA deletions, mtDNA copy number
DTOS 1822	85	MALE	OA HIP	CARTILAGE	mtDNA deletions, mtDNA copy number
DTOS 1823	79	MALE	OA KNEE	FAT PAD	mtDNA deletions, mtDNA copy number
DTOS 1823	79	MALE	OA KNEE	SYNOVIUM	mtDNA deletions, mtDNA copy number
DTOS 1823	79	MALE	OA KNEE	SYNOVIUM	mtDNA deletions, mtDNA copy number
DTOS 1828	57	FEMALE	OA KNEE	CARTILAGE	mtDNA deletions, mtDNA copy number
DTOS 1850	50	FEMALE	OA KNEE	CARTILAGE	mtDNA deletions, mtDNA copy number
DTOS 1850	50	FEMALE	OA KNEE	FAT PAD	mtDNA deletions, mtDNA copy number
T004	83	MALE	NOF	CARTILAGE	mtDNA deletions, mtDNA copy number
T005	69	FEMALE	NOF	CARTILAGE	mtDNA deletions, mtDNA copy number
T005	69	FEMALE	NOF	CARTILAGE	mtDNA deletions, mtDNA copy number
T010	86	MALE	NOF	CARTILAGE	mtDNA deletions, mtDNA copy number
T015	78	MALE	NOF	CARTILAGE	mtDNA deletions, mtDNA copy number
T016	79	FEMALE	NOF	CARTILAGE	mtDNA deletions, mtDNA copy number
T023	68	FEMALE	NOF	CARTILAGE	mtDNA deletions, mtDNA copy number
DTOS 1596	76	FEMALE	OA HIP	CARTILAGE	mtDNA deletions, TBARS, mtDNA copy number
DTOS 1622	67	FEMALE	OA HIP	CARTILAGE	mtDNA deletions, TBARS, mtDNA copy number
DTOS 1683	78	FEMALE	OA HIP	CARTILAGE	mtDNA deletions, TBARS, mtDNA copy number
DTOS 1734	83	FEMALE	OA HIP	CARTILAGE	mtDNA deletions, TBARS, mtDNA copy number
DTOS 1842	82	FEMALE	OA HIP	CARTILAGE	mtDNA deletions, TBARS, mtDNA copy number
DTOS 1906	72	FEMALE	OA HIP	CARTILAGE	mtDNA deletions, TBARS, mtDNA copy

					number
DTOS 1908	83	FEMALE	OA HIP	CARTILAGE	mtDNA deletions, TBARS, mtDNA copy number
T006	69	FEMALE	NOF	CARTILAGE	mtDNA deletions, TBARS, mtDNA copy number
T007	71	FEMALE	NOF	CARTILAGE	mtDNA deletions, TBARS, mtDNA copy number
T012	81	FEMALE	NOF	CARTILAGE	mtDNA deletions, TBARS, mtDNA copy number
T013	72	FEMALE	NOF	CARTILAGE	mtDNA deletions, TBARS, mtDNA copy number
T014	84	FEMALE	NOF	CARTILAGE	mtDNA deletions, TBARS, mtDNA copy number
T018	94	FEMALE	NOF	CARTILAGE	mtDNA deletions, TBARS, mtDNA copy number
T020	84	FEMALE	NOF	CARTILAGE	mtDNA deletions, TBARS, mtDNA copy number
T021	84	FEMALE	NOF	CARTILAGE	mtDNA deletions, TBARS, mtDNA copy number
T023	68	FEMALE	NOF	CARTILAGE	mtDNA deletions, TBARS, mtDNA copy number
T024	80	FEMALE	NOF	CARTILAGE	mtDNA deletions, TBARS, mtDNA copy number
T026	86	MALE	NOF	CARTILAGE	mtDNA deletions, TBARS, mtDNA copy number
T031	89	FEMALE	NOF	CARTILAGE	mtDNA deletions, TBARS, mtDNA copy number
T037	83	FEMALE	NOF	CARTILAGE	mtDNA deletions, TBARS, mtDNA copy number